

Report No. FHWA/RD-81/118

PB82140724



RAPID DETERMINATION OF THE CHLORIDE PERMEABILITY OF CONCRETE

August 1981
Final Report



Document is available to the public through
the National Technical Information Service,
Springfield, Virginia 22161



Prepared for
FEDERAL HIGHWAY ADMINISTRATION
Office of Research & Development
Materials Division
Washington, D.C. 20590

REPRODUCED BY
**NATIONAL TECHNICAL
INFORMATION SERVICE**
U.S. DEPARTMENT OF COMMERCE
SPRINGFIELD, VA 22161

Technical Report Documentation Page

1. Report No. FHWA RD-81/119	2. Government Accession No.	3. Recipient's Catalog No. PB82-140724
4. Title and Subtitle RAPID DETERMINATION OF THE CHLORIDE PERMEABILITY OF CONCRETE	5. Report Date August 1981	6. Performing Organization Code 355041
	7. Author(s) D. Whiting	8. Performing Organization Report No. CR-2056
9. Performing Organization Name and Address Construction Technology Laboratories A Division of the Portland Cement Association 5420 Old Orchard Road Skokie, Illinois 60077	10. Work Unit No. (TRIS) FCP-34K1-0' 2	11. Contract or Grant No. DOT-FH-11-9305
	12. Sponsoring Agency Name and Address Offices of Research and Development Federal Highway Administration U.S. Department of Transportation Washington, D. C. 20590	13. Type of Report and Period Covered Final Report
15. Supplementary Notes FHWA Contract Manager: T. M. Mitchell (HRS-21)		
16. Abstract Techniques have been developed for determination of the permeability of a variety of concretes to chloride ions in a relatively rapid period of time. The most promising method involves application of d.c. voltage in the range of 60.0-80.0 volts for 6-hours to either a section of a reinforced concrete bridge deck or a core taken from a concrete structure. Both variations involve conditioning of the specimen prior to test so as to eliminate test anomalies caused by low sample moisture contents. Core specimens can be tested at the rate of one specimen per day with a total of 2 days needed for a complete test including conditioning. The field apparatus is capable of conducting four tests within one working week on a given bridge deck. Results have been shown to yield reasonably good correlation with FHWA 90-day ponding data on companion specimens. Concretes can be ranked according to high, moderate, low, or very low chloride permeability. Further work is needed in order to make the test more applicable to field testing of bridge deck overlays.		
17. Key Words Concrete permeability, chlorides, latex, polymer concrete, internally sealed concrete, dense concrete overlays, bridge decks, non-destructive testing.	18. Distribution Statement No restrictions. This document is available to the public through the National Technical Information Service, Springfield, Virginia 22161	
19. Security Classif. (of this report) Unclassified	20. Security Classif. (of this page) Unclassified	21. No. of Pages 174
		22. Price


FOREWORD

This report describes a new method for rapid determination of the permeability of various concretes to chloride ions. It will be of interest to materials, bridge, and other engineers concerned with the construction of low permeability bridge deck protective systems.

The report covers the development of prototype equipment and includes the results of laboratory studies and of field and laboratory trials of the device on three bridges. The technique is suitable for use both on cores and in place on a deck. The results indicate the new procedure may be a very suitable replacement for the current 90-day ponding test for chloride permeability.

FHWA appreciates the assistance of the Wisconsin Department of Transportation in making field sites available to the researchers.

Sufficient copies of the report are being distributed by FHWA Bulletin to provide a minimum of one copy to each FHWA regional office, one copy to each FHWA division office, and two copies to each State highway agency. Direct distribution is being made to the division offices.


Charles F. Scheffey
Director, Office of Research
Federal Highway Administration

NOTICE

This document is disseminated under the sponsorship of the Department of Transportation in the interest of information exchange. The United States Government assumes no liability for its contents or use thereof. The contents of this report reflect the views of the contractor, who is responsible for the accuracy of the data presented herein. The contents do not necessarily reflect the official views or policy of the Department of Transportation. This report does not constitute a standard, specification, or regulation.

The United States Government does not endorse products or manufacturers. Trade or manufacturers' names appear herein only because they are considered essential to the object of this document.

TABLE OF CONTENTS

	<u>Page</u>		
1. INTRODUCTION	1	4.6 Results of Core Tests . .	62
2. LITERATURE STUDY	1	4.6.1 Specimen Preparation	63
2.1 Flow of Fluids and Ions Through Concrete	1	4.6.2 Current vs. Time	63
2.2 Permeability of Cement and Concrete	3	4.6.3 Temperature and Resistance	63
2.2.1 Hardened Cement Paste	3	4.6.4 Correlations with FHWA 90-Day Ponding Data	63
2.2.2 Concrete	4	4.6.5 Effects of Surface Finishing	71
2.3 Conventional Permeability Test Procedures	7	4.6.6 Effects of Heat Treatment on Internally Sealed Specimens	71
2.3.1 Water Permeability	7	4.6.7 Effect of Thickness	75
2.3.2 Air Permeability	7	4.6.8 Reproducibility of the Method	75
2.3.3 Water Vapor Transmission	7	4.7 Conclusions Derived from Laboratory Evaluations	75
2.3.4 Ion Diffusion	7	5. PROTOTYPE INSTRUMENT DEVELOPMENT	77
2.3.5 Resistivity Techniques	7	5.1 Desirable Features	77
2.4 Criteria for a Chloride Permeability Test Method	15	5.2 General Description	77
2.4.1 Nondestructive (Passive) Techniques	15	5.3 Construction	77
2.4.2 Direct Techniques	15	5.3.1 Electronics Module	77
2.4.3 Electrical Methods	17	5.3.2 Vacuum Saturation Module	79
2.5 Conclusions from Literature Search	18	5.3.3 Screen Assembly	79
2.6 Selection of Research Approach	18	5.3.4 Generator Set	79
2.7 Approach Selected	18	5.4 Electronic Circuitry	79
3. METHOD DEVELOPMENT	19	5.4.1 Locations of Components	79
3.1 Testing of Rocks, Cement Pastes, and Mortars	19	5.4.2 System Description	83
3.2 Concrete Slabs	24	5.4.3 Individual Circuit Descriptions	83
3.2.1 Slab Specimens	24	6. LABORATORY TESTING OF PROTOTYPE INSTRUMENT	86
3.2.2 Apparatus	24	6.1 Test Specimens	86
3.2.3 Preliminary Tests	24	6.2 Concrete Mixtures	87
3.2.4 Tests at Higher Voltages	30	6.3 Casting and Conditioning of Slabs	87
3.2.5 Conclusions Derived from Preliminary Experiments	32	6.4 Effect of Cover	87
4. LABORATORY TESTING	32	6.5 Effect of Reinforcing Cage Geometry	94
4.1 Test Specimens	32	6.6 Effect of Ambient Temperature	94
4.2 Concrete Mixtures	36	6.7 Test of Chloride-Laden Slab	96
4.3 Test Procedure-Slab Specimens	38	7. FIELD TRIALS	96
4.4 Results of Slab Tests	39	7.1 Bridge 1 - Conventional Concrete Deck	96
4.4.1 Moist and As-Received Slabs	39	7.1.1 Background	96
4.4.2 Correlations with FHWA 90-Day Ponding Data	40	7.1.2 Test Locations	97
4.4.3 Air-Dried Slabs	45	7.1.3 Functioning of Equipment	97
4.5 Re-Saturation Studies	45	7.1.4 Test Results	97
4.5.1 Apparatus	45	7.2 Bridge 2 - Dense Concrete Overlay	102
4.5.2 Preliminary Re-Saturation Tests	48	7.2.1 Background	102
4.5.3 Application to FHWA Slabs	55	7.2.2 Overlay and Test Locations	102
		7.2.3 Test Results	103
		7.3 Bridge 3 - Polymer-Concrete Overlay	108
		7.3.1 Installation of Overlay	108

7.3.2	Test Results . . .	108
7.4	Safety Considerations . . .	109
8.	OTHER TECHNIQUES	109
8.1	Water Vapor Transmission	109
8.2	Air Permeability	112
8.3	Depth of Impermeability-Resistivity Technique	115
9.	SUMMARY, CONCLUSIONS, AND RECOMMENDATIONS	115
9.1	Summary and Conclusions	115
9.1.1	General	115
9.1.2	Effects of Test Variables	116
9.1.3	Mode of Operation	116
9.1.4	Safety Considerations	117
9.2	Recommendations for Future Research	117
9.2.1	Improvement of Current Techniques	117
9.2.2	Basic Research	117
10.	REFERENCES	118
	APPENDIX 1	121
	APPENDIX 2	129
	APPENDIX 3	136
	APPENDIX 4	147
	APPENDIX 5	149
	APPENDIX 6	155
	APPENDIX 7	156

FIGURE 14	Chloride Profiles for Slabs Having w/c Ratio of 0.35	31
FIGURE 15	Chloride Profiles for Slabs Tested for 6 Hours	33
FIGURE 16	Current vs. Time for Slabs at 0.35 and 0.60 w/c Ratio Tested at 80.0 Vdc	34
FIGURE 17	Temperature Rise in Slab at 0.60 w/c Ratio Tested at 80.0 Vdc	35
FIGURE 18	Details of Slabs Supplied by FHWA	37
FIGURE 19	Temperature Rise in Slabs at 80.0 Vdc for Various Materials	40
FIGURE 20	Current vs. Time for Various Slabs Tested at 80.0 Vdc	41
FIGURE 21	Chloride Profiles for Slabs Tested for 6 Hours at 80.0 Vdc	42
FIGURE 22	Charge Passed vs. Average Free Moisture Content of As-Received and Air-Dried Slabs	46
FIGURE 23	Vacuum Chamber Used for Re-Saturation Studies	47
FIGURE 24	Sampling Locations	49
FIGURE 25	Relative Humidity Profiles During 36-Hour Ponding Period	51
FIGURE 26	Resistance vs. Time During Linewater Ponding on Slab Surface	52
FIGURE 27	Chloride Profiles for Various Re-Saturation Schemes	54
FIGURE 28	Resistance vs. Time During Re-Saturation of FHWA Slabs	56
FIGURE 29	Resistance vs. Time During Re-Saturation of Additional FHWA Slabs	57
FIGURE 30	Current vs. Time for Re-Saturated FHWA Slabs	58
FIGURE 31	Chloride Profiles for 0.60 w/c Ratio Slab Tested in Moist and Re-Saturated Conditions	59
FIGURE 32	Chloride Profile for Properly Consolidated Iowa Overlay Slab Tested in Moist and Re-Saturated Conditions	60
FIGURE 33	Chloride Profiles for Heated Full-Depth Internally Sealed Concrete Slab in Moist and Re-Saturated Conditions	61
FIGURE 34	Sectioning of Core Specimens	64
FIGURE 35	Current vs. Time for 2-inch Thick Core Slices Tested in Applied Voltage Cell	65

LIST OF ILLUSTRATIONS

FIGURE 1	Movement of Water Through Porous Materials	2
FIGURE 2	PCA Permeability Tests (1929) on Concrete	5
FIGURE 3	Kansas Permeability Cell	12
FIGURE 4	Test Results with Kansas Permeability Cell	13
FIGURE 5	Cell Used for Preliminary Experiments	20
FIGURE 6	Current vs. Time for Rock Slices	21
FIGURE 7	Current vs. Time for Paste Slices	22
FIGURE 8	Current vs. Time for Mortar Slices	23
FIGURE 9	Slab Specimen Details	25
FIGURE 10	Applied Voltage Apparatus Used on Slab Specimens	26
FIGURE 11	Electrical Block Diagram	27
FIGURE 12	Current vs. Time for 0.60 w/c Ratio Slabs Tested at Various Applied Voltages	28
FIGURE 13	Current vs. Time for 0.35 w/c Ratio Slabs Tested at Various Applied Voltages	29

FIGURE 34	Current vs. Time for 1-inch Thick Core Slices Tested in Applied Voltage Cell	66	FIGURE 63	WVT Test - Conventional Concrete	110
FIGURE 37	Current vs. Time for 1/2-inch Thick Core Slices Tested in Applied Voltage Cell	67	FIGURE 64	WVT Test - Full-Depth Treatments	111
FIGURE 38	Temperature Rise in Applied Voltage Cell for Core Slices of Varying Thickness	68	FIGURE 65	WVT Test - Overlays	113
FIGURE 39	Relationship Between Resistance and Temperature for 1/2-inch Thick Core Slice Tested in Applied Voltage Cell	69	FIGURE 66	Vacuum Saturation Apparatus	122
FIGURE 40	Effect of Various Heat Treatments on Charge Passed by Internally Sealed Concrete	73	FIGURE 67	Applied Voltage Cell - Face View	124
FIGURE 41	Effect of Surface Abrasion on Charge Passed by Internally Sealed Concrete	74	FIGURE 68	Applied Voltage Cell - Specimen Ready to Test	124
FIGURE 42	Effect of Thickness on Charge Passed	76	FIGURE 69	Electrical Block Diagram Applied Voltage Cell - (Construction Drawing)	128
FIGURE 43	Electronics Module - Overall View	78	FIGURE 70	Applied Voltage Cell - (Construction Drawing)	128
FIGURE 44	Readout Panel	78	FIGURE 71	Example of Dike Placement Over Test Area	131
FIGURE 45A	Vacuum Saturation Module	80	FIGURE 72	Chloride Profile Data Presentation	135
FIGURE 45B	Dike Used with Saturation Module	80	FIGURE 73	Relationship Between Total Integral Chloride Values for Rapid Test and 90-Day Results	137
FIGURE 46	Screen Unit	81	FIGURE 74	Relationship Between Charge Passed During Rapid Test and Total Integral Chloride Values in 90-Day Test	138
FIGURE 47	Field Generator Set with Auxiliary Gas Tank	81	FIGURE 75	Relationship Between Chloride Contents at the 0 to 3/8-in. Level for Rapid and 90-Day Test Results	139
FIGURE 48	Power Supply Circuitry	82	FIGURE 76	Relationship Between Chloride Contents at the 3/8 to 5/8-in. Level for Rapid and 90-Day Test Results	140
FIGURE 49	Control Circuitry	82	FIGURE 77	Relationship Between Chloride Contents at the 5/8 to 7/8-in. Level for Rapid and 90-Day Test Results	141
FIGURE 50	Electrical Block Diagram	84	FIGURE 78	Relationship Between Charge Passed for Re-Saturated and Moist Stored Slabs	142
FIGURE 51	Reinforcing Mats for Prototype Testing	88	FIGURE 79	Relationship Between Charge Passed During Cell Test on Cores and Total Integral Chloride from 90-Day Test	143
FIGURE 51	(Cont.) Reinforcing Mats for Prototype Testing	89	FIGURE 80	Relationship Between Loss from Solution During Cell Test on Cores and Total Integral Chloride from 90-Day Test	144
FIGURE 52	Chloride Profiles for Various Clear Covers	90	FIGURE 81	Wenner-Four-Electrode Configuration	150
FIGURE 53	Cover vs. Charge Passed	91	FIGURE 82	Apparatus for Resistivity Measurement	152
FIGURE 54	Comparison of Charge Passed between two Different Concrete Having Equal w/c Ratios	93	FIGURE 83	Resistivity Profiles for Base Concrete Slabs	154
FIGURE 55	Temperature Distributions in Concrete Slabs	95	FIGURE 84	Resistivity Profiles for Internally Sealed Concrete	155
FIGURE 56	Deck Plan - Plain Concrete Deck	98	FIGURE 85	Resistivity Summation for Unheated Internally Sealed Concrete Overlay	156
FIGURE 57	Charge Passed vs. Cover for Field and Laboratory Tests	99			
FIGURE 58	Chloride Profiles for Conventional Deck	100			
FIGURE 59	Comparison of Core Test Results with Previous Data	101			
FIGURE 60	Deck Plan - Dense Concrete Overlay	104			
FIGURE 61	Chloride Profiles - Dense Concrete Overlay	105			
FIGURE 62	Current vs. Time - Dense Concrete Overlay	106			

FIGURE 86	Resistivity Summation for Partially Melted Internally Sealed Concrete Overlay	157
FIGURE 87	Resistivity Summation for Full-Depth Internally Sealed Concrete-Partially Melted	158
FIGURE 88	Resistivity Profiles for Latex Modified Concretes	159
FIGURE 89	Resistivity Summation for Wet Latex Overlay	161
FIGURE 90	Resistivity Summation for Air-Dry Latex Overlay	162
FIGURE 91	Resistivity Profile for Polymer Concrete Overlay	163
FIGURE 92	Resistivity Profiles for Air-Dry and Wet Dense Concrete Overlays	164

TABLE 22	Test Results - Effect of Bar Spacing	94
TABLE 23	Test Results - Effect of Temperature	94
TABLE 24	Bridge Deck Concrete	96
TABLE 25	Field Test Results - Conventional Deck	102
TABLE 26	Core Test Results - Conventional Concrete Deck	102
TABLE 27	Dense Overlay Concrete	103
TABLE 28	Field Test Results - Dense Concrete Overlay	107
TABLE 29	Overlay Thickness	107
TABLE 30	Core Test Results - Dense Concrete Overlay	107
TABLE 31A	Resin Formulation - Polymer-Concrete Overlay	108
TABLE 31B	Sand Gradation - Polymer-Concrete Overlay	108
TABLE 32	Polymer-Concrete Cores - Test Results	109
TABLE 33	Water Vapor Transmission Results	112
TABLE 34	Air Permeability Results	114
TABLE 35	Applied Voltage Test - Interpretation of Results	127
TABLE 36	Field Equipment List	129
TABLE 37	Correlation Analyses - Summary Statistics	145
TABLE 38	Data Used for Correlation Analyses	146
TABLE 39	Structural Details - Test Bridge No. 1	165
TABLE 40	Structural Details - Test Bridge No. 2	165
TABLE 41	Slab Identification and Storage Conditions	166

LIST OF TABLES

TABLE 1	Chloride Penetration Data	7
TABLE 2	Ranking of Proposed Techniques	16
TABLE 3	Osmotic Cells	19
TABLE 4	Preliminary Concrete Mixtures	24
TABLE 5	Chloride Analyses	30
TABLE 6	Concrete Mixture Characteristics	38
TABLE 7	Permeability Characterization Parameters	43
TABLE 8A	Expected Error in Estimation of 90-Day Ponding Results from Charge Passed Data in Applied Voltage Test	44
TABLE 8B	Comparison Data - 90-Day Ponding	44
TABLE 9	Comparison Data - As-Received vs. Air-Dry	48
TABLE 10	Chloride Analyses - w/c = 0.60	50
TABLE 11	Chloride Analyses - w/c = 0.32	50
TABLE 12	Permeability Parameters - Various Treatments	55
TABLE 13	Permeability Parameters - Moist vs. Re-Saturated FHWA Slabs	62
TABLE 14	Applied Voltage Cell Results	70
TABLE 15	Comparison of Finished and Sawn Surfaces	71
TABLE 16	Internally Sealed Specimens - Reheated	72
TABLE 17	Replicate Specimens	75
TABLE 18	Reinforcement Details - Prototype Test Slabs	86
TABLE 19	Concrete Mixtures - Prototype Test Slabs	92
TABLE 20	Test Results - Effect of Cover	92
TABLE 21A	Slab A - Effect of Cover	92
TABLE 21B	Cores from Slab A - Effect of Thickness	92

PREFACE

The author would like to express his appreciation to the Wisconsin Department of Transportation, for making field sites available for part of the test program, and to Mr. James F. Hare, Jr., FHWA, Region 5, Director of the Office of Bridge, for his help in locating and selecting the field sites. Also, the work of several other people who contributed significantly to the project is gratefully acknowledged, namely: Messrs. Fred Blaul and John Steer, Expert Technicians, Construction Technology Laboratories; Mr. Hugh Love, Chemical Assistant, Construction Technology Laboratories; Mr. T. S. Young and Dr. C. Locke, University of Oklahoma; and Mr. Robert Carver, RLC Instruments.

CONVERSION FACTORS, U. S. CUSTOMARY TO METRIC (SI)
UNITS OF MEASUREMENT

U. S. customary units of measurement used in this report can be converted to metric (SI) units as follows:

Multiply	By	To Obtain
Angstroms	0.0000001 (10^{-7})	millimetres
inches	2.54	centimetres
feet	0.3048	metres
miles (U. S. statute)	1.609344	kilometres
square inches	0.00064516	square metres
square feet	0.09290304	square metres
cubic feet	0.02831685	cubic metres
cubic yards	0.7645549	cubic metres
grams	0.001	kilograms
pounds (mass)	0.4535924	kilograms
tons (2000 pounds)	907.1847	kilograms
pounds (mass) per cubic foot	16.01846	kilograms per cubic metre
pounds (mass) per cubic yard	0.59327631	kilograms per cubic metre
pounds (force)	4.448222	newtons
pounds (force) per square inch	6894.757	pascals
pounds (force) per square foot	4.882428	kilograms per square metre
miles per hour	1.609344	kilometres per hour
degrees (angle)	0.01745329	radians
Fahrenheit degrees	5/9	Celsius degrees or Kelvins*

* To obtain Celsius (C) temperature readings from Fahrenheit (F) readings, use the following formula: $C = (5/9)(F - 32)$. To obtain Kelvin (K) readings, use: $K = (5/9)(F - 32) + 273.15$.

1. INTRODUCTION

Deterioration of concrete bridge decks continues to be a serious problem for many state and Federal highway agencies. A report issued recently by the GAO (1) stated that nearly 6.3 billion dollars are needed to restore the Nation's Federal aid system bridge decks. The root of this problem lies in the deicing salts (primarily sodium chloride) used in many states during the winter months. The chloride ions (Cl^-) destroy the natural passivity of the reinforcing steel and promote the formation of corrosion products which exert large tensile forces on the concrete cover. These forces can cause delamination and spalling of the riding surface.

The problem can be solved by providing a barrier which can retard, or halt, the migration of chloride ions to the steel surface. This barrier may either be on the steel, as in galvanized or epoxy coated bars, or in the concrete itself. This project was directed towards evaluation of the effectiveness of techniques based on the latter approach.

Materials used as barriers to chloride ions include, but are not limited to, the following:

- Polymer Impregnated Concrete
- Latex Modified Concrete
- Dense Portland Cement Concrete
- Internally Sealed Concrete
- Polymer Concrete

Rapid test procedures are needed to judge the effectiveness of these treatments. The two major objectives of this project were:

1. To develop and test a rapid destructive permeability device which can be used in the laboratory on sections of concrete,

such as cores, taken from structures.

2. To develop and test a rapid non-destructive permeability device which can determine the permeability of rigid concrete members (such as bridge decks) in field installations.

2. LITERATURE STUDY

Prior to initiation of method development work, a literature survey was conducted. The objective of the survey was to assemble all available data concerning the permeability of concrete to fluids and dissolved ions, and to select those techniques which held the most promise for fulfilling the contract objectives. If suitable techniques were not currently available, the knowledge gathered from the literature survey would be used as a basis for development of novel methods.

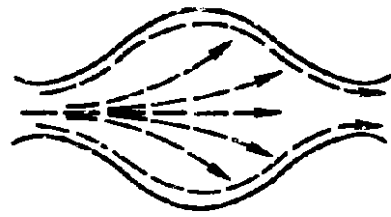
2.1 Flow of Fluids and Ions Through Concrete

Flow of fluids and ions through concrete can take place via a number of mechanisms, depending upon the initial state of the concrete, nature of the permeating substances, temperature, and pressure. Rose (2) has broken down the movement of water in porous materials into seven distinct stages (Figure 1). After initial surface adsorption, movement of water vapor is via diffusion. Diffusion is mathematically expressed by Fick's first law:

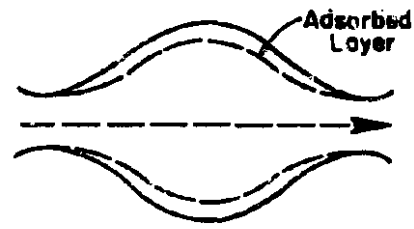
$$J = -D \frac{dc}{dx} \quad (1)$$

where: J = flux ($g/cm^2 \cdot s$)
 D = diffusion coefficient (cm^2/s)

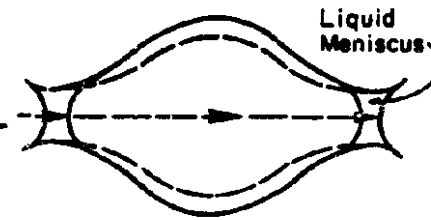
$\frac{dc}{dx}$ = concentration gradient ($g/cm^3/cm$)



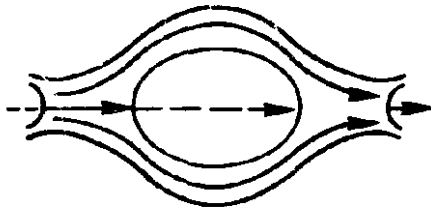
Stage 1: Adsorption And Surface Diffusion



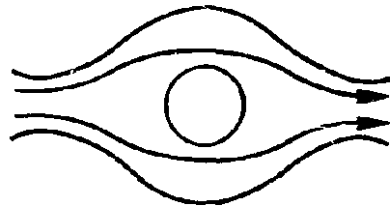
Stage 2: Vapor Diffusion



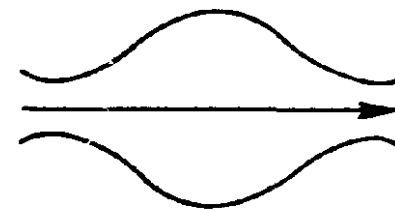
Stage 3: Film Transfer



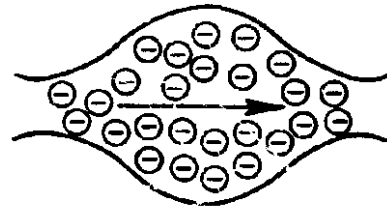
Stage 4: Surface Creep Plus Vapor Diffusion



Stage 5: Partially Saturated Liquid Flow



Stage 6: Liquid Flow



Stage 7: Ionic Diffusion

FIGURE 1. MOVEMENT OF WATER THROUGH POROUS MATERIALS.

Although chloride ions obviously cannot transfer via vapor-phase diffusion, the measurement of water vapor transmission may be an effective means of assessing relative materials permeability. Additionally, chloride ions can transfer within the liquid phase via self-diffusion along the chloride concentration gradients existing within the concrete porewater.

As relative humidity increases, water begins to condense within capillary spaces. Forces then arise as a result of the pressure differential across the meniscus in the capillary and induce a flow through the capillary, the rate of which is given by Washburn's Equation (3):

$$v = (rV_L/4dn) \cos \theta \quad (2)$$

where: v = flow rate (cm/s)
 r = capillary radius (cm)
 V_L = surface tension (Pa·cm)
 d = depth of penetration (cm)
 n = fluid viscosity (Pa·s)
 θ = the contact angle

Once the pore system is completely saturated, water may flow as a fluid. In materials having very finely divided pores, however, significant flow will occur only under high pressure heads. In this case Darcy's Law (4) governs the flow rate:

$$Q = -KA \Delta h/L \quad (3)$$

where: Q = volume outflow (cm³/s)
 A = area (cm²)
 Δh = fluid head (cm)
 L = path length (cm)
 K = permeability constant (cm/s)

As previously mentioned, ionic species, such as chlorides, can migrate through free water within the concrete

pore structure. This may occur via diffusion in Stages 3 and 4 (Figure 1), although probably at low velocity due to ionic interaction with the electrical double layer on the cement paste surface. Ionic diffusion will be most effective in the fully saturated state (Stage 7).

A special case of diffusion occurs when an electric potential is applied across an electrolytic solution, free or contained within a porous material. The ions will then be transported towards the electrode of opposing sign (5). Ionic mobility is given by the following expression:

$$\mu = \frac{x}{t(dE/dx)} \quad (4)$$

where: μ = ionic mobility (cm²/V·s)
 x = distance (cm)
 t = time (s)
 $\frac{dE}{dx}$ = electric field strength (V/cm)

2.2 Permeability of Cement and Concrete

A comprehensive search for data on the permeability of hardened cement and concrete was conducted. Representative results will be presented in this section, discussion of specific techniques used to develop the data will be given in a later section.

2.2.1 Hardened Cement Paste

Permeability of a variety of cement pastes to water at approximately 50 psi (345 kPa) was studied by Powers and co-workers (5). Their results indicate that permeabilities of hardened, mature pastes range from 1×10^{-13} to 1×10^{-9} cm/sec for water-to-cement ratios (w/c) ranging from 0.3 to 0.7 by weight. Permeabilities also vary greatly over the period of hydration, ranging from 4×10^{-8} cm/s at 5 days to 0.6×10^{-10} cm/s ultimately, for a paste of w/c = 0.7.

Additionally, permeabilities of cement pastes were compared with various rock types used as concrete aggregates. Their data indicate that an increase in w/c ratio from 0.38 to 0.71 will span the range of permeabilities generally encountered in concrete aggregates. Although total porosities of cement paste are far higher than rocks, permeabilities may be equivalent.

In a study of water vapor transmission through cement pastes equilibrated to various internal relative humidities, Sorensen and Radjy (7) found values ranging from 4×10^{-8} cm/s for very dry conditions (RH ~ 10%) to 1×10^{-8} cm/s for values close to saturation. Diffusion coefficients for water vapor through hardened cement paste (8) of w/c = 0.28 range from 15×10^{-8} cm²/s at 2 days to 8×10^{-8} cm²/s at 28 days, remaining constant up to 90 days.

The movement of ions through hardened cement paste has also been studied, and is of particular interest in the present study. Berman (9) exposed hardened cement pastes (w/c = 0.4 and 0.5, age = 28 days) to various chloride, fluoride, and chromate solutions, holding humidities on the downstream side of a 4-in. long specimen at 72% RH and 100% RH. Results showed penetration of sodium chloride to a greater depth than any of the other salts tested. Additionally, his data showed that the dissolved ions penetrated more rapidly into the pastes than the water did. Similar studies have been carried out by Kondo, et al. (20), Kondo's results indicate diffusion coefficients for Cl⁻ through hardened cement pastes at w/c = 0.4 cured for 28 days to be greater than that of the associated cation, leading him to conclude that, "hardened cement paste seemed to behave as an electro-positive semi-permeable membrane." For NaCl solutions

at 20°C the diffusion coefficient for chloride ion was 6×10^{-8} cm²/sec.

2.2.2 Concrete

Much of the early work on permeability of concrete dealt with flow of bulk water through concrete under the influence of relatively large pressure heads. One of the earliest comprehensive studies (11) used concretes of varying mix proportions cured for up to 1 year and subject to a water pressure of 100 psi (690 kPa). Results showed the expected trends of reduction in permeability with decreasing w/c and increasing age. Permeability ranged from 0.19 ft/day (6.9 cm/s) at 7 days to less than 8.5×10^{-3} ft/day (3.0×10^{-6} cm/s) at 1 year. Effects of aggregate gradation, when realistic gradings were used, were minor.

Early studies at PCA (12) utilized pressurized water at somewhat lower pressures applied to 6-in. (152 mm) dia. x 2-in. (51 mm) thick specimens. Decreasing flow with period of test was found (Figure 2). Results at 24 hours show permeabilities decreasing from about 2.7×10^{-7} cm/s at w/c = 0.80 to values too small to measure below w/c of about 0.5.

The classic paper among the early studies is that of Ruettgers, Vidal, and Wing at USBR (13). Concrete specimens up to 18x18 in. (457x457 mm) in size were subjected to water pressures of 400 psi (2.8 MPa). In addition to the usual increase in permeability with w/c ratio, the investigators found an increase of about 30 times when going from 1/4 in. (6 mm) to 9 in. (229 mm) maximum aggregate size. Although the authors attribute this to greater probability of voids occurring beneath larger aggregate particles, it is also possible

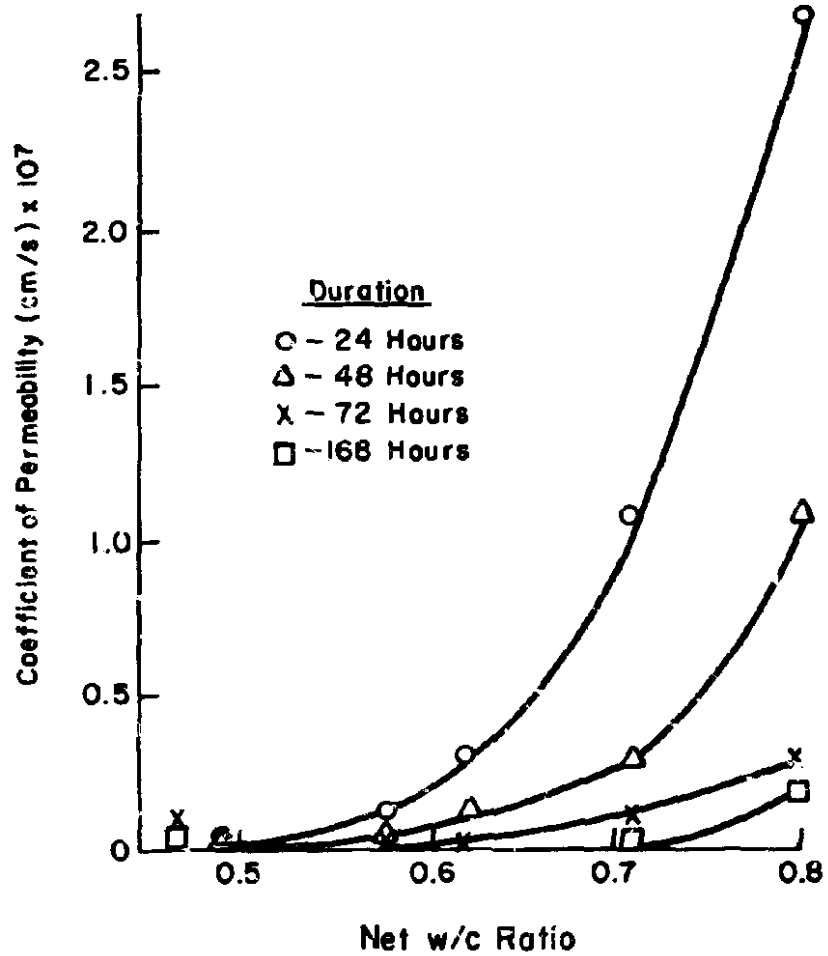


FIGURE 2. PCA PERMEABILITY TESTS (1929)
ON CONCRETE.

that flow occurred through the aggregates, (limestone in their case) and, therefore, total flow would increase in proportion to the aggregate content, which would be greater as the maximum aggregate size was increased.

Later work in the area of permeability under high water heads was reported by Cook (14). His tests involved lean mass concretes subjected to pressure of 200 psi (1.4 MPa). Specimens with cement contents ranging from 188 to 282 lb/yd³ (112-167 kg/m³) with w/c from 0.50 to 0.86, were tested at 3 and 12 months age. Permeabilities at 3 months ranged from 1.5×10^{-8} cm/s for w/c = 0.86 to 6×10^{-9} cm/s for w/c = 0.50. Specimens which were vacuum saturated prior to test gave higher permeabilities (by a factor of 2) than those tested in the moist-cured condition.

In many areas of the construction industry the permeability of concrete to water under high heads is not applicable; rather what is needed are data on water vapor transmission (WVT) of concrete. Also included in this general area are absorption and capillary flow testing. Early tests by Wiley and Coulsen (15), although devised as a rapid test for water permeability, were in actuality a measure of capillary flow and vapor transmission through the concrete pipe sections used. Their coefficients ($3-40 \times 10^{-8}$ cm/s) were from 10^2 to 10^3 higher than previous (13) data for mixes ranging in w/c from 0.53 to 1.1. In effect, this says that capillary forces can move water through concrete at a higher rate than can pressures of up to 400 psi (2.8 MPa). Barre (16) using 1.5x10x10-in. (4x25x25 cm) specimens exposed on one side to air at 50% RH and 73°F (23°C) and on the other side to a chilled condensing surface at 32°F (0°C) found WVT to range from 4.66 X

10^{-9} gm/cm².s at w/c = 0.46, to 6.19 X 10^{-9} gm/cm².s at w/c = 0.82.

More recent work in this area has been reported in a report by the U.S. Naval Civil Engineering Laboratory (17). A "wet cup" technique was employed where a 1-1/2-in. (38 mm) thick x 4-in. (101 mm) diameter concrete disc is exposed to a saturated atmosphere on one face and varying RH on the opposite face. Flow is measured by weighing the entire apparatus to the nearest gram. They concluded that WVT increases with w/c, decreases with RH, and is reduced by addition of NaCl to the concrete mix. Studies were also done on the various rock types contained within the San Gabriel gravel used as the aggregate source. Values ranged from 2.1×10^{-8} gm/cm².s for a medium grained biotite granite to 3.5×10^{-9} gm/cm².s for a hiatal porphyry. Unfortunately, all concretes were prepared with a mixture of rock types, therefore, no conclusions can be drawn as to the relative effects of aggregate WVT on concrete WVT from this study.

The movement of chloride ions (Cl⁻) through concrete has also been the topic of several investigations. Monfore and Ost (18) monitored chloride levels in 2x4-in. (51x102 mm) concrete cylinders exposed on one face to 23% and 8% CaCl₂·2H₂O solutions. The results indicated that after 12 months of ponding Cl⁻ levels will be significant at the 1-in. (25 mm) level at w/c of 0.40 and above. At the 2-in. (51 mm) level Cl⁻ levels will still remain at baseline levels at 12 months if w/c is held to 0.44 or less. Clear (19) has studied Cl⁻ penetration of a number of special concretes as well as conventional portland cement concrete. Some of his data are reproduced in Table 1. The

TABLE 1
CHLORIDE PENETRATION DATA
(REF. 19)

Cl⁻ at Level Indicated (lbs/yd³)^{1/-}
Average

Conventional Concrete - 830 saltings

Depth ^{2/} (in.)	w/c = 0.4	w/c = 0.5	w/c = 0.6
0.28	20.0	22.1	27.9
1.0	1.58	11.4	13.7
2.0	BL*	1.76	3.85
3.0	BL	0.55	0.77
4.0	BL	BL	0.53

"Iowa Method" - w/c = 0.32 - 830 saltings

Depth ^{2/} (in.)	Properly Consolidated	Improperly Consolidated
0.28	15.2	17.9
1.0	1.29	6.25
2.0	BL	3.34
3.0	BL	1.00
4.0	BL	BL

Latex Modified Concrete - 830 saltings

Depth ^{2/} (in.)	
0.28	6.52
1.0	0.44
2.0	BL
3.0	BL
4.0	BL

Polymer Impregnated Concrete - 938 saltings

Depth ^{2/} (in.)	
0.28	1.06
1.0	BL
2.0	BL
3.0	BL
4.0	BL

*BL = Baseline reading
1/ kg/m³ = lb/yd³ X 0.5935
2/ mm = inches X 25.4

data indicate that the specialty concretes, when properly prepared, greatly reduce the ingress of Cl⁻ into the slabs. Coppelardi et al. (20) using techniques similar to that of Monfore,

calculated Cl⁻ diffusion coefficients from the rate of penetration of the chloride front through the concrete cylinder. Values determined were 1.7 X 10⁻⁸ cm²/s for portland cement concrete of w/c = 0.50 (vibrated) and 3.3 X 10⁻⁶ cm²/s for w/c = 0.60 (nonvibrated). Pozzolanic cements exhibited somewhat lower diffusion coefficients.

2.3 Conventional Permeability Test Procedures

In the following section permeability test methods will be briefly described with references to more complete descriptions included. Only methods judged to be applicable to the current project will be discussed. An outline of the procedures and apparatus to be discussed follows:

- 2.3.1 Water Permeability
 - 2.3.1.1 High Water Heads
 - 2.3.1.2 Variable Head
 - 2.3.1.3 Initial Surface Absorption Test (ISAT)
 - 2.3.1.4 Water Injection
- 2.3.2 Air Permeability
 - 2.3.2.1 High Pressure Air
 - 2.3.2.2 Pressure Corline
 - 2.3.2.3 Vacuum Methods
- 2.3.3 Water Vapor Transmission
- 2.3.4 Ion Diffusion
- 2.3.5 Resistivity Techniques

- 2.3.1 Water Permeability
 - 2.3.1.1 High Water Heads
Typical of the apparatus developed to determine water permeabilities of concretes under high hydrostatic heads is that used by the U.S. Bureau of Reclamation (21). Pressure regulators can be varied to supply up to 450 psi (3.1 MPa) to any one specimen. The specimen containers are designed so that distilled water covers the upper surface of the specimen, and flow is lateral

through standard 6x12-in. (152x305 mm) specimens or 18x18-in. (457x457 mm) specimens when mass concrete is to be tested. The test is usually carried out to 500 hours.

The above technique works well with conventional concretes, although long times (up to 25 days) are necessary to achieve constant flow conditions. Permeability values of PIC gathered using this apparatus are suspect, due to extremely low flow rates and inability to achieve equilibrium.

Murata (23) has devised a more rapid test based on calculation of the water diffusion coefficient through a concrete specimen 6-in. (152 mm) in diameter x 6-in. (152 mm) long. A water head (dye being added to the water) of from 142 psi (0.98 MPa) to 287 psi (2.0 MPa) is applied to the specimen for 48 hr, the specimen being subsequently fractured and the average depth of penetration calculated from planimeter measurements of the area of penetration of the dye. Diffusion coefficient (B^2) is calculated as:

$$B^2 = \frac{D_m^2}{4t \cdot c^2} \quad (5)$$

where: B^2 = diffusion coefficient (cm²/s)
 D_m^2 = average depth of penetration (cm)
 t = time at which D is measured (s)
 c^2 = constant of integration

2.3.1.2 Variable-Head Technique

In the variable-head technique (24), the rate of passage of water through a specimen is monitored by the fall of the water level in a manometer connected to the specimen under test.

Care must be taken to saturate the sample prior to test; otherwise the measurement will be a function of the

capillary force developed in the sample at varying degrees of saturation and not a true measure of permeability, per se. As flow through concrete materials is very slow even at high pressure heads it was felt that the variable head technique would be inapplicable to the present project.

2.3.1.3 Initial Surface Absorption Test (ISAT)

The Cast Concrete Products Association (Great Britain) recognized that high pressure permeability tests do not simulate the real action of deleterious agents on concrete surfaces (which occurs mainly due to capillary flow), and may indeed alter the pore structure where sufficiently high pressures are used. For these reasons the initial surface absorption test (ISAT) (25) was developed.

It was shown that flow of water into a surface under low heads follows an inverse power law:

$$\frac{dr}{dt} = at^{-n} \quad (6)$$

where: $\frac{dr}{dt}$ = flow rate (ml/s)
 t = time (s)
 a = a dimensional constant (cm)

n has been found to vary from 0.3 to 0.7, being constant for a specific concrete mix.

The test apparatus consists of a gasketed cap which is clamped or otherwise affixed to the concrete test surface. Water is poured into the inlet until the outlet runs clear. A capillary tube (bore 0.7 mm - 1.3 mm) is then affixed to the outlet tube, an initial reading is taken at 10 min, 30 min, 1 hr, and 2 hr. To date, the apparatus has been used on reinforced concrete, paving, and architectural concrete with

good results. It should be noted that the objective of this test is to predict the durability of a surface layer of concrete, and gives no information on the interior material.

2.3.1.4 Water Injection

The British Building Research Establishment (BRE), recognizing that the ISAT values are highly dependent on the permeability of the first few millimeters of surface, developed a technique (26) which could be used to assess the permeability of concrete at any depth below the surface. The procedure consists of drilling a hole 30-mm deep x 5.5-mm diameter into the concrete, sealing the hole with a silicone rubber plug, ensuring an air tight seal by means of a hypodermic needle placed through the silicone plug, and then monitoring the rate of fall of water in a capillary after injecting water by means of the hypodermic syringe into the small cavity in the concrete.

The moisture content of the concrete had a significant effect on the results, especially at high (w/c = 0.6) w/c ratios. Scatter in the data is quite high indicating aggregate effects to be substantial). The method has also been adapted to measure air permeabilities. This will be discussed in the next section.

2.3.2 Air Permeability

2.3.2.1 Air Flow Under Pressure

Air permeameters have been devised to cover large ranges of applied pressure. In principle, all that is needed is a suitable specimen holder which will confine the flow to the longitudinal direction, accurate pressure gages, stable gas supply, and accurate flow meter on the downstream side. ASTM C577-68 (27) describes equipment and test procedures necessary for the determination of air permeabilities of

refractory materials at 240 mm Hg (31.9 kPa) pressure on 2-in. (51 mm) specimens.

When highly permeable samples or high pressures are utilized Darcy's law may be invalid due to the presence of turbulent flow conditions. At very low pressures, flow will also deviate from Darcy conditions, due to the so-called "Klinkenberg Effect." This is most apparent for materials of fine pore structure and low permeability, when the layer of gas nearest to the surface will move relatively freely, especially if inert gases such as helium are used, yet liquids such as water will be immobilized at the surface layer by dispersion forces. This slip-effect is an inverse function of the mean pressure, and can be corrected for by measurement at a number of pressures and extrapolation to infinite mean pressure.

2.3.2.2 Pressure Decline Technique

Air permeability may also be calculated in the non-steady state region by measuring the pressure drop in a vessel sealed by the specimen itself to the outside atmosphere. This is termed the constant-volume technique (27).

The need for a simpler and more rapid test for air permeability led to the development of a technique in which air is caused to permeate from the atmosphere through the specimen into a container by draining water from the container. This technique, termed the "variable volume-decay-rate" method, was criticized on the grounds that restricted outflow of fluid from the container causes a head loss which has an indeterminate effect on the results. Drennan (28), however, was able to formulate an equation of flow which included that head loss term and thus achieve favorable results. Although the apparatus is simplified over the constant

volume technique, the mathematics are greatly complicated, and tables are needed to perform the calculations due to the many correction terms needed.

2.3.2.3 Vacuum Methods

A negative pressure may also be utilized in the determinations of air permeability. One such apparatus is that developed by Whiteway (29). The apparatus consists of three 100 cc bulbs connected through the test piece to a vacuum pump, the drop in pressure being sensed by a manometer equipped with electrical contacts so arranged as to allow timing of the interval between any two chosen pressures. This elapsed time is a measure of the permeability. Whiteway recognized that at low pressures Darcy's law might not apply and the predominant transfer mechanism may be molecular or "slip" flow. The predominant type of flow for any given specimen can be ascertained by performing the determination using air and then repeating the run using helium. The ratio of time increments (Δt (air)/ Δt (He)) theoretically should be 2.69 for pure molecular flow. Whiteway determined the ratio to be 2.59 for a series of low-permeability magnesia specimens, indicating the flow in this case to be mostly of the molecular type, which occurs when the mean pore diameter is of the same order as the mean free path of the gas molecules (0.3 μm at 2.4 kPa for air). For cement pastes ranging from w/c ratios of 0.6 to 0.4, Winslow and Diamond (30) have determined mean pore diameters less than 0.05 μm at 28 days of age. Even at 1 day age, mean diameters were less than 0.3 μm . For polymer impregnated cement pastes (w/c = 0.60) cured for 3 days and subsequently dried and polymerized, mean pore diameters (31) were less than 0.1 μm . It therefore appears that this technique

might be applicable to the materials of interest in this study.

Concurrent with the work on the water injection method (26), the BRE developed a device for determination of air permeability of concrete in-situ. The hole and sealant are the same as previously described for the water injection method. The test is started by turning a 3-way stopcock to allow air to be withdrawn from the concrete until a vacuum of 112 mm Hg (14.9 kPa) is reached. The pump is then isolated and the time required for the pressure to rise to 150 mm Hg (20.0 kPa) is recorded. This value (Δt) is taken as a relative measure of the air permeability of the concrete.

The results obtained were found to be a strong function of the moisture content of the concrete. Variations in moisture content from 1.0 to 1.8% lead to a maximum difference in Δt of 20 s. Typical test times run from 100 to 500 s, indicating errors of up to 20% are to be expected if the moisture content of the concrete has not previously been determined. Although it is possible in the laboratory to determine moisture content by subsequent oven-drying, a satisfactory field technique is not yet generally available.

2.3.3 Water Vapor Transmission

A standard method (ASTM C355-64, Standard Test Methods for Water-Vapor Transmission of Thick Materials) is available for testing materials up to 1-1/4-in. (32 mm) thick. The details of the method are given in the ASTM Standard so only a general description will be given here. The test specimen, in the form of a flat plate, is sealed into a wide, shallow pan containing either a desiccant or water. The specimen is sealed onto the pan by means of molten

asphalt or wax. The rate of change of weight of the entire apparatus contained in a controlled atmosphere with time is taken as a measure of the WVT.

$$WVT = \frac{G}{t} \times \frac{1}{A} \quad (7)$$

where: WVT = water vapor transmission, grains/hr-ft² (gm/s·cm²)
 $\frac{G}{t}$ = rate of water gain or loss, grains/hr (gm/s)
 A = area of test specimen exposed to desiccant or water, ft² (cm²)

Results may also be expressed in terms of water vapor permeance, defined as the ratio of the WVT to the vapor pressure differential (WVT/p). The average permeability (for homogeneous specimens) is the product of the permeance times thickness of the specimen.

It is apparent, that in order to obtain reproducible results, the specimens must be brought to some uniform moisture state prior to test. For concretes the obvious choice would be the oven-dry state, and the desiccant method would likely yield the most favorable results.

The results of USNCEL (17) previously discussed (see page 6) indicate that this technique may be applicable to concretes, although it is very slow. Morrison, et al. (32) have developed a variation on the desiccant method using a water reservoir instead of a controlled atmosphere on the opposite specimen face. A schematic illustration of the apparatus and some results on conventional, polymer impregnated, and latex modified concretes are shown in Figs. 3 and 4, respectively. In this case the concrete discs 1-in. (25 mm) thick x 2-in. (51 mm) dia. are brought to the moist condition (15 days in water) prior to test. Good temperature control ($\pm 0.1^\circ\text{C}$) is necessary if reproducible results are to be obtained,

necessitating the use of a large temperature bath if many cells are to be operated simultaneously.

2.3.4 Ion Diffusion

Though not fully documented, it is highly probable that one of the major transport pathways for chlorides into concrete is via ionic diffusion. The process is likely not one of pure diffusion, as chemical reactions with hardened cement constituents and electrokinetic effects due to interactions within the gel pores are likely to affect the rate of transport.

The earliest work on ionic (electrolyte) diffusion through porous substances was done by Northrop and Anson (33), who were not interested in the ability of the porous material to transport ions, per se, but rather in a substrate which could be used to separate two reservoirs of vastly different concentrations, thus reducing the time required for a measurement. This was termed the "Diaphragm Cell Method," and its theory, operation, and limitations were discussed in a comprehensive article by Gordon (34). These workers were interested in determining diffusion constants in free solution; thus they precalibrated their solid diaphragms with ions of known diffusion, and assumed no interaction between ions and diaphragm. Workers such as Garrels (35) also assumed free solution behavior, and used this assumption to obtain information on diffusion of chloride ions through various rocks.

Another means used to calculate ionic diffusion coefficients is by radioactive tracer studies. This method is especially useful when the material already contains substantial amounts of the ion of interest, and chemical techniques would, therefore, be "swamped

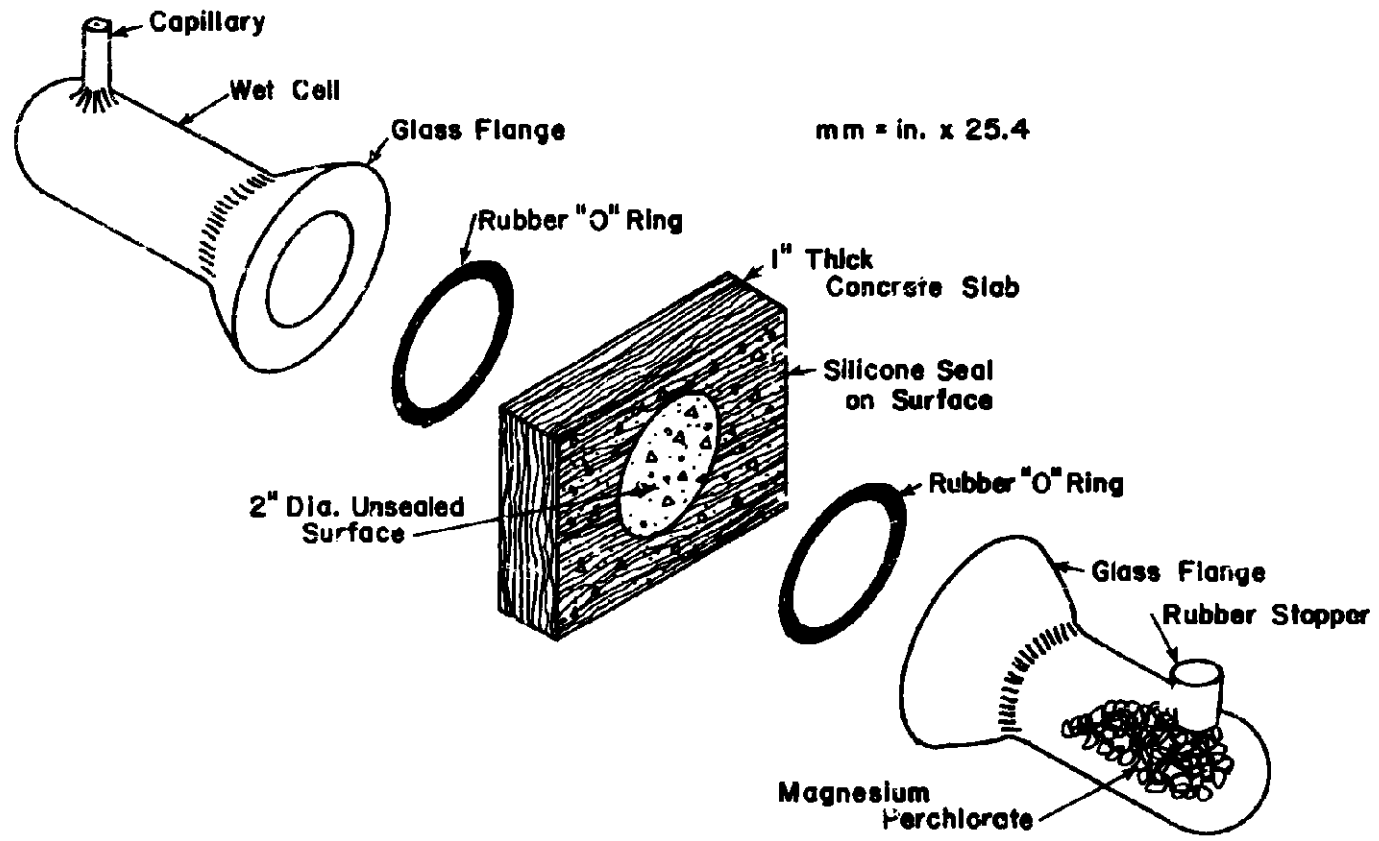


FIGURE 3. KANSAS PERMEABILITY CELL (REF. 32).

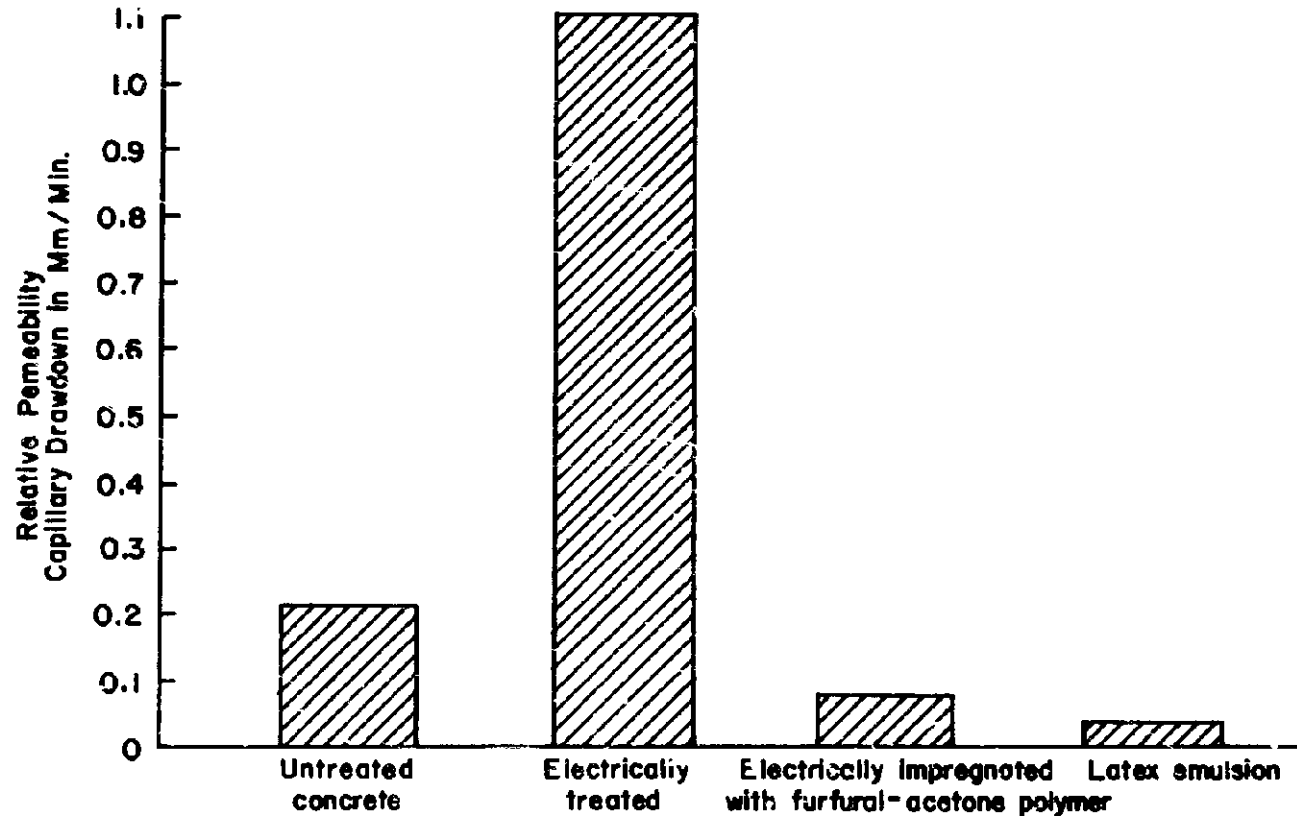


FIGURE 4. TEST RESULTS WITH KANSAS PERMEABILITY CELL (REF. 32).

out" by the presence of initially large quantities of mobile ions in the sample. Spinks, et al. (36), have used a tracer technique used to monitor diffusion of $^{22}\text{Na}^+$, $^{143}\text{Ca}^{++}$, $^{131}\text{I}^-$, and $^{35}\text{SO}_4^-$ tracers into neat cement and mortar. The measured activity gradient then gave a reasonably accurate measure of the ionic concentration gradient, assuming the distance of penetration of tracer ion was large compared to the range of radioactive particles emitted from the material.

2.3.5 Resistivity Techniques

In some applications it is not necessary to measure the exact amount of material (be it fluid, gas, vapor, or ions) permeating through a sample, but all that is desired is a relative indication of the permeabilities of various porous materials. It is known that the electrical resistivity (ρ) is a strong function of the moisture content and electrolyte concentration of concrete (37). Thus, by bringing a specimen to a reproducible initial moisture condition, exposing the specimen to an electrolytic solution, and then monitoring the change of resistivity with time, an estimate of the relative "permeability" can be obtained.

A technique incorporating these principles has been described by Astbury and Vyse (38). The apparatus consists of a lucite tank, the base of which has a rectangular opening into which the specimen can be placed and sealed. To start the run a 0.1N K_2SO_4 solution is poured into the tank. Voltage is supplied to electrodes on both faces of the specimen and current monitored across an appropriate shunt. Increase in current indicates decrease in resistivity and passage of solution into the test specimen. Data presented for a mullite brick

specimen indicate a current increase from 0 to 28 ma over a period of 25 min.

Manheim and Waterman (39) have used resistivity techniques to determine formation factors of Indian Ocean limestone cores. Formation factor (F) is the ratio of the electrical resistivity of the interstitial water (ρ_w) in a given sediment to the bulk resistivity (ρ_s) of that sediment.

$$F = \frac{\rho_w}{\rho_s} \quad (8)$$

The apparent diffusion coefficient (d) of a given ionic species is related to the diffusion coefficient in free solution (d_o) by

$$d = \frac{d_o}{F} \quad (9)$$

The technique requires that the specimen be saturated and that it is possible to extract the interstitial fluid so that its resistivity can be measured in a calibrated cell. The method obviously works best on unconsolidated or partially consolidated materials, and it is doubtful whether this could be applied to hardened concrete.

The State of Vermont (40) is currently evaluating a resistivity technique first proposed by Spellman and Stratfull (41), which is designed to test integrity of bridge deck membrane sealing systems. Resistance is measured between the reinforcing steel mat and a copper plate placed on top of a sponge in contact with the concrete deck surface.

Vermont reports reliability of the method to be about 60% when compared with actual long-term chloride measurements. Variations in pavement porosity and moisture content are believed to be

the major interferences. The method has been accepted as an ASTM Standard Method (ASTM D3633-77, Standard Test Method for Electrical Resistivity of Membrane Pavements) in spite of the poor correlation with chloride penetration, presumably for lack of any more precise method at this time.

Locke (42) has used a four-pin resistivity technique to determine the depth of partial impregnation of concrete with methyl methacrylate resins. This technique may be adaptable to determining depth of impermeability of overlay materials and depth of wax melting in internally sealed concretes. It relies on a large difference in electrical resistivity between two adjacent layers.

2.4 Criteria for a Chloride Permeability Test Method

In the preceding section the currently available techniques for determination of various types of permeabilities in concrete and other materials were presented and discussed. After careful consideration, it was concluded that none of the currently available techniques met the requirements of this project. Ideally, the technique should meet the following criteria:

1. Results should correlate directly with the long term permeability of the member.
2. Test should be rapid.
3. Device should be portable.
4. Device should preferably measure permeability in-situ, without disturbing concrete.
5. If in-situ measurement is impossible, tests on cores should be performed in laboratory.
6. Test should measure depth as well as degree of impermeability.

In the following section, available and proposed methods are divided into

general categories and the ability of the methods to satisfy these criteria are discussed. A value of 1 point is assigned for each of the criteria met by the test method and ranking is presented in Table 2. The methods are broken down into the following categories.

2.4.1 Non-Destructive Techniques

Purely Passive

2.4.2 Direct Techniques

Water Permeability

Air Permeability

Water Vapor Transmission

Electrical Methods

2.4.1 Non-Destructive (Passive) Techniques

Ideally, the test itself should not disturb the in-place concrete or subject the concrete to chemical solutions, moisture, electric current, or other factors which might possibly affect the performance of the protective system. A variety of non-destructive techniques have been developed or are under development for assessing strength, modulus, moisture content, chloride content, depth of cover, corrosion potential of reinforcement, void areas, and other properties of concrete. These methods either directly measure the property of interest or are based on the fact that there is a unique relationship between the property of interest and some other property which can be related to the measurement in question. For example, the velocity of propagation of acoustic waves through a material is proportional to the elastic modulus and unit weight of the material (43). This has a sound theoretical basis and has been experimentally verified. Therefore, measurement of acoustic wave velocity can be used with a certain degree of confidence to predict in-place moduli of concrete (44). As another

TABLE 2
RANKING OF PROPOSED TECHNIQUES

Technique	Reference(s)	Basis for Method	Advantages	Disadvantages	Assigned Points
Chloride Migration (Electrical Test)	47, 48	Migration of Cl ⁻ under imposed potential causes increase of current with time due to electrolyte flow	Rapid Should correlate with long term permeability Portable Relatively non-destructive	Heating effects Difficulty in passing current Cannot measure depth of impermeability	5
Water Permeability (Low-Head)	25, 26	Capillary action	Simple Non-destructive	Slow Sensitive to temperature and initial moisture content May not correlate w/long term permeability Cannot measure depth of impermeability	3
Air Permeability (Vacuum Method)	26, 29	Vacuum declines as air flows out of concrete	Relatively simple Portable	May not correlate w/long term permeability Very sensitive to moisture content High test variance Requires holes drilled into concrete	3
Water Vapor Transmission	ASTM C355 17, 32	Diffusion of water vapor under humidity gradient	Relatively simple Proven applicability to some materials of interest	Sensitive to temperature Sensitive to initial moisture content Destructive Not readily adaptable to field Slow test	2
Four-Pin Resistivity	42	Difference in electrical resistivity between layers	Simple to use Rapid Applicable to P.I.C.	Requires large difference in resistivity between adjacent layers Sensitive to moisture content Only measures depth	1

example, there is an approximately linear relationship between attenuation of x-rays and density of material. Thus, in-place density of concrete can be measured using transmission of backscatter type radiometer equipment (45).

This review of the literature, however, has indicated that there are no unique fundamental relationships between permeability and relatively easily measured properties such as density, chemical composition, porosity, or electrical properties. Indeed, "permeability" is not a property at all, but merely an operationally defined quantity which relates the amount of any given substance which can pass through any one material under a single set of test conditions. Witness the discrepancies between air and water permeabilities on the same material (46).

It, therefore, appears that in order to satisfy Criterion #1, tests must be made using the substance of interest, in this case chloride ion. It is quite possible that there may be an empirical correlation between air, water, or other types of permeability and chloride permeability (Criterion #1), however, there is no way of knowing beforehand whether this is the case. Passive methods, however, appear totally unpromising.

2.4.2 Direct Techniques

2.4.1.2 Water Permeability

The high pressure techniques fail to meet most of the criteria, since they are destructive, time-consuming, not adaptable to in-situ work, and do not necessarily satisfy Criterion #1. The low pressure techniques suffer from their sensitivity to initial moisture content, and are mainly a measure of capillary rise. Techniques such as the BRG method (26), however, do deserve further study.

2.4.2.2 Air Permeability

The high pressure techniques suffer from the same disadvantages as the water methods. Low pressure techniques are very sensitive to moisture content and problems arise with effecting adequate seals in an in-situ test. They may be more rapid than water methods, however, and deserve a limited amount of pilot testing.

2.4.2.3 Water-Vapor Transmission

The work of Morrison (32) indicates that these techniques may be applicable to the materials to be considered in this study and deserve further investigation. Slowness of test, however, gives these methods low priority.

2.4.3 Electrical Methods

It is obvious that chloride migration into even high w/c ratio conventional concretes is a very slow process, and in itself would not constitute a rapid test. Recent studies (47,48), however, indicate that chloride can be caused to migrate out of a concrete slab quite rapidly under application of an external electric field imposed across a concrete slab.

This technique could be utilized as a chloride permeability method if the polarity were reversed, that is, by making the reinforcing steel anodic (+); chloride ion, having a negative charge, would migrate into the concrete. As the electrical resistivity of concrete decreases with increasing chloride ion concentration, a measure of the increase in current with time could be correlated with the amount of chloride entering the concrete. Additionally, at the termination of the test, samples could be taken to verify the ingress of chloride by subsequent wet chemical analysis.

2.5 Conclusions from Literature Search

1. Although many accepted techniques are available for determination of the permeability of concrete to high water heads, water vapor, and air, only long-term ponding methods are currently available for determination of chloride permeability.
2. While it may be possible to establish an empirical correlation between water and air permeability and chloride ion permeabilities, the differences in transport mechanisms preclude the use of data gathered via conventional techniques in predicting long-term chloride permeability without extensive cross-correlations.
3. As permeability is an operationally defined parameter, there are no fundamental theoretical relationships between it and basic physical properties. Thus, the measurement of such properties as density, porosity, wave velocity, or other physical properties holds little promise.
4. Chloride ion can be forced to rapidly migrate into concrete under the influence of an electric potential. This technique is especially appealing as the test permeant is the substance of interest, i.e., chloride ions.
5. Change of electrical resistivity with depth may be used to assess the thickness of an impermeable layer. This could be used to determine "depth of impermeability".
6. The permeability of concrete is influenced by its moisture content at the time of testing.

Therefore, it is likely that some type of conditioning will be necessary prior to testing so that all specimens can be tested at approximately the same degree of saturation.

2.6 Selection of Research Approach

2.6.1 Option 1

Evaluate all possible techniques for determining permeability of concrete materials. As this would leave little time or funding for method development, only conventional techniques could be studied.

2.6.2 Option 2

Study the mechanism of flow of chloride ions through concrete and concrete materials under applied voltage. Rigorously define all variables (i.e., aggregate type, cement, moisture content, temperature, etc.) as to their effects on ion flow. Then proceed to develop an instrument capable of measuring chloride ion flow in laboratory and field situations.

2.6.3 Option 3

Devote a limited effort to evaluation of conventional techniques for water, air, and water-vapor transmission. Develop the applied voltage technique on an empirical basis to the point where field and laboratory testing can be carried out using a set routine, and results can be correlated with 90-day ponding data on comparison specimens.

2.7 Approach Selected

It was felt that restriction of the project to use of conventional techniques might result in failure to develop a reliable method. Devotion of all research to the study of chloride ion flow, while certainly commendable from a

basic research standpoint, might be so laborious a task that no practical instrument could be developed within the original project funding and time limitations. For these reasons, a mission oriented approach (Option 3) was chosen. Development of the applied voltage technique had to be carried out in as efficient a manner as possible, with the study of the basic mechanism of the technique de-emphasized. This would allow time for limited evaluation of the most promising conventional techniques, and also an evaluation of the test used by Locke (42) for measurement of the depth of impermeability.

3. METHOD DEVELOPMENT

3.1 Testing of Rocks, Cement Pastes, and Mortars

An initial series of experiments was designed to yield information on the relative chloride permeability of small specimens of various aggregates, cement pastes, and mortars prepared from these crushed aggregates and cements. Initially, the specimens were tested in the form of discs 0.175-in. (4 mm) thick x 2 in. (51 mm) in diameter in small cells previously used at PCA in alkali/aggregate research (49) (see Figure 5). The specimens were exposed to a 30% NaCl solution on one side of the membrane, and distilled water on the other. This was chosen so as to maximize osmotic forces. The concentration of NaCl on the distilled water side was monitored at daily intervals using Quantab^(R)* chloride strips. Results after 7 days of test are given in Table 3. It is seen that all rocks tested exhibited higher permeability than all but the most permeable cement paste (w/c = 0.6). In the

mortar series when the lower permeability rock was used as aggregate, the permeability of the mortar was apparently determined mainly by the permeability of the paste. When a high permeability aggregate was used, the permeability of the aggregate had a large effect even at low w/c ratios.

TABLE 3
OSMOTIC CELLS

% NaCl in Left Side at 7 Days

<u>Rock #</u>	<u>1</u>	<u>2</u>	<u>3</u>	<u>4</u>	<u>5</u>	<u>6</u>
	9.0	6.8	0.28	0.31	0.17	0.12
<u>Paste w/c</u>	<u>0.3</u>	<u>0.4</u>	<u>0.5</u>	<u>0.6</u>		
-28d moist	0.02	0.03	0.07	0.30		
1:2 Mortars with <u>Rock #</u>	<u>5</u>	<u>2</u>				
- 28d moist w/c	0.4	0.02	0.29			
	0.5	0.15	0.29			
	0.5	0.32	0.46			

The osmotic cell was then modified by placing copper mesh screens on both sides of the test specimen. The screen immersed in 30% NaCl was connected to the negative lead of a 10.0 Vdc constant voltage power supply, the screen immersed in distilled water connected to the positive lead. The current (in milliamperes) generated at 10 Vdc was monitored as a function of time. Plots of current vs. time for rock, paste, and mortar specimens are shown in Figures 6 through 8. Although the precise significance of the shape of the curves is unknown, it is evident that the magnitudes of the current are generally proportional to the chloride permeabilities determined in the osmotic cell tests. The results of these preliminary experiments indicated, therefore, that further development work on the applied voltage technique was warranted.

*Registered trademark, Ames Co., Elkhart, Indiana.

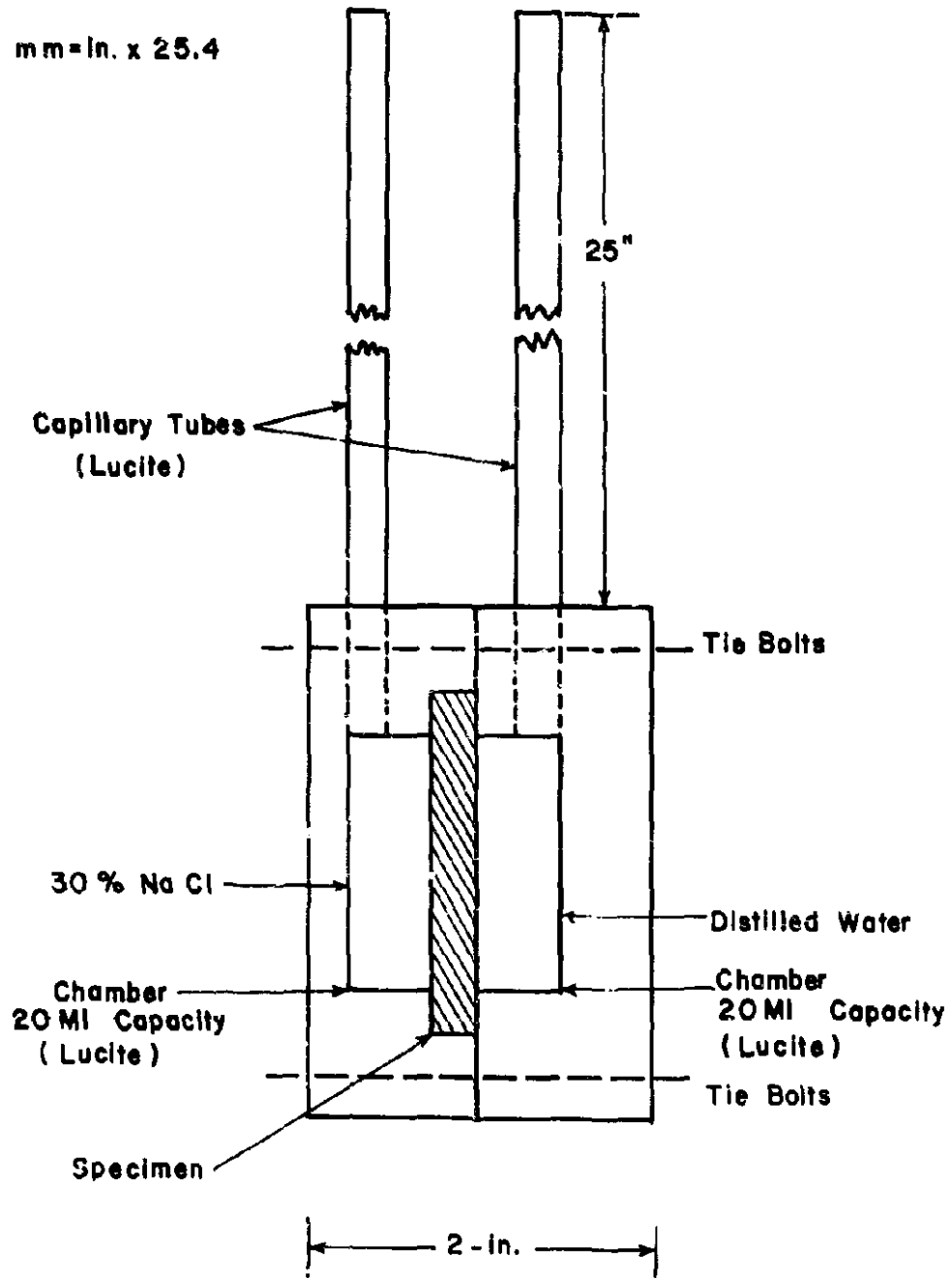


FIGURE 5. CELL USED FOR PRELIMINARY EXPERIMENTS.

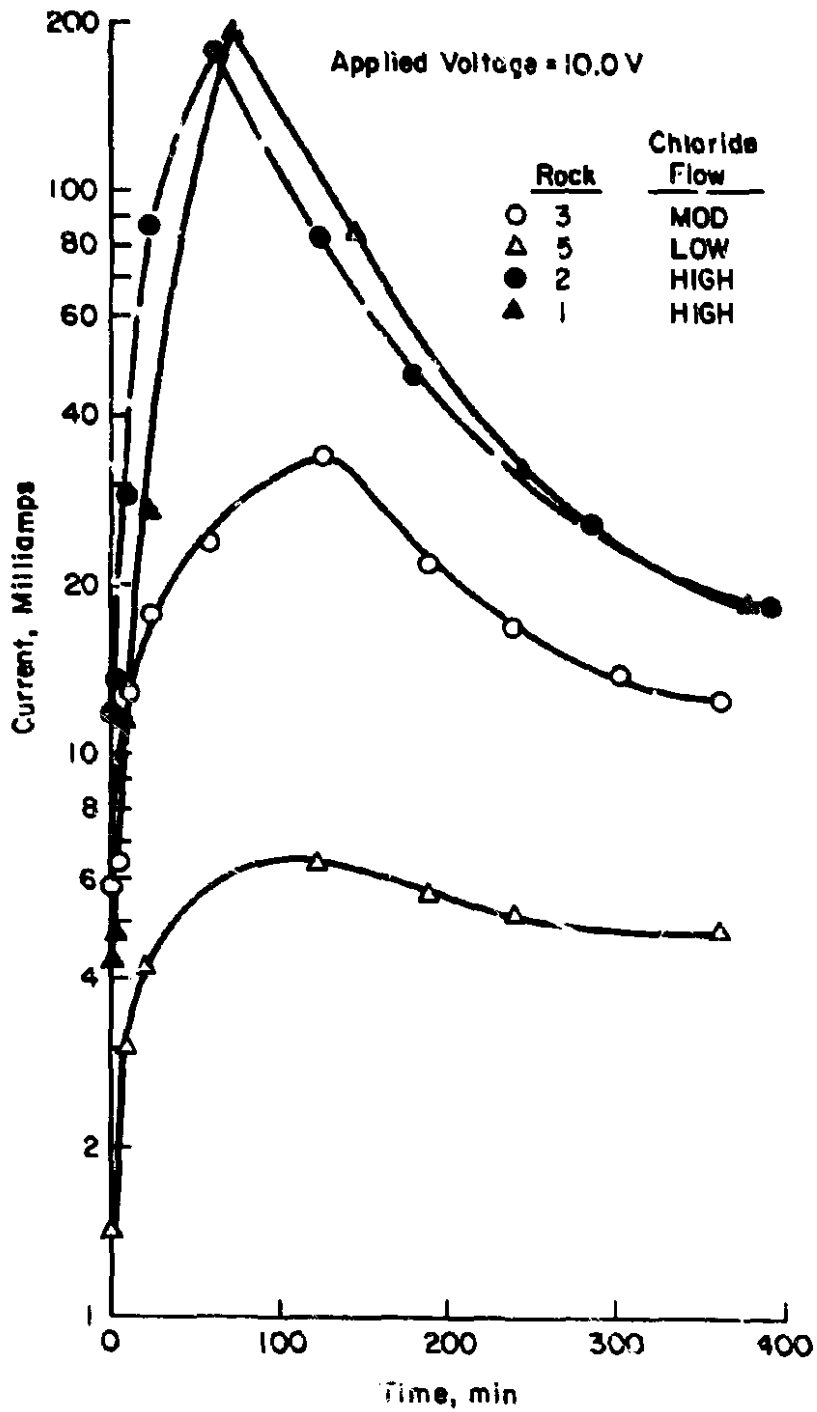


FIGURE 6. CURRENT VS. TIME FOR ROCK SLICES.

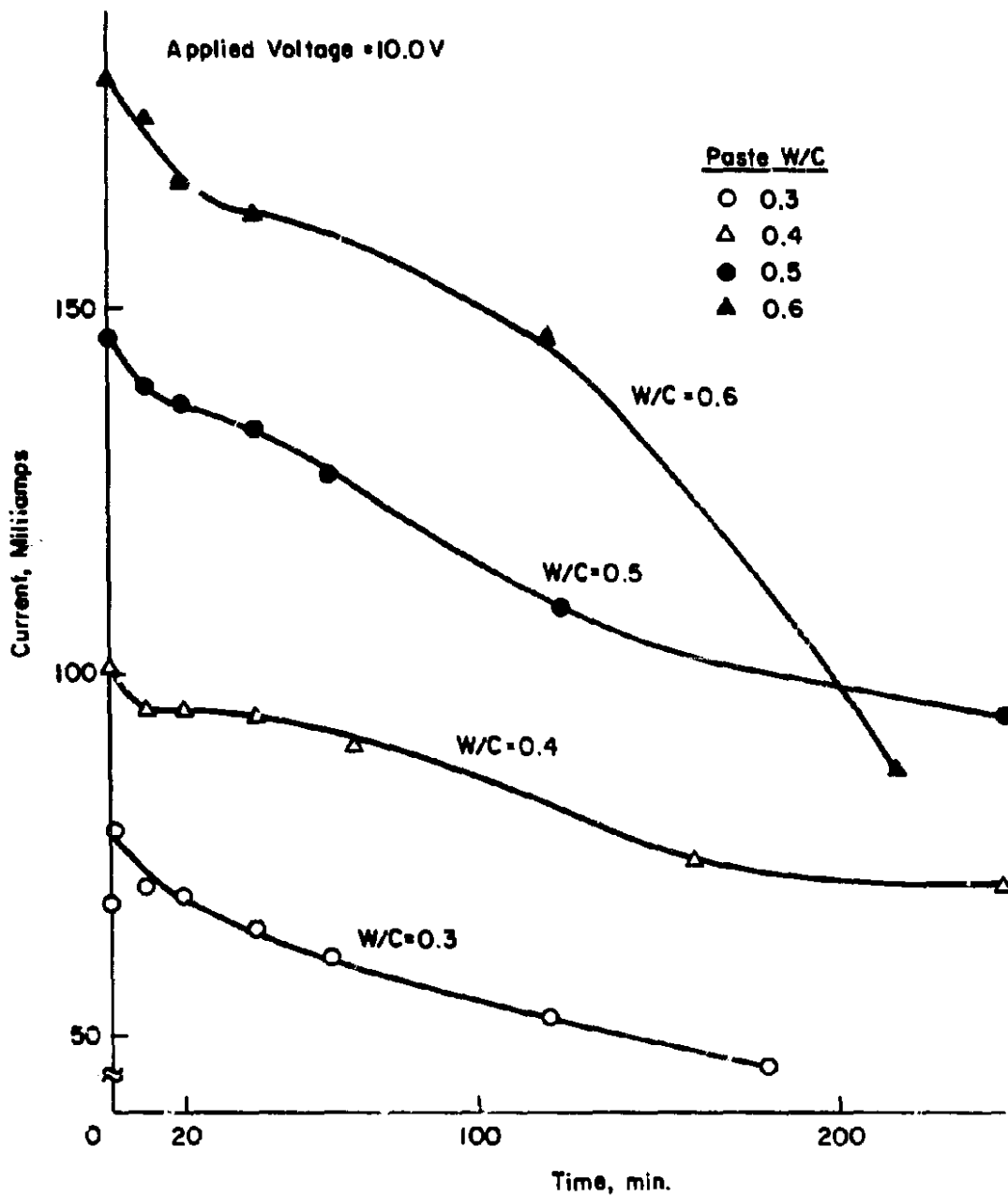


FIGURE 7. CURRENT VS. TIME FOR PASTE SLICES.

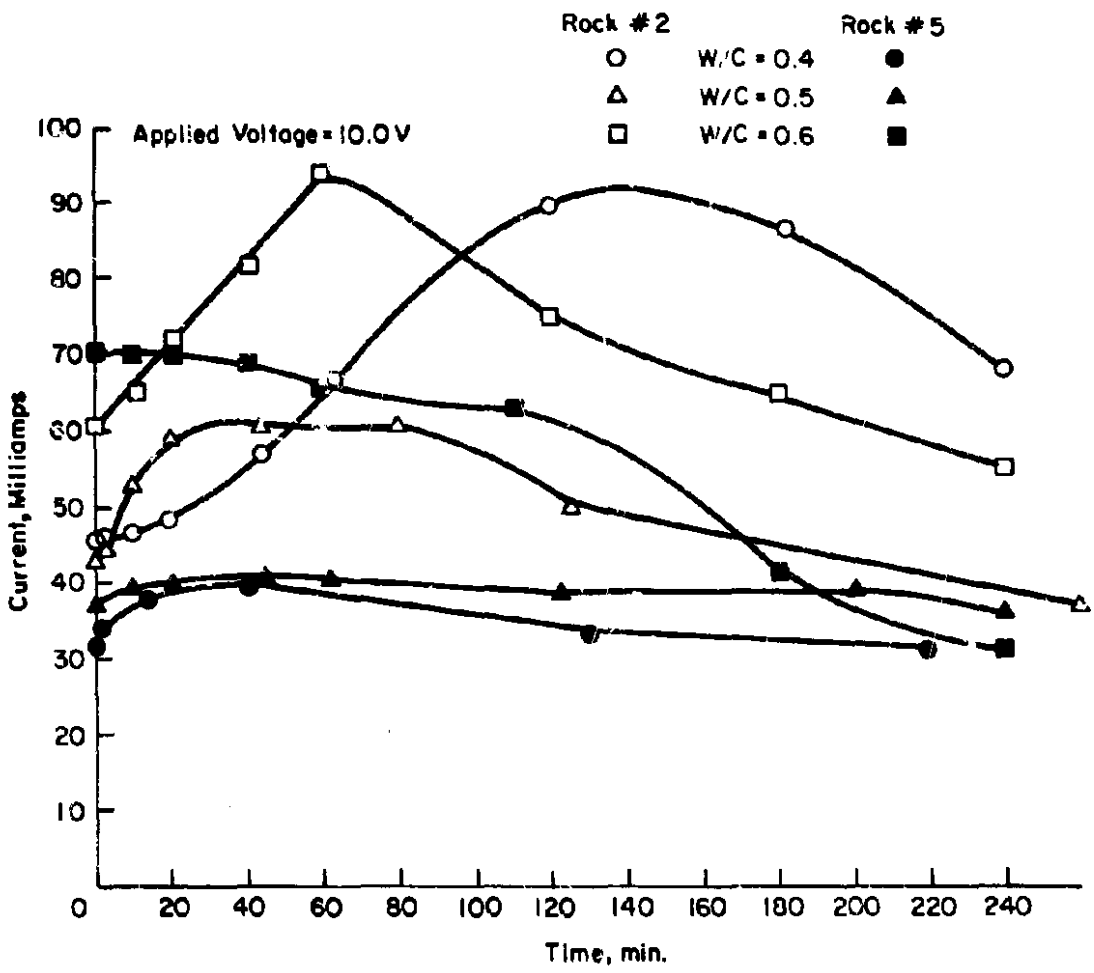


FIGURE 8. CURRENT VS. TIME FOR MORTAR SLICES.

3.2 Testing of Concrete Slabs

3.2.1 Slab Specimens

In order to assess the applicability of the applied voltage method to larger scale specimens, a series of tests was conducted on reinforced concrete slabs. These were 0.5 ft³ (0.014 m³) specimens having the dimensions shown in Figure 9. Two mats of No. 5 (16 mm) bars were tied together with wire. The upper ("transverse") mat was set at 4-in. (102 mm) centers, the lower ("longitudinal") at 8-in. (203 mm) centers. A knurled steel pin was used for the electrical connection. Thermocouples were placed at 1/2- (13 mm), 1- (25 mm), and 2-in. (51 mm) depths. Clear cover over the top mat was 2 in. (51 mm). Two concrete mixes were utilized, the first (E-60) being a high water-cement ratio permeable mix, the second (E-35) a low water-cement ratio dense concrete. Batch quantities and characteristics are shown in Table 4. Specimens were moist cured for 28 days prior to test.

poured into the dike. A No. 4 (4.75 mm) mesh copper screen was used as the negative electrode. The electronic components used are shown in Figure 11. A dc power supply is used to apply a constant voltage between the copper screen and steel reinforcing mat. The current flow is monitored by placing a digital voltmeter (DVM) across a 100- μ v shunt in series with the copper screen. This affords a sensitivity of 1 ma/0.01 mv; thus current in milliamps can be read directly from the digital voltmeter. Initial and final resistances between the steel mat and the copper screen were measured on some of the test slabs using an AC resistance meter (Nilsson Model 400).

3.2.3 Preliminary Tests

The concrete slabs were subjected to applied potentials of 10, 20, and 40 volts for periods of 1, 2, and 4 hours. Plots of current vs. time are shown in Figure 12 for w/c = 0.6 and Figure 13 for

TABLE 4
PRELIMINARY CONCRETE MIXTURES
Mix Quantities (lbs/yd³)

Mix	w/c	Cement	Water	Sand	Gravel	Slump ₂ / (in.) ²	Air (%)
E-60	0.60	322	193	1,314	2,144	1.0	5.3
E-35	0.35	670	241	968	2,056	2.0	5.6

$$1/ \text{ kg/m}^3 = \text{ lb/yd}^3 \times 0.594$$

$$2/ \text{ mm} = \text{ in.} \times 25.4$$

3.2.2 Apparatus

The apparatus used to conduct the tests on these slabs is shown in Figure 10. An acrylic dike was affixed to the concrete surface with silicone caulking compound. The silicone was air-cured overnight, and the following morning 1,500 ml of sodium chloride solution (30% used in initial tests) was

w/c = 0.35. The breaks in the curves represent times when chloride drill samples were taken, the test being interrupted for approximately 45 min to allow for drilling and backfill of the drill hole with rapid-setting epoxy. Except for the highest voltage applied to the high w/c mix, all curves appear relatively flat throughout the test period.

mm = in. x 25.4

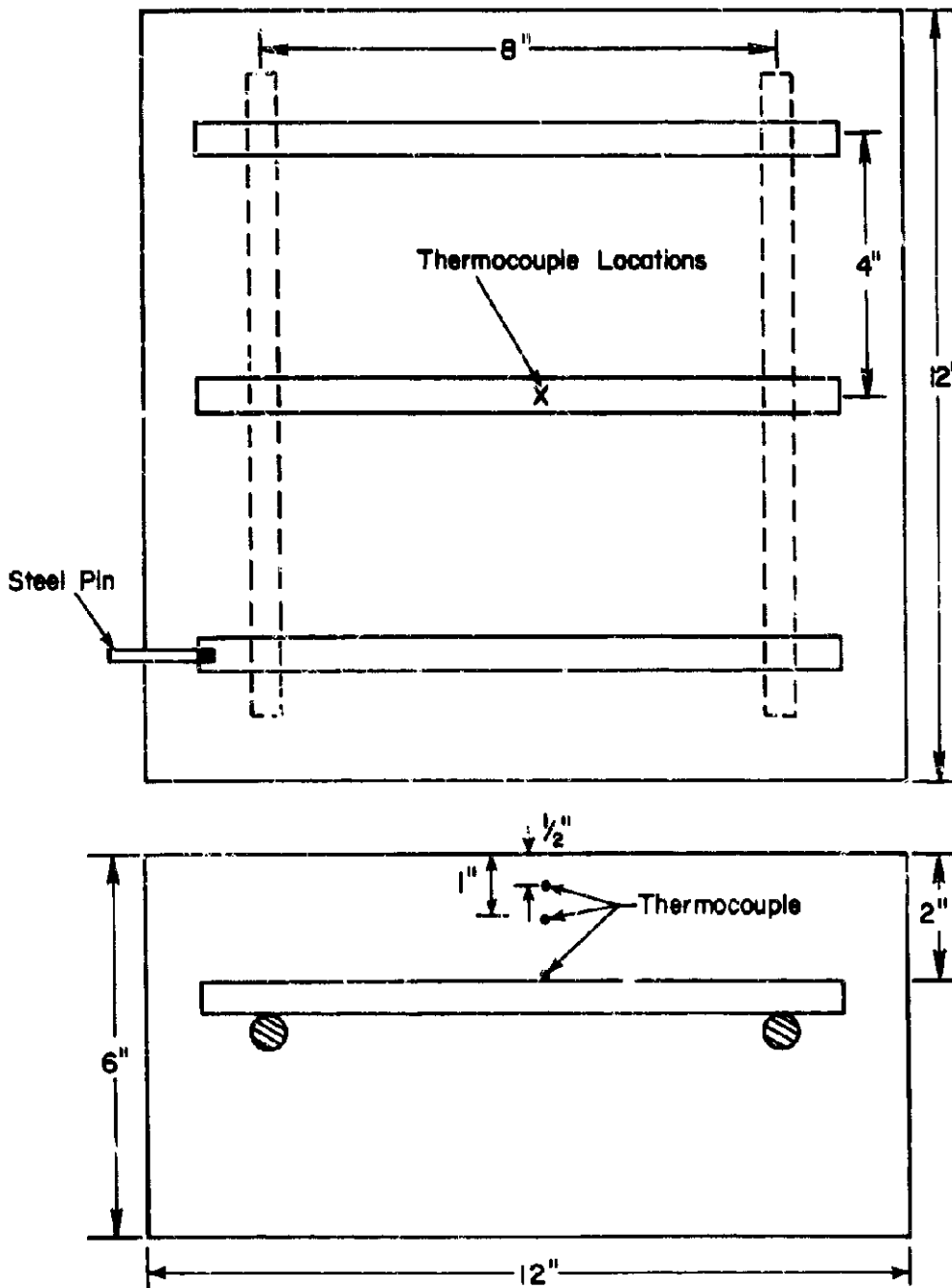


FIGURE 9. SLAB SPECIMEN DETAILS.

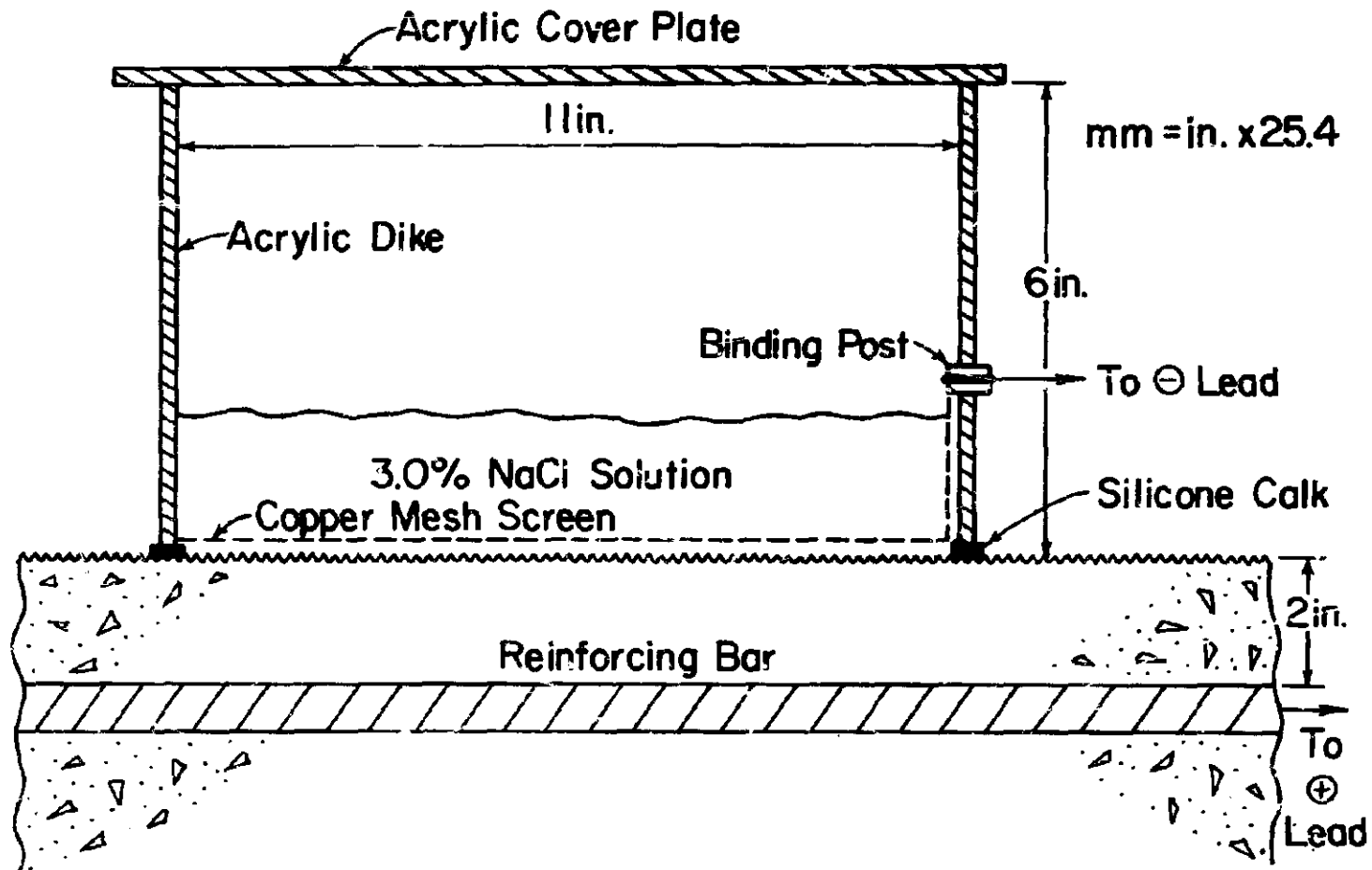


FIGURE 10. APPLIED VOLTAGE APPARATUS USED ON SLAB SPECIMEN.

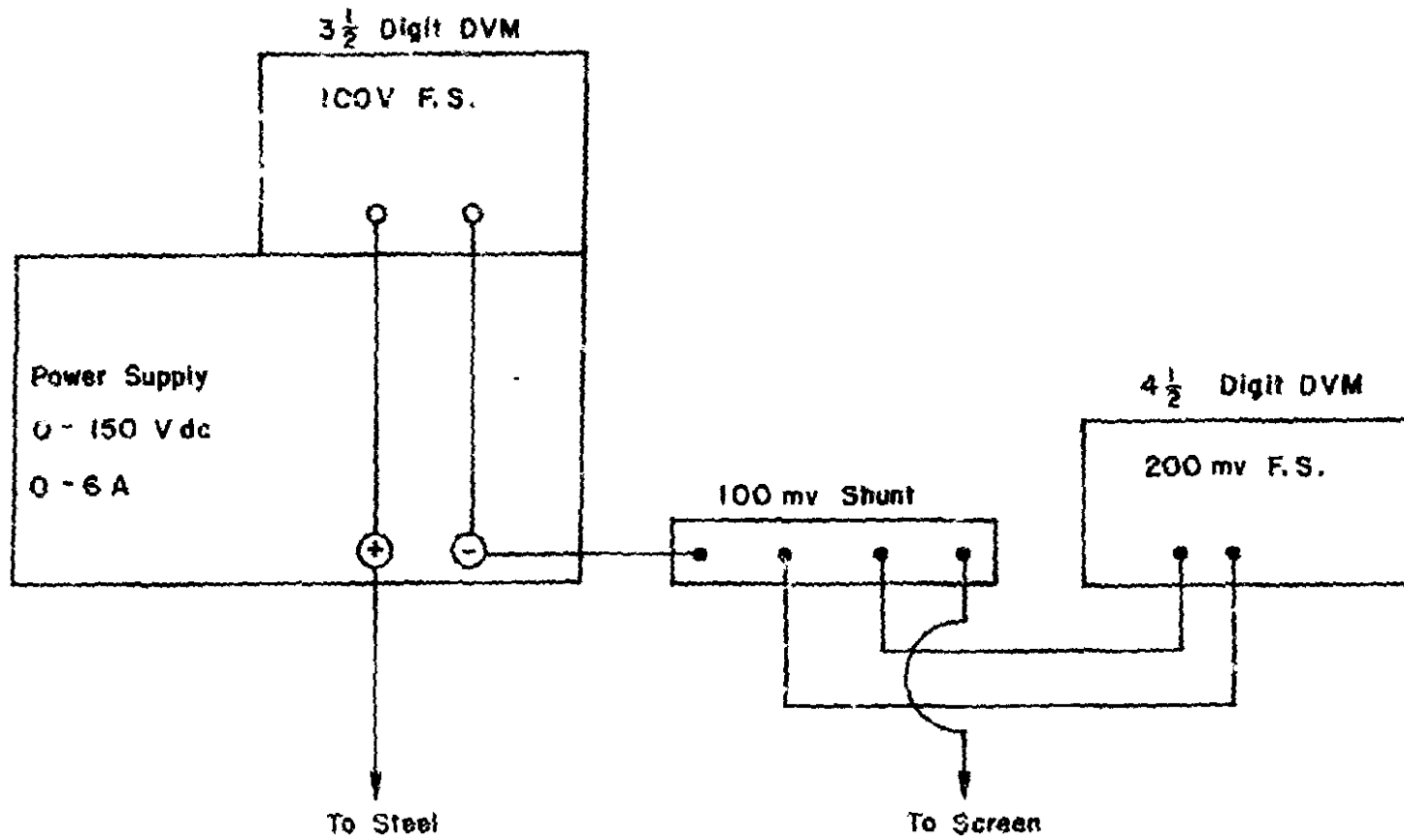


FIGURE II. ELECTRICAL BLOCK DIAGRAM.

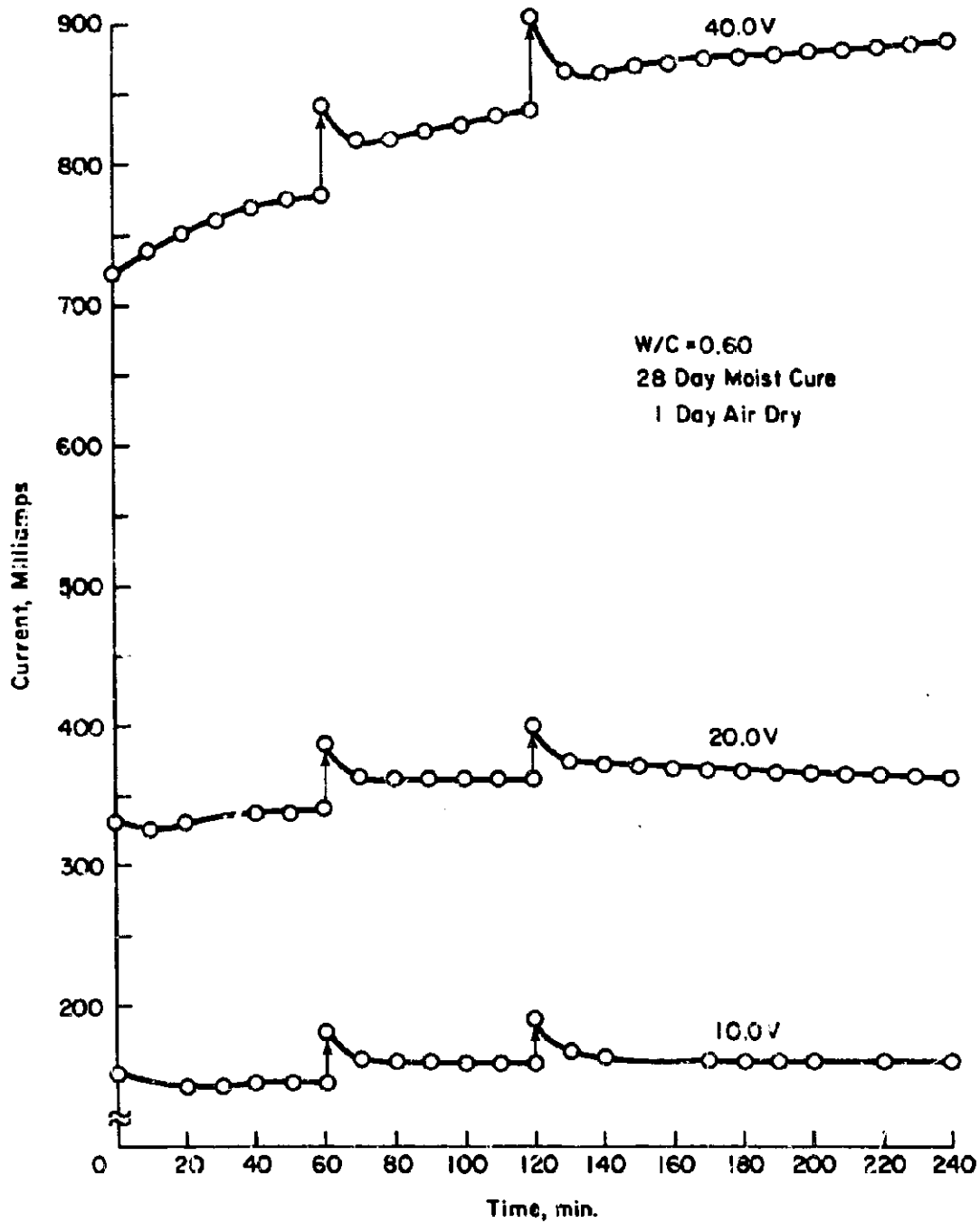


FIGURE 12. CURRENT VS. TIME FOR 0.60 W/C RATIO SLABS TESTED AT VARIOUS APPLIED VOLTAGES.

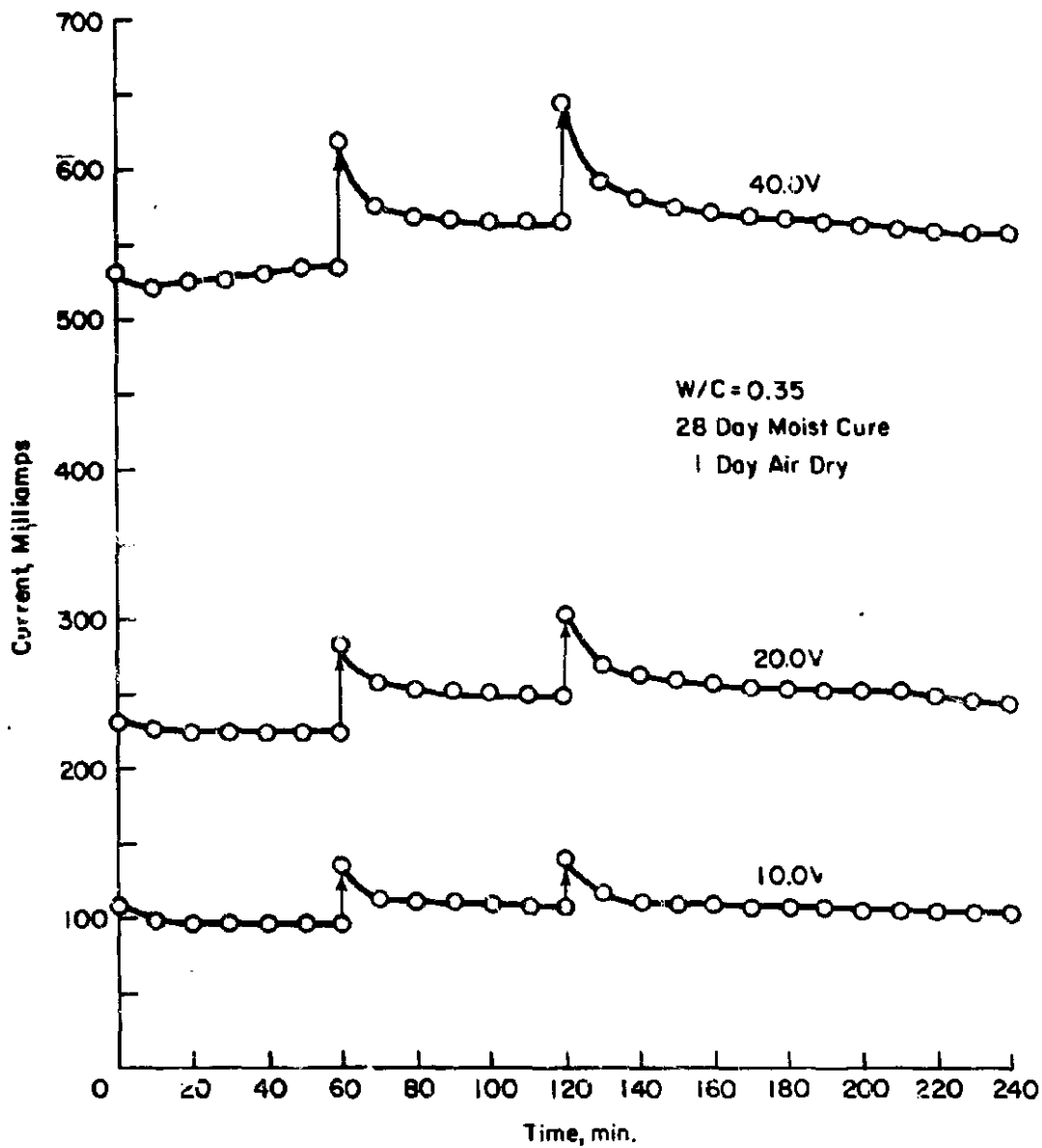


FIGURE 13. CURRENT VS. TIME FOR 0.35 W/C RATIO SLABS TESTED AT VARIOUS APPLIED VOLTAGES.

Chloride samples were obtained using a 1-1/8-in. (28 mm) diameter carbide bit on a rotary-impact hammer. Samples were ground to pass a 100 mesh sieve and analyzed using the Gran Plot technique (50).

Results of chloride sampling (Table 5) taken at depths of 0 to 3/8 in.

significant amounts of chloride into highly permeable concrete, little difference between simple ponding and applied voltage could be found for concretes of lower permeability. In order to increase the sensitivity of the test, therefore, it was necessary to inves-

TABLE 5
CHLORIDE ANALYSES
0-3/8-in. ^{1/} Depth
(% by Weight of Sample)

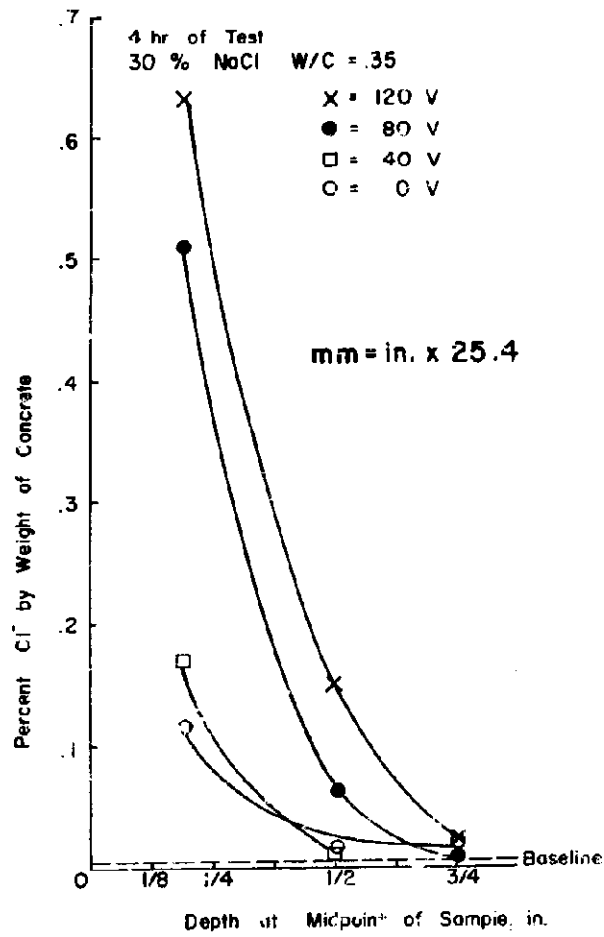
<u>Applied Voltage</u>					
<u>w/c = 0.60</u>					
<u>Time</u>	<u>0 V</u>	<u>10 V</u>	<u>20 V</u>	<u>40 V</u>	
1 hr	-	0.062	0.157	0.142	
2 hr	-	0.125	0.298	0.206	3/4 - 1 in. 1-1/2 - 1-3/4 in.
4 hr	0.130	0.208	0.356	0.394	0.0131 0.0108
<u>w/c = 0.35</u>					
1 hr	-	0.067	0.029*	0.082	
2 hr	-	0.130	0.152	0.105	3/4 - 1 in. 1-1/2 - 1-3/4 in.
4 hr	0.150	0.181	0.282	0.174	0.0088 0.0122
<u>Baseline</u>					
w/c = 0.35 / 0.00449, 0.00679					
w/c = 0.60 / 0.00630, 0.00871					
*Questionable result					
1/ mm = in. X 25.4					

(0-10 mm), 3/8 to 5/8 in. (10-16 mm), and 3/4 to 1 in. (19-25 mm) indicate that at shallow depths chloride penetration increases both with voltage and time, but at lower depths little chloride has penetrated even at the highest voltage employed. Control slabs (ponded with 30% NaCl but not subjected to voltage) showed approximately equal chloride concentrations in the first 3/8 in. (9 mm) for both concretes, and no significant chloride at lower levels. This set of results indicated that although 40 Vdc applied for 4 hr would migrate

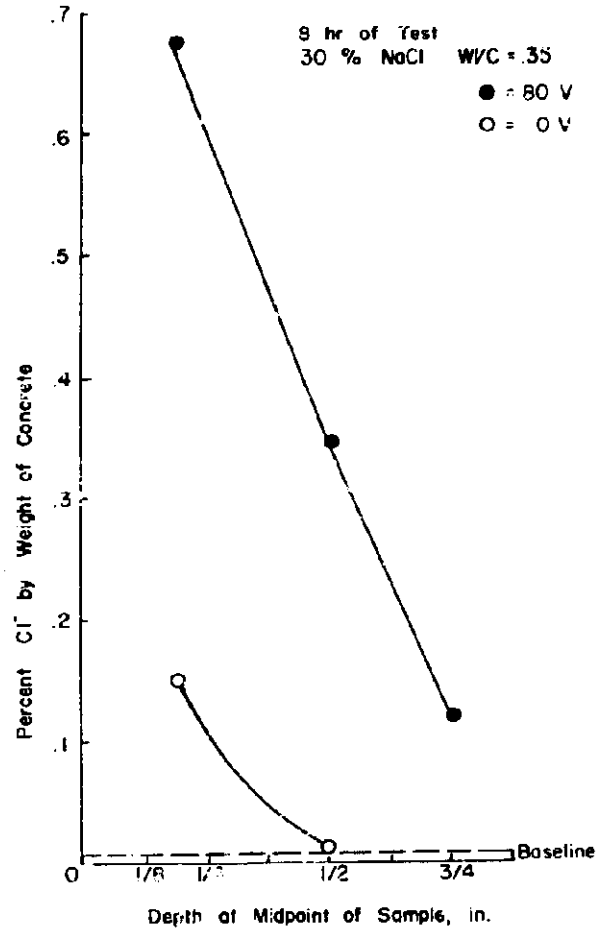
investigate the use of higher voltages and longer test periods.

3.2.4 Tests at Higher Voltages

Concrete slabs having w/c = 0.35 were treated by ponding a 30% NaCl solution on top of the slabs and applying direct current at fixed voltages of 40, 80, and 120 Vdc for periods of 4 hr and 8 hr. Results, shown in Figure 14A, indicate a steady increase in Cl⁻ detected at the 3/16- and 1/2-in. (8 and 13 mm) levels as voltage is increased. Figure 14B indicates a large increase in



(A) TESTED FOR 4 HOURS.



(B) TESTED FOR 8 HOURS.

FIGURE 14. CHLORIDE PROFILES FOR SLABS HAVING W/C RATIO OF 0.35.

Cl⁻ detected at 1/2 and 3/4 in. (13 and 19 mm) as time at 80 Vdc is extended from 4 hr to 8 hr. As 8 hr may be inconvenient for a field test situation (requiring overtime to setup and break-down) a test period of 6 hr was also tried. Results (Figure 15A) are also very promising, indicating about 0.35% Cl⁻ at 1/2 in. (13 mm) after 6 hr of test at 80.0 V.

As the relative change in actual solution concentration during the period of test is very small if one starts with a highly concentrated (30%) NaCl solution, we decided to try a 3.0% initial solution under the same conditions. This might allow one to dispense with chloride drill sampling in the field if the change in concentration of the ponding solution was great enough. The Cl⁻ profile for this test (Figure 15A) also indicates a high concentration of Cl⁻ at 1/2 in. (13 mm). Solution concentration decreased 0.5% in NaCl measured using Quantab^(R) chloride indicator strips. Although later testing showed these strips to be inaccurate, they did indicate that some measurable change in concentration had taken place.

The test was repeated using concrete with w/c = 0.60. Results, shown in Figure 15B, show a reverse chloride gradient. This indicates that chloride is beginning to accumulate at lower depths faster than it can be pulled in from solution, which would be expected in a very permeable system. This test also shows that a series of samples must be taken at increasing depths. Otherwise, if one were to simply sample at say, 1/2 in. (13 mm), the concretes would appear to have the same chloride permeabilities on the basis of the single point result.

Current rise as a function of time at 80 Vdc is shown in Figure 16. The

higher currents encountered in the 0.60 w/c concrete can be attributed to the lower circuit resistance (initial = 65 Ω) relative to the 0.35 w/c concrete (initial = 120 Ω). It is interesting to note that final circuit resistances were much closer (32 Ω for w/c = 0.60 vs. 42 Ω for w/c = 0.35).

Temperature rise as a function of time for w/c = 0.60 concrete at 80.0 Vdc is shown in Figure 17. Final temperatures after 6 hr of test range from 150°F (66°C) at the surface to 170°F (77°C) at 2 in. (51 mm). These can be considered conservative estimates, as on an actual structure the heat sink would be substantially greater than that of an 0.5 ft³ (0.14 m³) specimen.

3.2.5 Conclusions Derived from Preliminary Experiments

1. It is possible to accelerate migration of chloride ions into concrete by application of potential between the surface of a slab and the topmost reinforcing mat.
2. In order to distinguish between highly permeable and moderately impermeable concretes, a test period of 6 hr at 80.0 Vdc has been selected. Rapid heating due to IR losses precludes the use of higher voltages.
3. The permeability of the test specimen may be assessed by examination of plots of current vs. time, chloride concentration vs. sampling depth, or loss of chloride from the surface solution.

4. LABORATORY TESTING

4.1 Test Specimens

Specimens of various types of concretes were prepared at the FHWA

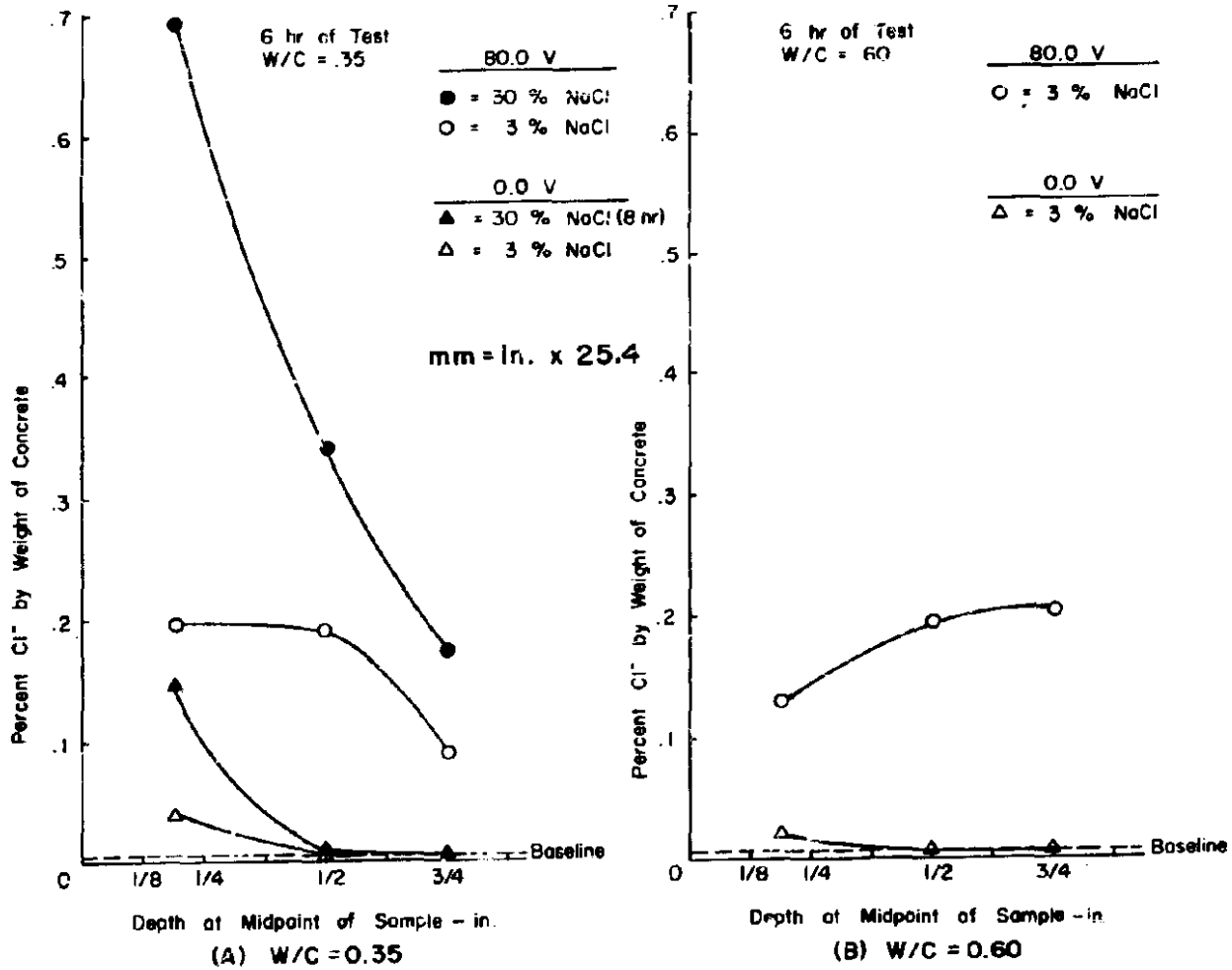


FIGURE 15. CHLORIDE PROFILES FOR SLABS TESTED FOR 6 HOURS.

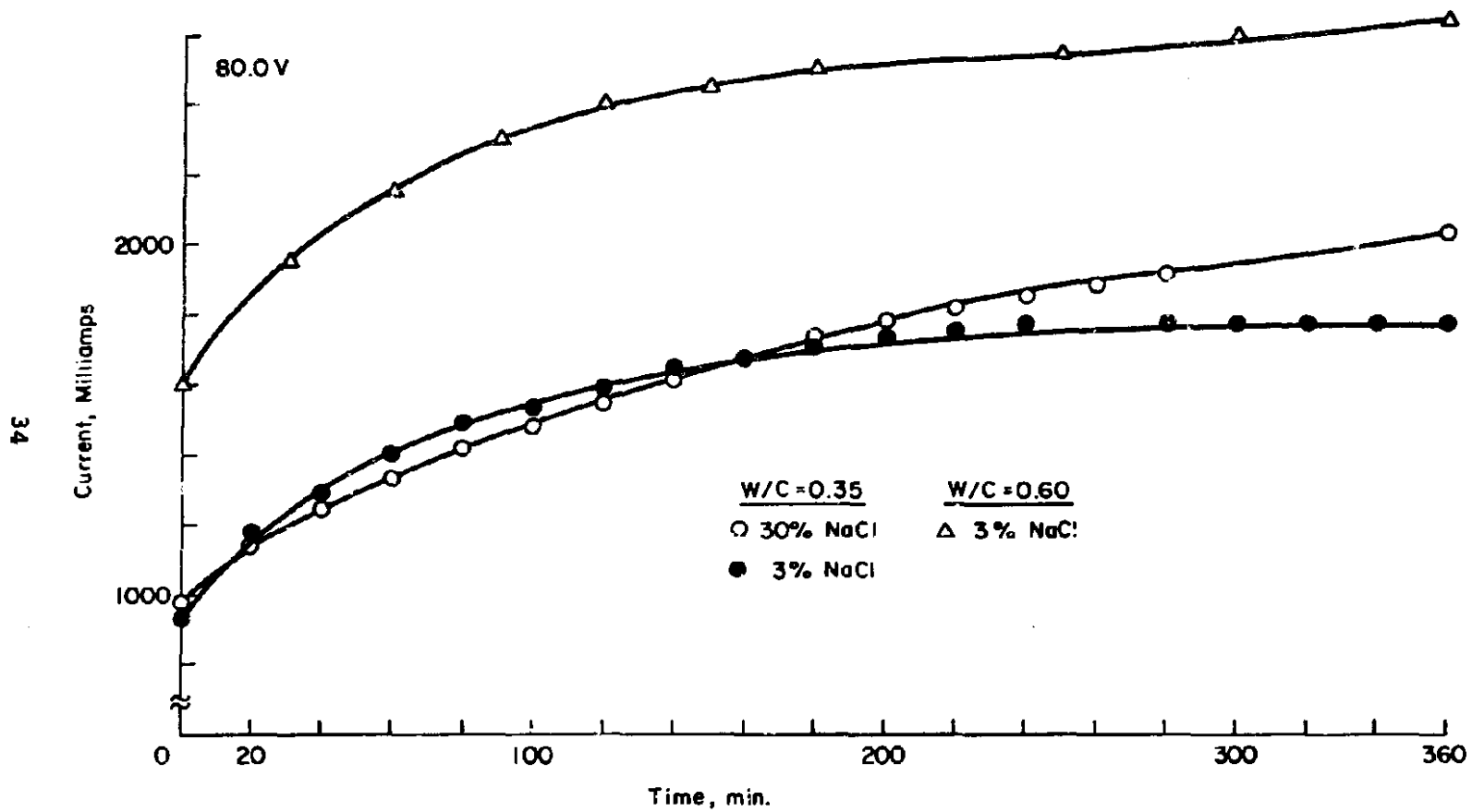


FIGURE 16. CURRENT VS. TIME FOR SLABS AT 0.35 AND 0.60 W/C RATIO TESTED AT 80.0 VDC.

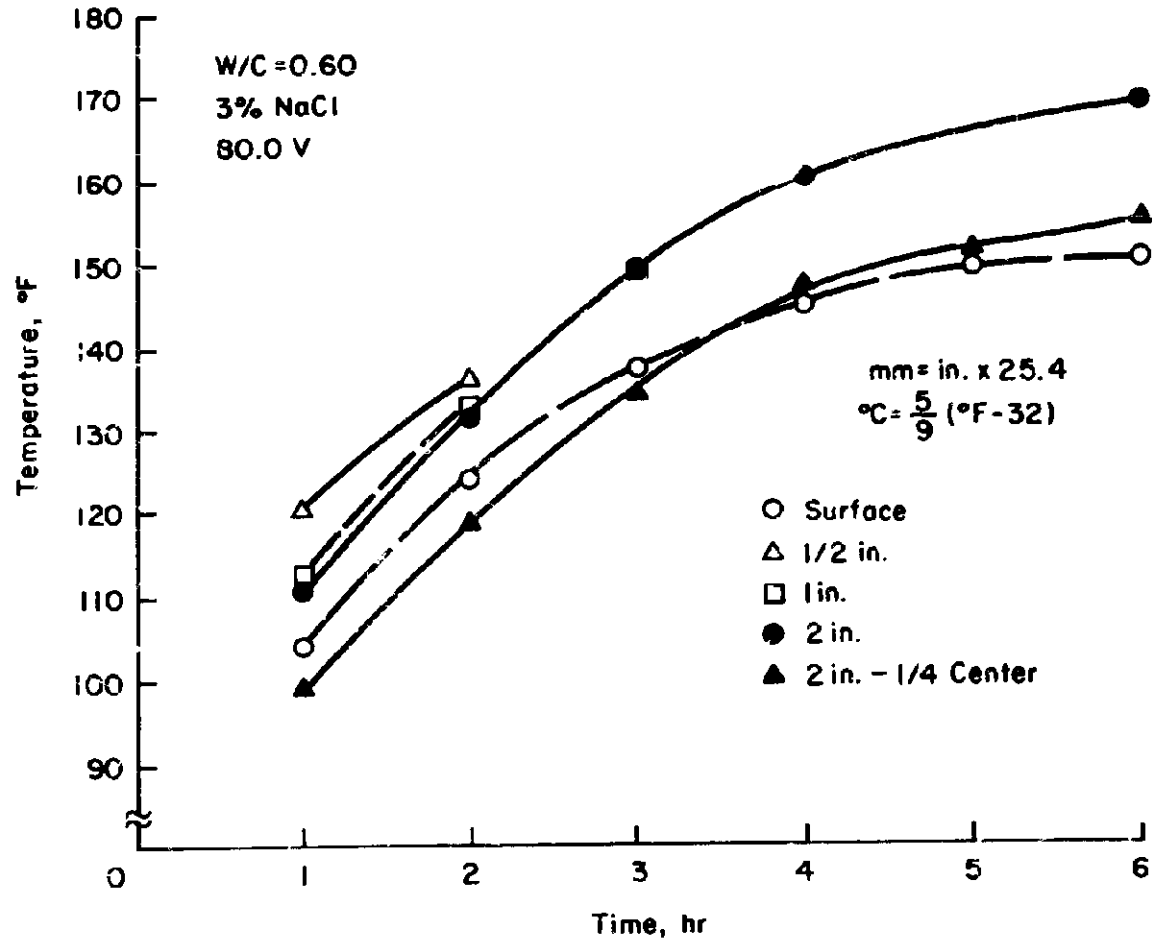


FIGURE 17. TEMPERATURE RISE IN SLAB AT 0.60 W/C RATIO TESTED AT 80.0 VDC.

laboratories. The specimens were in the form of slabs having dimensions of 23-1/2-in. (597 mm) long x 12-in. (305 mm) wide x 6-in. (152 mm) deep. Five of these slabs were cast from each concrete mixture. Two contained a mat of reinforcement consisting of No. 5 (16 mm) bars on 5-in. (127 mm) centers (top) and No. 4 (13 mm) bars on 10-in. (254 mm) centers (bottom) (see Figure 18). The two mats were joined with steel wire ties. One out of each set of these reinforced slabs contained a set (A) of embedded thermocouples located at depths of 1/2 in. (13 mm), 1 in. (25 mm), and 2 in. (51 mm) and directly above a steel reinforcing bar, and a single thermocouple (B) located midway between two bars at the level of the steel. The remaining three slabs were unreinforced. All slabs (with the exception of the latex modified mixes) were cured for 14 days under wet burlap, then wrapped in plastic sheet and shipped to our facilities for testing. Latex modified specimens were burlap cured for 1 day, followed by air curing. One plain slab from each mix was retained at FHWA for 90-day chloride ponding. The remaining four were shipped to CTL/PCA and stored as follows:

Set

No.

Storage Conditions

- 1 Stored in fog room approximately 3 months prior to test, "moist" (reinforced slabs with thermocouples).
- 2 Stored in air freezer in heavy plastic bags at 0°F (-18°C) to maintain moisture content in the "as-received" condition (reinforced slabs).
- 3 Stored in air at 70-75°F (21-24°C) and 50-60 percent RH (plain slabs only).
- 4 Eight cores, 3.75 in. (95 mm) in diameter were taken from these

slabs, then placed in the air freezer.

Slab numbers, descriptions, and storage conditions are given in Table 41 (Appendix 7).

4.2 Concrete Mixtures

Ten concrete mixtures were produced for this study (Table 6). They consisted of conventional concretes (Mixtures 1-3), specialty concretes (Mixtures 4-6) and overlays (Mixtures 7-10).

Overlays were placed over base course slabs having w/c = 0.50. Base slabs were sandblasted to remove all laitance prior to applying the overlays. Portland cement grout was used as a bonding agent for the Iowa and internally sealed overlays. Latex grout was used to bond the latex overlays, and a "quick seal" (R)^{*} resin containing 1% accelerator used to bond the polymer concrete overlay.

All internally sealed specimens (overlays and full-depth slabs) were air dried for one week after curing, then surface heated with blankets until the temperature reached 185°F (85°C) at 2 in. (51 mm) from the surface. A set of internally sealed concretes was left unheated.

Polymer impregnated concrete were produced at Brookhaven National Laboratories. The slabs were dried for 72 hr at 151°F (66°C) followed by 48 hr at 250°F (121°C). They were then evacuated at 76 cm Hg for 24 hr, and a monomer system containing 95% MMA - 5% TMPTMA was used to impregnate the slabs. They were then soaked 36 hr, followed by heating at 190°F (88°C) for 4 hr. Polymer loading (by weight) averaged approximately 5%.

Polymer concrete overlays consisted of a mixture of "quick-deck" (R)^{*} resin,

^{*}Registered Trademark, ODT, Inc., Pittsburgh, Pennsylvania.

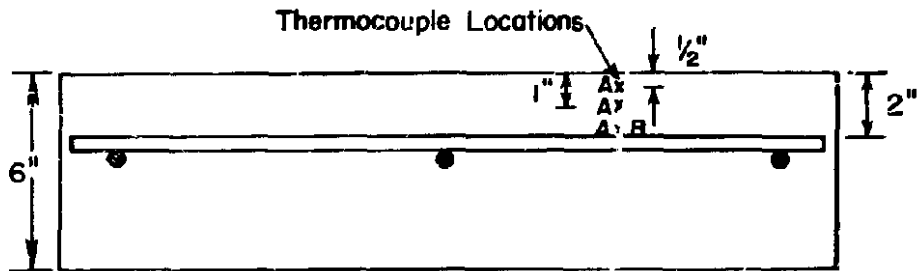
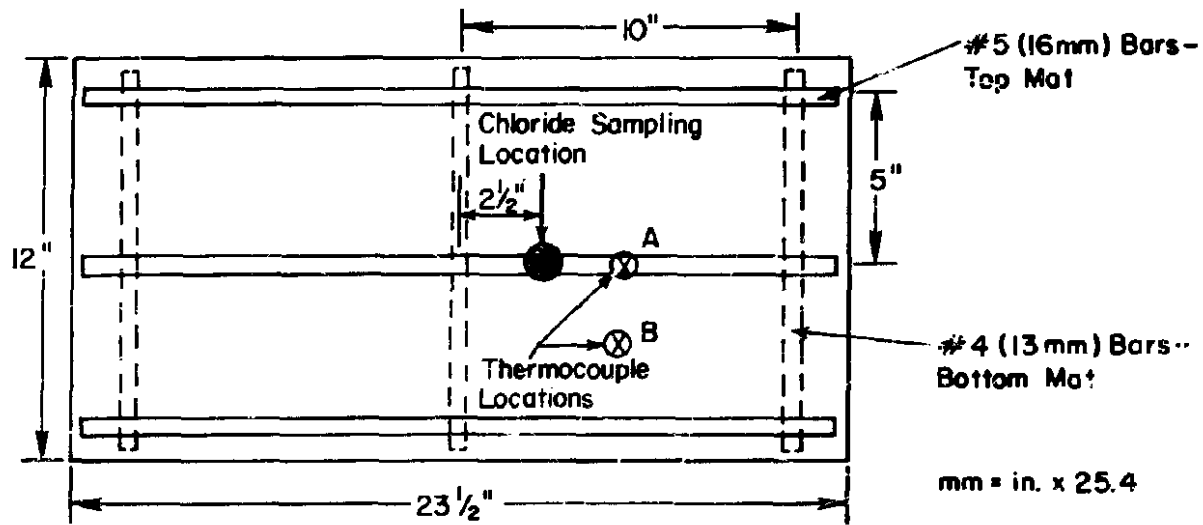


FIGURE 18. DETAILS OF SLABS SUPPLIED BY FHWA.

TABLE 6
CONCRETE MIXTURE CHARACTERISTICS

Batch Quantities (lb/cu yd)^{1/}

Mix No.	Type	Cement	Water	Additive(s)	Slump ^{2/} (in.)	Air (%)	Overlay Depth ^{2/} (in.)	Depth to Steel Mat (in.) ^{2/}
1	w/c = 0.60	658	395	--	7.8	8.0	--	2.0
2	w/c = 0.50	658	329	--	3.4	5.5	--	2.0
3	w/c = 0.40	658	263	--	2.0	7.9	--	2.0
4	Latex Modified	658	158	Latex Emulsion - 198	7.2	7.7	--	2.0
5	Internally Sealed	658	364	Wax Beads - 119	3.4	3.7	--	2.0
6	Polymer Impregnated Concrete	658	329	PMMA 5% by wt. of Dry Concrete	3.2	5.2	--	2.0
7	Latex Modified Overlay	658	158	Latex Emulsion - 198	4.0	3.7	1.25	2.25
8	Internally Sealed Overlay	658	365	Wax Beads - 119	3.2	3.3	2.0	3.0
9	Iowa Overlay	830	272	--	0	6.7	2.0	3.0
10	Polymer Concrete Overlay:	19.9%	"quick-deck" resin		-	-	0.5	1.5
		0.4%	accelerator					
		79.7%	-8 sand					

^{1/} kg/m³ = lb/yd³ X 0.594
^{2/} mm = in. X 25.4

and minus 8 (-2.4 mm) mesh sand in proportions of 20:80 by weight. Accelerator was added at 2% by weight of resin.

4.3 Test Procedure - Slab Specimens:

The apparatus previously used on the smaller slabs (see Figures 10 and 11) was also used on Sets 1 and 2 of the FHWA slab specimens. In this case 3 percent NaCl solution was used. A voltage of 80.0 ± 0.1 Vdc was applied for 6 hrs in all cases. Current and thermocouple readings were monitored at 30-minute intervals.

At the conclusion of each test 200 ml of the surface solution was collected into a polyethylene sample bottle. Initial analysis for chloride concentration was done using a calibrated direct-reading chloride electrode (Orion Model 94-17). In some solutions the pH increased to highly alkaline levels during the test period. It was later found that this resulted in a shift of the chloride calibration curve, resulting in reported readings of solution loss (%) being greater than the true losses. It was possible to overcome

these problems by acidification of the test solution to a pH between 4-5 prior to taking the electrode readings; however, this acidification was tedious and time-consuming and no more efficient than simple potentiometric titration of an acidified solution. Therefore, the values reported for "solution loss %" in the moist and as-received slab series are to be taken as relative indications of concentration changes only. In later studies the values are more accurate, as they were obtained by potentiometric titration (Gran Plot).

Chloride drill samples were taken after the test surface had been flushed with water and dried. Samples were taken above the centrally located upper rebar. Samples were taken at the following increments: 0-1/8 in. (0-10 mm), 1/8-3/8 in. (10-16 mm), 3/8-7/8 in. (16-22 mm), 7/8-9/8 in. (22-29 mm), 9/8-13/8 in. (29-41 mm). The final sample is a 1/2-in. (13 mm) increment, as little chloride is usually detected at such a depth. All samples were ground to -100 (-150 μ m) mesh prior to extraction and analysis.

Samples for free water content determination were taken prior to each test on the untested half of the slab. These consisted of drill samples taken at 1/2-in. (13 mm) increments. Samples were placed in plastic vials immediately after drilling. Free water was determined by loss on drying for 48 hr at 221°F (105°C).

4.4 Results of Slab Tests

4.4.1 Tests on Moist and As-Received Slabs

The apparatus and technique described on page 24 was applied to Sets 1 and 2 of the reinforced slabs. The dike covered one-half the surface of the slab under test, allowing the remainder to be

tested at a later date if desired. A voltage of 80.0 V_{ac} was applied in each case for 6 hr. The following parameters were used to characterize the permeability of each specimen:

1. Charged passed in coulombs = integral of current vs. time under test.
2. Solution loss = decrease in concentration of NaCl solution ponded on surface of slab.
3. Chloride concentrations = percent Cl⁻ by weight of concrete at a given sampling depth.
4. Total chloride = integral of chloride profile (concentration vs. depth).

Additionally, by utilizing the embedded thermocouples, the temperature of one set of reinforced slabs (Set 1) was monitored during the period of test. Plots of temperature at the 1-in. (25 mm) level vs. time for selected slabs are shown in Figure 19. The 1-in. (25 mm) level was found to yield the highest temperatures of all positions monitored. The rate of temperature rise is highest in the most permeable, high water-cement ratio concrete. The temperature rise can be attributed to the higher levels of current which are passed through the concrete as its permeability increases (Figure 20). It was noted that in the high permeability concretes (w/c = 0.6), there appeared to be a peak in the plots of current vs. time, while for the other concretes current increased continuously with time at various rates.

Some examples of chloride profiles with depth are shown in Figure 21. The highly permeable concrete (water-cement ratio = 0.6) shows a concentration increasing with depth up to about 0.5 in. (13 mm), then decreasing. Other concretes show a rapid decrease with depth.

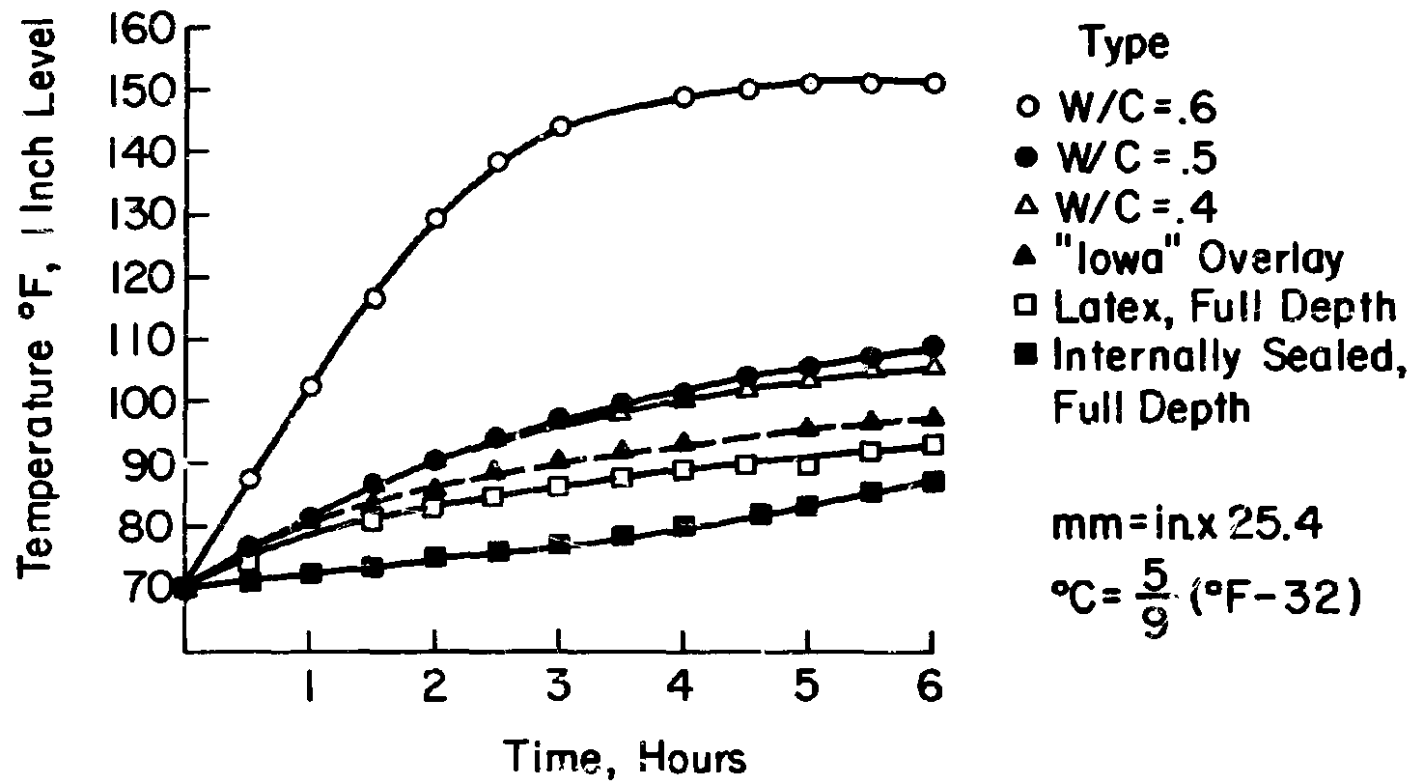
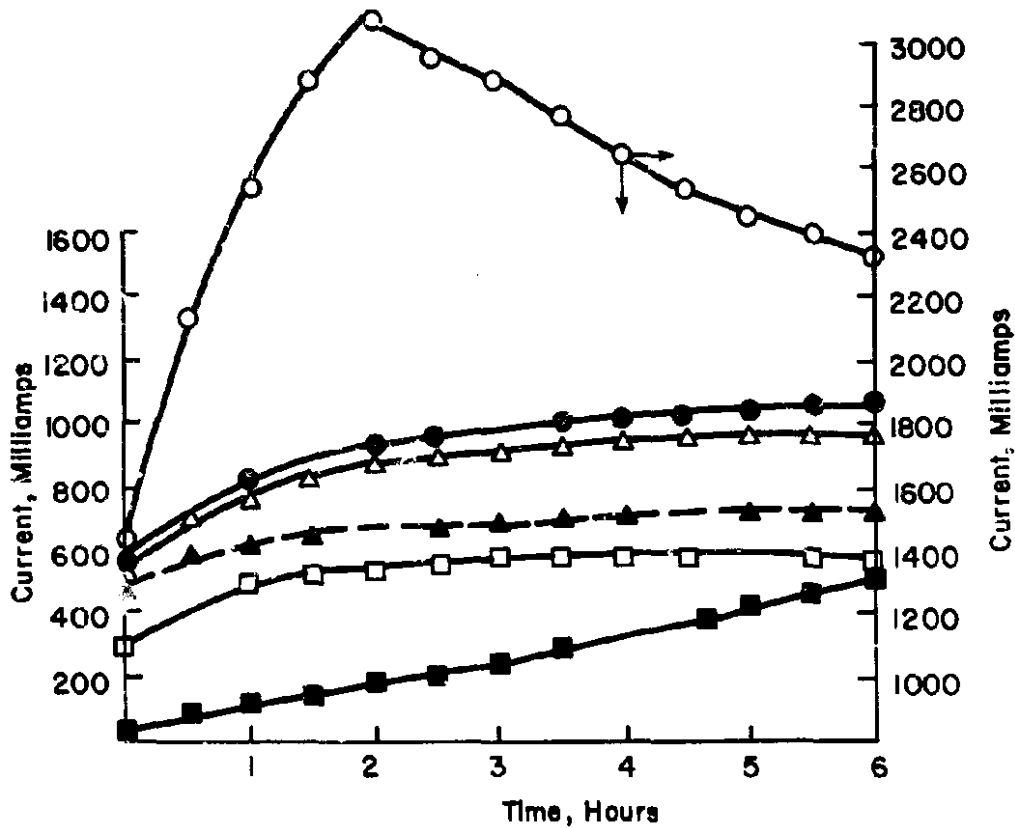


FIGURE 19. TEMPERATURE RISE IN SLABS AT 80.0 VDC FOR VARIOUS MATERIALS.



● W/C = .5 △ W/C = .4 □ Latex, Full Depth
 ○ W/C = .6 ▲ "low" Overlay ■ Internally Sealed, Full Depth

FIGURE 20. CURRENT VS. TIME FOR VARIOUS SLABS TESTED AT 80.0 Vdc.

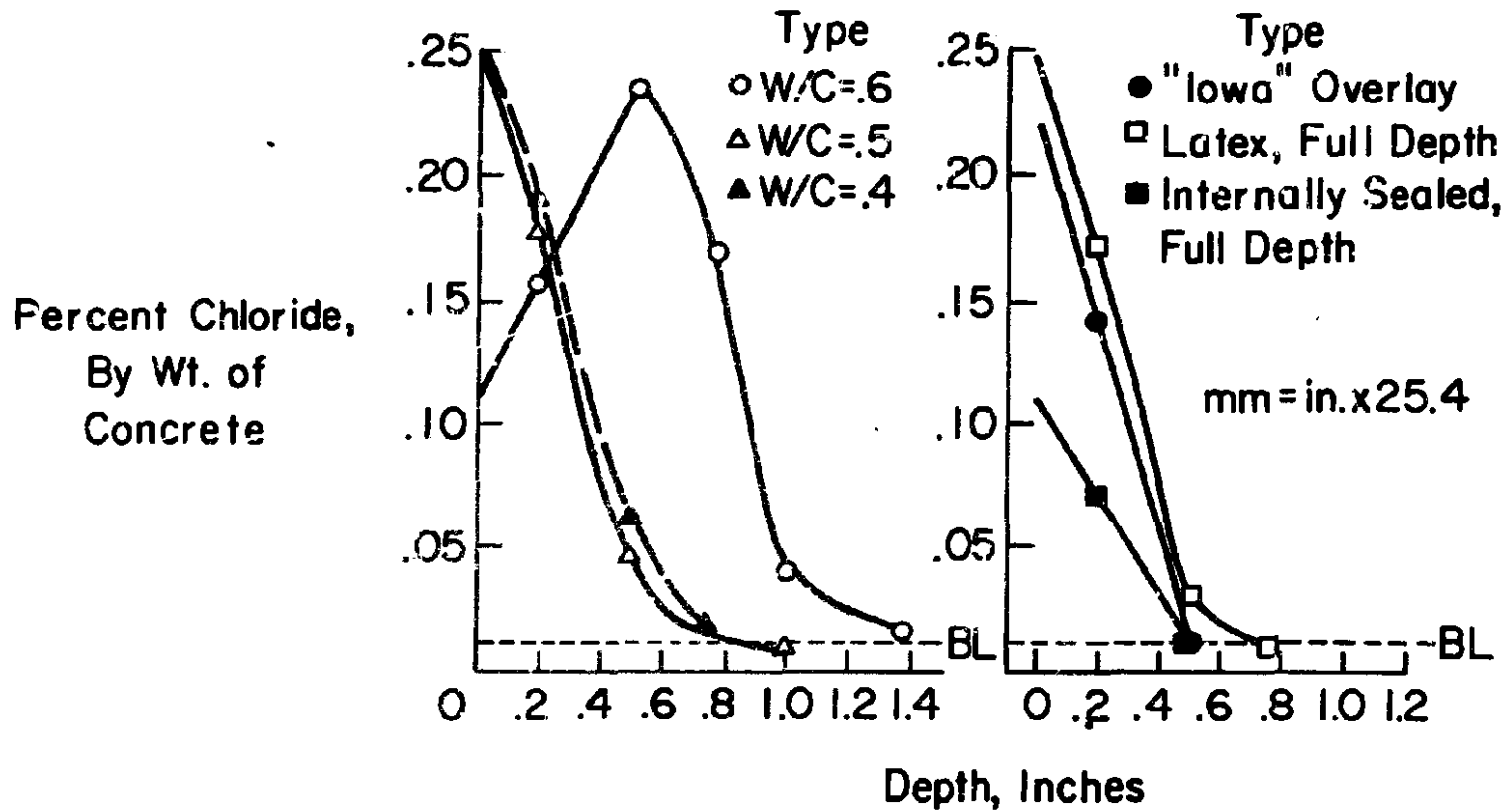


FIGURE 21. CHLORIDE PROFILES FOR SLABS TESTED FOR 6 HOURS AT 80.0 VDC.

The least permeable materials, such as internally sealed and "Iowa" concretes, show no significant amounts of chloride below the 0.5-in. (13 mm) level.

Results of total integral chloride, solution loss, and charge passed are presented in Table 7. The various concretes seem to arrange themselves into four major groups. The first, conventional concretes, exhibit relatively high total chloride levels, solution losses, and charge passed. In the next group, encompassing latex modified and Iowa concretes, values of total chloride, charge passed, and solution loss run about 20-30% lower than the "best" of the conventional concretes. It should be noted, however, that subsequent experimentation showed that concrete cover could have a

significant influence on the test results. For the "Iowa" overlay slabs the total distance from the test surface to the steel was 3.0 in. (76 mm), versus 2.0 in. for the conventional slabs. Therefore, the charge passed through the "Iowa" slab is thus artificially lowered due to the increased cover. If the "Iowa" slab had been tested at a cover of 2.0 in. (51 mm) it is likely that the charge passed would have been comparable to the conventional 0.40 w/c ratio slab. This was verified in results of core tests in the applied voltage cell (Table 14), where there was little apparent difference between 2.0 in. (51 mm) slices of "Iowa" and 0.40 w/c ratio concretes. It is likely that these "Iowa" concretes were not completely consolidated, which would tend to increase

TABLE 7
PERMEABILITY CHARACTERIZATION PARAMETERS

Description	Total Chloride		Chloride Solution Loss - %		Charged Passed - Coulombs		Chloride Permeability
	Moist	As-Rec'd	Moist	As-Rec'd	Moist	As-Rec'd	
w/c = 0.60	0.81	0.77	0.65	0.53	56,010	52,570	High
w/c = 0.50	0.39	0.47	0.33	0.38	20,230	22,500	High
w/c = 0.40	0.40	0.37	0.27	0.34	18,680	20,410	High
Latex-Overlay	0.34	0.37	0.18	0.38	13,820	16,950	Moderate
Latex-Full Depth	0.31	0.27	0.20	0.18	11,330	6,670	Moderate
Iowa-Overlay	0.26	0.31	0.22	0.27	14,260	15,270	Moderate ^{3/}
Int. Seal-Full Depth-Heated	0.10	--	0.10	--	5,770	--	Low
Int. Seal-Full Depth-Unheated	--	0.93	--	0.53	--	36,070	High
Int. Seal-Overlay-Heated	0.09	--	0.03	--	3,020	--	Low
Int. Seal-Overlay-Unheated	--	0.47	--	0.28	--	22,418	High
Polymer Impregnated ^{1/}	0	--	0	--	220	--	Very Low
Polymer Impregnated ^{2/}	--	--	--	--	--	0	Very Low
Polymer Concrete Overlay	--	--	--	--	--	0	Very Low

Moist = stored 3 months in moist room
 As-Rec'd = stored at 0°F (-18°C) immediately after receipt
 1/ "Time-to-Corrosion" slab-previously salted by FHWA
 2/ Slabs prepared at Brookhaven National Laboratories for this project
 3/ Cover over steel has a significant effect on test result. See above discussion.

their permeability. The third group, internally sealed concretes, show a dramatic drop in all parameters. Note that when internally sealed concrete is not heat treated, its permeability is of the same order as conventional concretes. The final group, polymer impregnated concrete, shows negligible permeability to chlorides.

4.4.2 Correlations with FHWA 90-Day Ponding Data

Correlation analyses were performed between the as-received data sets and 90-day ponding results obtained by FHWA on companion slabs. The parameters compared are given in Table 35 (Appendix 3), along with summary statistics. The raw data used for the analyses are given in Table 36. The parameter of "Total Integral Chloride" is in arbitrary units, being expressed as the integral of chloride concentration vs. unit depth increments rather than actual depth in inches (mm). This approach was chosen

because sufficient results were not available on the lateral distribution of chloride within the test slabs for the applied voltage test; thus an integration using the actual depth values would only indicate how much chloride was contained in the particular drill hole sampled, not in the slab as a whole. Linear regression plots are shown in Figures 73 through 80.

Examination of the data indicates that the closest relationship is between the charge passed (coulombs) in the rapid test and the total integral chloride in the 90-day test (see Figure 74). A correlation coefficient of 0.92 was calculated. While the relationship is highly significant, the quantitative error estimate (percent standard error) is relatively high, about ±31 percent. Applying the 95 percent confidence limits to charge levels representative of high, moderate, low, and very low permeabilities, the data in Table 8 are developed. For a test result of 30,000 coulombs passed, one would be 95 percent confident

TABLE 8A

EXPECTED ERROR IN ESTIMATION OF 90-DAY PONDING RESULTS FROM CHARGE PASSED DATA IN APPLIED VOLTAGE TEST

X Charge (coulombs x 10 ⁻³)	Permeability Designation	Y		+ Total Integral Cl ⁻	- Total Integral Cl ⁻
		Calculated 90-Day Total Integral Chloride	1/ 95% C.L.		
30	High	1.06	0.19	1.27	0.89
15	Moderate	0.65	0.15	0.80	0.50
5	Low	0.37	0.19	0.56	0.18
0	Very Low	0.24	0.22	0.46	0.02

$Y = 2.96 \times 10^{-2} X + 0.226$

TABLE 8B

COMPARISON DATA - 90-DAY PONDING

Type of Concrete	Total Integral Chloride - 90-Day Ponding
Conventional	1.0-1.5
Iowa, Latex	0.4-0.6
Internally Sealed, PIC	0.1-0.4
PC	0.1

that the 90-day total integral chloride would be between 0.9 and 1.3 units. Reference to comparison data indicates this is indeed within the range of conventional concrete. For a test result of 15,000 coulombs, which we have selected as representing "moderately" permeable concrete, one would be 95 percent confident that the 90-day total integral chloride would lie between 0.5 and 0.8 units. This is close to the range expected for Iowa and latex concretes. For low values of charge passed (5,000 coulombs), the confidence limits span the 0.18-0.56 range. This encompasses (but exceeds somewhat on the high side) high quality internally sealed and polymer impregnated concretes. For very low values of charge passed (such as for the polymer concretes), however, the upper confidence limit is rather high (0.46 units). This can be attributed to the fan-shaped nature of the confidence band at the extremities, where estimates based on the regression line are not advisable.

4.4.3 Air-Dried Slabs

One problem anticipated in the application of the proposed procedure to actual field testing is that of variable concrete moisture content. As the method requires an electrolytic path between the reinforcement and the concrete surface, moisture content will influence the electrical resistance of this path which in turn will influence the amount of current and chloride flow into the concrete. In order to develop some information on the extent of this effect, a few slabs were dried in air at 130°F (54°C) so that moisture contents were reduced to 40-60 percent of the initial (as-rec'd) levels in the conventional concretes. Published results (51) show that the top 2 in. (51 mm) of bridge

deck slabs may reach these moisture levels during dry summer seasons.

Results of tests conducted on the air-dried slabs are given in Table 9. It is quite apparent that there are significant differences between tests on slabs in the moist and air-dried conditions. In most, though not all, cases the parameters of total integral chloride, solution loss, and charge passed are significantly reduced in the air-dried series. Analysis of the data with respect to moisture content and each of these parameters indicates that the relationship is unique for each "material" (see Figure 22). Therefore, since one does not know prior to test what "material" is being tested (i.e., what the w/c is or what the extent of heating has been), an analytical correction for moisture content cannot be applied. The only approach left is to bring the test area back close to saturation moisture content prior to actual testing.

4.5 Re-Saturation Studies

4.5.1 Apparatus

A sketch of an apparatus designed to affect such a re-saturation of a concrete slab is shown in Figure 23. The chamber is constructed of 1/4-in. (6 mm) thick aluminum plate, with an inner liner of 1/8-in. (3 mm) acrylic. Internal dimensions are 10-3/4 x 10-3/4 in. (273x273 mm). The chamber is bonded to the concrete slab with silicone caulking (Dow Corning RTV-632). The lid of the chamber is also bonded to the side walls with the same sealant. Brass tubes threaded and sealed to the chamber lid are used as inlet and outlet ports. A terminal post threaded through the chamber wall can be used for an electrical connection to a resistance meter (Nilsson Model 400). Thus, the extent of re-saturation can be estimated by

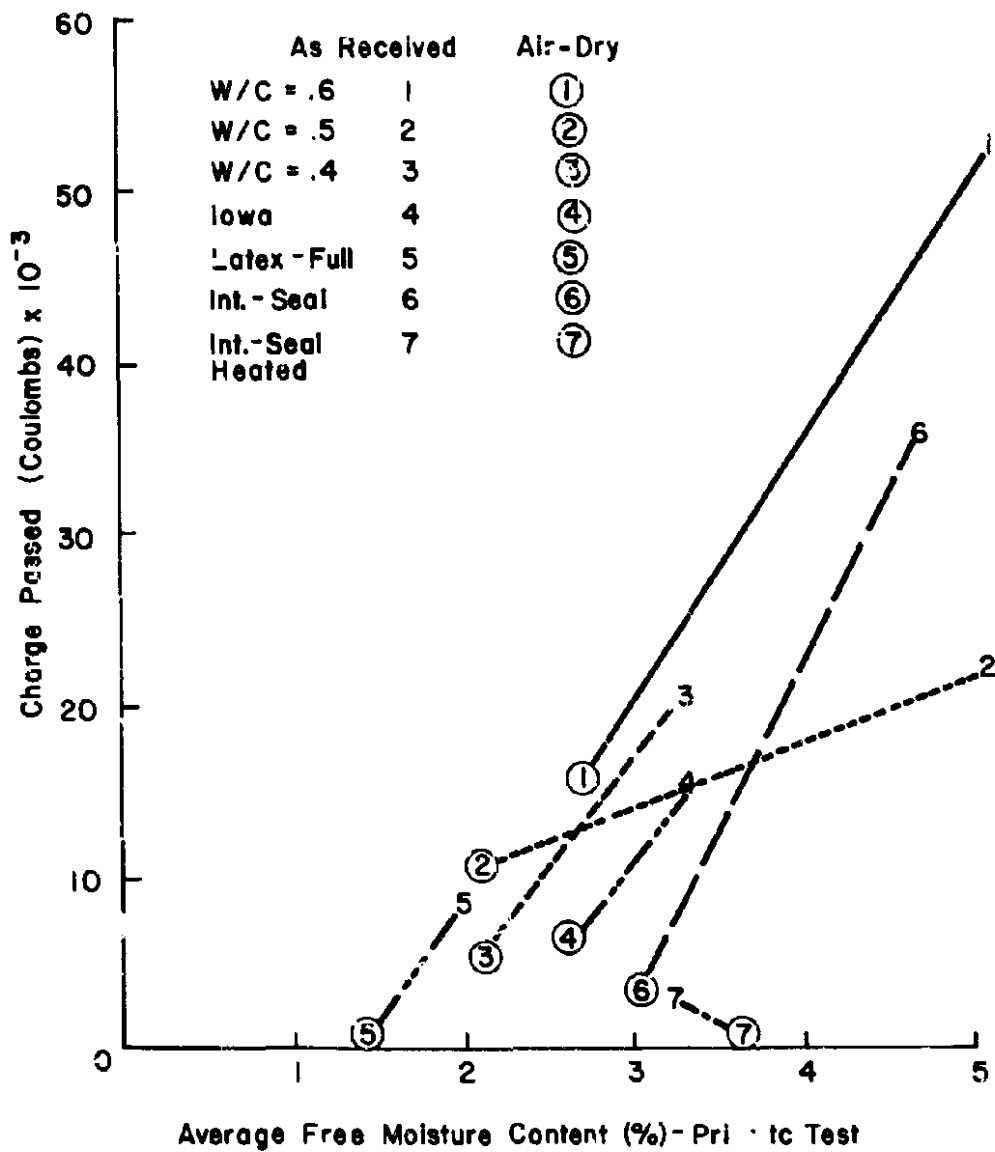


FIGURE 22. CHARGE PASSED VS. AVERAGE FREE MOISTURE CONTENT OF AS-RECEIVED AND AIR-DRIED SLABS.

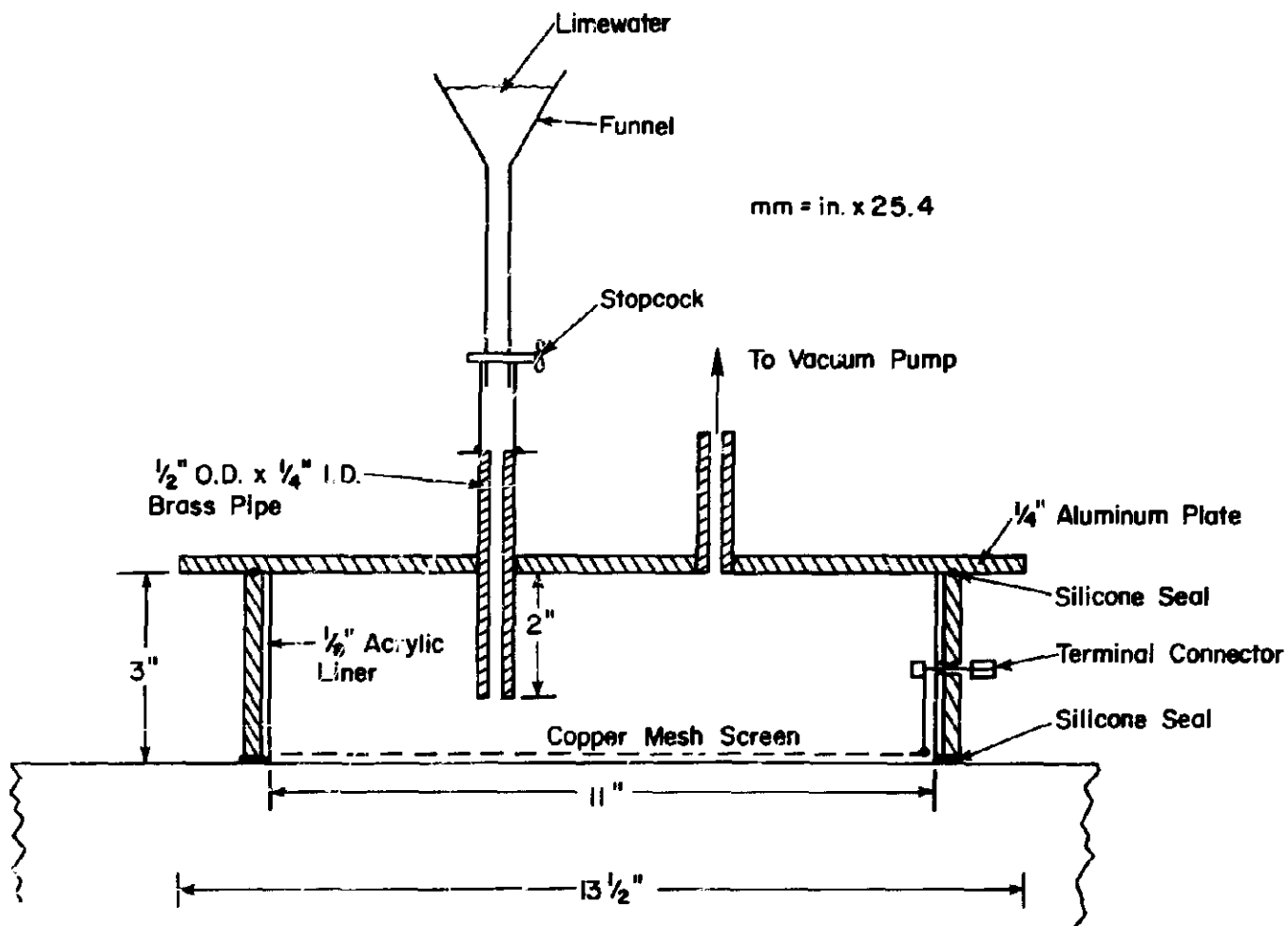


FIGURE 23. VACUUM CHAMBER USED FOR RE-SATURATION STUDIES.

TABLE 9
COMPARISON DATA
As-Received (AR) vs. Air-Dry (AD)

Type	Free Moisture*			Total Integral Cl			Solution Loss (% Chloride)			Charge Passed (coulombs)		
	AR	AD	% of Initial	AR	AD	%	AR	AD	%	AR	AD	%
w/c = 0.60	5.1	2.7	53	0.77	0.85	+10	0.53	0.36	-32	52,570	15,790	-70
w/c = 0.50	5.1	2.1	41	0.47	0.39	-17	0.38	0.23	-39	22,500	10,370	-54
w/c = 0.40	3.3	2.1	64	0.37	0.30	-19	0.34	0.14	-59	20,410	5,420	-73
Iowa	3.3	2.6	79	0.31	0.34	+10	0.27	0.15	-44	15,270	6,060	-60
Latex-Full Depth	2.0	1.4	70	0.27	0.02	-93	0.18	0.02	-89	7,670	610	-93
Int. Seal-Overlay -Unheated	4.7	3.0	64	0.47	0.23	-51	0.28	0.10	-64	22,410	3,610	-84
Int. Seal-Overlay-Heated	3.2	3.6	--	0.09	0.09	0	0.03	0	-100	3,020	400	-87

*Powdered samples dried 72 hours at 221°F (105°C)

monitoring the decrease in resistance of the concrete between the copper mesh and the steel reinforcing mat.

4.5.2 Preliminary Re-Saturation Tests

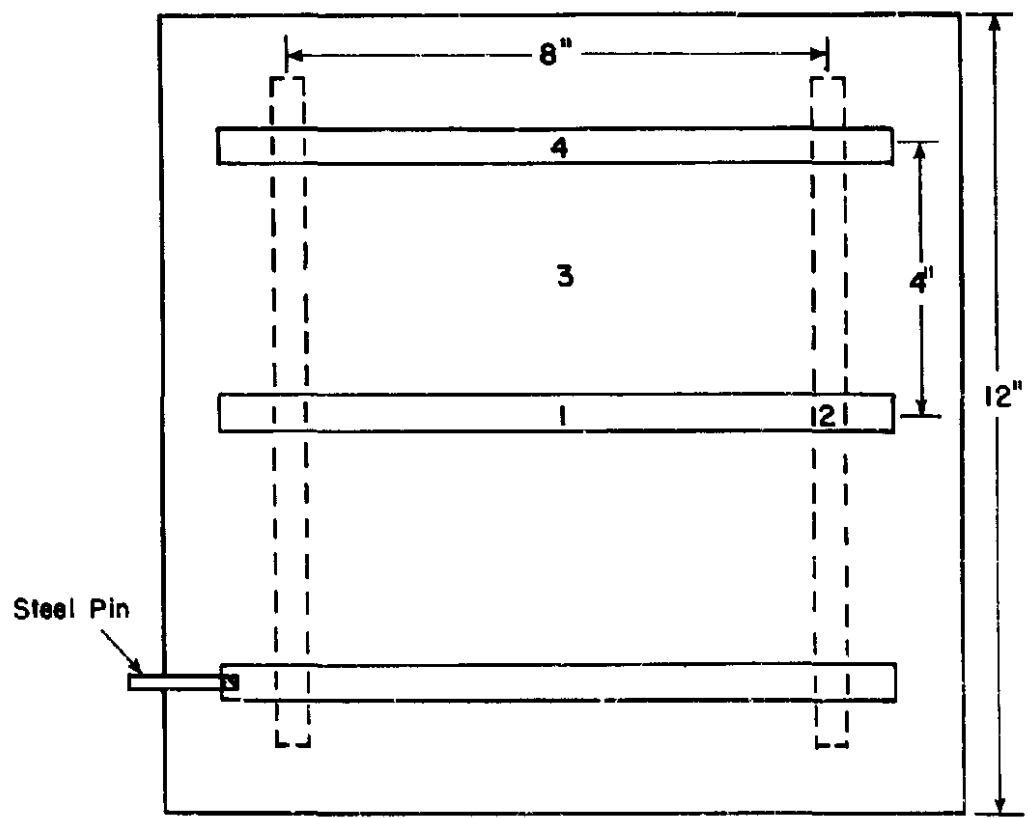
A number of reinforced concrete slabs were produced from batches similar to those used in earlier studies (Table 4). One slab from each of the batches was tested in the moist condition at 14 days. The remaining slabs were placed in a forced-air drying room at 130°F (54°C) for 1 week, at which time they had reached 60-70 percent of their initial moisture content. They were then placed in thick plastic bags until ready to test.

Results on moist slabs tested at 14 days are shown in Tables 10 and 11. For these slabs it was felt desirable to take chloride drill samples at a number of locations (see Figure 24), as all previous work had been done on samples taken directly above the centrally located bar. Although the results are

somewhat scattered, little consistent difference between sampling locations can be discerned. This indicated that the lines of current flow, and hence of chloride migration, are relatively uniform even in areas between the steel rebars.

An initial test of the re-saturation apparatus was performed on a slab which had been exposed to 50% RH and 73°F (23°C) for about 14 months. Water-cement ratio was 0.6, and initial cure period was 28 days. The initial resistance (at 28 days) between the surface and rebar mat was 65 ohms. Humidity wells had previously been cast into this slab at depths of 0.5 in., 1.0 in., and 2.0 in. A miniature hygrometer probe developed by Monfore (52) was used to measure internal relative humidities.

A vacuum of -25.5 in. Hg (14.9 kPa) was pulled on the slab for 60 min. With the pump still running, 1500 ml of saturated limewater were let into the chamber. Saturated limewater was used so



mm = in. x 25.4

FIGURE 24. SAMPLING LOCATIONS.

TABLE 10
CHLORIDE ANALYSES
w/c = 0.60
Moist - 14 Days

Location (See Fig. 24)	<u>% Cl⁻ by Weight of Concrete</u>					<u>Integral</u>	
	<u>Depth</u>					<u>Arithmetic Mean</u>	<u>Arbitrary Units</u>
	1	2	3	4	5		
1	0.133	0.086	0.042	0.093	0.061	0.083	0.652
2	0.126	0.109	0.077	0.040	0.024	0.075	0.528
3	0.087	0.084	0.077	0.093	0.045	0.077	0.548
4	0.099	0.087	0.084	0.077	0.052	0.080	0.589
Mean	0.111	0.092	0.070	0.076	0.046	0.079	0.579
Blank	-	0.008	-	-	-	-	-

<u>Sample</u>	<u>Depth₁ (in.)</u>
1	0-3/8
2	3/8-5/8
3	5/8-7/8
4	7/8-9/8
5	9/8-13/8

1/ mm = in. X 25.4

TABLE 11
CHLORIDE ANALYSES
w/c = 0.32
Moist - 14 days

Location (see Fig. 24)	<u>% Cl⁻ by Weight of Concrete</u>					<u>Integral</u>	
	<u>Depth</u>					<u>Arithmetic Mean</u>	<u>Arbitrary Units</u>
	1	2	3	4	5		
1	0.175	0.042	0.018	0.020	0.009	0.053	0.383
2	0.215	0.088	-	-	-	-	-
3	0.235	0.065	0.019	0.015	0.007	0.068	0.496
4	0.197	0.048	0.021	0.007	0.007	0.056	0.424
Mean	0.206	0.061	0.019	0.014	0.008	0.059	0.436
Blank	-	0.009	-	-	-	-	-

<u>Sample</u>	<u>Depth₁ (in.)</u>
1	0-3/8
2	3/8-5/8
3	5/8-7/8
4	7/8-9/8
5	9/8-13/8

1/ mm = in. X 25.4

that the electrical resistance of the slab could be monitored using a copper screen immersed in the solution. Pumping was continued for 60 min. Air was

let into the chamber, and RH and resistance monitored vs. time. RH profiles at various times are shown in Figure 25, resistance vs. time in Figure

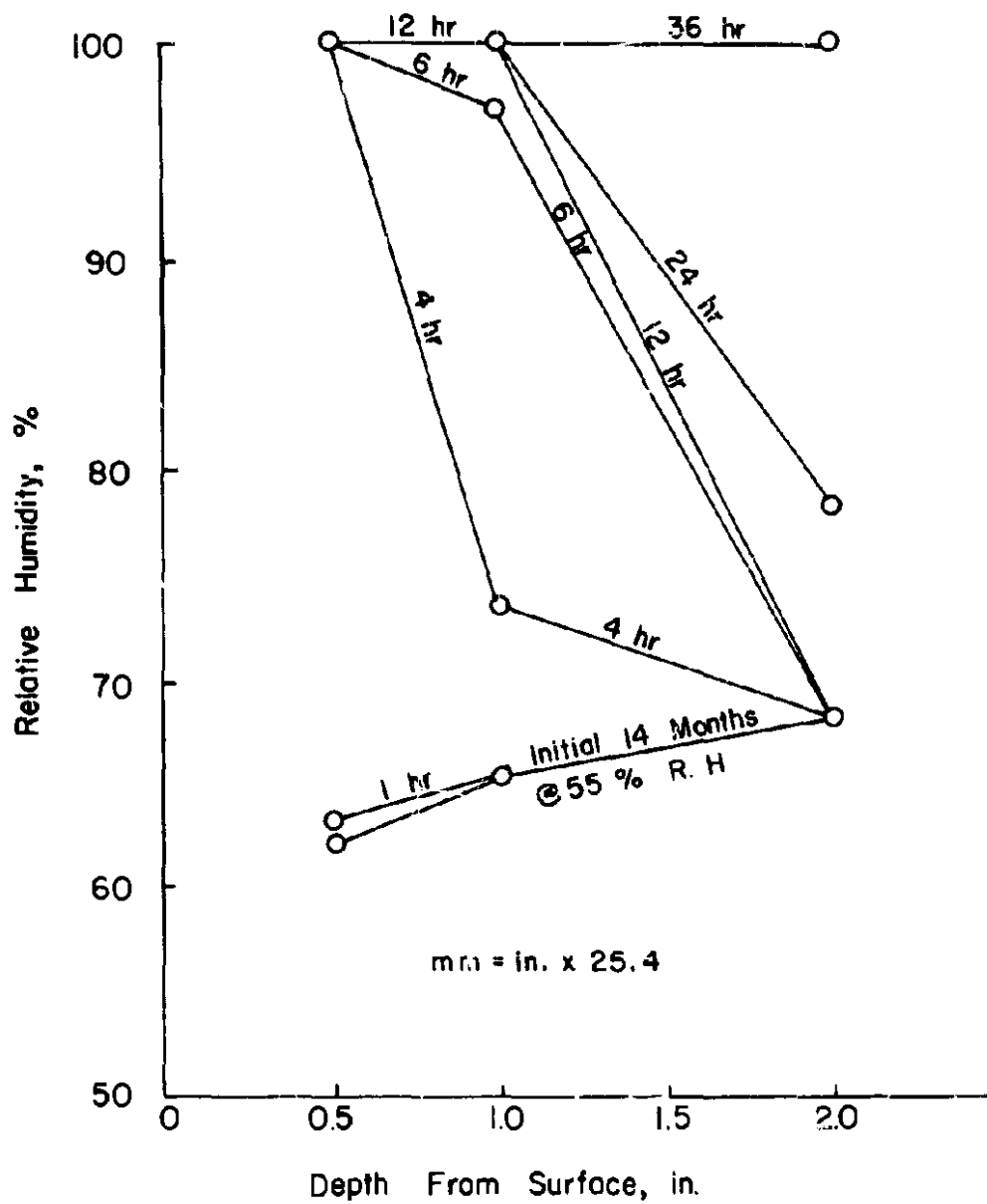


FIGURE 25. RELATIVE HUMIDITY PROFILES DURING 36 HOUR PONDING PERIOD.

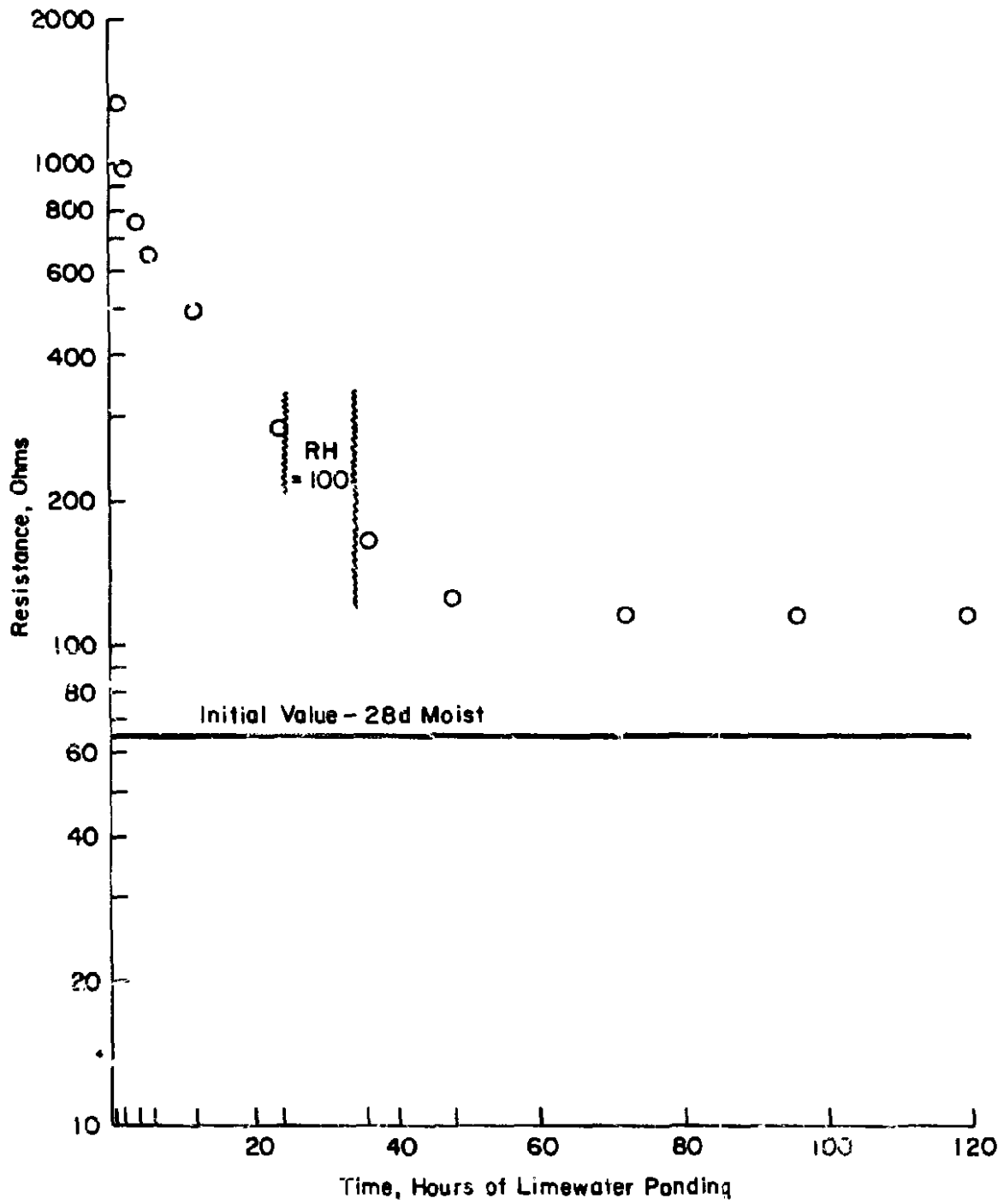


FIGURE 26. RESISTANCE VS. TIME DURING LIMEWATER PONDING ON SLAB SURFACE.

26. It is seen that constant relative humidity of 100% is achieved down to 2 in. (51 mm) somewhere between 24 hr and 36 hr. Resistance, however, continues to slowly decrease beyond 36 hr, leveling off at 115 ohms at 72 hr. This is still 50 ohms higher than the value initially measured after 28-days of moist cure.

Testing then proceeded to the set of slabs dried 1 week at 130°F (54°C). The first slab was subjected to limewater ponding only. Results were similar to the previously tested slab, that is, resistance did not return to the initial value even after 4 days of ponding. Measured free water contents on drill samples, however, indicated that the moisture content had returned to that of the 14 day moist-cured slab, except perhaps at the lowest depth. A second slab was then subjected to the vacuum-saturation procedure, using limewater. In this case, resistance dropped more rapidly, but still remained above 100 ohms after 3 days of ponding. In order to facilitate the ingress of water and decrease the resistance more rapidly, a third slab from this set was subjected to the same vacuum saturation technique, this time using limewater heated to 140°F (60°C).

After vacuum pumping was discontinued, the chamber lid was removed and a heating coil placed into the solution. A commercial thermoregulator was used to maintain the temperature at $140 \pm 1^\circ\text{F}$ ($60 \pm 0.5^\circ\text{C}$) for 24 hrs. Some problems with the stirrer led to termination of the test and the slab was allowed to cool back to room temperature 73°F (23°C). Although resistance had decreased to 75 ohm at 140°F (60°C), it increased back to 110 ohm after cooling to 73°F (23°C). Thus, part of the resistance decrease is due to heating of the solution, and

indicates that the chloride test should be run without allowing the slab to cool back to room temperature. A second slab was treated in a similar manner, in this case resistance at 140°F (60°C) had dropped to 58 ohm after 24 hours of heating. A comparison of the various re-saturation schemes indicates that vacuum re-saturation for 24 hr using limewater maintained at 140°F (60°C) yields the most rapid reduction of resistance in the shortest time period.

After the 24 hour heating period had elapsed, the limewater was removed from the dike and a 3.0% NaCl solution applied. The slab was then subjected to 80.0 Vdc for 6 hours. Results of Cl⁻ solution loss, charge passed, and total chloride for three slabs are shown in Table 12. These are:

1. Initial test on 14-day moist-cured slab.
2. Test on dried slab re-saturated with 73°F (23°C) limewater for 4 days.
3. Test on dried slab re-saturated with 140°F (60°C) limewater for 24 hours.

Chloride profiles (average of drill holes #1 and #2 - see Figure 24 for locations) are shown in Figure 27. Although there are differences between the three treatments, the parameters are all sufficiently high so that all three concretes would fall into the highly permeable range, which they should at such a high water-cement ratio. The chloride profiles are all what would be expected for a permeable concrete, i.e., high levels of Cl⁻ even below 0.5-in. (13 mm) depth. To summarize, the use of vacuum saturation followed by 24 hours of ponding with limewater at 140°F (60°C) allows one to return a dry concrete to moisture levels sufficient to obtain essentially the same results as if the concrete were tested in the moist-cured condition.

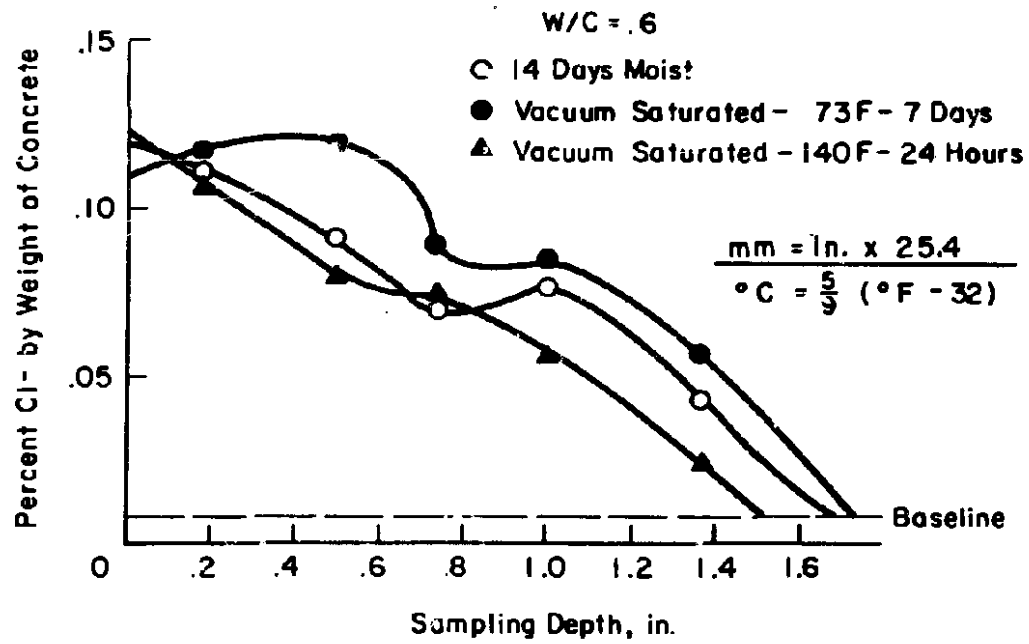


FIGURE 27. CHLORIDE PROFILES FOR VARIOUS RE-SATURATION SCHEMES.

TABLE 12
PERMEABILITY PARAMETERS
VARIOUS TREATMENTS

Slab	Charged Passed (Coulombs)	Cl ⁻ Solution Loss (%)	Total Integral Chloride (Arbitrary Units)
14 day moist	37,570	0.21	0.58
73°F limewater - 4 day	30,000	0.14	0.65
140°F limewater - 24 hr	30,950	0.31	0.45

$$^{\circ}\text{C} = 5/9(^{\circ}\text{F} - 32)$$

4.5.3 Application to FHWA Slabs

Selected FHWA slabs, previously tested in the moist condition (Set 1) were dried for 2 weeks at 130°F (54°C). The slabs were then subjected to the re-saturation procedure described in the previous section. Plots of resistance vs. time are shown in Figures 28 and 29. Resistance in the initial moist condition is shown for comparison purposes. In all cases, resistance after the 24 hr re-saturation had dropped below the original moist-cured values.

After the 24-hr heating period was over the limewater was removed from the slabs and 1,500 ml of 3.0% NaCl was poured into the chamber. A potential of 80.0 Vdc was applied for 6 hr. Plot of current vs. time are shown in Figure 30. The curves all reach a peak (or plateau) in current value between 1 and 2 hr of test, then begin to decrease. The decrease is sharpest for the most permeable (w/c = 0.6) concrete. These are to be compared with previous runs on the same slabs in the initial moist-cured condition (Fig. 20). Similar types of curves are seen for the w/c = 0.6 slab in both cases; however, for the other slabs in the moist condition a gradual increase in current is seen, rather than a decrease as seen for the re-saturated slabs. The current decreases seen in the re-saturated slabs correspond with increases in resistance between the time

at which the current peaked and the final reading of 6 hr. Although surface temperature was monitored, this did not appear to explain the increases in resistance. It is possible, however, that heat was flowing out of the concrete (initially close to 140°F at beginning of the test) and that the internal temperature was decreasing during the test period.

Typical chloride profiles for both the moist and re-saturated conditions are given for some of the slabs tested in Figures 31 through 33. The data represent the average of drill samples taken from sampling Locations 1 and 2 (see Figure 24). It is seen that the profiles are quite different in many cases. Higher chloride concentrations were detected at lower depths for the re-saturated tests. For the heated internally sealed slab, the re-saturated chloride profile is much higher. This indicates that the 140°F (60°C) limewater ponding somehow increased the permeability of the system. For internally sealed concrete, therefore, one may need to use a lower temperature during re-saturation.

Test parameters (total integral Cl⁻, solution loss, and charge passed) are given in Table 13. It is seen that for Slabs 3357, 3392, and 3372 a higher chloride content in the slab corresponds with a lower solution loss. This could

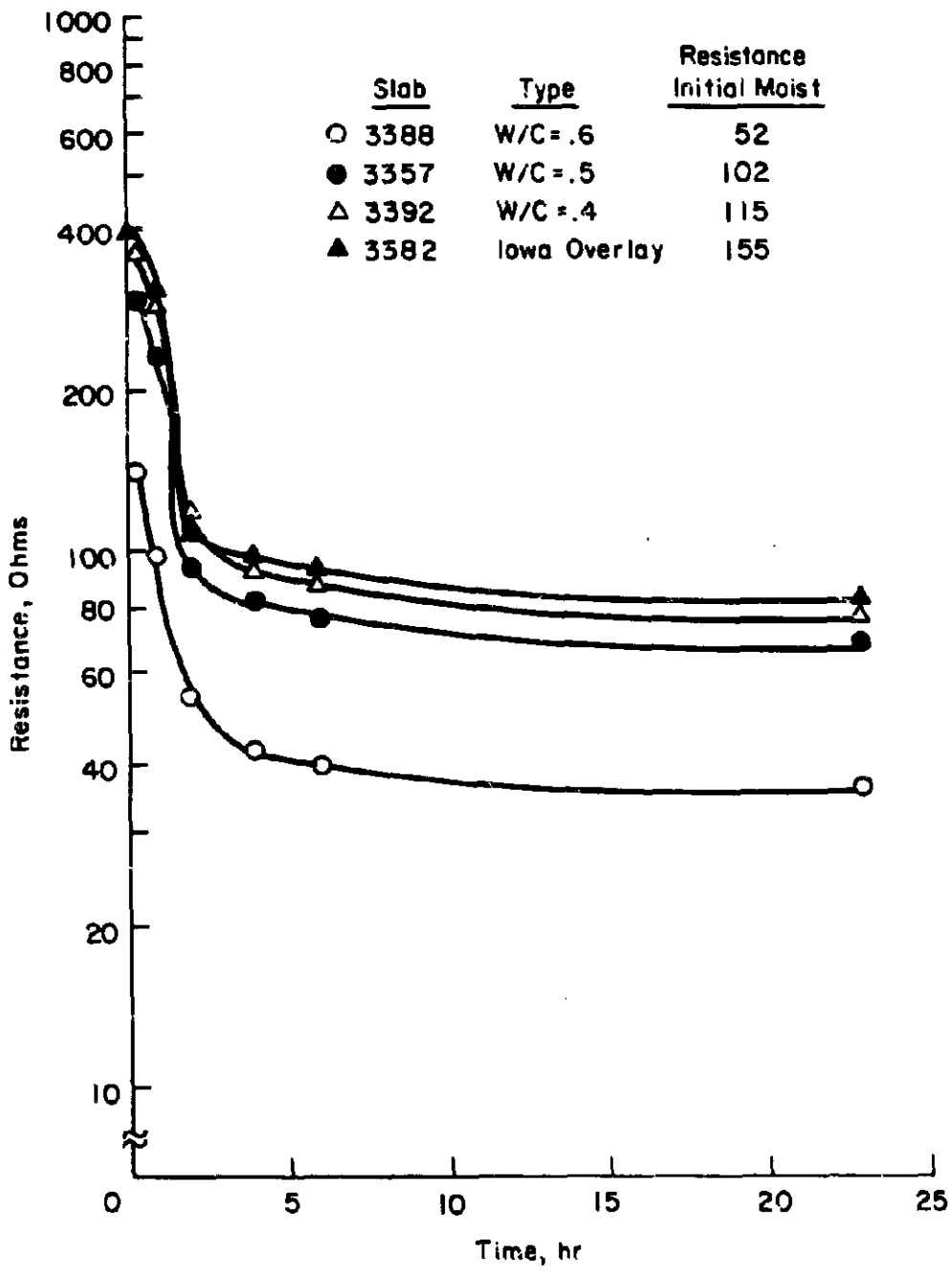


FIGURE 28. RESISTANCE VS. TIME DURING RE-SATURATION OF FHWA SLABS.

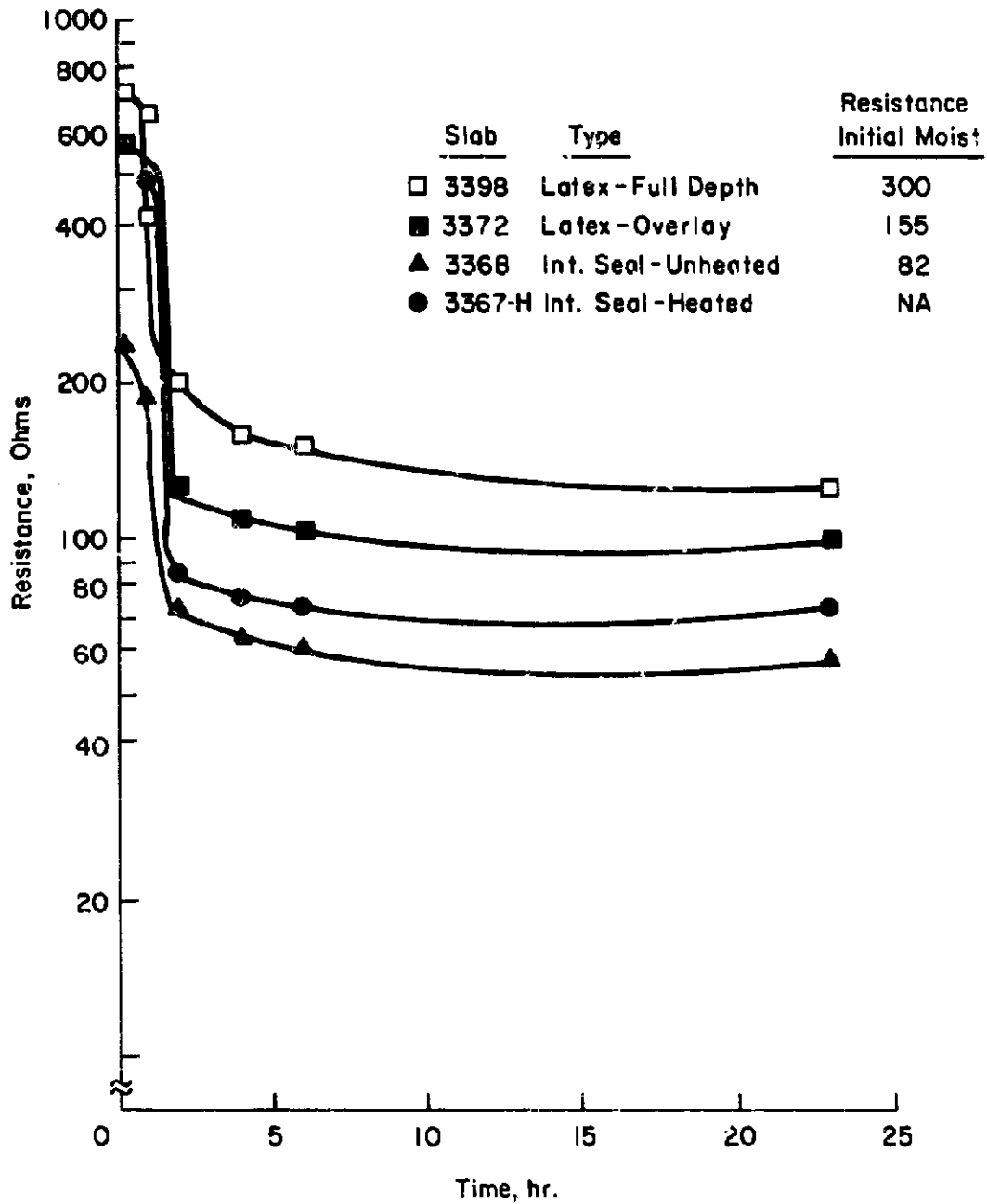


FIGURE 29. RESISTANCE VS. TIME DURING RE-SATURATION OF ADDITIONAL FHWA SLABS.

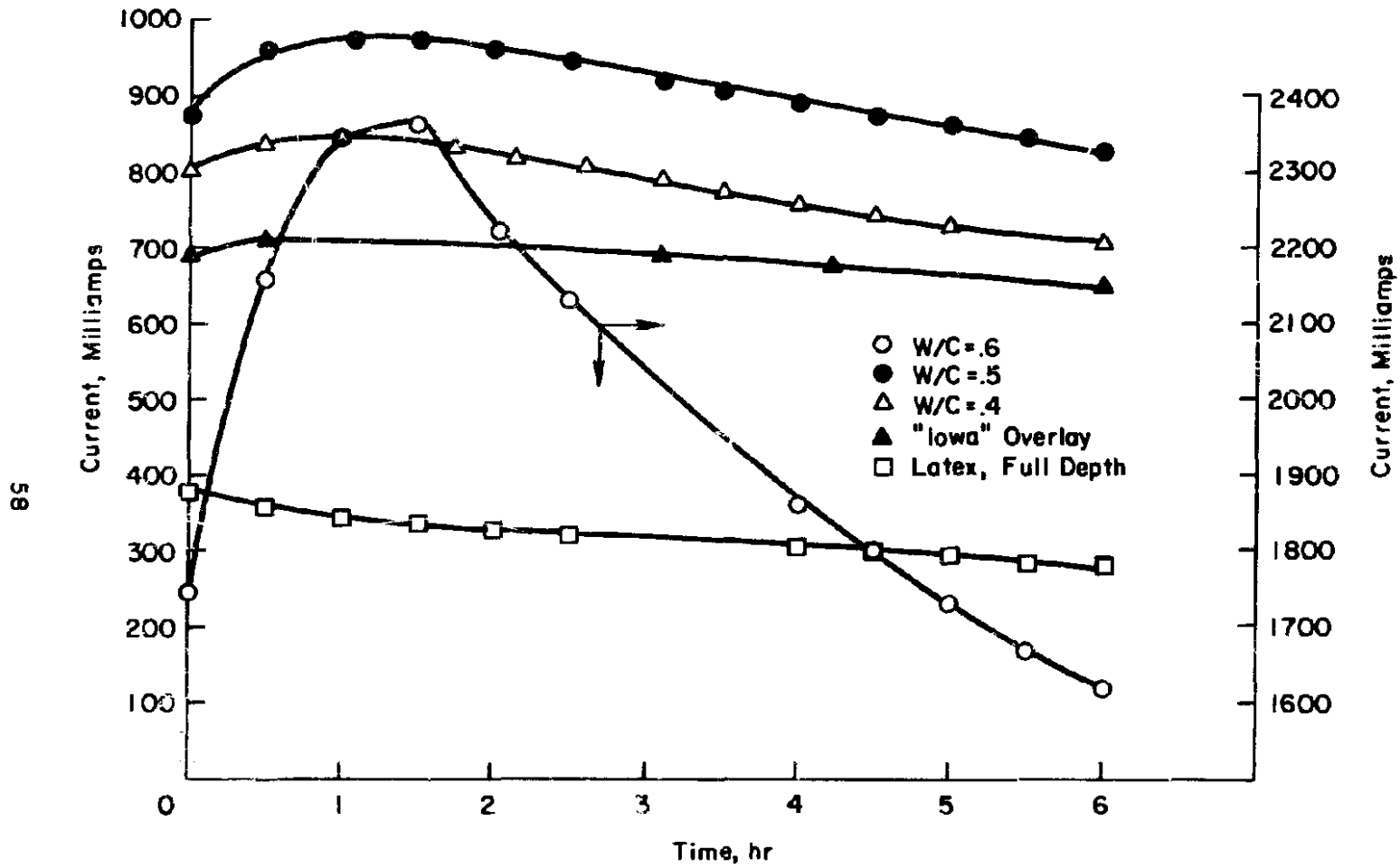


FIGURE 30. CURRENT VS. TIME FOR RE-SATURATED FHWA SLABS.

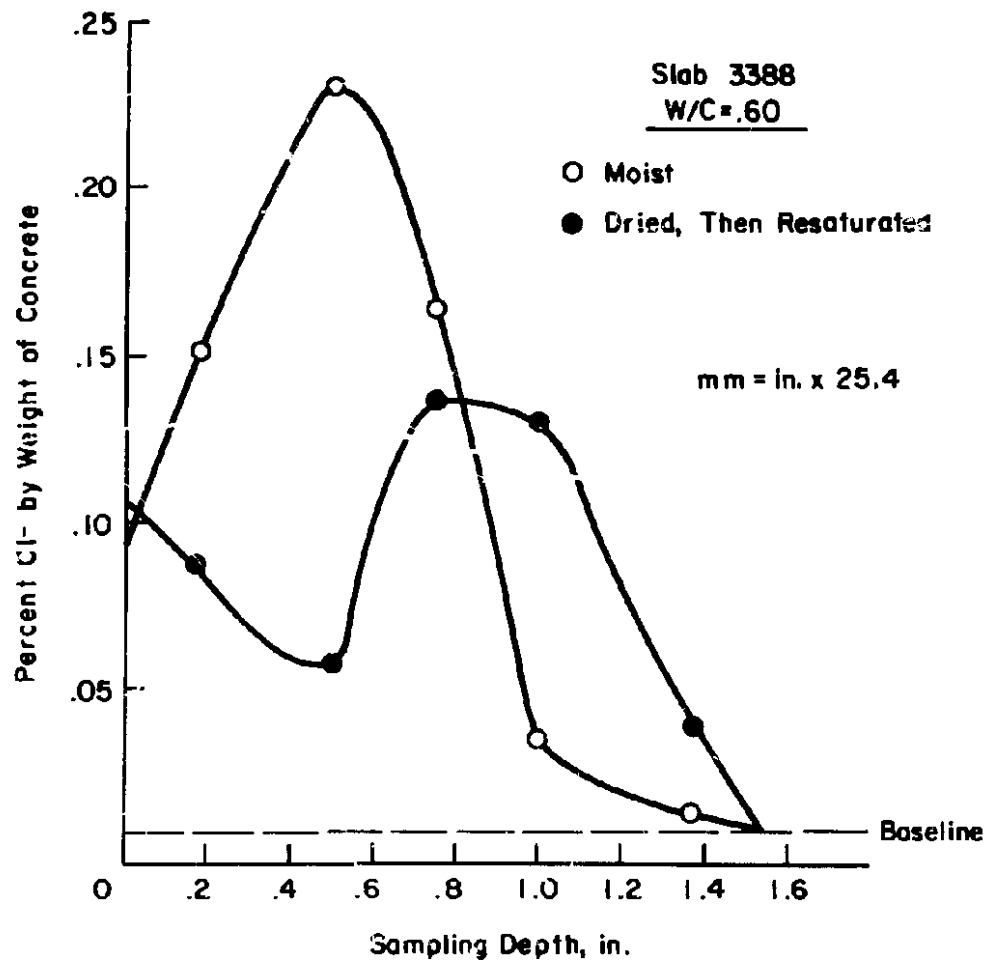


FIGURE 31. CHLORIDE PROFILES FOR .60 W/C RATIO SLAB TESTED IN MOIST AND RE-SATURATED CONDITIONS.

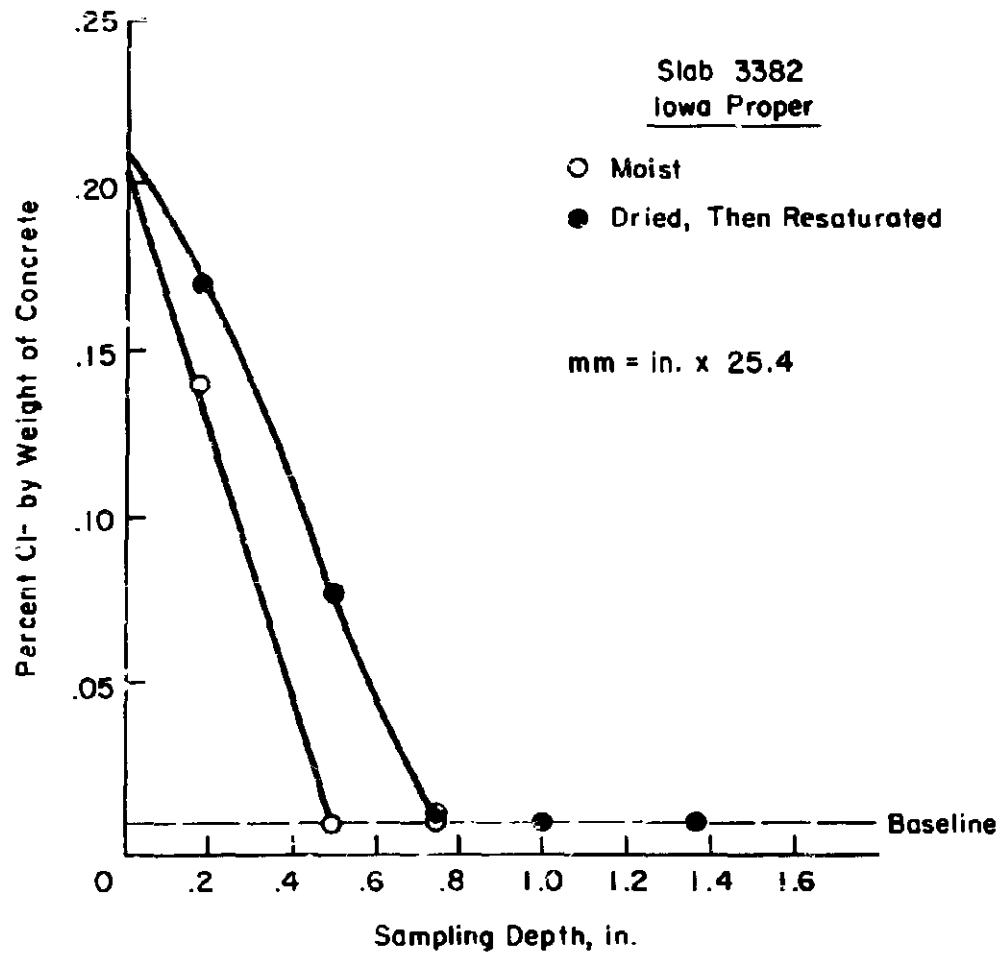


FIGURE 32. CHLORIDE PROFILES FOR PROPERLY CONSOLIDATED IOWA OVERLAY SLAB TESTED IN MOIST AND RE-SATURATED CONDITIONS.

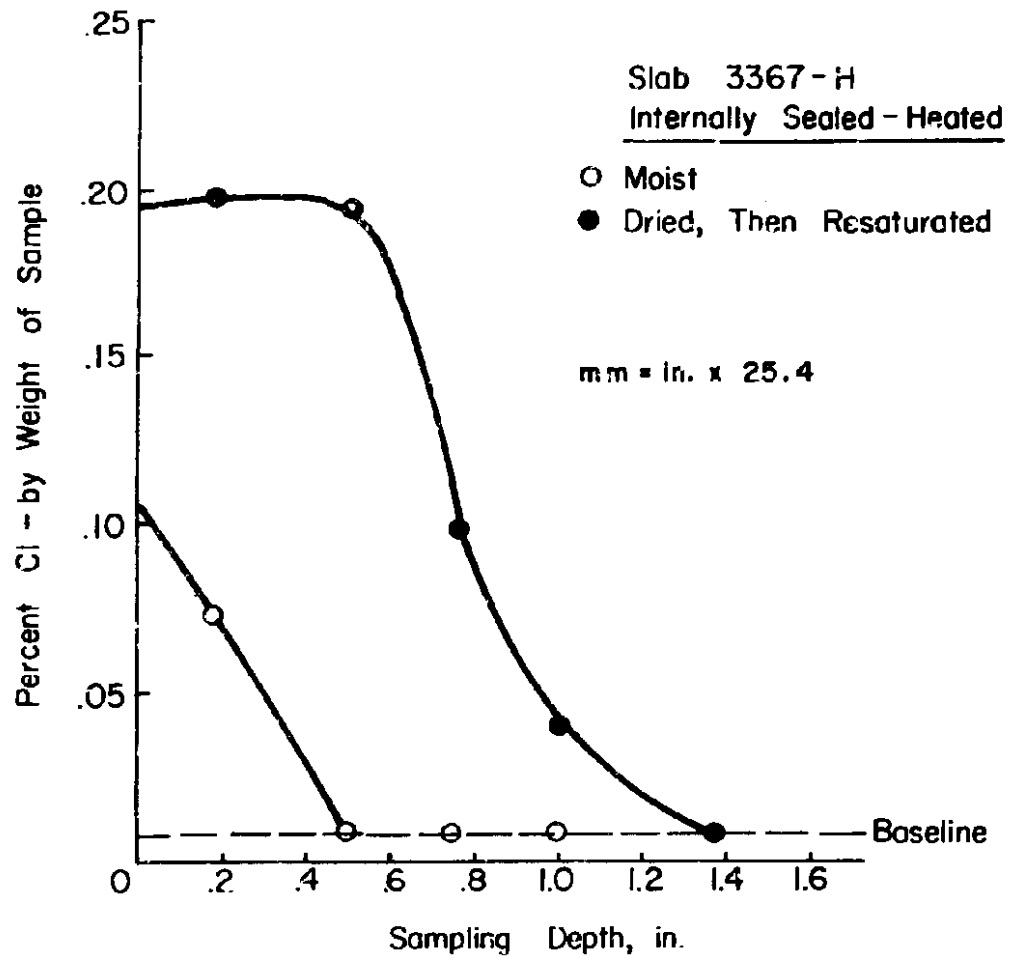


FIGURE 33. CHLORIDE PROFILES FOR HEATED FULL-DEPTH INTERNALLY SEALED CONCRETE SLAB IN MOIST AND RE-SATURATED CONDITIONS.

TABLE 13

PERMEABILITY PARAMETERS

Moist vs. Re-Saturated FHWA Slabs

Slab	Type	Total Integral Cl ⁻		Cl ⁻ Solution Loss (%)		Charge Passed (Coulombs)	
		Moist	Re-Sat'd	Moist	Re-Sat'd	Moist	Re-Sat'd
3388	w/c = 0.6	0.81	0.63	0.65	0.29	56,010	43,157
3357	w/c = 0.5	0.39	0.58	0.33	0.16	20,230	19,690
3392	w/c = 0.4	0.40	0.57	0.27	0.16	18,675	16,985
3382	Iowa	0.26	0.39	0.22	0.18	14,260	14,783
3398	Latex-Full Depth	0.31	0.17	0.20	0.07	11,330	6,989
3372	Latex-Overlay	0.34	0.52	0.18	0.13	13,820	11,851
3368	Int. Seal-Unheated	0.93	0.64	0.53	0.22	36,070	24,803
3367H	Int. Seal-Heated	0.10	0.74	0.10	0.21	5,770	18,400

occur only if there were chloride in the slab to begin with. We tested one-half of the slab in the moist state, then placed the slabs in the freezer. However, during the initial part of the drying period some chloride may have migrated to the other half of the slab. Additionally, in order to intercept the same rebar geometry as in the first set of tests, the chamber had to be placed so that the left edge spanned the central transverse bar. As the right edge of the chamber spanned the same bar in the earlier moist tests, we were in fact including an area of about 1x11 in. (25x280 mm) which had previously been exposed to chloride. During the 24-hr ponding with hot linewater, some of this chloride most likely leached out into the linewater and re-entered the slab, thus accounting for the anomalously high chloride levels in the re-saturation tests.

The charge passed comparison data (Table 13) are much more favorable, however. The amounts of charge passed are fairly comparable for both the moist and re-saturated test conditions. This

is reasonable, as chloride ions constitute only a portion of the charge carriers in the high ionic strength pore water. This relationship is shown in Figure 78 (Appendix 3). Summary statistics (Appendix 3) show a high correlation between the two data sets. Standard error is about 16 percent of the mean value. Thus, in slabs which have been previously exposed to chloride (which we expect to find in many field situations), one could use the charge passed as an indicator of chloride permeability, but actual measurement of chloride concentrations would not be advisable. This hypothesis was verified in later field testing (see page 97). For slab No. 3367H, the charge passed is anomalously high, presumably due to the increase in permeability after ponding at 140°F (60°C).

4.5 Results of Core Tests

The apparatus and test procedure described in Appendix 1 was used to test 3.75-in. (95 mm) diameter x 2-in. (51 mm) long core slices taken from FHWA slabs.

4.6.1 Specimen Preparation

For the full-depth materials, four slices were taken from each core (Figure 34A). For the overlay materials slices were taken both at the bondline (Figure 34B) including the surface layer, and at the bondline with 1/8 in. (3 mm) of the surface removed (Figure 34C). Finally, the polymer concrete overlay and latex overlay cores were also sectioned so as to include all of the overlay plus enough base course to yield a total thickness of 2 in. (51 mm) (see Figure 34D).

Briefly, the testing procedure is as follows: The slice is first allowed to air dry for a short time and the sides are coated with an epoxy formulation. After 3 hr of curing the slice is weighed, then placed in a vacuum desiccator. The chamber is evacuated for 3 hr. De-aerated water is then let into the chamber sufficient to cover the specimen, and the pump is run for an additional hour. The vacuum is then broken and the chamber brought back to atmospheric pressure. After soaking overnight, the specimen is ready for testing the following day.

Prior to test the specimen is surface-dried and weighed. A very rapid-setting silastic rubber is used to form an in-place gasket between the specimen and the liquid reservoirs. After allowing the rubber to cure for 10 min, the reservoir connected to the negative lead is filled with 3.0% NaCl, and the reservoir connected to the positive lead is filled with 0.3N NaOH. This is done to achieve approximately equal conductances, approximately $5 \times 10^{-2} \text{ mho}\cdot\text{cm}^{-1}$ ($5 \text{ S}\cdot\text{cm}^{-1}$), on both sides of the specimen. The specimen is then subjected to 50.0 Vdc for 6 hr.

4.6.2 Current vs. Time

Plots of current vs. time for 2-in. (51 mm), 1-in. (25 mm), and 0.5-in.

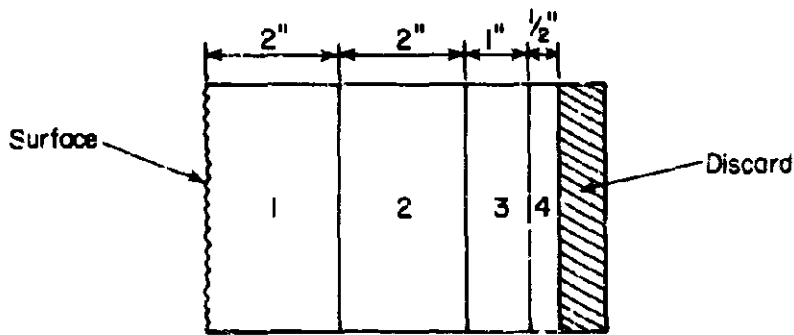
(13 mm) slices are shown in Figures 35 through 37. It should be noted that, as slice thickness decreases, the number of materials which can be tested also decreases, as high permeability samples exhibit excessive heating during the test. The plots in Figure 35 are for 2-in. (51 mm) slices taken off the top surface of the core (see Figure 34A, Section 1). Results for 2-in. (51 mm) slices taken from the core interior (Section 2) were similar for conventional concretes, but differed somewhat for modified concretes. This will be discussed later.

4.6.3 Temperature and Resistance

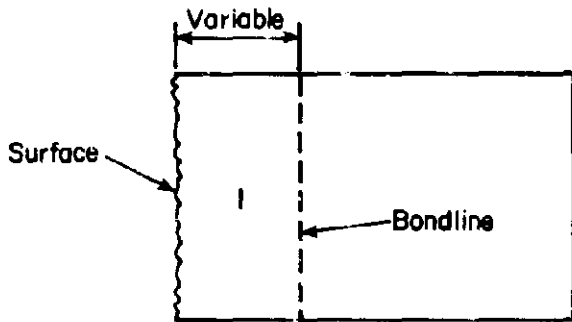
The high current flow in the more permeable specimens leads to a rapid temperature rise (see Figure 38). Even at 1-in. (25 mm) thickness, the test on the specimen with $w/c = 0.60$ had to be terminated before the 6-hr test period had elapsed in order to prevent damage to the cell. In most runs the current increase during the test period was proportional to a decrease in resistance. One of the test slices ($w/c = 0.40$, 0.5 in. (13 mm)) was left in the cell after the 6-hr period and allowed to cool. Figure 39 indicates that although most of the drop in resistance is due to the temperature increase, the hysteresis indicates that the resistivity of the specimen had been irreversibly lowered, most likely by the increase in chloride ion concentration during the test period.

4.6.4 Correlations with FHWA 90-Day Ponding Data

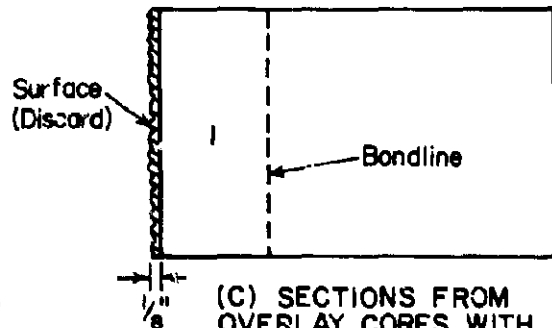
In order to obtain more quantitative results, various parameters were used to afford a measure of impermeability. These are:



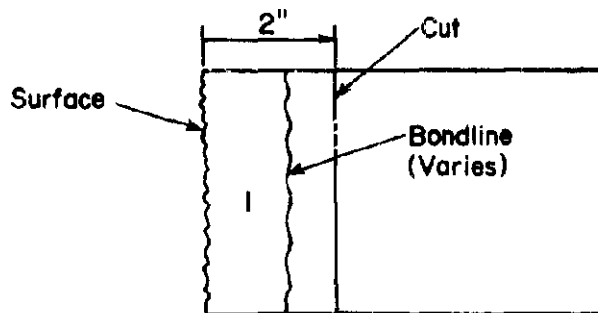
(A) SECTIONS FROM FULL-DEPTH CORES.



(B) SECTIONS FROM OVERLAY CORES.



(C) SECTIONS FROM OVERLAY CORES WITH SURFACE REMOVED.



(D) SECTIONS FROM OVERLAY CORES INCLUDING BASE COURSE.

mm = in. x 25.4

FIGURE 34. SECTIONING OF CORE SPECIMENS.

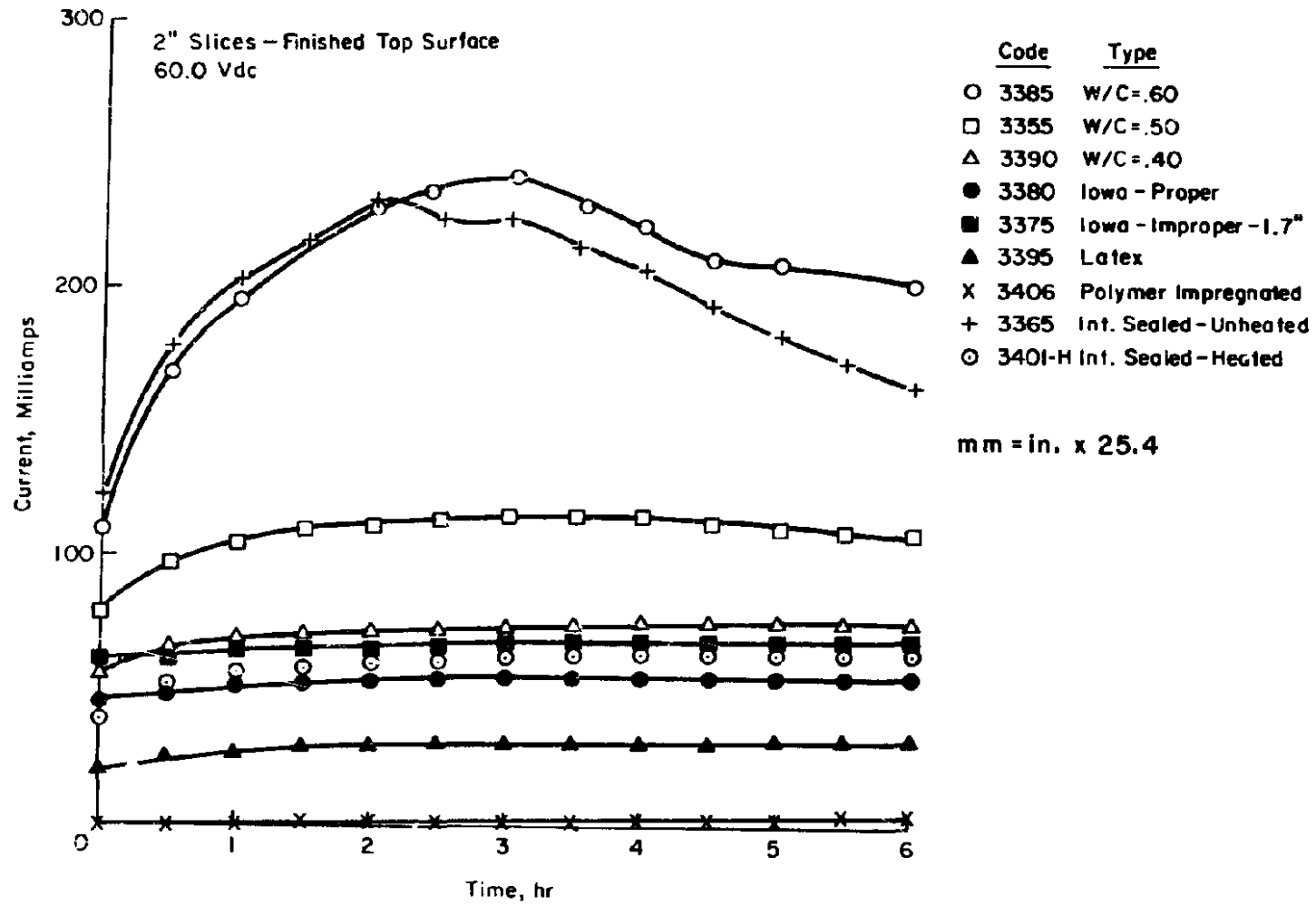


FIGURE 35. CURRENT VS. TIME FOR 2-IN. THICK CORE SLICES TESTED IN APPLIED VOLTAGE CELL.

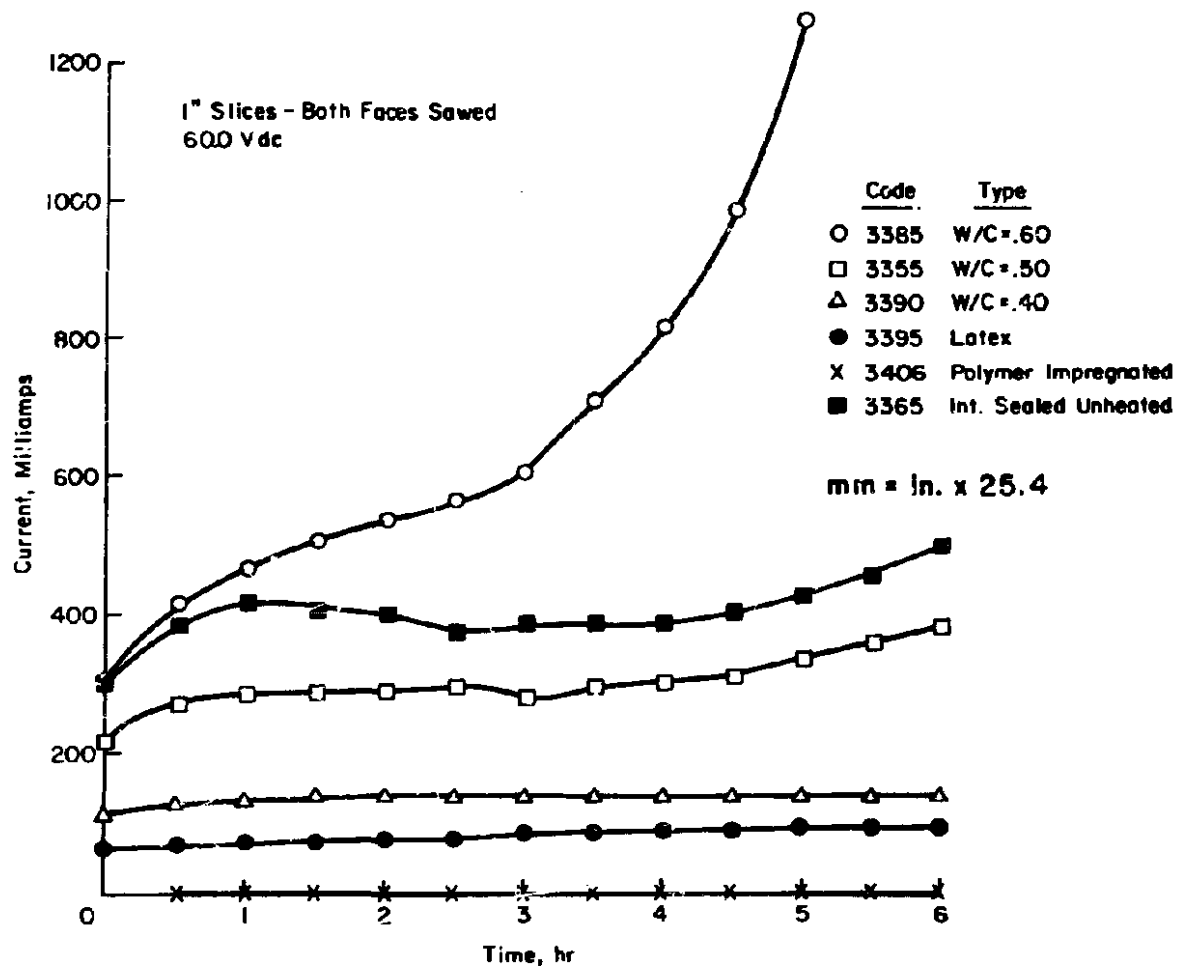


FIGURE 36. CURRENT VS. TIME FOR 1-IN. THICK CORE SLICES TESTED IN APPLIED VOLTAGE CELL.

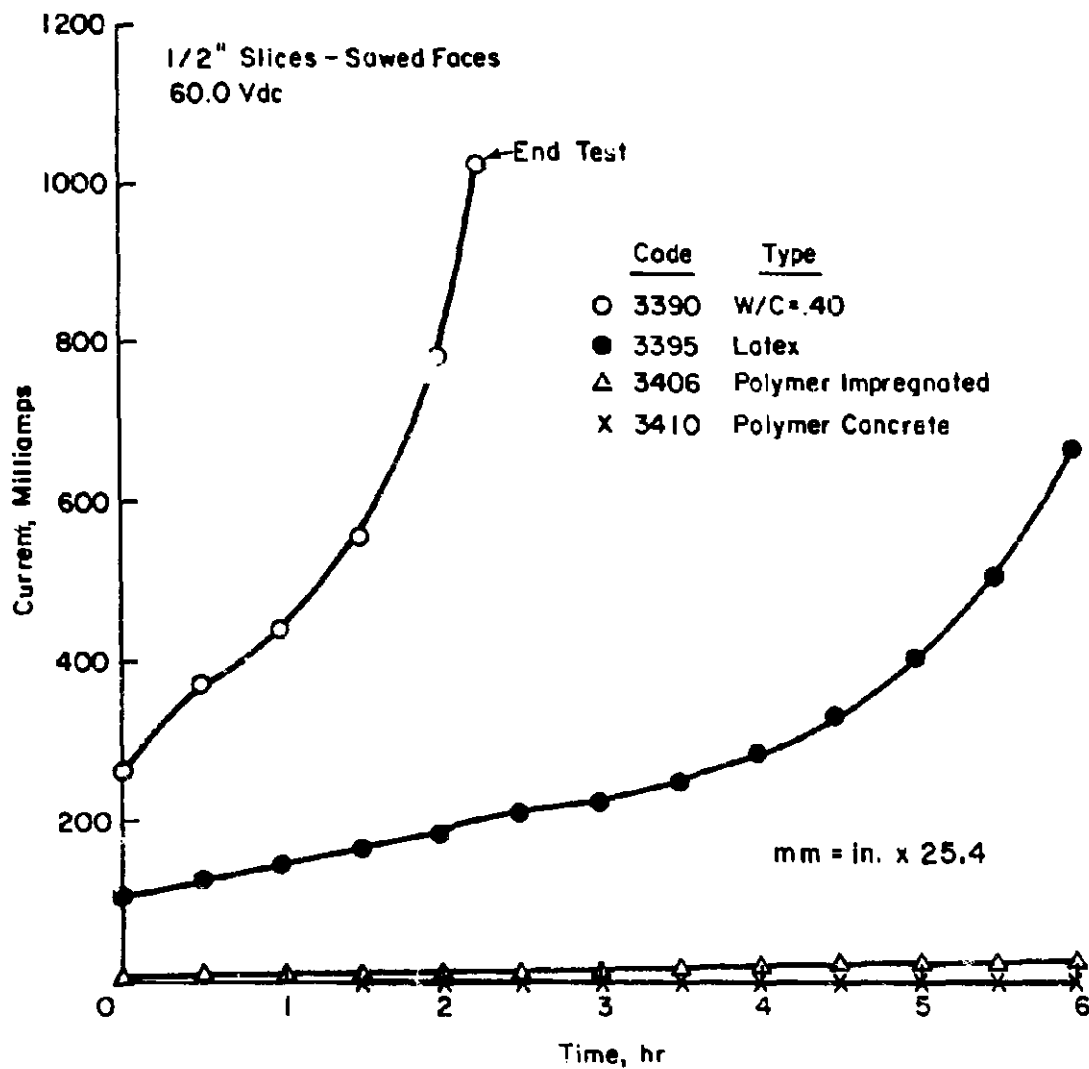


FIGURE 37. CURRENT VS. TIME FOR 1/2 -IN. THICK CORE SLICES TESTED IN APPLIED VOLTAGE CELL.

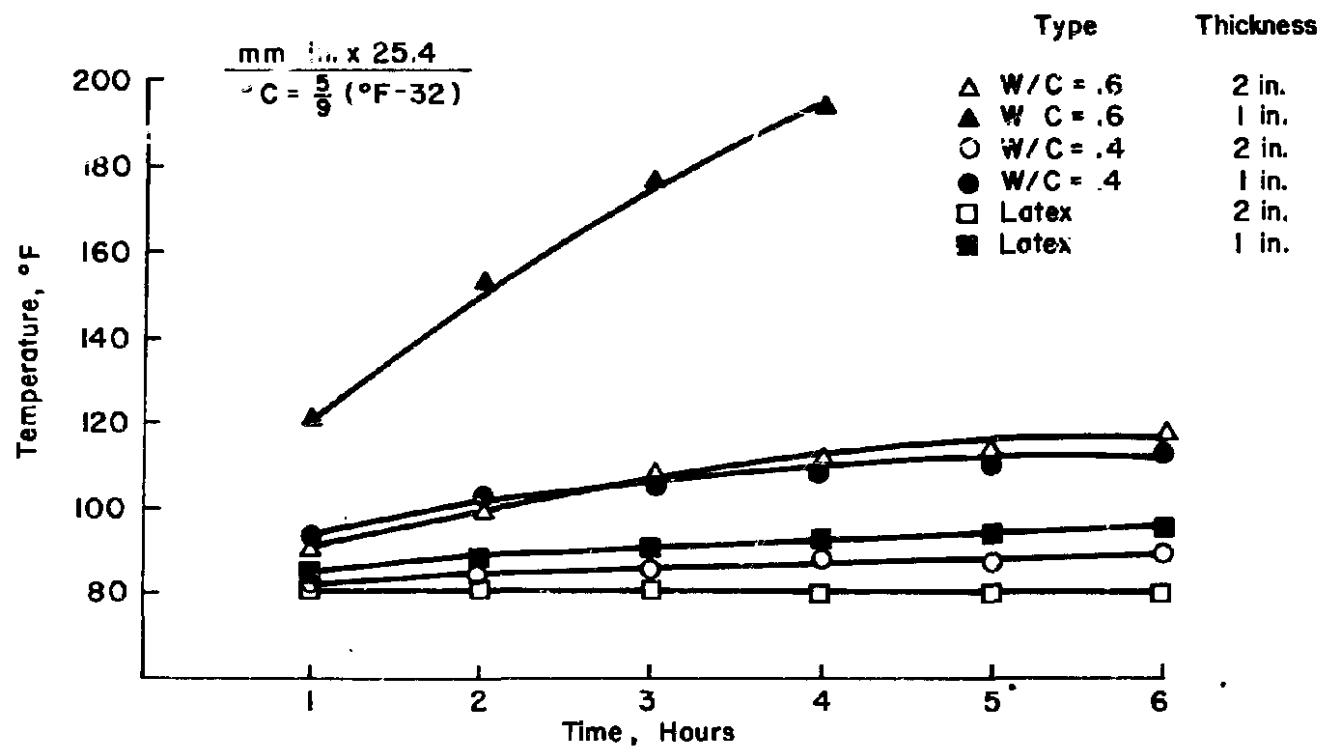


FIGURE 38. TEMPERATURE RISE IN APPLIED VOLTAGE CELL FOR CORE SLICES OF VARYING THICKNESS.

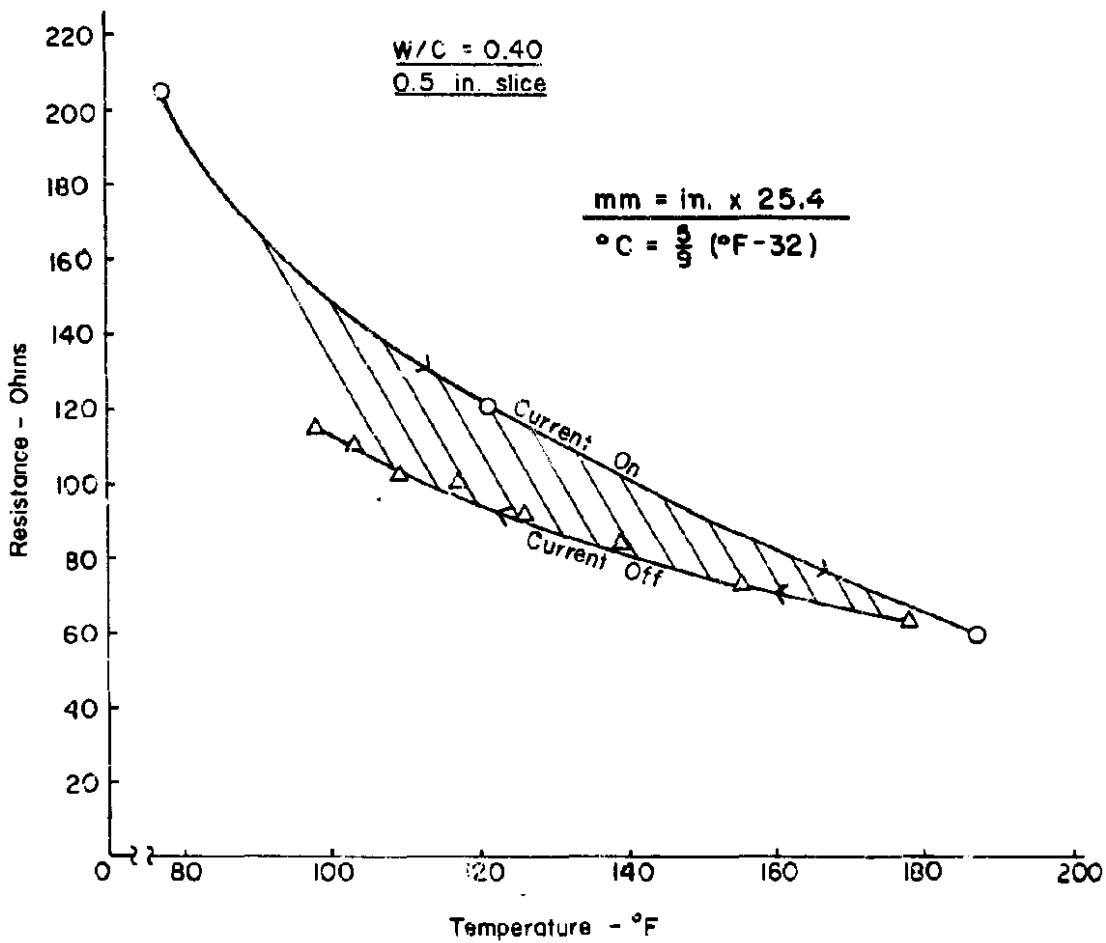


FIGURE 39. RELATIONSHIP BETWEEN RESISTANCE AND TEMPERATURE FOR 1/2-INCH THICK CORE SLICE TESTED IN APPLIED VOLTAGE CELL.

1. Cl⁻ solution loss: drop from initial 1.8 percent chloride (3.0% NaCl) concentration.
2. Cl⁻ (+): rise in chloride concentration in the right hand (positive pole) side of the cell.

3. Charge passed: coulombs of charge transferred during the test period - integral of current vs. time curve.

These parameters are presented in Table 14 for all specimens tested in the cell. Those slices where thickness is 2 in. (51 mm) represent Section 2

TABLE 14
APPLIED VOLTAGE CELL RESULTS

Type	Thickness ^{1/}	Cl ⁻ Solution Loss (%)	Cl ⁻ Positive Half Cell (%)	Charge Passed (coulombs)
w/c = 0.60	2 in.	0.45	BL	4,430
w/c = 0.60	1 in.	0.78	0.44	22,980
w/c = 0.50	2 in.	0.27	0.01	2,560
w/c = 0.50	1 in.	0.58	0.21	6,620
w/c = 0.40	2 in.	0.10	0.007	1,210
w/c = 0.40	1 in.	0.27	0.22	2,960
w/c = 0.40	1/2 in.	0.37	0.40	2/
Iowa Overlay	2 in.	0.08	0.002	1,170
Latex-Full Depth	2 in.	0.11	0.002	876
Latex-Full Depth	1 in.	0.32	0.002	1,631
Latex-Full Depth	1/2 in.	0.42	0.30	5,911
Polymer Impregnated	2 in.	0.01	NA	35
Polymer Impregnated	1 in.	0	NA	91
Polymer Impregnated	1/2 in.	0.03	0.04	401
Int. Seal-Full Depth -Unheated	2 in.	0.36	0.03	4,720
Int. Seal-Full Depth -Unheated	1 in.	0.58	0.27	8,830
Int. Seal-Full Depth Surface-Heated	2 in. including surface	0.15	NA	1,330
Int. Seal-Full Depth -Fully Heated	2 in.	0.05	NA	280
Latex-Overlay	1.3 in. including surface	0.19	NA	1,510
Latex-Overlay	1.0 in. - 1/8 in. removed from surface	0.26	0.02	2,490
Latex-Overlay	2 in. - includes base course	0.11	NA	1,079
Polymer Concrete Overlay	0.4 in overlay only	NA	NA	0
Polymer Concrete Overlay	Overlay + 1 in. base course	NA	NA	0

^{1/} mm = in. X 25.4

^{2/} Test terminated at 135 minutes due to rapid temperature rise

NA = not analyzed

(Figure 34A) and do not include the finished surface. Correlation analyses were performed between the charge passed and the Cl^- solution loss data sets for the slices and the total chloride data set for the FHWA 90-day results. These relationships are shown in Figures 79-80 (Appendix 3), respectively. Summary statistics (Table 35, Nos. 7 and 8) show lower correlation coefficients than those obtained in the slab tests. Standard errors are higher, about 40 percent of the mean value. These data indicate that the cell test would yield a rougher estimate of the long-term permeability than the slab test, which may be attributed to the difference in specimen size.

4.6.5 Effects of Surface Finishing

The data in Table 15 are presented so as to afford a quantitative evaluation of the effect of the finished surface on the test results. As mentioned previously, results are comparable for conventional concretes of w/c = 0.6 and 0.5, but are significantly different for w/c = 0.4, latex modified, and surface heated internally sealed concretes. The different results for the Iowa concrete

specimens are most likely attributable to the thickness differential. For the w/c = 0.4 and the latex modified concretes, however, the thickness differential is small compared with the difference in charge passed. This indicates the presence of a more impermeable surface layer in these concretes. This corroborates observations on latex field jobs where latex particles are sometimes seen to concentrate at the surface. The surface densification of the w/c = 0.4 concrete could be attributable to the paste-rich surface layer. Of course, there would also be paste-rich surface layers in the w/c = 0.6 and w/c = 0.5 specimens; however, these pastes would be of high permeability due to their high water-cement ratios.

4.6.6 Effects of Heat Treatment on Internally Sealed Specimens

The very large difference between the surface and sawed internally sealed specimens prompted further investigation. Some of the partially heated (surface heated) internally sealed core slices were placed in an oven at 190°F (88°C) for 2 hr. Upon cooling, microscopic

TABLE 15
COMPARISON OF FINISHED AND SAWED SURFACES

Slice	Type	Charge Passed (coulombs)		ΔQ	Thickness Differential
		Incl. Surface	Sawed ^{2/}		
3385	w/c = 0.60	4,573	4,430	-3.1	+1.1
3355	w/c = 0.50	2,371	2,556	+7.8	-0.6
3390	w/c = 0.40	1,543	1,214	-21.3	+1.8
3395	Latex	613	876	+42.9	-7.2
3365	Int. Sealed- Full Depth-Unheated	4,310	4,720	+9.5	-0.5
3401H	Int. Sealed- Full Depth-Heated	1,333	2,284	+71.3	-6.7
3380	Iowa - Proper	1,167	1,349	+15.6	-11.5

^{1/} mm = in. X 25.4

^{2/} 0.25 in. (6 mm) of material removed from surface by diamond saw

examination indicated some shrinkage of the wax beads, but no extensive melting. The slices were, therefore, returned to the oven and heated to 210°F (99°C) for 6 hr. Subsequent examination indicated melting and migration of the wax had taken place. The surfaces of the slices were abraded on fine sandpaper prior to test. The slices were then tested in the cell at 60.0 Vdc for 6 hr. Results are presented in Table 16. The surface heated 2-in. (51 mm) slice was included for comparison. It is seen that reheating dramatically lowers the permeability. In addition, there is no increase in permeability with decreasing thickness, as was seen for other materials. This may reflect a more complete sealing in the thinner slices. A pictorial representation of the effects of various types of heating is shown in Figure 40. The difference between Slices #1 and #2 indicates a more complete melting in the surface layer, which was verified by microscopic examination. At a depth of 2 in. (51 mm) or more, however, there is still some melting taking place, as Slice #2 shows lower permeability than the unheated core.

TABLE 16

INTERNALLY SEALED SPECIMENS - REHEATED

<u>Specimen</u>	<u>Thickness (in.)^{1/}</u>	<u>Cl⁻ Solution Loss (%)</u>	<u>Charge Passed (coulombs)</u>
3401H-4 (not reheated)	2.1	0.15	1,330
3401H-5-2 (reheated)	1.9	0.05	280
3401H-5-1 (reheated)	1.0	0	290
3401H-1/2 (reheated)	0.56	0.02	160

^{1/} m² = in. X 25.4

Work was also done on testing Slice #1 at various depth increments, that is, slicing off approximately 1/8-in. (3 mm) layers and retesting each time. Results, shown in Figure 41, indicate an increase in slope at about 0.2 in. (5 mm). This corresponds with microscopic examinations at each level, which revealed that melting was complete only to about 1/4-in. (6 mm) below the surface. Below this level wax beads were darkened and partially melted, but complete migration of the beads into the surrounding paste was not evident. It should be emphasized that the applied voltage cell, when used for this purpose, (i.e., in determining depth of complete heating), is no more accurate than simple microscopic examination, and is far more time-consuming and expensive. One drawback to reliance solely on microscopic examination is that, due to an excess of wax above that being necessary to fill the capillaries being present, the presence of unmigrated material may reflect the inability of the wax to migrate into already filled capillary space. Thus, detection of unmelted beads in the interior concrete may not necessarily mean that complete filling of capillaries has not been achieved. At the surface some of the excess wax may be driven out due to the high temperatures employed, in the range of 300°F (150°C). It should also be noted that this depth of relatively complete melting, 0.2 in. (5 mm), in the surface heated slab is much less than the depth of melting indicated by the resistivity technique (see Appendix 5). Apparently, the resistivity technique is measuring the total overlay depth, and not the depth of melting.

Because of the difficulties encountered in the interpretation of results when testing internally sealed concrete in the applied voltage cell,

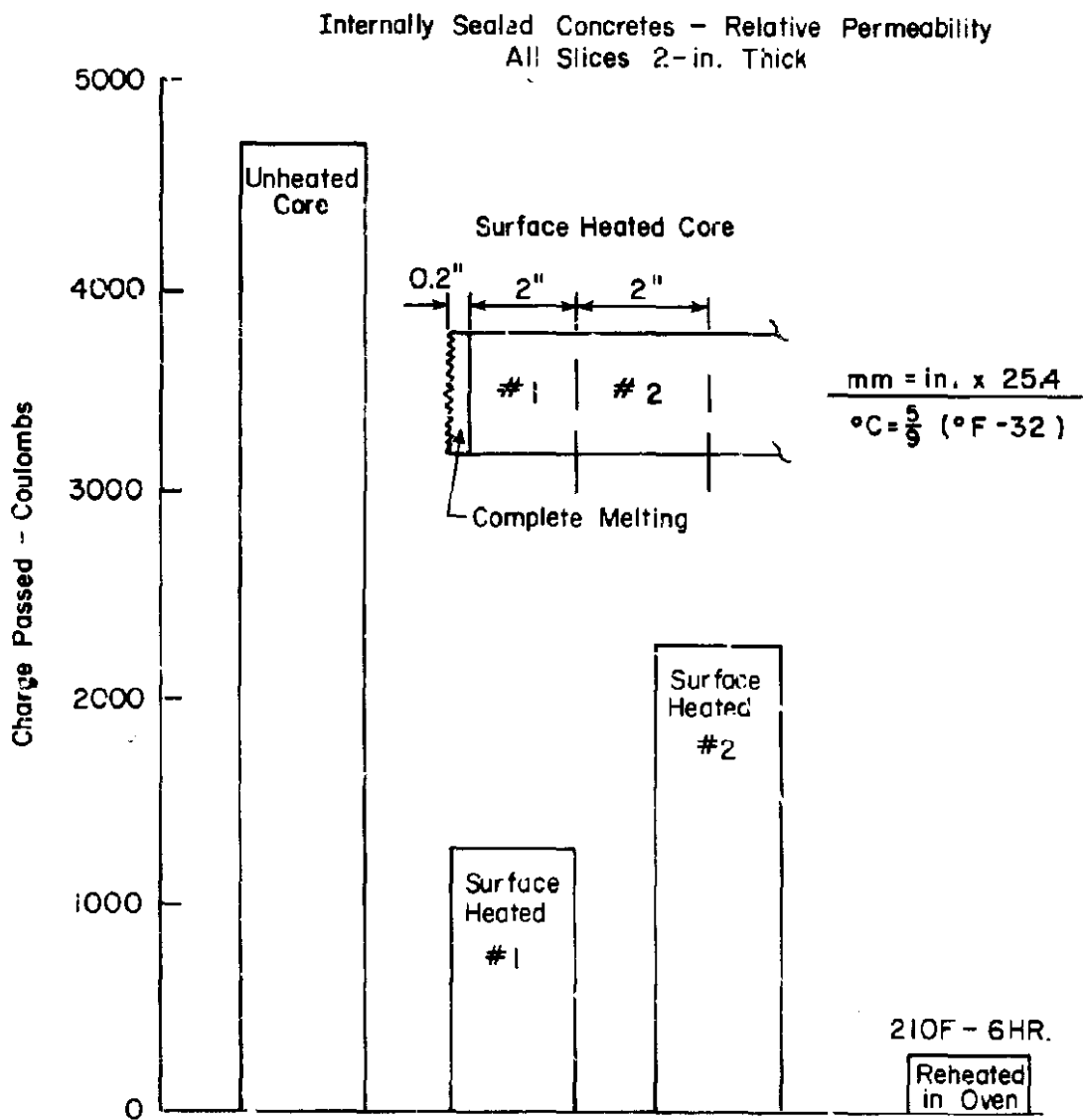


FIGURE 40. EFFECT OF VARIOUS HEAT TREATMENTS ON CHARGE PASSED BY INTERNALLY SEALED CONCRETES.

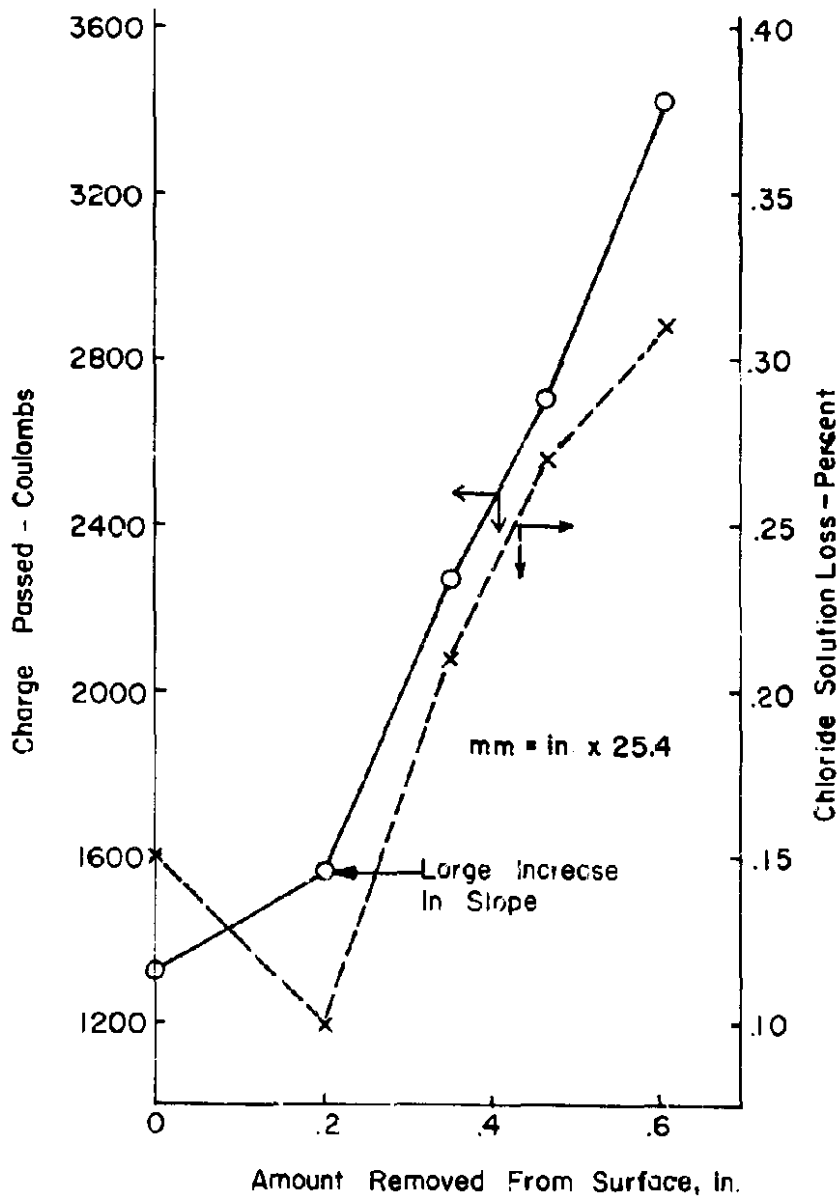


FIGURE 41. EFFECT OF SURFACE ABRASION ON CHARGE PASSED BY INTERNALLY SEALED CONCRETES.

additional research is desirable to establish the optimum method for applying the rapid test procedure to internally sealed concrete.

4.6.7 Effect of Thickness

The relationships between charge passed and thickness of the core specimens are plotted in Fig. 42. The various types of concrete are seen to separate out very nicely. For the very permeable concretes (w/c = 0.6) only 2-in. (51 mm) thick slices can be tested under the voltage chosen, thinner slices leading to excessive heating. For highly impermeable concrete (such as PC and PIC) negligible charge is passed even for thin (approximately 0.5 in. (13 mm)) slices. Obviously, both charge passed and thickness must be known in order to effectively use the test data.

4.6.8 Reproducibility of the Method

To evaluate the reproducibility of the test, six 4-in. (102 mm) cores were taken from slabs 3386 (w/c = 0.60) and 3396 (latex full depth). These represent very high and very low permeability concretes. Slices 2-in. (51 mm) thick were taken off the top of each core, placed in limewater for 14 days, and then stored in plastic sample bags until ready to test.

Results are given in Table 17. The data show the coefficient of variation to range from 6 to 7 percent. Most of the test variance is likely due to differences in moisture content, aggregate distribution, and other specimen-to-specimen variations.

4.7 Conclusions Derived from Laboratory Evaluations

4.7.1 Application of a potential in the range of 60-80 Vdc to a 3 percent

TABLE 17

REPLICATE SPECIMENS

Specimen	Charge Passed (coulombs)	
	w/c = 0.60	Latex Modified
1	4,577	539
2	4,721	569
3	4,669	522
4	3,994	572
5	4,444	540
6	4,340	631
Mean	4,458	562
Std. Dev.	267	38.8
C.V. - %	6.0	6.9

sodium chloride solution can accelerate the ingress of chloride ions into concrete slab and core test specimens.

4.7.2 In highly permeable concretes, significant quantities of chloride ion (greater than 0.02%) can be detected at the 1 in. (25 mm) depth level after 6 hrs of test at 80 Vdc.

4.7.3 The total amount of electrical charge passed during the test shows a high degree of correlation with the total amount of chloride ion which penetrates a companion specimen during a conventional 90-day ponding test.

4.7.4 The moisture content of the concrete has a large influence on the test results. Air-dry specimens will exhibit less chloride penetration during the test period than moist-cured specimens.

4.7.5 An equilibration procedure for slab specimens involving vacuum saturation with heated (140°F (60°C)) limewater has been developed in order to re-establish

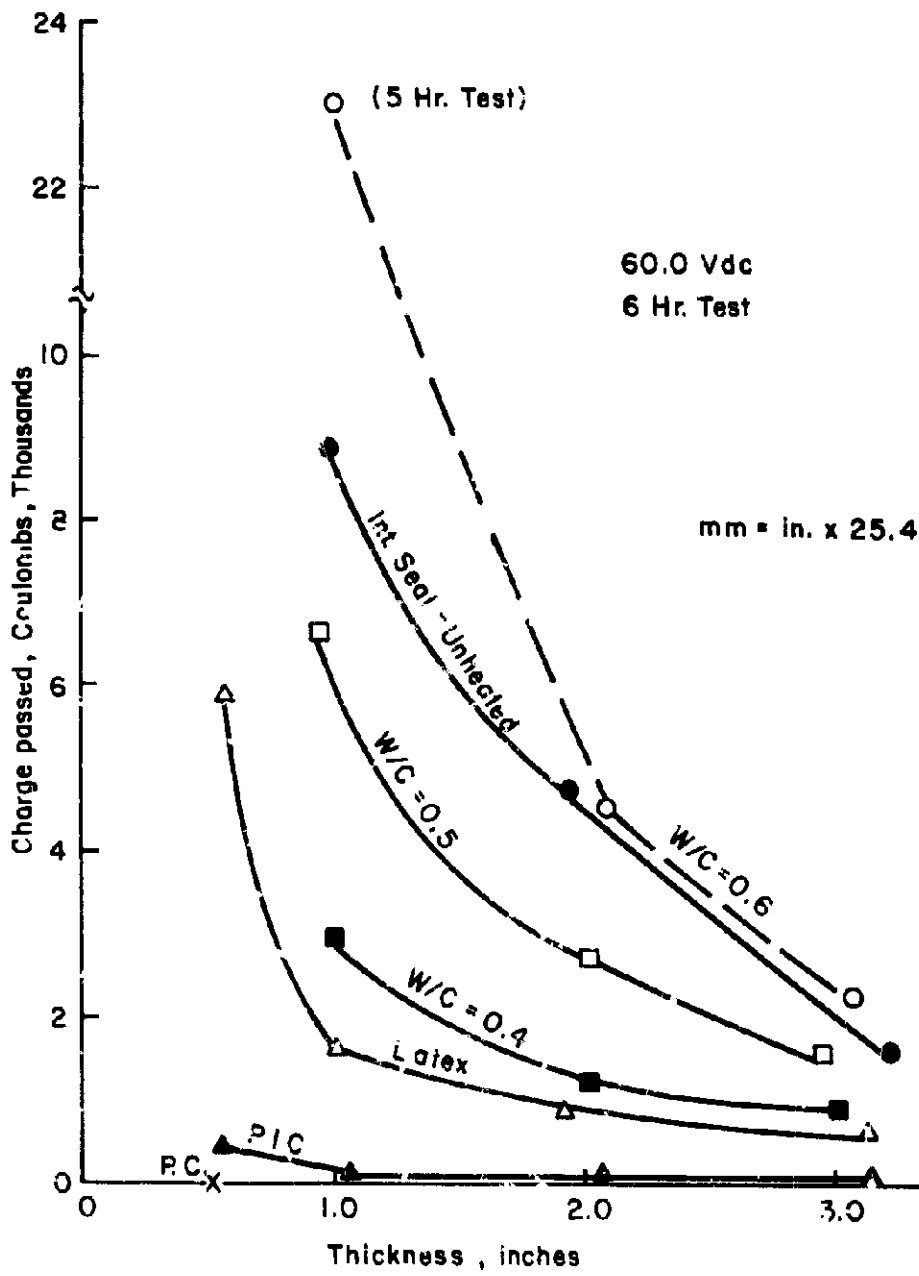


FIGURE 42. EFFECT OF THICKNESS ON CHARGE PASSED .

a high moisture content in the specimen prior to test. Additional research is needed, however, if this technique is to be successfully applied to internally sealed concrete.

- 4.7.6 High rates of heating may be encountered when utilizing the technique for testing of small (4-in. (102 mm) diameter) core specimens. For very permeable specimens the test may have to be terminated before the standard 6-hr period has elapsed, due to excessive heating ($>190^{\circ}\text{F}$ (88°C)) in the test cell.
- 4.7.7 The thickness of the core test specimen has a large effect on the test results. In order to adequately rank a series of concretes in terms of their chloride permeabilities, all specimens must be tested at equal thickness. A 2-in. (51 mm) thick core slice has been found adequate for most of the concretes tested to date.
- 4.7.8 Differences may be encountered when comparing sawed and finished surfaces, especially for latex modified and cement-rich concretes.

5. PROTOTYPE INSTRUMENT DEVELOPMENT

5.1 Desirable Features

The aim of this phase of the project was to incorporate the components of the applied voltage technique into a single portable electronics package capable of operating off of a field generator set. In addition, a unit incorporating vacuum pump, heater, stirrer, and temperature controller was also felt to be desirable. Finally, the dike used to contain the 3.0% NaCl solution and the electrode screen was redesigned for ease of

operation. Various fail-safe features included over-temperature and over-current cut-outs, time run-out, and battery backup for data storage in case of loss of line power. Detailed requirements are given in Appendix 4.

5.2 General Description

The field instrumentation consists of three separate modules. The first houses the electronics package (this can also be used in the laboratory), the second allows for vacuum saturation prior to test, and the third is designed to apply voltage to the salt solution used as the permeant. All instrumentation was designed with portability in mind, and the entire field set (along with auxiliary generator, tools, and chemicals) can be transported in a van-type vehicle having a storage area of 8x6x4 ft (2.4x1.8x1.2 m). Configurations of the equipment and functioning of the electronic circuitry are described in this section. The field test procedure is set forth in Appendix 2. Current price (November 1980) of the complete system is estimated at \$10,400.

5.3 Construction

5.3.1 Electronics Module

The complete electronics module is shown in Figure 43. The module consists of two NEMA-4 weatherproof enclosures mounted on a lightweight pneumatic-tired aluminum dolly. Overall dimensions are 49x29x24.5 in. (124x74x62 cm). Total weight is 166 lb (75 kg). The lower enclosure houses the power supplies. A cooling fan prevents overheating of the unit. The upper enclosure houses all electronics, operating controls, and the readouts (Figure 44). The elapsed time and coulomb meters are LED's constructed for visibility even in strong sunlight. The digital panel meters, used for the



FIGURE 43. ELECTRONICS MODULE. OVERALL VIEW.

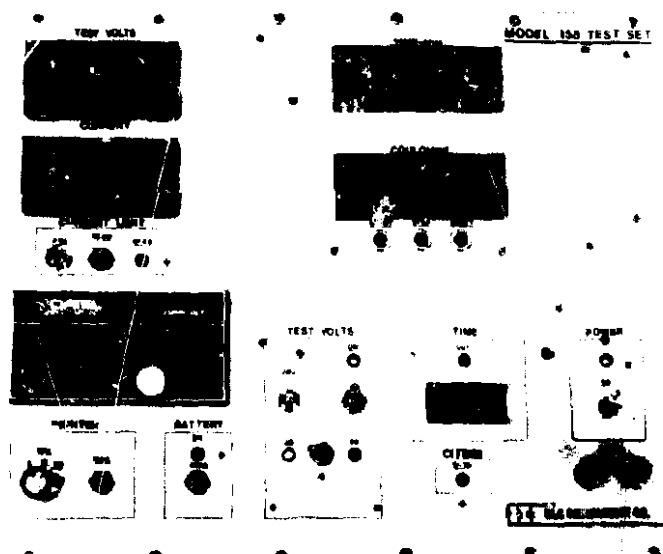


FIGURE 44. READOUT PANEL

current and voltage meters, have LED's not visible in sunlight; therefore, a sunshield was constructed. A rain shield can be placed over the entire panel (Figure 43).

5.3.2 Vacuum Saturation Module

The vacuum saturation module and associated dike are shown in Figure 45A and B. A compact single-stage vacuum pump (Sargent-Welch Model 8803) is mounted onto a 1/4-in. (6 mm) thick anodized aluminum plate along with a dial-type vacuum gage. Also included are a thermocouple based temperature controller (RFL Model 70A), a 550 watt, resistance heater (Watlow #1-47-7-68), a pyrometer (Simpson Model 2123), a magnetically coupled stirrer, and a fluid entry valve. The mounting plate is raised above the main dike cover by 7/8 in. (22 mm) so as to allow for air flow around the vacuum pump and temperature controller. The dike is constructed from 1/4-in. (6 mm) thick anodized aluminum plate having a Teflon coating. Wing nuts are provided to obtain a tight seal between the dike and the vacuum saturation cover. The dike serves the dual purpose of containing both the linewater solution used in the saturation phase and the chloride solution used during the actual test period.

5.3.3 Screen Assembly

The screen assembly (Figure 46) is fabricated from 4 mesh (4.75 mm) stainless steel fabric reinforced along its outer edge with 1/8-in. (3.2 mm) stainless steel rod. The screen is bolted to Teflon standoffs and sits approximately 1/32-in. (0.8 mm) off the concrete surface during the test. The negative electrode is a 1/2-in. (13 mm) stainless steel rod bolted to the screen at one end and terminating in a female "banana"

jack at the other. A high limit thermostatic switch (Fenwal 1A322-1) is housed in a 5/8-in. (16 mm) diameter stainless steel well which extends into the chloride solution and terminates on the cover in an amphenol-type connector.

5.3.4 Generator Set

A 3.5 kW, single cylinder, air-cooled, 4 cycle portable gas generator (Kohler Model 3.5MM65) is used to power all instrumentation (Figure 47). The generator is supplied with a wheel kit to permit easy transport across the test bridges. An auxiliary 6-gal gas tank (Kohler A-238-712-6) allows the vacuum-saturation unit to run unattended for at least 14 hours.

5.4 Electronic Circuitry

5.4.1 Locations of Components

The electronic circuitry is housed in two weatherproof NEMA-4 enclosures. In the lower enclosure (Figure 48) are located the three power supplies (Power One F24-12, HE24-7.2, HAA24-.6) delivering a maximum of 80 volts DC at 6 amperes. A fan (Rotron MU2A1) is used to maintain the supplies within their specified temperature limit (0-50°C).

The active circuitry is mounted on two printed circuit boards packaged in the sloped face of the upper enclosure mounted on the dolly (Figure 49). Both boards are hinged to the back of the front panel to allow ready access for parts replacement and trouble shooting.

The Time and Coulomb Counter Board, mounted against the front panel, houses the Crystal Clock, the Time Counter with display, the precision Current Amplifier, the Voltage Controlled Oscillator (VCO), the Coulomb Counter with display, the Power-Up Reset Circuit, and the Current Limit and Latch Circuit. The Multiplexer board, mounted on stand-offs over

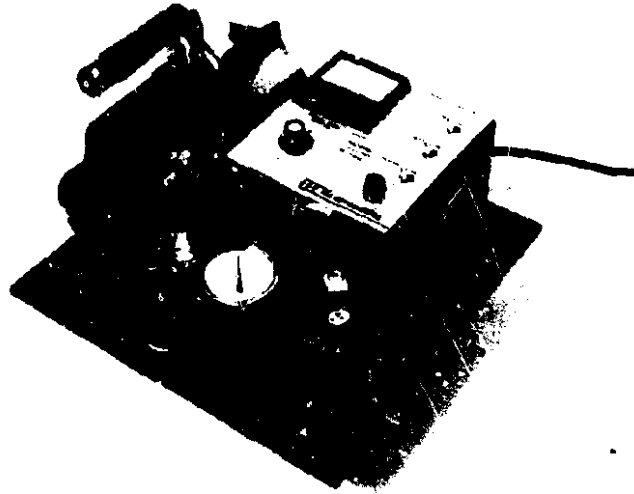


FIGURE 45A. VACUUM SATURATION MODULE

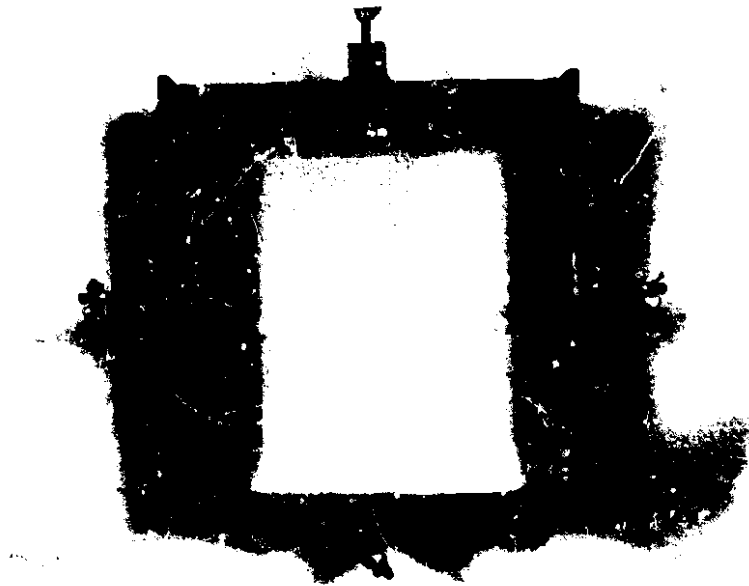


FIGURE 45B. DIKE USED WITH SATURATION MODULE.

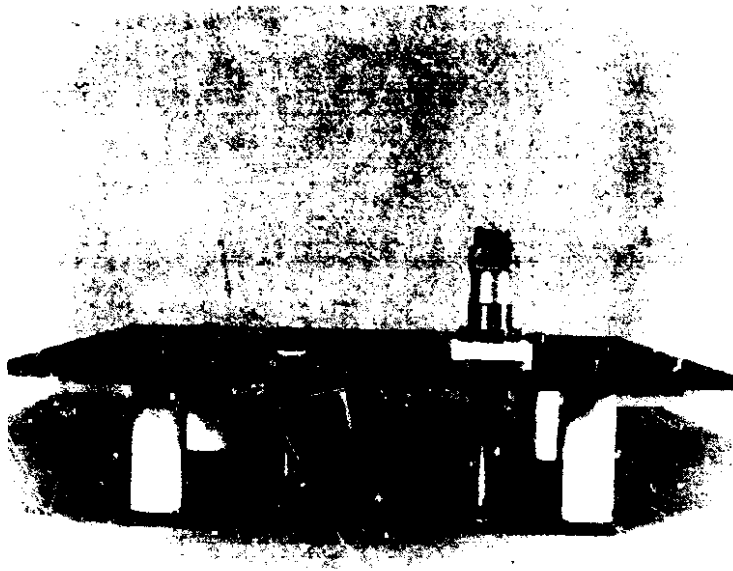


FIGURE 46. SCREEN UNIT.



FIGURE 47. FIELD GENERATOR SET WITH AUXILIARY GAS TANK .

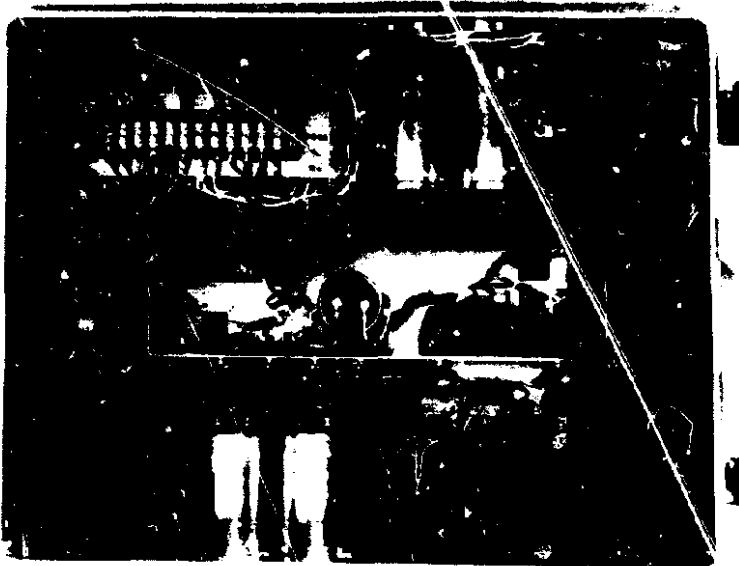


FIGURE 48. POWER SUPPLY CIRCUITRY.

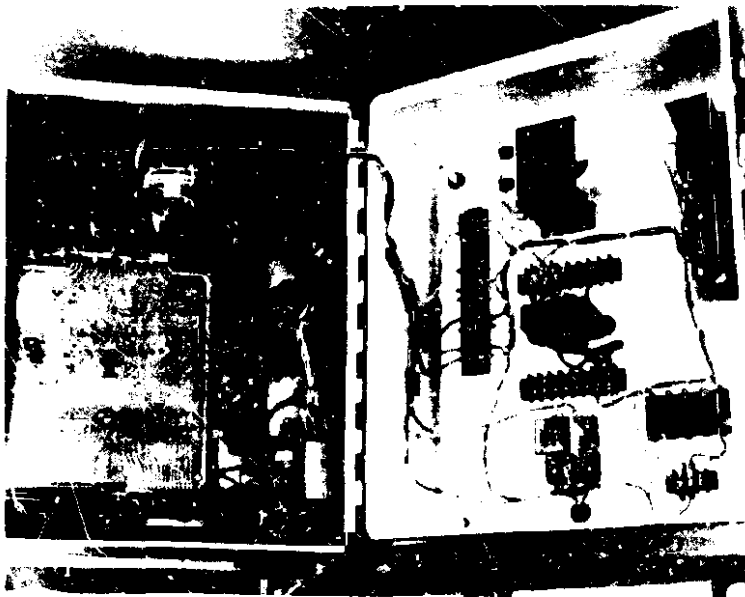


FIGURE 49. CONTROL CIRCUITRY.

the counter board, contains the Printer Multiplexer, the Start-Stop Circuit, the Over Temperature Limit Stop Circuit, the Test Time Stop circuit, the Battery Switching Circuit, and the Battery Charging Circuit.

5.4.2 System Description

The overall Block Diagram of the Model 158 Test Set is shown in Figure 50. Current flow through the current shunt is amplified by an instrumentation amplifier. The amplifier output is scaled to read current by a 4-1/2 digit DPM and also drives a precision integrator-voltage controlled oscillator. The oscillator output is scaled to read directly in coulombs on a five digit readout.

A crystal based clock is used to allow display of elapsed test time, selection of recurrent printout periods, and test time selection. At each printout interval the information in the storage registers of the current, time and coulomb displays are latched while the printer is multiplexed through the readouts. The printout cycle does not interrupt the accumulation of new data. Data may be printed out at any time by use of the manual printout switch.

5.4.3 Individual Circuit Description

5.4.3.1 Time and Coulomb Counter

5.4.3.1.1 Crystal Based Clock:

The crystal based clock provides an accurate one pulse per minute clock pulse. It is used to define the total test time and printout periods and is used to drive the Auto Print circuit on the Multiplexer board and the Test Time Counter.

5.4.3.1.2 Current Amplifier: The current amplifier functions as a voltage amplifier for the voltage developed across the current shunt. With 5 amps

flowing through the current shunt the output is 5 volts.

5.4.3.1.3 VCD Integrator: The output of the current amplifier is filtered by the integrator. The output of the integrator is connected to the voltage to frequency converter, which is adjusted to give a DC frequency conversion of exactly 1K Hz per ampere drawn by the test cell and sample.

The frequency output of the voltage to frequency counter is directly related to the current flow through the current shunt. For example, 5 amps of current flow will generate a frequency of 5,000 cycles per second. A current flow of 5 amps for one second is equal to 5 coulombs.

5.4.3.1.4 Time Counter and Display:

The output of the time counter feeds its 1 pulse per minute output to cascaded decade counters which drive the appropriate Test Time displays. The same outputs are interfaced with 3 BCD thumb-wheel switches on the front panel to allow selection of test time from 1 to 999 minutes. The "time" BCD outputs are also interfaced through a connector to tri-state latches on the Multiplexer board.

5.4.3.1.5 Coulomb Counter and Display: The pulse output of the coulomb counter represents the direct coulomb measure of amp-sec. and is connected to trigger five BCD counters. The BCD output of these counters drives the appropriate coulomb display digits. The five counter BCD outputs are also connected to a board connector and interfaced with Tri-State latches on the Multiplexer board for printout purposes.

5.4.3.1.6 Current Limit and Latch Circuit: The purpose of this circuit is to limit the maximum current to a selected value in the range of 0-7.2 amps. A comparator continuously compares the

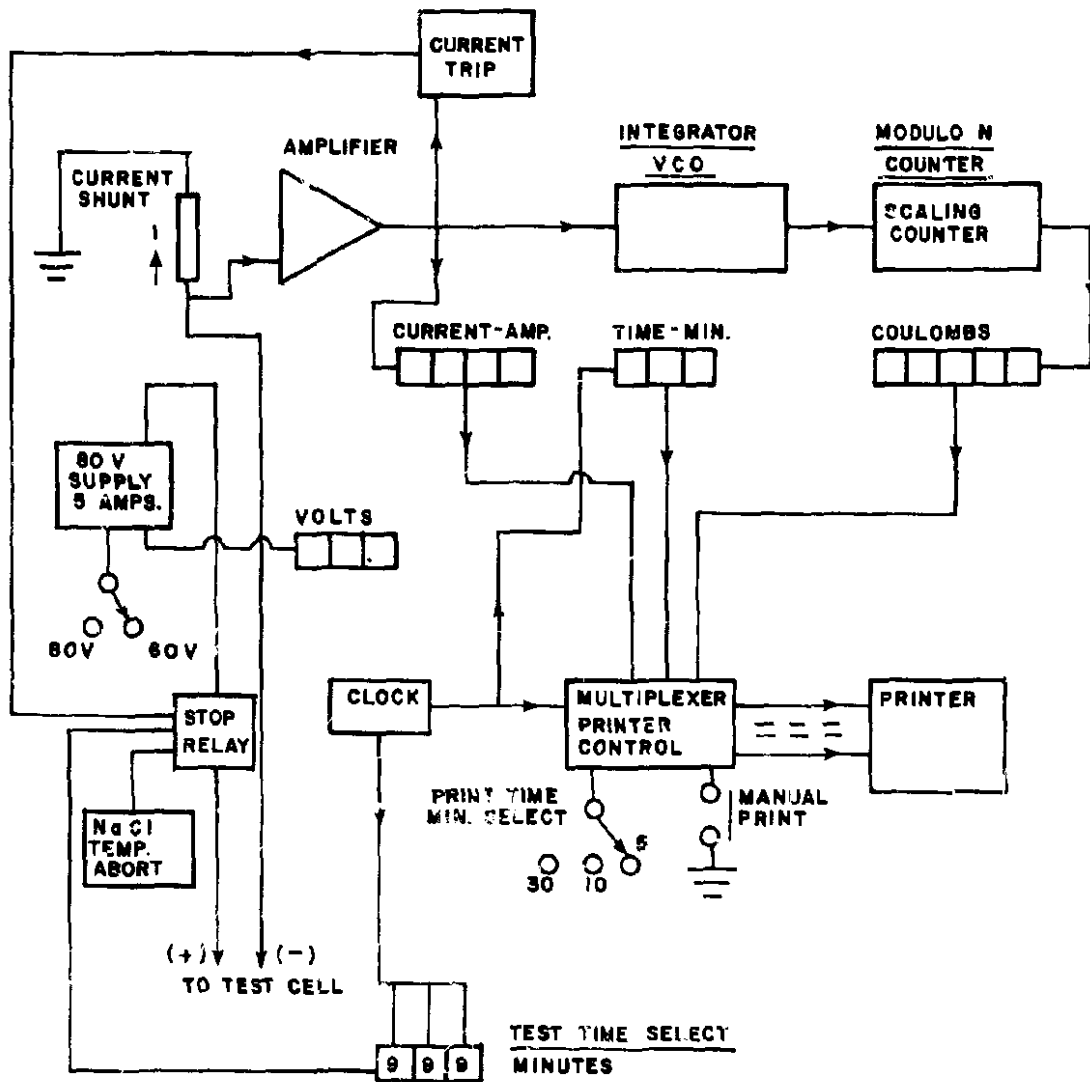


FIGURE 50. ELECTRICAL BLOCK DIAGRAM.

current through the current shunt with a voltage set by the front panel current limit-adjust potentiometer. When current exceeds the set point, the front panel Over Current LED is turned on and the stop circuit on the Multiplexer board is triggered, thus stopping the test. The circuit can be reset by simultaneously pushing the Stop and Reset switches on the front panel.

5.4.3.1.7 Power Up Reset: The power up reset circuit is provided to reset all counters to the 0 state when power is first applied.

5.4.3.2 Multiplexer Board

5.4.3.2.1 The Printer Multiplexer Circuit functions to sequentially scan and print out the Time, Current, and Coulomb displays. The multiplexer circuit is energized by either Manual push button command or automatically by the printout select switch at 5, 10 or 30 minute intervals.

There are four tri-state dual 4 bit latches at the output of the multiplexing circuit. The input to these latches is connected to the time and coulomb BCD data lines. The output of the latches is connected to the printer data input lines. The current DPM tri-state BCD data lines are also connected directly to the printer data input lines.

The printer data input lines are inputted from tri-state logic which allows multiple connection to the same point. Gating of the tri-state data sources permits these multiple connections.

Data Printout is accomplished via a miniature 7-column thermal printer (Datel Model DPP-Q7). At the selected printout time^{1/}, time in minutes is printed on the first line, current (in amperes) on the second line and coulombs on the

^{1/} At the initiation of test the manual print button must be depressed to obtain readings at zero elapsed time.

third line. The paper automatically advances one blank line between each set of readings.

5.4.3.2.2 Start-Stop Circuit: The start-stop circuit performs two functions. It enables and disables the counters and simultaneously operates the 80 volt power relay.

When the Start push button on the front panel is actuated, both the 80V relay and all counting functions at the counter board are enabled at this time.

Depressing the Stop push button reverses the above action to terminate the counting and application of 80V power to the test cell. During a normal test cycle the test may be started and stopped at any time by the front panel Start and Stop push buttons. Also, during a normal test cycle the Reset push button is inactive. That is, the stored data cannot be erased unless both the Stop and Reset button are actuated together.

A test cycle may be stopped by actuating the Stop push button, having test time run out, exceeding the over current limit setting, having the salt solution exceed 180°F (82°C) or having the AC operated DC supply fall below 11 volts.

5.4.3.2.3 Over Temperature Limit Stop Circuit: The Test Cell cover used for the salt solution phase of the test contains a high limit normally closed thermostat set at about 180°F (82°C). If the salt solution exceeds 180°F, (82°C) the thermostat contacts open. This action turns on the Over Temperature LED on the front panel and stops the test. The test cannot be restarted until the over temperature condition is eliminated.

5.4.3.2.4 Test Time Stop Circuit: The test time is settable from 1 to 999 minutes. When elapsed test time is equal to the selected test time, the common lines of the BCD thumbwheel switches go

to 1; this pulls the reset line to 0 and stops the test.

5.4.3.2.5 Battery Switching Circuit: The Battery Switching Circuit energizes a relay and transfers the 12 Vdc supply for all counters over to the battery backup system. The displays are turned off to conserve battery power.

The test is automatically stopped when the unit goes to battery backup. No further counting takes place, but the data accumulated prior to the low voltage condition is retained for up to 40 hours. These data may be displayed by pushing the Read push button on the front panel.

5.4.3.2.6 Battery Charging Circuit: The Battery Charging Circuit is operative whenever the test set is connected to 115V AC and the power switch is on. The batteries require 12-hours to reach full charge initially, or if the unit has been stored for more than four months. The battery is in use only when the internal 12V DC supply falls below about 11V. This generally will occur only when the AC line voltage falls below 100V.

5.4.3.3 Further Circuit Details

The preceding sections have described the operation of each separate circuit without detailing the electronic logic flow between subsection components. Those requiring exact component-by-component descriptions and electrical schematics are advised to consult the Operation Manual-Model 158 Chloride Permeability Test Instrument available as a separate publication.

6. LABORATORY TESTING OF PROTOTYPE INSTRUMENT

Before proceeding to actual field testing, it was desirable to test the prototype on slabs intermediate between the small specimens tested in the earlier phases of the project and full-scale bridge decks. This would allow a more

realistic heat sink and also allow the evaluation of a number of variables within a single slab.

The variables which needed to be studied in more detail were:

1. Concrete cover
2. Ambient test temperature
3. Geometry of reinforcing cages
4. Presence of chloride in concrete prior to test.

6.1 Test Specimens

Three test slabs were prepared. These were 4-ft x 5-ft x 7-in. (1.2 m x 1.5 m x 17 cm) slabs, each having one mat of No. 4 (13 mm) reinforcing bars (Grade 40) located 1 in. (25 mm) clear from the bottom of the slab and spaced at 5-in. (127 mm) centers running the 5-ft (1.5 m) length of the slab and 10-in. (254 mm) centers running the width. The topmost reinforcing mat varied for each slab as given in Table 18.

**TABLE 18
REINFORCEMENT DETAILS
PROTOTYPE TEST SLABS**

Slab	Mat	Bar Spacing		Clear Cover (in.)
		(in.) ^{1/}		
		Top	Bottom	Nominal (actual)
A	1	5	10	1 (1.125)
	2A	5	10	2 (2.25)
	2B	5	10	2 (not tested)
	3	5	10	3 (3.50)
B	1	6	14	2 (2.50)
	2	5	5	2 (2.375)
	3	5	10	2 (2.375)
	4	5	10	2 (2.4375)
C	1	5	10	1 (1.25)
	2	5	10	2 (not tested)

^{1/} mm = in. x 25.4

Grade 40, No. 4 (13 mm) bars were used in all the mats. The mats were secured to the plywood bases of the forms by securely wiring them to bar

chairs. Actual covers (measured on the exposed bar used to make the positive electrical connection) were greater than originally planned. This was attributed to placement of the topmost bars on the chairs rather than securing the bottom bars to the chairs. As the objective of this task was to simply obtain a range of known covers the forms were left intact and casting was done using the somewhat greater covers. Photographs of the reinforcement in each slab are shown in Figure 51A-C.

Thermocouples were installed in each mat at the locations denoted by an "X" in Figures 51A-C. Copper-Constantan thermocouples (Type T) were first cast into 1x1x7-in. (25x25x178 mm) mortar bars, then these bars were wired at the indicated location just prior to placing the concrete in the slab. Thermocouples were located 1/2, 1, 2, and 3 in. (13, 25, 51, and 76 mm) from the concrete surface.

6.2 Concrete Mixtures

Batch analysis of the concretes used to pour each slab are given in Table 19. Chloride-free materials (less than 0.01% by weight as Cl^-) were used, except in Slab C where chloride was intentionally added to the mix. The concretes were designed for a w/c ratio of 0.5, slump of $3\frac{1}{2}$ in. (76 ± 13 mm) and air content of $6\pm 1\%$.

6.3 Casting and Conditioning of Slabs

Each slab was cast in two lifts. A spud vibrator was used to consolidate the concrete. Slabs were struck off with a magnesium screed. Wooden trowels were used to obtain a rough surface on one of the slabs (Slab B) to evaluate the ability of the silicone adhesive to obtain a good seal. No further finishing was done on the slabs.

The specimens were cured under moist burlap for 24 hours, then transferred outside and set on concrete blocks. Curing was continued for 14 days, then the burlap was removed and the slabs allowed to come to equilibrium with the natural environment. Approximately 6 weeks elapsed between the time the curing was ended and the time each slab was tested; prior to test each slab was allowed to equilibrate at least 2 days in the environment of interest.

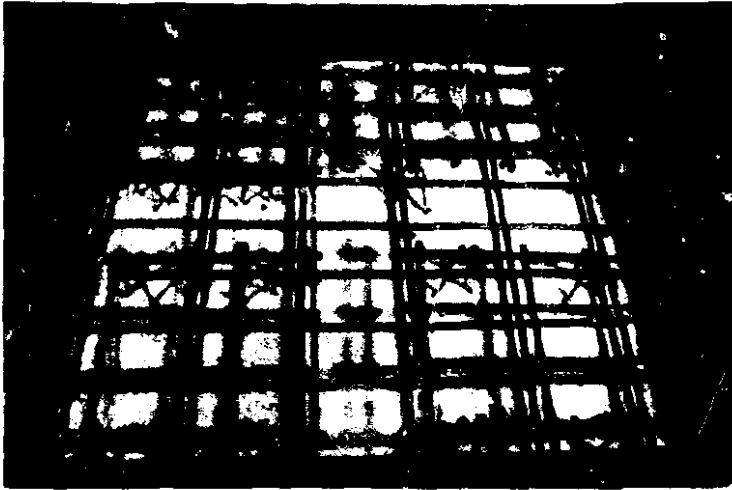
6.4 Effect of Cover

Tests were conducted on Slab A using the equipment and procedures described in Section 5. Ambient temperature was maintained between 70-75°F (21-24°C)

Test results are shown in Table 20. There is a difference of approximately 20,000 coulombs between the areas of highest and lowest cover. There is a good correlation between solution loss, total chloride, and charge passed. Chloride profiles are shown in Figure 52. The high chloride levels close to 1 in. (25 mm) for the slab with 1-in. (25 mm) cover indicate a concentration of chloride at the positively charged rebar. For the deeper covers it is evident that the chloride has not penetrated to the steel during the test period.

The relationship between clear cover and charge passed is shown in Figure 53. The plot was used to obtain the charge passed at nominal covers of 1.0, 2.0, and 3.0 in. The ratios of the charge passed at 1 and 3 in. (25 and 76 mm) to the charge passed at 2 in. (51 mm) are shown in Table 21A.

Cores were taken from this slab and sliced to 1, 2, and 3-in. (25, 51, and 76 mm) thickness. They were then tested



(A) REINFORCING MATS-SLAB A .



(B) REINFORCING MATS-SLAB B

FIGURE 5J. REINFORCING MATS FOR PROTOTYPE TESTING .



(C) REINFORCING MATS - SLAB C

FIGURE 5I. (CONT.) REINFORCING MATS FOR PROTOTYPE TESTING.

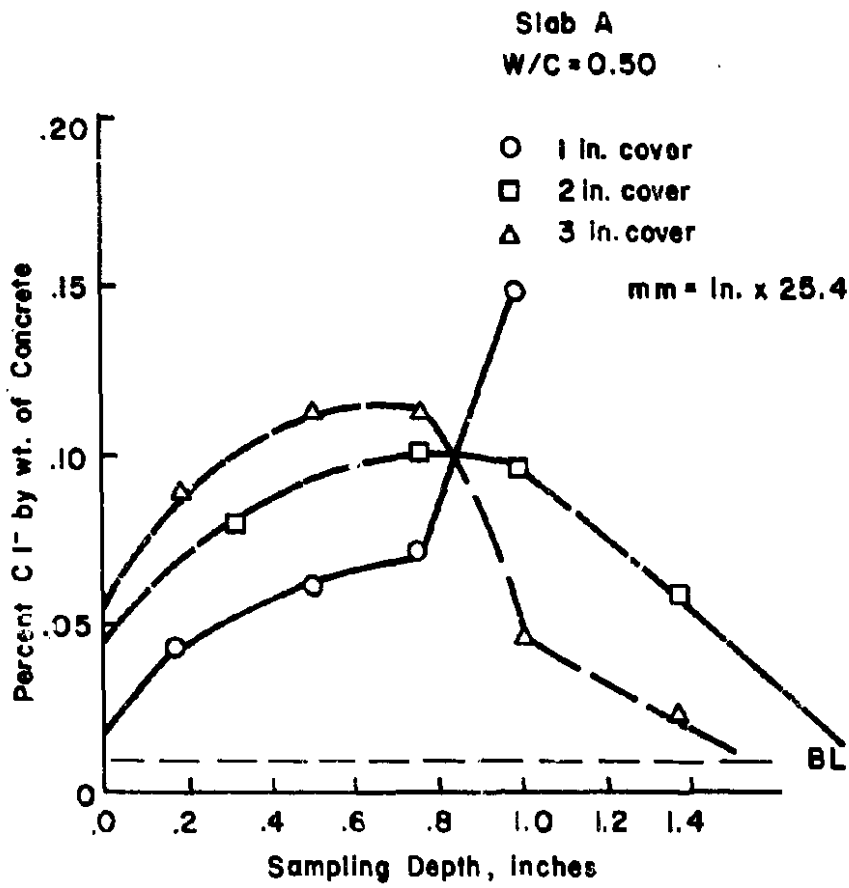


FIGURE 52. CHLORIDE PROFILES FOR VARIOUS CLEAR COVERS.

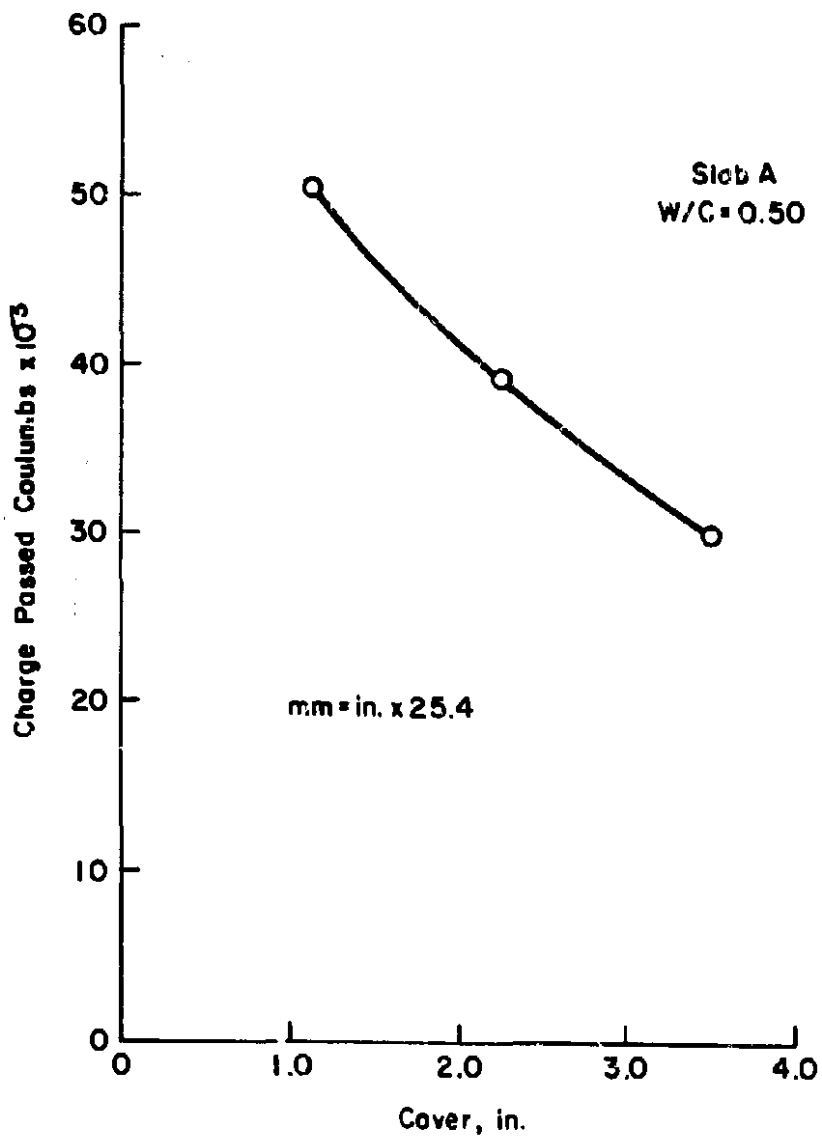


FIGURE 53. COVER VS. CHARGE PASSED.

TABLE 19
CONCRETE MIXTURES
PROTOTYPE TEST SLABS

Mix Quantities (lb/cu yd)^{1/}

	<u>Cement</u>	<u>Water</u>	<u>Sand</u>	<u>Gravel</u>	<u>Cl^{-2/}</u>	<u>Slump^{3/}</u> (in.)	<u>Air</u> (%)
A	422	211	1,311	1,968	0	2.5	6.3
B	423	212	1,316	1,975	0	2.6	6.0
C	423	212	1,306	1,958	5.0	3.5	5.9

1/ kg/m³ = lb/yd³ X 0.594
 2/ Added as CaCl₂ · 2H₂O (40% solution)
 3/ mm = in. X 25.4

TABLE 20
TEST RESULTS
EFFECT OF COVER

<u>Cover</u> (Actual-Inches) ^{1/}	<u>Solution Loss</u> (% Cl ⁻)	<u>Total Integral Cl⁻</u> (Arbitrary Units)	<u>Charge Passed</u> (coulombs)
1.125	0.49	--2/	50,300
2.25	0.37	0.56	39,380
3.50	0.30	0.48	30,008

1/ mm = in. X 25.4
 2/ Samples not taken below 1-in. (see chloride profile - Figure 1)

in the "applied voltage cell" (Appendix 1). Results are shown in Table 21B. Table 21A shows results for the slab tests. The effect of cover in the slab test is less severe than the effect of thickness in the core test. Also shown

(Figure 54) is the relationship between slice thickness and charge passed for both the cores taken from Slab A, where the cement content was 422 lb/yd³ (250 kg/m³) and rounded siliceous

TABLE 21A
SLAB A
EFFECT OF COVER

<u>Cover^{1/}</u> (in.)	<u>Charge Passed^{2/}</u> (coulombs)	<u>Ratio^{3/}</u> (2"/)
1	52,000	0.80
2	41,500	1.00
3	33,200	1.25

TABLE 21B
CORES FROM SLAB A
EFFECT OF THICKNESS

<u>Thickness</u> (in.) ^{1/}	<u>Charge Passed^{2/}</u> (coulombs)	<u>Ratio^{3/}</u> (2"/)
1	6,200	0.49
2	3,050	1.00
3	1,800	1.69

1/ mm = in. X 25.4
 2/ Taken from Figure 53
 3/ Ratio of charge passed at 2 in. (51 mm) of cover to charge passed at indicated cover.

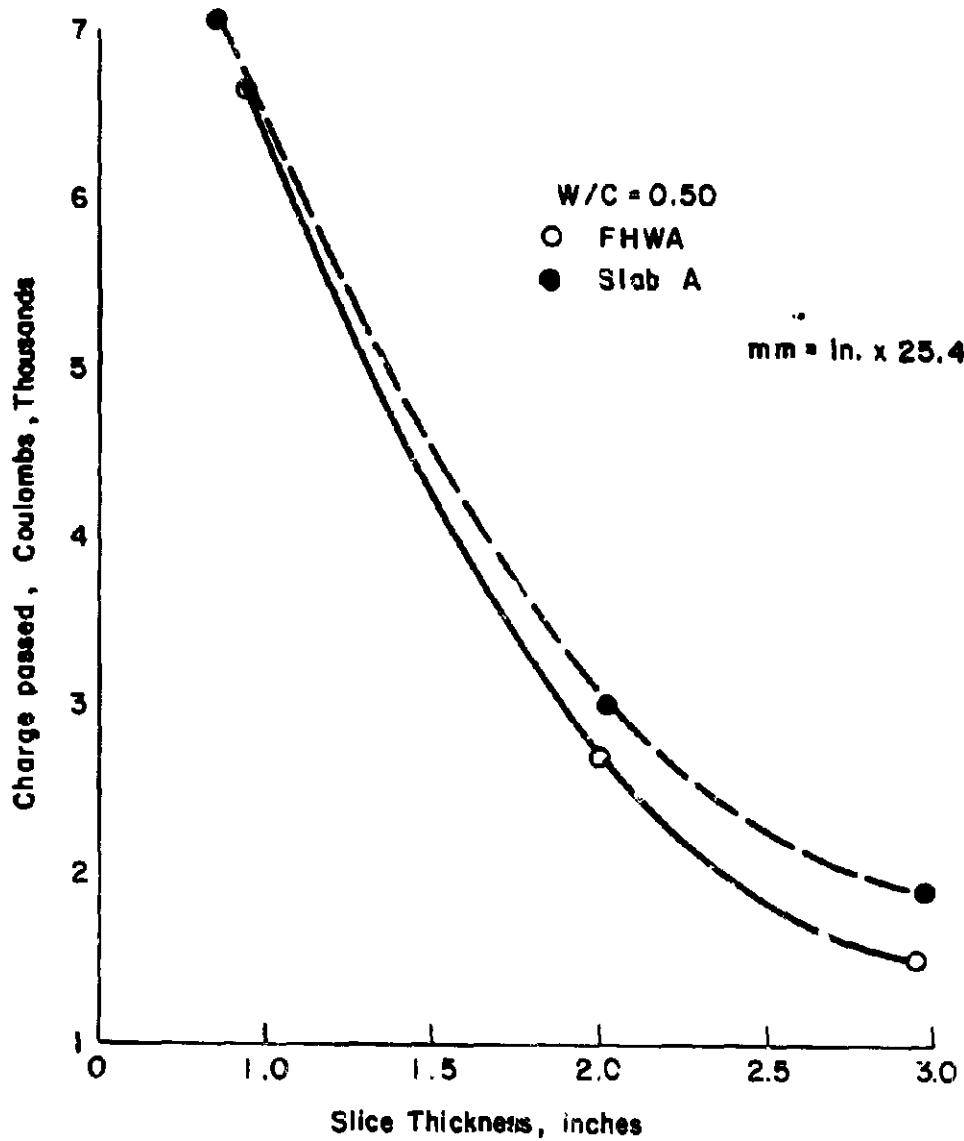


FIGURE 54. COMPARISON OF CHARGE PASSED BETWEEN TWO DIFFERENT CONCRETES HAVING EQUAL W/C RATIOS.

aggregate was used, versus cores taken from the previously tested FHWA slabs, where the cement content was 658 lb/yd³ (390 kg/m³) and angular carbonate aggregate was used. There is very good agreement between the two sets, indicating that mix factors other than w/c ratio have only a minor effect.

6.5 Effect of Reinforcing Cage Geometry

Test results on sections having varying rebar spacings are shown in Table 22. Chloride profiles (not shown) were essentially identical. These results indicate that rebar spacings, at least within the ranges encountered in practice, have no significant effect on the test.

6.6 Effect of Ambient Temperature

The temperature distributions reached after 18 hours of heating the concrete surfaces to 140°F (60°C) are shown in Figure 55. As would be expected, the highest temperatures are reached on the slab stored at 100°F (38°C). The differences between the three conditions are less at the 0.5-in. (13 mm) level and increase at greater depths. A malfunctioning thermocouple prevented obtaining readings at 2.0 in. (51 mm) for the slab stored at 100°F (38°C).

Results for tests conducted at the three temperature levels are shown in Table 23. As expected, charge passed during the test increases with the

TABLE 22
TEST RESULTS
EFFECT OF BAR SPACING

<u>Spacing - top Mat</u>		<u>Solution Loss</u> (% Cl ⁻)	<u>Total Integral Cl⁻</u> (Arbitrary Units)	<u>Charge Passed</u> (coulombs)
<u>Top Steel</u> (inches) ¹	<u>Bottom Steel</u> (inches)			
5	10	0.37	0.56	39,380
6	14	0.34	0.57	41,577
5	5	0.35	0.56	41,404

¹/ mm = in. X 25.4

TABLE 23
TEST RESULTS
EFFECT OF TEMPERATURE

<u>Ambient Temperature</u> (°F) ¹	<u>Solution Loss</u> (% Cl ⁻)	<u>Total Integral Cl⁻</u> (Arbitrary Units)	<u>Charge Passed</u> (coulombs)
40	0.32	0.44	29,292
72	0.37	0.56	39,380
100	-	0.46	42,006

1. °C = 5/9(°F - 32)

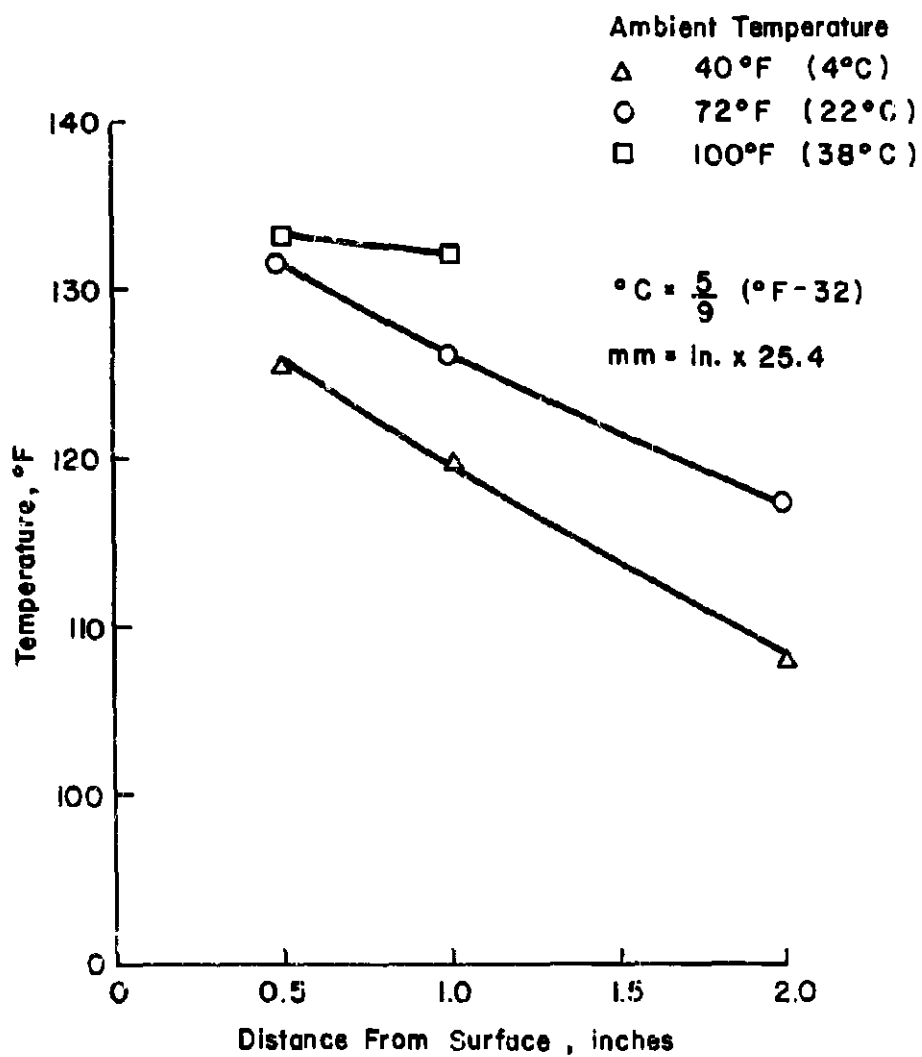


FIGURE 55. TEMPERATURE DISTRIBUTIONS IN CONCRETE SLABS.

increasing ambient temperature. Due to the pretest heat soak of the test area, however, the differences are not as great as would be obtained if one started the test on slabs at the ambient temperature. Results for all temperatures place the concrete into the range of moderately high permeability (30,000 to 50,000 coulombs).

6.7 Test of Chloride-Laden Slab

A slab prepared with 5 lb/yd³ (3 kg/m³) Cl⁻ and 1-in. (25 mm) of concrete cover was subjected to the applied voltage test. The test was carried out in an outdoor test plot, ambient temperature ranged from 80°F (27°C) at the start of test to 87°F (31°C) at the termination. Total charge passed was 52,300 coulombs, close to the value of 50,300 coulombs measured on a chloride-free slab of equal clear cover indoors at 72°F. No signs of concrete distress were seen during the test period. A core taken through the steel at the conclusion of the test showed only very slight corrosion of the steel reinforcing bar, the corrosion products being contained within a 45° arc from top-center of the bar and exuding about 1 mm into the adjacent concrete.

7. FIELD TRIALS

Field trials using the Model 158 Chloride Permeability Instrument were conducted on two bridge decks in the State of Wisconsin during the summer of 1980. The major objective of these field trials was to evaluate the performance of the instrument under actual field conditions. On both sites construction was on-going, thus providing "worst case" conditions for ruggedness testing. A secondary objective was to

interpret the test results in order to gain some information on the permeability of the test sections. The fact that some influences, such as variable overlay depths, are still relatively unquantified limited this objective. Finally, cores were obtained from these two bridges plus one additional structure for evaluation in the laboratory using the applied voltage cell.

7.1 Bridge 1 - Conventional Concrete Deck

7.1.1 Background

The first bridge chosen (Wisconsin B-36-73) was a four-span, conventional poured concrete deck on 70-in. (178 mm) prestressed I-girders. The deck was poured in July of 1979, and is part of a newly constructed interstate highway (I-43). No deicing salt has been applied to this deck. Structural details are given in Appendix 6.

The deck was poured from south to north abutments using crane and bucket techniques. The entire pour was completed in one day. Concrete mix proportions are shown in Table 24.

TABLE 24
BRIDGE DECK CONCRETE

	Quantity (lb/cu yd) ^{1/}
Cement (Type I)	- 658
Sand	- 1,200 (P.M. = 2.72)
Gravel	- 1,800 (3/4-in. ^{2/} maximum size)
Water	- 297 (w/c = 0.45)
WRDA	- 3.81 fl oz/cwt ^{3/}
AEA	- 0.74 fl oz/cwt ^{3/}

1/ kg/m³ = lb/yd³ X 0.594
2/ mm = in. X 25.4
3/ ml/kg = fl oz/cwt X 0.65

Slump and air contents were monitored at frequent intervals during the pours. Slump ranged from a low value of 1.5 in. (38 mm) to a high of 3.25-in. (83 mm). Air contents ranged from an initial low of 2.0% to a high of 7.3%, although the remainder of the readings were much closer to specifications (5.3 to 7.0%). Inspection of the job tickets indicated that the initial truckload (10 cu yd - 7.6 m³) of concrete had approximately 8 gal (30.3 L) more water than the rest of the loads. This load corresponds to approximately the first 10 linear feet of concrete placed from the south bridge abutment. The deck was cured for 7 days under wet burlap after placement. It has been closed to the public since construction, and no deicing salt has been applied.

7.1.2 Test Locations

The bridge plan showing test locations is shown in Figure 56. Field tests were conducted on locations 1-4. Cores 4 in. (102 mm) in diameter were taken approximately 1 ft (0.3 m) away from the test areas and also at location 5. Because of high-speed construction traffic (gravel trucks) all field tests were conducted in the 10-ft (3 m) shoulder area.

7.1.3 Functioning of Equipment

No major problems were encountered with the equipment. The pyrometer, however, used to monitor temperature during the heat/soak period was found to read low due to a heat-sink effect. For this reason, an auxiliary thermocouple was inserted into the chamber through the fluid filling valve and a portable digital thermometer (Fliuke Model 2176A) was used to monitor the temperature of the limewater and saltwater solutions.

The generator was capable of running for up to 14 hours off the 6-gal (22.7 L) auxiliary fuel tank. This required that the investigators return to the test site between 1800 and 1900 hours to refill the gasoline supply.

7.1.4 Test Results

Results of the field testing are shown in Table 25. Values for charge passed and solution loss lie between previous laboratory values for concretes having w/c ratios of 0.4 to 0.5. Although ambient temperature appears to have little significant effect, the effect of clear cover is substantial (see Figure 57). The field results appear more sensitive than previous lab tests. The results do show that at all covers the results for the concrete bridge deck with stated w/c ratio of 0.45 do fall between those for w/c ratios of 0.4 to 0.5.

Analyses of "blank" chloride powder samples taken prior to testing at locations 1 and 3 indicated baseline chloride contents of 0.055 and 0.078% Cl⁻, respectively. This could explain the erratic results for total integral chloride obtained by integration of the chloride profiles (Figure 58), and subtracting the baseline values from the result. As this deck had not been salted, the chloride most likely was due to chloride bearing aggregates used in the concrete mixture. These results indicate that chloride sampling after test is inappropriate where large amounts (> 0.01%) of chloride are detected in the blank samples.

Results on cores taken from locations 1-5 are shown in Table 26.

Reference to Figure 59 shows the core test results (open triangles) in

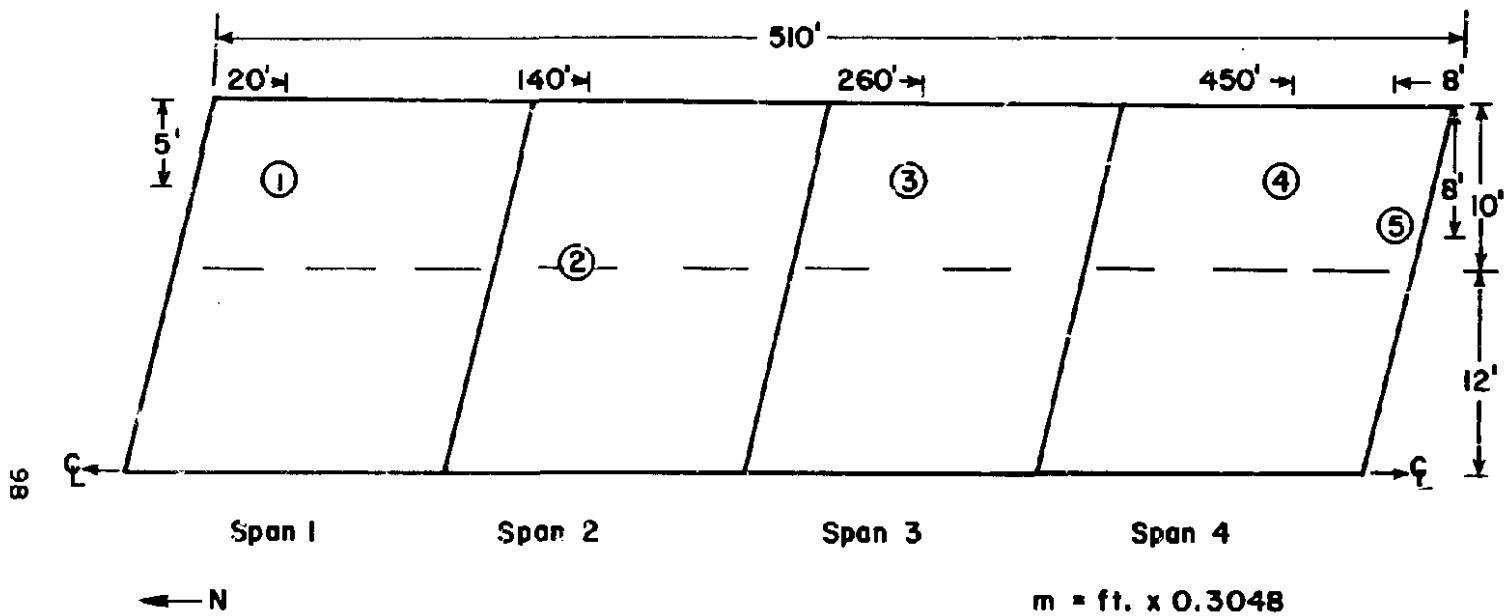


FIGURE 56. DECK PLAN.
 B-36-73 (I-43)
 MANITOWOC, WISCONSIN
 PLAIN CONCRETE DECK

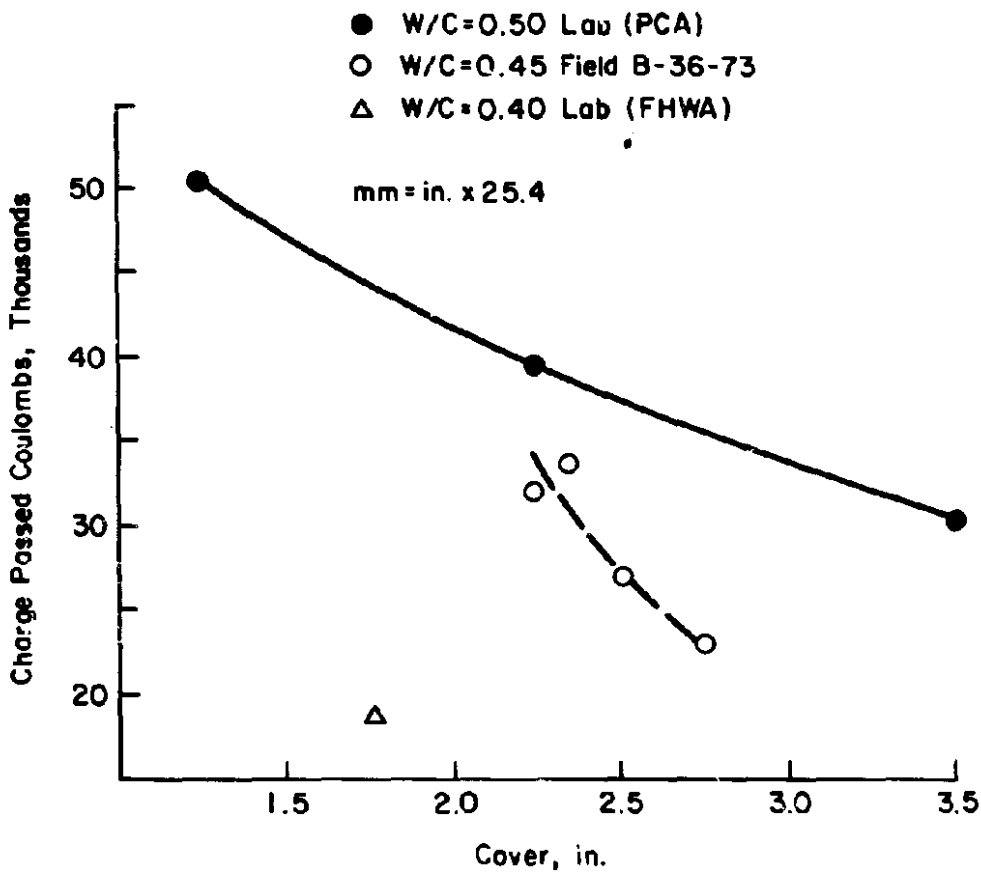


FIGURE 57. CHARGE PASSED VS. COVER FOR FIELD AND LABORATORY TESTS,

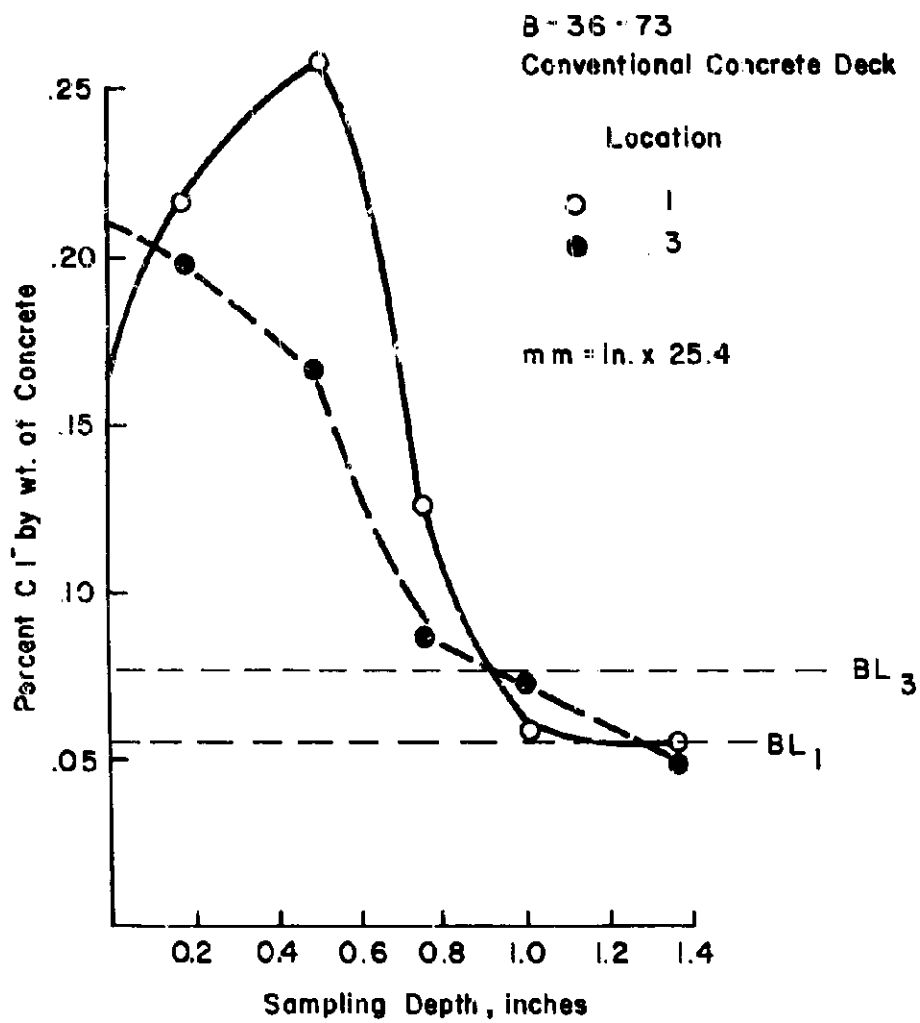


FIGURE 58. CHLORIDE PROFILES FOR CONVENTIONAL DECK.

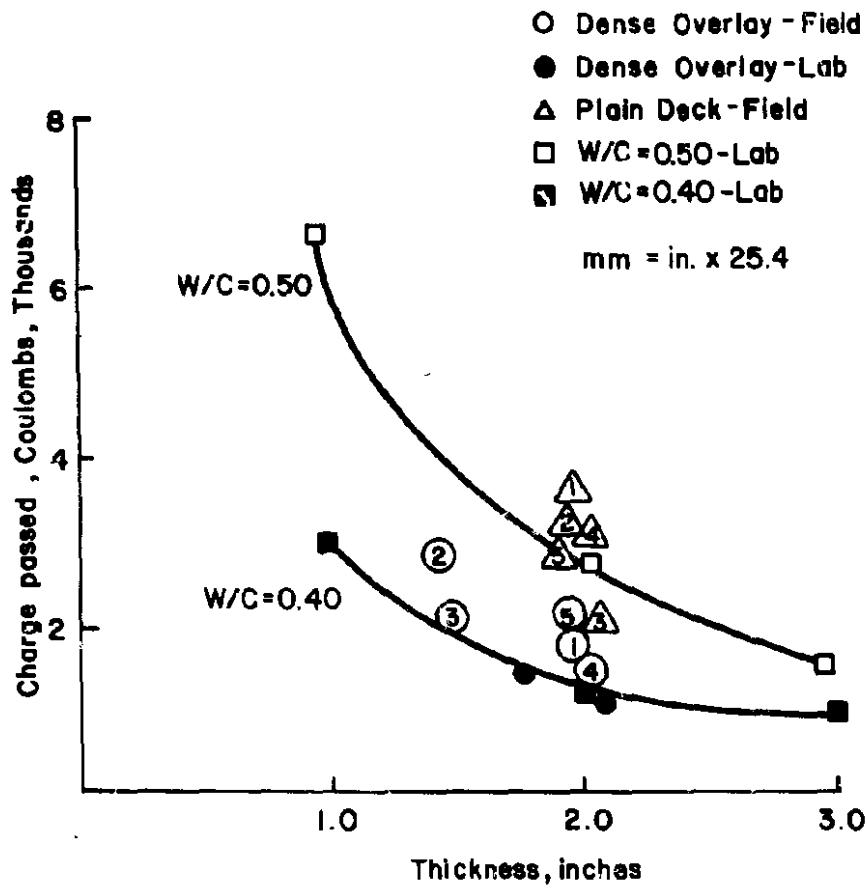


FIGURE 59. COMPARISON OF CORE TEST RESULTS WITH PREVIOUS DATA.

TABLE 25**FIELD TEST RESULTS****Conventional Deck - Manitowoc Rapids, Wisconsin**

Location	Cover ^{1/2/} (in.)	Air Temp. Range (°F) ^{3/}	Charge Passed (coulombs)	Solution Loss (% Cl ⁻)	Total Integral Chloride ^{4/}
1	2-1/4	72-87	31,990	0.30	0.66
2	2-1/2	61-68	26,680	0.25	-
3	2-3/4	66-71	22,672	0.22	0.33
4	2-3/8	54-69	33,646	0.35	-

1/ Measured approximately 5 in. (127 mm) outside actual test area on transverse bar
2/ mm = in. X 25.4

3/ °C = 5/9(°F - 32)

4/ Corrected for baseline values

comparison to previous data. With the exception of location 3, all results are close to those obtained on w/c = 0.50 in previous tests. This result for location 3 is much lower, checking the low field test result at this location. In general, the core test results when compared with previous data would indicate an effective w/c ratio equal to or slightly greater than 0.50. The field results, at covers close to 2.0 in., indicate an effective w/c ratio somewhat less than 0.50.

TABLE 26**CORE TEST RESULTS****Conventional Concrete Deck**

Location	Slice Thickness (in.) ^{1/}	Charge Passed (coulombs)	Solution Loss (% Cl ⁻)
1	1.98	3,462	0.35
2	1.93	3,160	0.33
3	1.98	1,972	0.21
4	1.96	2,938	0.34
5	1.96	2,623	0.29

1/ mm = in. X 25.4

7.2 Bridge 2 - Dense Concrete Overlay**7.2.1 Background**

The second bridge (Wisconsin B-41-62) was a three-span conventional poured concrete deck on 36-in. (914 mm) prestressed I-girders. A dense concrete overlay had recently been applied to the deck as part of a highway rehabilitation program, encompassing approximately 15 mi. (24.1 km) of Eastbound I-94 between Millston and Warrens, Wisconsin. The initial structure was completed in 1965. The overlay was placed in June of 1980. No deicing salt had been applied to the overlay; chloride contents had not been determined on the original deck. Structural details are given in Appendix 6.

7.2.2 Overlay and Test Locations

A dense ("Iowa Method") portland cement concrete overlay was placed over the original deck surface in June 1980. Mix design is shown in Table 27.

TABLE 27

DENSE OVERLAY CONCRETE

Quantity (lb/cu yd)^{1/}

Cement - 823
 Sand - 1,372 (P.M. = 2.73)
 Gravel - 1,372 (3/4-in.^{2/} maximum size)
 Water - 206 (w/c = 0.25)

Quality Control Testing

Slump (45 min. intervals) - 3/4 in.
 1/2 in., 3/4 in.

Air (45 min. intervals) - 5.6%, 5.8%,
 5.4%

^{1/} kg/m³ = lb/yd³ x 0.594
^{2/} mm = in. x 25.4

Slump and air content tests taken during the 2-hour pour indicate good uniformity. The concrete was mixed in a "Concrete-Mobile." The overlay was placed to a plan depth of 2.375 in. (60 mm). Transverse grooves 0.125-in. (3 mm) wide, 0.0625-in. (2 mm) deep and spaced 0.75 in. (19 mm) apart were made in the fresh concrete in order to provide improved skid resistance.

The overlay was approximately 2 months old at time of testing. Bridge deck plan and test locations are shown in Figure 60. Complete tests were carried out on locations 1 to 4. On location 5 a core only was obtained for later lab testing. Heavy construction traffic restricted our testing for the most part to the 5-ft-6-in. (1.7 m) shoulder lane.

7.2.3 Test Results

Test results are shown in Table 28. Results range from a high of 17,690 coulombs at location 1 to a low of 9,250

coulombs at location 2. Solution loss values correlate well with charge passed. Chloride profiles for locations 1 through 4 are shown in Figure 61. They are closer than would be expected from the difference in charge passed and solution loss between four locations. The highest total integral chloride value (location 4) is 50% greater than the lowest (location 2), but the highest charge passed value (location 1) is almost double the lowest (location 2). Additionally, the highest total chloride (location 4) is not associated with the highest charge passed (location 1). The lowest chloride values, however, are associated with the lowest charge passed (location 2). Current vs time curves are shown in

Figure 62. The cause of the high currents associated with location 1 could not be readily ascertained. Maximum air temperature was somewhat higher for this location, but cover for location 1 was greater than any of the other locations. Additionally (see Table 29), a core taken 1 ft (305 mm) from the test section showed an overlay thickness of 2.52 in. (64 mm), greater than that of the other test sections. It is perhaps possible that immediately inside the actual test area the overlay thickness was less; this could not be verified because no additional coring was allowed from this deck.

Cores taken from this deck were then tested in the applied voltage cell. Core slices were cut at the substrate/overlay interface. Test results are shown in Table 30. Figure 59 (page 101) shows the test results in comparison with previous tests in the cell. Locations

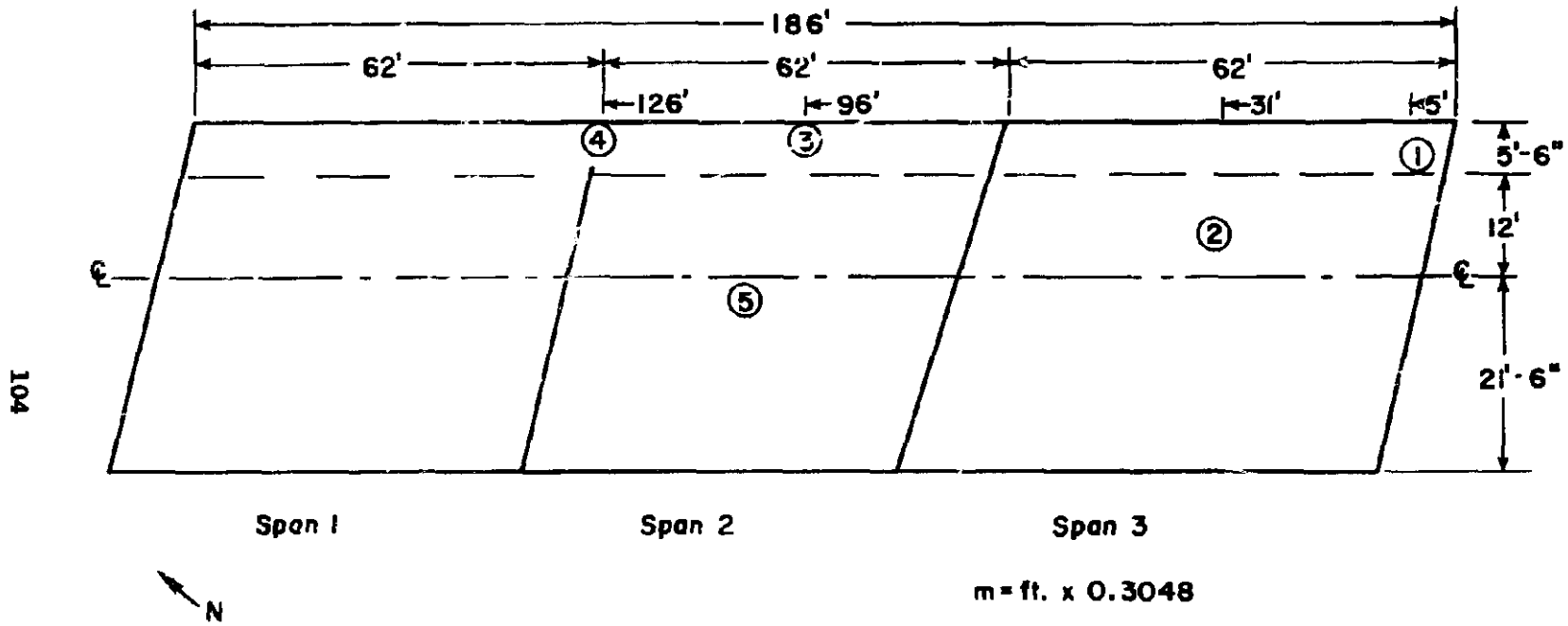


FIGURE 60. DECK PLAN.
 B-41-62 (1-94)
 LINCOLN, WISCONSIN
 DENSE CONCRETE OVERLAY

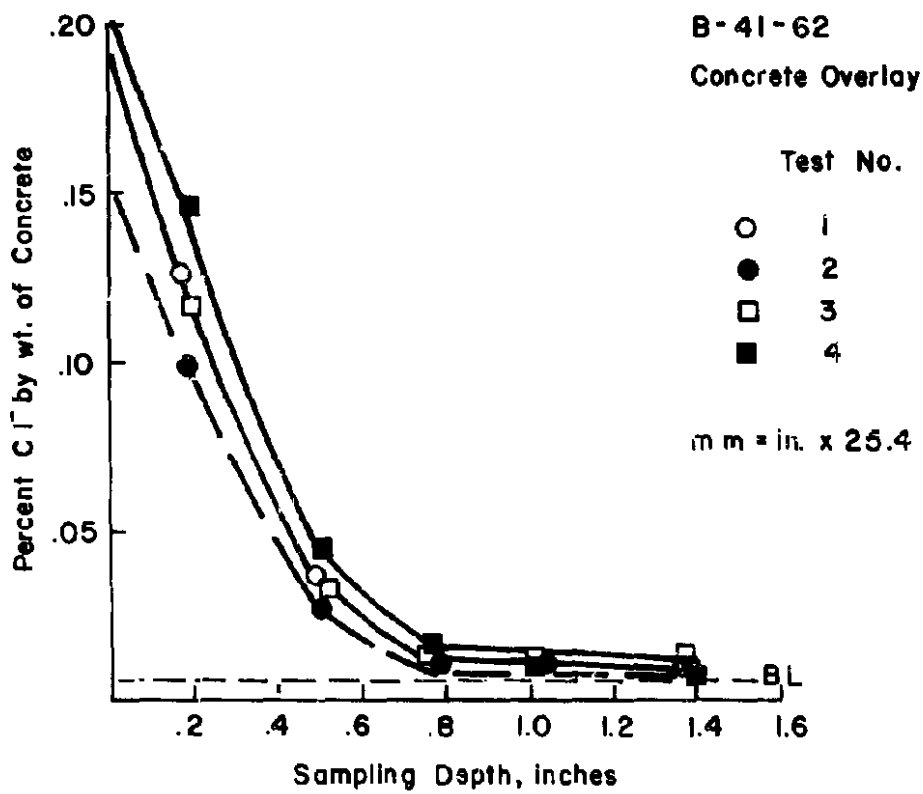


FIGURE 61. CHLORIDE PROFILES - DENSE CONCRETE OVERLAY.

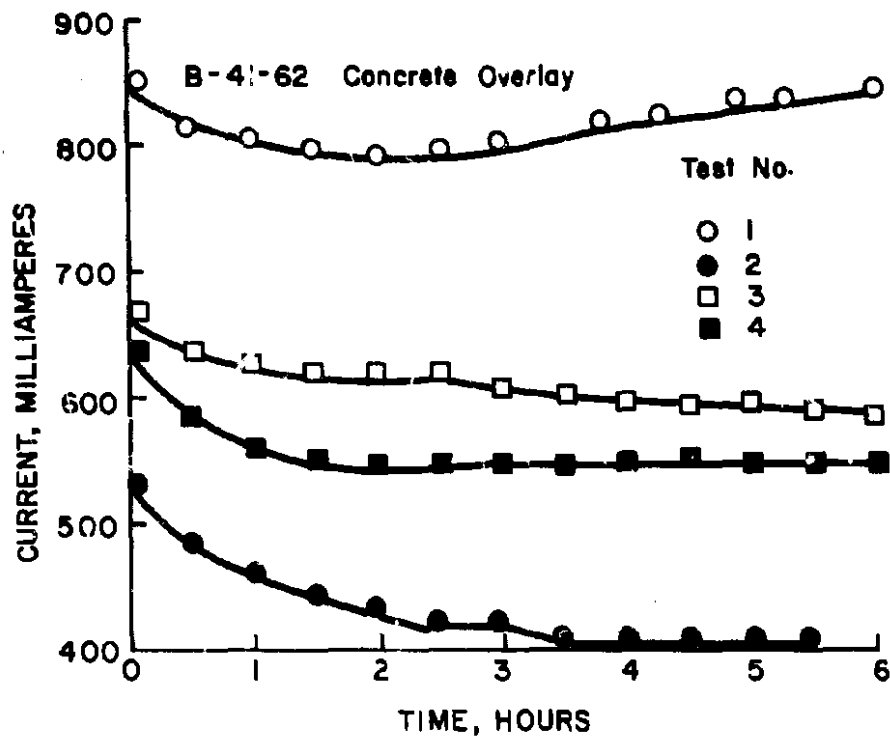


FIGURE 62. CURRENT VS. TIME DENSE CONCRETE OVERLAY.

TABLE 28

FIELD TEST RESULTS

Dense Concrete Overlay - Lincoln, Wisconsin

Location	Cover ^{1/} (in.) ^{2/}	Air Temp. Range (°F) ^{3/}	Charge Passed (coulombs)	Solution Loss (% Cl ⁻)	Total Integral Chloride
1	4-1/2	65-88	17,690	0.29	0.27
2	4-1/8	67-79	9,250	0.10	0.22
3	3-7/8	73-82	13,390	0.24	0.27
4	4-1/4	67-79	12,190	0.17	0.33
Average	4-3/16		13,130	0.20	0.27

^{1/} Measured approximately 5 in. (127 mm) outside actual test area on transverse test bar

^{2/} mm = in. X 25.4

^{3/} °C = 5/9 (°F - 32)

TABLE 29

OVERLAY THICKNESS^{1/} - Inches^{2/}

Location	Maximum	Minimum	Average
1	2.75	2.43	2.52
2	2.04	1.51	1.78
3	1.75	1.50	1.60
4	2.56	2.125	2.30
5	2.90	2.40	2.57

^{1/} Measured on cores taken approximately 1 ft (305 mm) from test area

^{2/} mm = in. X 25.4

TABLE 30

CORE TEST RESULTS

Dense Concrete Overlay

Location	Slice Thickness (in.) ^{1/}	Charge Passed (coulombs)	Solution Loss (% Cl ⁻)
1	1.98	1,846	0.07
2	1.45	2,846	0.17
3	1.48	2,015	0.06
4	1.98	1,480	NA
5	1.97	1,988	0.13

^{1/} mm = in. X 25.4

are denoted by numerals inside the open circles on the plot. All results lie above the line denoting a w/c ratio of 0.40. Locations 2 and 5 appear to suggest a w/c ratio close to 0.45.

These results indicate higher permeabilities than previously encountered with dense overlay materials prepared in the lab (closed circles), and also conflict with the field test results. The

field tests, however, included approximately 2 in. (51 mm) of substrate material in the test sections. The tests done on slabs prepared by FHWA had only 1 in. (25 mm) of substrate concrete beneath the 2-in. (51 mm) overlay. Therefore, the total concrete thickness between the surface solution and the steel was approximately 1 in. (25 mm) greater in the field tests than in the lab tests. The field test results are thus overly optimistic if one makes a direct comparison without considering

the difference in cover. Obviously, much more work will have to be done in the future so that a data base encompassing various overlay and substrate thicknesses can be compiled.

In summary, the core (cell test) results are more reliable than the field test results for this deck. These results indicate that this concrete is comparable to an ordinary high quality concrete (w/c = 0.40 - 0.45) and not to a low permeability, low w/c ratio (less than 0.35) dense mixture.

7.3 Bridge 3 - Polymer-Concrete Overlay

On the third structure, cores for evaluation via the laboratory applied voltage cell were obtained. No field testing was done.

7.3.1 Installation of Overlay

The overlay was installed on South Fork Ash Creek Bridge (No. 491A) in Independence, Oregon. The bridge roadway was 81-ft (24.7 m) long by 38-ft (11.6 m) wide. The deck condition was good with no delaminations detected. Chloride content was below 0.003% by weight of concrete. The deck was sandblasted prior to polymer-concrete application in order to remove dirt, oil and surface moisture.

The monomer chosen was a thermosetting, medium viscosity vinyl ester resin (Derakane 411-C-50, Dow Chemical Corp.). Other chemical constituents added to the mix are given in Table 31A, showing the amount added to each layer of the overlay system. The aggregate used was Wedron E1-8 washed and dried sand, having the gradation given in Table 31B.

Just prior to application of the first resin coat, the initiator (MEK) was added. The resin was then poured onto two, 20-ft long (6.1 m) sections of two lanes. The resin was brushed across the surface, resulting in an application rate

TABLE 31A
RESIN FORMULATION
POLYMER CONCRETE OVERLAY

Chemical Component	Layer	
	1	2-4
	% of Monomer by Weight	
Surfynol 400	1.0	0.0
Silane A174	1.0	1.0
Cobalt Naphthronate (12% Cobalt)	0.15	0.15
Dimethyl Aniline	0.05	0.05
Methyl Ethyl Ketone Peroxide	1.0	1.0

TABLE 31B
SAND GRADATION
POLYMER CONCRETE OVERLAY

Sieve Size	% Passing
8 (2.36 mm)	96
12 (1.70 mm)	66
16 (1.18 mm)	19
20 (850 μ m)	6
30 (600 μ m)	2.5

of 2.0 lb/yd² (1.1 kg/m²). Aggregate was then spread over the resin at a rate of 15 lb/yd² (8.2 kg/m²) and compacted with a larger pneumatic roller. The first layer was allowed to cure for 2 hours, unbonded aggregate was removed, and the second layer was then cast. Resin loading on this and subsequent layers was 3.5 lb/yd² (1.9 kg/m²); aggregate loading was the same as for the first layer. A two hour cure was allowed between the second and third, and the third and fourth layers. Three hours after placing the fourth layer the lane was reopened to traffic. The remaining sections of the deck were completed the next day.

7.3.2 Test Results

Four cores were extracted from the deck and shipped to PCA/CTL for testing in the applied voltage cell. Total core

slice thickness, overlay thickness, and charge passed are shown in Table 32. It is easily seen that all cores exhibited zero charge passed during the test period of 6 hours. Resistance measured across the cell was greater than 10^6 ohms in all cases, confirming the dielectric nature of the overlay.

TABLE 32
POLYMER-CONCRETE CORES
TEST RESULTS

Cores	Thickness - Inches ^{1/}		Charge Passed (coulombs)
	Total Slice	Overlay	
1	1.92	0.82	0
2	1.97	0.80	0
3	1.95	0.80	0
4	1.98	0.82	0

^{1/} mm = in. x 25.4

7.4 Safety Considerations

The possibility always exists that external metallic bridge members, such as handrails, guardrails, steel beams, and electrical conduit may be electrically connected with the reinforcing mats in the deck slab. If the return path to the test area were sufficiently conductive, personnel might achieve a lethal shock by touching an exposed metallic surface. To check this possibility, voltage drops between an aluminum handrail and the concrete surface were determined during an actual test. The curb area was wetted prior to test. Except for areas less than 8 in. (200 mm) from the test dike, the voltage drop between the railing and the deck was less than 1 volt. Assuming that the pin connection and test cell are covered, a potentially hazardous situation would arise only if the test area were immediately adjacent to the exposed metallic member, such as at a curb line. In this case, nonconductive footwear should be

worn and personnel should stay clear of the cell during application of the 80.0 volts.

8. OTHER TECHNIQUES

Although the major aim of this project was to develop the applied voltage technique, a limited amount of effort was devoted to evaluation of other candidate techniques. These included water-vapor transmission (WVT), air permeability, and four-pin resistivity. Brief summaries of the testing and results follow. The four-pin resistivity method is described in more detail in Appendix 5.

8.1 Water Vapor Transmission (WVT)

Core slice specimens, 2x4 in. (51x102 mm), were prepared in a manner similar to that used for the applied voltage cell test, the periphery being coated with epoxy and the specimen then vacuum saturated overnight. The test apparatus was identical to the applied voltage cell (minus the mesh screens and electrical connectors), with the exception that the left side reservoir was fitted with a 4 mm I.D. capillary sight tube approximately 36-in. long. A mm scale was affixed to the tube. Prior to test, the left side of the cell was filled with tap water and into the right side was placed approximately 60 gm of "drierite" desiccant (CaSO₄) contained in a nylon mesh bag. The entire apparatus (with the exception of the sight tube) was then placed in a water bath maintained at $80 \pm 0.2^\circ\text{F}$ ($27 \pm 0.1^\circ\text{C}$). The apparatus was allowed to equilibrate for 2 hours, then capillary readings were taken at hourly intervals. Results on slices where 1/4 in. (6 mm) of material was removed from the surface are presented in Figures 63 and 64 for full-

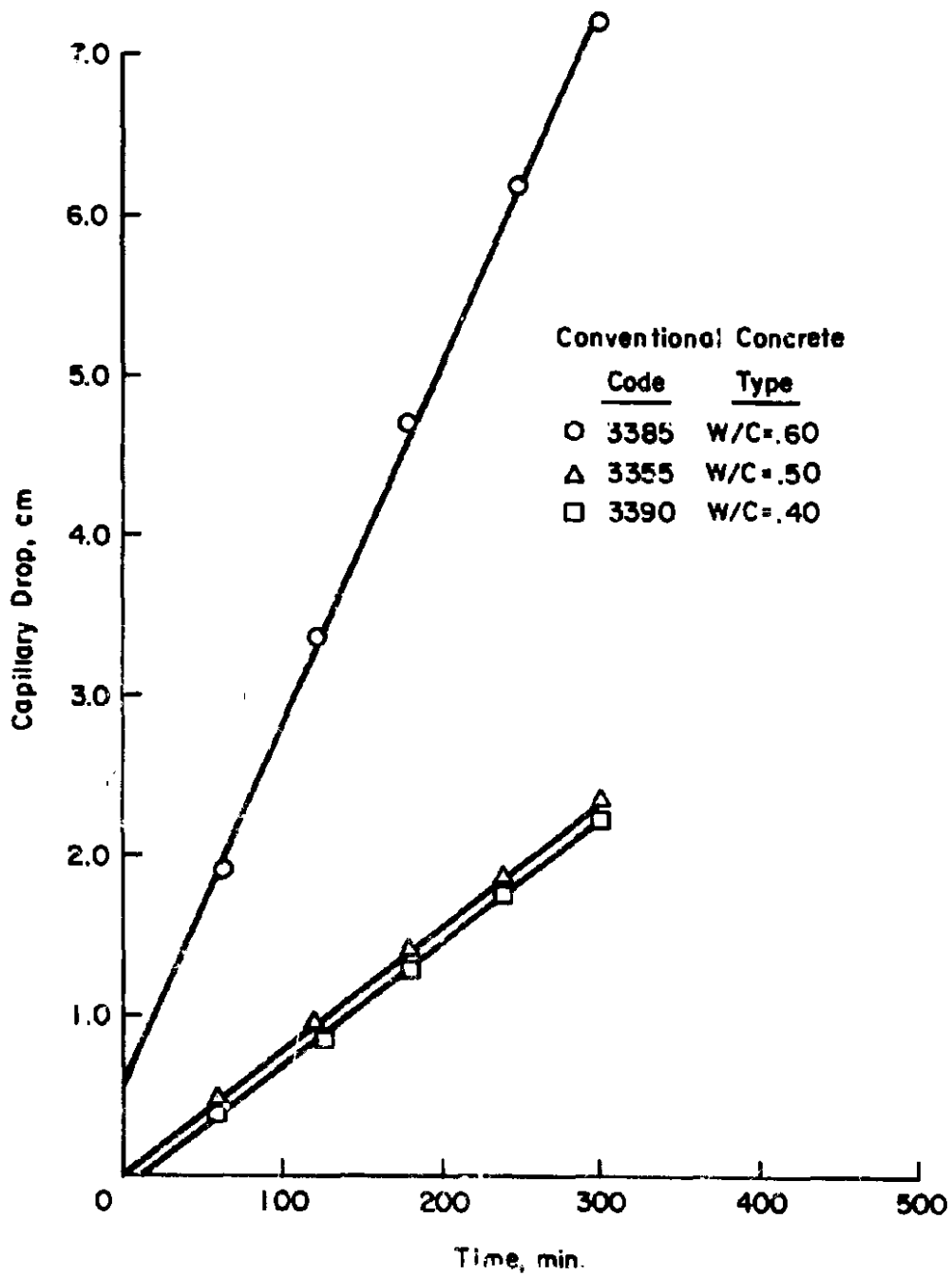


FIGURE 63. WVT TEST - CONVENTIONAL CONCRETES.

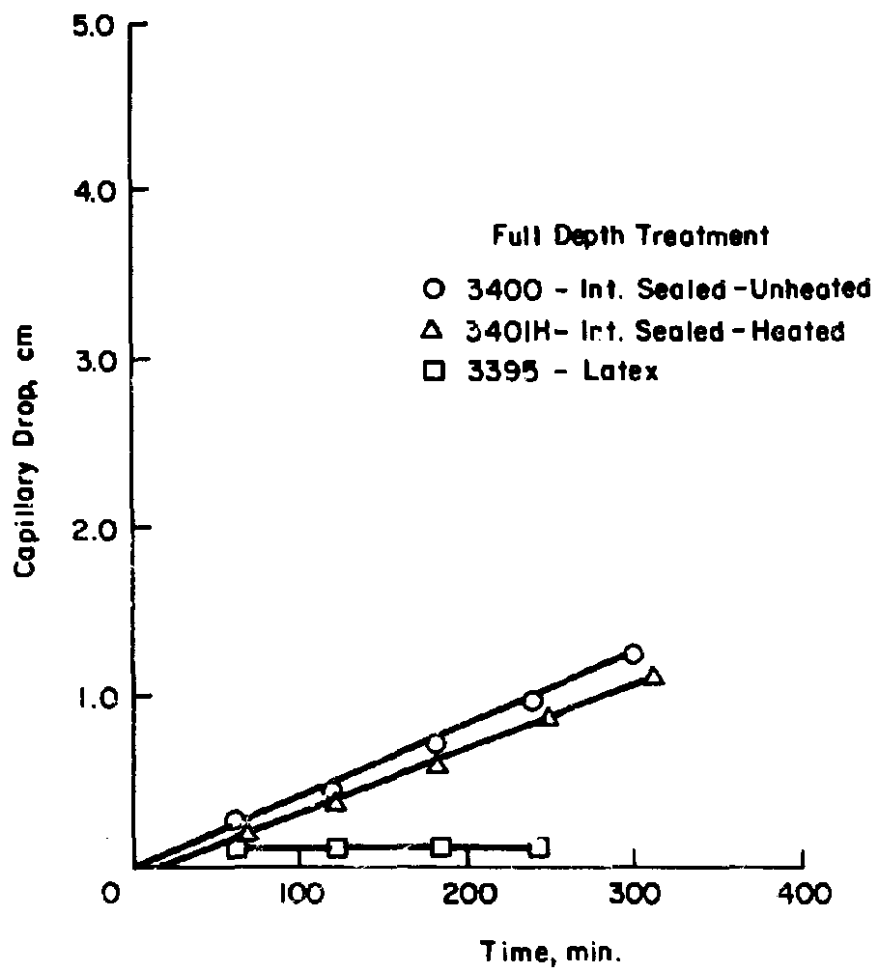


FIGURE 64. WVT TEST - FULL-DEPTH TREATMENTS.

depth materials and Figure 65 for overlays. In order to quantify the results, the drop in the level of water in the capillary was converted to a permeability coefficient by the following formula:

$$K = \frac{P \cdot F \cdot L}{A}$$

where K = permeability coefficient (g/cm²·s)
 p = mass of water per unit capillary length (g/cm)
 F = rate of capillary drop (cm/s)
 L = length of specimen (cm)
 A = area of specimen (cm²)

Permeability coefficients are given in Table 33. The materials appear to line up generally in the expected order of permeabilities. The essentially equal

TABLE 33
 WATER VAPOR TRANSMISSION RESULTS

Slab	Description	Permeability Coefficient K (gm/s·cm X 10 ⁻⁷)
3385	w/c = 0.60	19.9
3355	w/c = 0.50	5.87
3390	w/c = 0.40	6.65
3400	Int. Seal - Unheated	3.81
3401H	Int. Seal - Heated	3.37
3395	Latex - Full Depth	0.30
3380	Iowa - Proper	0.39
3375	Iowa - Improper	0.21
3370	Latex Overlay	0.16
3360	Int. Seal - Overlay-Unheated	0.51
19-93	P.I.C. - Full Depth	0

permeabilities of the 0.5 and 0.4 water-cement ratio concretes were confirmed by later FHWA 90-day chloride ponding tests. The technique, however, failed to distinguish between heated and unheated internally sealed concretes, and showed anomalous results when applied to

properly and improperly consolidated "Iowa" concretes. Furthermore, some specimens exhibited an anomalous rise in capillary column height during the test period. As workers at the Kansas Department of Transportation (32) were developing more refined techniques for WVT testing, it was decided to terminate this phase of the investigations at PCA and devote principal emphasis to development of the applied voltage technique.

8.2 Air Permeability

Two sets of 2x4-in. (51x102 mm) slices (one set with two sawed faces and one set with one finished face) were dried in a forced-draft oven at 140°F (60°C) for 24 days. At this point weight loss was less than 0.5 gm per 48-hour period. The specimens were then individually wrapped in Saran and aluminum foil, sealed in "Ziplok" bags containing a small amount of drierite, and shipped to a commercial laboratory for air permeability testing.

The specimens were tested at 32 psig (220 kPa) using dried air. They were sealed into a test chamber by application of external pressure to a rubber boot surrounding the periphery of the specimen. In this manner air flow was restricted to the longitudinal direction. Readings were taken on flow meters until a steady-state was achieved. For these specimens this equilibration time was about 15 minutes. The permeability (in millidarcys) was then calculated from the following expression:

$$k = \frac{2\mu \cdot Q_2 \cdot P_2 \cdot L}{A(P_1^2 - P_2^2)} \times 10^3 \quad (11)$$

where k = permeability, millidarcys (m²)
 μ = gas viscosity, centipoise (Pa·s)

1/ Core Laboratories, Inc., Dallas, Texas.

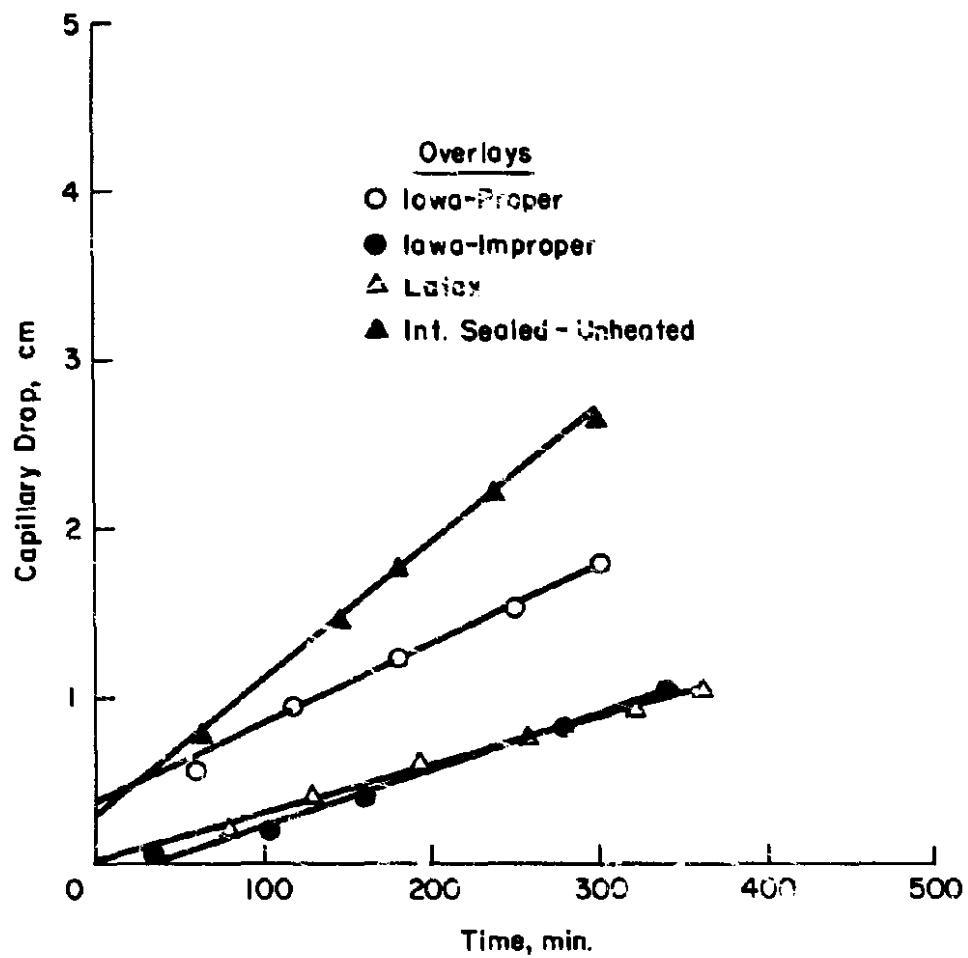


FIGURE 65. WVT TEST - OVERLAYS.

Q_2 = volume flow rate, cc/s (m^3/s)
 P_1 = inlet pressure, atmos (Pa)
 P_2 = outlet pressure, atmos (Pa)
 L = flow length, cm (m)
 A = test specimen area, cm^2 (m^2)

Unfortunately, it was not possible to obtain further details on the specific equipment or test procedures used to perform the air permeability testing.

Results are presented in Table 34. Although results for conventional con-

crete are reasonable, there are discrepancies for the data on the modified concrete systems. For example, latex concrete shows lower air permeability than heated internally sealed concrete. It is possible that, if the capillary spaces in internally sealed concrete are only partially filled with melted wax, then relatively high air permeabilities could be maintained, while water (or chloride solution) permeability would decrease due to a hydrophobic effect.

TABLE 34

AIR PERMEABILITY RESULTS

<u>Slice</u>	<u>Type</u>	<u>Air Permeability</u> <u>(nd)</u>	<u>Average</u> <u>(nd)</u>
3385 - 1A - 1B	w/c = 0.60	0.12 0.16	0.14
3355 - 1A - 1B	w/c = 0.50	0.10 0.12	0.11
3390 - 1A - 1B	w/c = 0.40	0.03 0.09	0.06
3400 - 1A - 1B	Int. Seal. Full Depth	0.05 0.06	0.06
3400H - 1A - 1B	Int. Seal. Full Depth-Heated	0.01 0.01	0.01
3395 - 1A - 1B	Latex - Full Depth	<0.01 <0.01	<0.01
3380 - 1A - 1B	Iowa - Proper	0.04 0.03	0.04
3375 - 1A - 1B	Iowa - Improper	0.04 0.07	0.06
3370 - 1A - 1B	Latex Overlay	0.04 <0.01	
3360 - 1A - 1B	Int. Seal. Overlay	0.01 <0.01	
19-93 - 1A - 1B	P.I.C. - Full Depth	<0.01 0.03	
3410 - 1	P.C. Overlay + Base Course 2 in. total thickness	<0.01	<0.01
3410 - 2	P.C. Overlay Only 0.5 in. thickness	<0.01	<0.01

NOTE: A = slice includes top finished surface
 B = 0.25 in. cut off finished surface

$\frac{1}{2} \frac{nd}{cm} = \frac{nd}{in.} \times 1.01 \times 10^3$
 $\frac{1}{2} \frac{nd}{cm} = \frac{nd}{in.} \times 25.4$

Unheated internally sealed concrete has an air permeability essentially the same as conventional concrete with w/c = 0.40; a higher value is expected. In addition, the duplication appears to be poor in some cases (see results for Slices 3370-1A and 1B, 19-93 1A and 1B).

It is possible that some of these anomalies can be traced to the drying given to the slices prior to test. Drying is a necessity prior to air permeability testing. The literature review showed that moisture content can have a strong influence on results. In view of the somewhat questionable results, the lack of precise information on test equipment and procedures, and the difficulty of adapting such a test to a field situation, further developmental work on this technique was halted.

8.3 Depth of Impermeability - Resistivity Technique

A method previously used (42) for determining depth of polymer impregnation using a four-pin resistivity technique was applied to some of the FHWA slabs. This work was carried out by Professor Carl Locke of the University of Oklahoma and a student assistant. A description of the tests and analysis of the data is included as Appendix E.

The general conclusion derived from these tests was that the technique was not sufficiently sensitive to determine the difference in resistivity occurring at the overlay/base course interfaces for the materials used in this study. Additionally, we have seen that surface-heated internally sealed concrete has no sharp line of demarcation separating heated and unheated levels, but rather contains a continuum of material heated to various degrees, which reflects the temperature gradient established in the slab at the time of heat treatment.

Thus, there is no unique "depth of impermeability" for this case.

9. SUMMARY, CONCLUSIONS AND RECOMMENDATIONS

9.1 Summary and Conclusions

9.1.1 General

A portable instrument has been developed for measuring chloride permeability of various types of concrete both in-situ and in the laboratory. The instrument relies on the accelerated migration of negatively charge chloride ions toward a positive electrode under the influence of an applied voltage field. In the field mode the topmost reinforcing mat is used as the positive electrode; in the laboratory a specially designed test cell is used to hold a 3.75-in. (95 mm) diameter core test specimen. Both modes utilize a 3.0% sodium chloride solution as the permeant.

The field (in-situ) test is carried out over a two-day period. Although the application of voltage lasts only 6 hours, laboratory testing indicated that extremely dry concrete would produce anomalous test results. For this reason, a vacuum/heat soak cycle utilizing lime-water was developed and a portable field vacuum/heat chamber was constructed. Prior to actual test, the test area, measuring approximately 121 in.² (780 cm²), is placed under vacuum for 1 hour and then ponded with lime-water maintained at 140°F (60°C) for 10 hours. The lime-water is then removed and 80.0 Vdc is applied to the chloride solution for a period of 6 hours. After completion of the test, the concrete may be sampled for chloride content using standard techniques.

For the laboratory test, a similar procedure is used although the soak solution is not heated. In this case,

60.0 Vdc is applied across the core specimen. The reproducibility of the test was established for multiple specimens taken from the same concrete slab. It is of the order of 6-8 percent coefficient of variation.

Data which can be generated include total electrical charge (in coulombs), loss of chloride from the test solution, and total chloride contained in the drill sample (field test only). Correlations have been established between these parameters and FHWA 90-day ponding data. For the field technique, a correlation coefficient of 0.92 and standard error of 31% have been established for the relationship between charge passed and total chloride after 90-days of ponding. For the laboratory test, a correlation coefficient of 0.83 and standard error of 39% have been established for the same relationship. Because of the relatively high standard errors, the test is best utilized to rank concretes in terms of their relative expected permeability rather than as a predictor of 90-day ponding results.

9.1.2 Effects of Test Variables

The most important variable to be considered is that of clear cover. In the laboratory version, where core specimens are utilized, a standard thickness, usually 2 in. (51 mm) can be specified. When cores taken from overlays are to be tested, the core can be sectioned so as to include only the overlay material. Test results can then be compared to results obtained on specimens of the same thickness from a variety of concrete. The laboratory procedure shows obvious advantages over the field test because effects of cover and temperature can be eliminated.

For the field test the only complete set of data encompassing all concrete

types are for slabs having 2 in. (51 mm) of clear cover. Limited laboratory testing on a single concrete type over a range of covers from 1-3 in. (25-75 mm), indicates that charge passed may vary ± 20 percent from the values obtained at 2-in. (51 mm) cover. It is not yet known whether this can be universally applied. Additionally, no means are yet available for analyzing field test results where overlay and substrate thicknesses vary from those obtained on laboratory specimens.

Ambient temperature has been found to be important over the range of 40-100°F (4-38°C) but had little apparent influence under the smaller diurnal fluctuations encountered during actual field testing. In order to make the test applicable to a wide variety of environments and concretes, however, more data will need to be developed on this aspect of the testing.

Other variables, such as reinforcement cage geometry, concrete mix design factors, and chloride content of concrete prior to test have been found to exert only minor influences on the test results.

9.1.3 Ease of Operation

The entire field test can be conducted by one person plus an assistant. No specialized knowledge other than instruction and training in the use of the equipment is needed. Obtaining cores for the laboratory test presents no problems not ordinarily encountered in coring highway structures. Running the field test in-situ, however, requires that the section being tested be closed to traffic for at least 30 hours continuously for each test. Additionally, the test chamber and auxiliary generator must be left in operation at the test site overnight.

9.1.4 Safety Considerations

As with all electrical devices operating off line voltage, caution must be exercised. Personnel should keep clear of the test cell, pin connection, and lead wire terminations while the 80 volts is being applied. If the test area is close enough to exposed metallic surfaces (such as handrails, steel beams, etc.) that one could stand immediately adjacent to the cell and simultaneously touch the guardrail, nonconductive footwear should be worn. As standard practice personnel should keep clear of the cell and an area about 1 yd² (0.8 m²) surrounding it.

9.2 Recommendations for Future Research

9.2.1 Improvement of Current Techniques

The instrumentation for these measurements is straightforward and does not need additional refinement at this stage. What is needed is the development of a more complete body of data concerning the effects of concrete type, clear cover, overlay depth, and temperature on the test results. Also, more work needs to be done in establishing a routine for obtaining and verifying the existence of a uniform moisture content in the test specimen. Some work is needed to attempt to reduce the time needed to carry out the field test. A research program designed to meet these objectives could take the following form:

Laboratory Test

1. Obtain core specimens from a variety of concrete materials, similar to those prepared by FHWA for the present study. Obtain known moisture contents by a variety of vacuum saturation routines and run 6 hour, 60.0 Vdc tests on all specimens. These results, coupled with a knowledge of the saturation moisture content of each material, could be

used to determine the optimum conditioning to be used for laboratory tests. This would remove some of the uncertainties present in the current procedure, where one does not know whether different types of concrete are being brought to the same percentage saturation during the conditioning phase.

Field Test

1. Prepare concrete slabs similar to those used in the present study. Investigate effects of ambient temperature on test results for a wide variety of concretes. Investigate a number of combinations of overlay depth/substrate covers in order to encompass a wider range of possible field conditions.
2. Establish the minimum concrete moisture content above which resaturation of the slab is not necessary prior to test.^{1/} This would significantly reduce field test time and make the procedure more applicable to work on bridges already open to traffic.
3. If possible, develop correction factors to use in bringing field test results to standard conditions.

9.2.2 Basic Research

Applications of the applied voltage techniques and interpretation of the results are seriously hampered by the lack of understanding of the mechanism of ion flow through concrete. The present study, being goal-oriented, did not allow in-depth investigation of many basic materials variables which can

^{1/} Although satisfactory techniques for determination of in-situ moisture content do not now exist, instrumentation is currently under development under contract to FHWA which may lend itself to such research.

influence the test. Effects of cement composition and hydration state, aggregate characteristics, mix design, saturation, and temperature need to be more fully understood. Polarization effects, which apparently are manifested in a decreasing rate of current flow, are not well-defined. A better understanding of the entire process will put the test on a more rational basis and most likely allow further improvements in procedure and an increase in test efficiency.

10. REFERENCES

1. Solving Corrosion Problems of Bridge Surfaces Could Save Billions. Comptroller General's Report to the Congress of the United States, PSAD-79-10, January 19, 1979.
2. Rose, D.A., "Water Movement in Unsaturated Porous Materials," RILEM Bulletin No. 29, pp. 119-25, 1965.
3. Washburn, E.W., "The Dynamics of Capillary Flow," Physical Review, Series 2, 17, pp. 273-83, 1921.
4. D'arcy, H., "Les Fontaines Publiques de la Ville de Dijon," 1856.
5. Daniels, F. and Albery, R., Physical Chemistry, 3rd Edition, Chapter 11, p. 394, Wiley, N.Y., 1967.
6. Powers, T.C., Copeland, L.E., Hayes, J.C., and Mann, H.M., "Permeability of Portland Cement Pastes," Journal of the American Concrete Institute, Vol. 26, No. 3, pp. 285-98, November 1954.
7. Sorensen, E.V. and Radjy, F., "Permeability of Hardened Cement Paste in Relation to Pore Structure," Hydraulic Cement Pastes: Their Structure and Properties, C&CA Publication 15.12, pp. 52-54, 1976.
8. Glover, G.M. and Raask, E., "Water Diffusion and Microstructure of Hydrated Cement Paste," Materials and Structures, 5 (29), pp. 315-22, September 1972.
9. Berman, H.A. and Chaiken, B., "Techniques for Retarding the Penetration of Deicers into Cement Paste and Mortar," PHWA-RD-72-46, 1972.
10. Kondo, R., Satake, M., and Ushiyama, H., "Diffusion of Various Ions in Hardened Portland Cement," Japan, Review of the 28th General Meeting - Technical Session, pp. 41-43, May 1974.
11. Clanville, W.H., "The Permeability of Portland Cement Concrete," Bldg. Res. Tech. Paper No. 3, London, 1926.
12. McMillan, F.R. and Lyse, I., "Some Permeability Studies of Concrete," Proc. American Concrete Institute, Vol. 26, p. 101, 1930.
13. Ruettggers, A., Vidal, E.N., and Wing, S.F., "An Investigation of the Permeability of Mass Concrete with Particular Reference to Boulder Dam," Proc. American Concrete Institute, Vol. 31, p. 382, 1935.
14. Cook, H.R., "Permeability Tests of Lean Mass Concrete," Proc. American Society for Testing and Materials, Vol. 51, p. 1156, 1951.
15. Wiley, G. and Coulson, E., "A Simple Test for Water Permeability of Concrete," Proc. American Concrete Institute, Vol. 34, p. 65, 1938.
16. Barre, H.J., "Some Observations of the Water-Vapor Permeability of Concrete," Proc. American Society for Testing and Materials, Vol. 39, p. 860, 1939.
17. Henry, R.L. and Kurtz, G.K., "Water-Vapor Transmission of Concrete and Aggregates," U.S. Naval Civil Engineering Lab. Report No. R-244, June 1963.
18. Monfore, G.E. and Ost, B., "Penetration of Chloride into Concrete," Journal of the PCA Research and Development Laboratories, Vol. 8, No. 1, p. 46, January 1966.
19. Clear, K.C., "Time-to-Corrosion of Reinforcing Steel in Concrete Slabs," Report No. PHWA-RD-76-70, April 1976.
20. Collepardi M., Marcialis, A., and Turniziani, R., "The Kinetics of Penetration of Chloride Ions into Concrete," Journal of the American Ceramic Society, Vol. 55, No. 10, p. 534, 1972.

21. U.S. Bureau of Reclamation, Materials Laboratory Procedures Manual, Paragraphs 5.35B-5.40, 1951.
22. USBR, personal communication.
23. Murata, J., "Studies on the Permeability of Concrete," RILEM Bulletin, No. 29, pp. 47-54, December 1965.
24. Johnson, A.I., "Application of Laboratory Permeability Data," U.S. Department of Interior, Water Resources Division, pp. 3-4, 1963.
25. Levitt, M., "The Permeability and Absorption of Precast Concrete Products," Civil Engineering and Public Works Review, Vol. 55, No. 642, pp. 88-90, 1960.
26. Figg, J.W., "Methods of Measuring the Air and Water Permeability of Concrete," Magazine of Concrete Research, Vol. 25, No. 85, pp. 213-19, 1973.
27. Davies, L.J. and Booth, H., "An Unsteady Flow Method for Air-Permeability Measurement of Refractory Materials," Ceramic Bulletin, Vol. 40, No. 12, pp. 744-47, 1961.
28. Drennan, J.A., "A Variable Volume-Decay-Rate Permeameter with Restricted-Outflow," Brit. Ceramic Society, Transactions, Vol. 61, No. 10, pp. 623-35, 1962.
29. Whiteway, S.G., "Measurement of Low Permeability in Ceramic Test Pieces," Ceramic Bulletin, Vol. 39, No. 11, pp. 677-79, 1960.
30. Winslow, D.H. and Diamond, S., "A Mercury Porosimetry Study of the Evolution of Porosity in Portland Cement," Journal of Materials, Vol. 5, No. 3, pp. 564-85, 1970.
31. Whiting, D. and Kline, D.E., "Pore Size Distribution in Epoxy Impregnated Hardened Cement Paste," Cement and Concrete Research, Vol. 7, pp. 53-60, 1977.
32. Morrison, G.L., et al., "An Evapo-Transmission Method for Determining Relative Permeability of Concrete," Report No. FHWA-RS-79-1, April 1979.
33. Northrop, J.N. and Anson, J., "Method for Determination of Diffusion Constants and Calculation of Radius and Weight of Hemoglobin Molecule," J. General Physiology, Vol. 12, pp. 543-542, 1929.
34. Gordon, A.R., "The Diaphragm Cell Method of Measuring Diffusion," Annals of the New York Academy of Sciences, Vol. 46, pp. 285-308, 1945.
35. Garrels, R.M., Dreyer, R.N., and Howard, A.L., "Diffusion of Ions Through Intergranular Spaces in Water-Saturated Rocks," Bulletin of the Geological Society of America, Vol. 60, pp. 1809-28, 1949.
36. Spinks, J.W., Baldwin, H.W., and Thorvaldson, T., "Tracer Studies of Diffusion in Set Portland Cement," Canadian Journal of Technology, Vol. 30, pp. 20-28, 1952.
37. Monfore, G.E., "The Electrical Resistivity of Concrete," Journal of the FCA Research and Development Laboratories, Vol. 10, No. 2, pp. 35-48, 1968.
38. Astbury, N.F. and Vyse, J., "A New Method for the Study of Pore Size Distribution," Journal of the British Ceramic Society, Vol. 70, No. 3, pp. 77-85, 1971.
39. Manheim, F.J. and Waterman, L.S., Initial Reports of the Deep Sea Drilling Project, Vol. 11, Washington, D.C., 1974.
40. Frascoia, R.I., Evaluation of Bridge Deck Membrane Systems and Membrane Evaluation Procedures, Report 77-2, Vermont Department of Highways, 1977.
41. Spellman, D.L. and Stratfull, R.F., An Electrical Method for Evaluating Bridge Deck Coatings, Research Report NC. M&R 635116-5, State of California, Division of Highways, 1971.
42. Locke, Carl, E., "Measurement of the Depth of Partial Polymer Impregnation of Concrete," Polymers in Concrete, American Concrete Institute, Special Publication No. 58, pp. 25-35, 1978.
43. Love, A.E.H., A Treatise on the Mathematical Theory of Elasticity, p. 297, Chapter XIII, Dover, N.Y., 1944.
44. Whitehurst, E.A., "A Review of Pulse Velocity Techniques and Equipment for Testing Concrete," Proceedings, Highway Research Board, Vol. 33, p. 226, 1954.

45. Harland, D.C., "A Radio-Active Method for Measuring Variations in Density in Concrete Cores, Cubes, and Beams," Magazine of Concrete Research, Vol. 18, No. 55, pp. 95-101, 1965.
46. Pollard, T.A. and Reichertz, P., "Core-Analysis Practices - Basic Methods and New Developments," Bulletin of the American Association of Petroleum Geologists, Vol. 36, No. 2, pp. 230-252, 1952.
47. Slater, J., Lankard, D., and Moreland, P.J., "Electrochemical Removal of Chlorides from Concrete Bridge Decks," Materials Performance, Vol. 15, No. 11, pp. 21-26, 1974.
48. Morrison, G.L., Virmani, Y.P., Stratten, F.W., and Gilliland, W.J., "Chloride Removal and Monomer Impregnation of Bridge Deck Concrete by Electro-Osmosis," Report No. FHWA-RS-RD-74-1, 1976.
49. Verbeck, G. and Gramlich, C., "Osmotic Studies and Hypothesis Concerning Alkali-Aggregate Reaction," Proceedings, American Society for Testing and Materials, Vol. 55, p. 1110-28, 1955.
50. Clear, K.C. and Harrigan, E.T., "Sampling and Testing for Chloride Ion in Concrete," Report No. FHWA-RD-77-85, August 1977.
51. Carrier, R. Pu, D.C., and Cady, P., "Moisture Distribution in Concrete Bridge Decks and Pavements," American Concrete Institute, Special Publication 47, pp. 169-90, 1975.
52. Monfore, G.E., "Small Probe-Type Gage for Measuring Relative Humidity," Journal of the PCA Research and Development Laboratories, Vol. 5, No. 2, pp. 41-47, 1963.
53. Conten, S.D., Elementary Numerical Analysis, Chapter 4, pp. 134-135, McGraw Hill, N.Y., 1965.
54. Wenner, F., "A Method of Measuring Earth Resistivity," Bulletin of the Bureau of Standards, pp. 469-79, July, 1915.
55. Moore, R.W., "Earth-Resistivity Tests Applied as a Rapid, Nondestructive Procedure for Determining Thickness of Concrete Pavements," Highway Research Record NO. 218, pp. 49-55, 1968.

APPENDIX 1

APPLIED VOLTAGE TEST - CORE SPECIMENS

The test consists of a number of steps, starting from obtaining a specimen and ending with interpretation of data. The materials, equipment, and procedures necessary to complete each step are described so that the user may run this test utilizing "off the shelf" components.^{1/} It is necessary, however, to machine the acrylic applied voltage cell as this is a custom component.

Step 1 - Obtaining Specimen

Equipment

1. Core Drilling Rig.
2. 4-in. (102 mm) diameter (3.75 in. (95 mm) I.D.) diamond dressed core bit.^{2/}

Procedure

Obtain core from structure in conventional manner. Place core in plastic bag and return to laboratory. Core should be of a sufficient length so that a 2-in. (51 mm) slice can be taken off the surface in the next step.

Step 2 - Sizing of Specimens

Equipment

1. Movable bed diamond saw (Highland Park Model 24SS or equivalent).
2. Specimen clamping holder (Optional).

^{1/} The electronic unit (RLC Instruments Model 158) used for field testing (Appendix 2) may also be used in the laboratory test. In this case "Test Volts" is set at 60.0 Vdc, and a short jumper wire is inserted into the over temperature sensor connector. All other functions remain the same as when the unit is used for field testing.

^{2/} If the core bit has a 4.00-in. (102 mm) I.D., the dimensions of the applied voltage cell (Step 4 and Figure 70) should be adjusted accordingly.

Procedure

1. Place core in saw and align face of core parallel to saw blade. Set bed so as to obtain a slice 2 in. (51 mm) in length. Cut specimen at slow speed so as to obtain a clean cut.
2. Remove any burrs on belt sander.

Step 3 - Preparation of Specimen

Materials

1. Rapid setting epoxy. (CIBA 6010 Resin/XU-225 hardener at 1:1 by weight is recommended).
2. De-aerated water (Boiled water).
3. Vacuum pump oil.

Equipment

1. Vacuum Saturation Setup - See Figure 66.
 - 1.1 500 ml separating funnel.
 - 1.2 1,200 ml stainless steel beaker.
 - 1.3 250 mm I.D. vacuum desiccator with sleeve type stopcock.
 - 1.4 Laboratory vacuum pump (Sargent Welch "Duo-Seal" Model 1405-6 or equivalent).
 - 1.5 U-tube vacuum manometer 0-260 mm Hg (-346 kPa) (Sargent Welch Model 5-39745 or equivalent).
 - 1.6 Vacuum hose, clamps, rubber stopper, glass tubing, stopcocks, support stand.
2. Epoxy coating equipment. Gram balance, paper cups, wooden spatulas, disposable glue brushes, small support studs.



FIGURE 66. VACUUM SATURATION APPARATUS.

Procedure

1. Vigorously boil tapwater in a large (2 L) Florence flask. Cap tightly a short while after removing from hotplate and allow to cool overnight.
2. Allow specimen to surface dry in air for 1 hour. Thoroughly mix 5 grams of epoxy resin with 5 grams of hardener and brush onto sides of specimen (placing specimen on a small stud while applying coating will help). Allow coating to cure 3 hours at lab temperature.
3. Check coating for tack-free surface. Place specimen in 500 ml w.s. beaker, and place beaker into vacuum desiccator. Seal desiccator and turn on vacuum pump. Vacuum should reduce to less than 1 mm Hg (1330 kPa) within a few minutes. Run pump for 3 hours.
4. Fill 500 ml separatory funnel with de-aerated water. With pump still running open stopcock and drain sufficient water into stainless steel beaker to cover specimen (do not allow air to enter desiccator through stopcock).
5. Close stopcock and allow pump to run for an additional hour.
6. Close desiccator sleeve, turn off pump, allow air to re-enter desiccator.
7. Drain oil from vacuum pump and replace with fresh oil.
8. Allow specimen to soak under water for 17-19 hours (overnight).

Step 4 - Testing of Specimen

Materials

1. Silastic Rubber (Dow Corning 3112 RTV +0.5% catalyst F).

2. 3.0% by weight sodium chloride (Reagent grade) solution.
3. 0.3N sodium hydroxide (pellets - Reagent grade) solution.
4. Paper discs - 3-in. diameter.

Equipment

1. Applied Voltage Cell (Figures 67 and 68).
2. 4-1/2 digit DVM - 200.00 mv full scale (Fluke Model 8630A or equivalent).
3. 3-1/2 digit DVM - 99.9 v full scale (Fluke Model 8020A or equivalent).
4. 100 mv shunt resistor - 10 amp rating (3E 50-140-034-MTAA).
5. D.C. constant voltage power supply. 0-80 Vdc 0-6 A (Sorenson Model 80-6 or equivalent).
6. No. 14 (1.6 mm) two conductor insulated 600 V cable.
7. Miscellaneous electrical components, hookup wire, banana jacks.
8. Long stem plastic funnel.
9. Thermocouple wire and readout device (Optional).

Note: An electrical block diagram of the equipment is shown in Figure 69. All wires carrying the current which passes through the cell should be No. 14 (1.6 mm) high voltage cable. Wires leading to the meters can be standard electrical hookup wire.

Procedure

1. Remove specimen from water, blot off excess water, transfer to sealed can.
2. Mix 20 grams of RTV rubber with 0.1 gram of Catalyst F.
3. Place paper disc over one cell screen; trowel RTV rubber over screen borders adjacent to

Reproduced from
best available copy

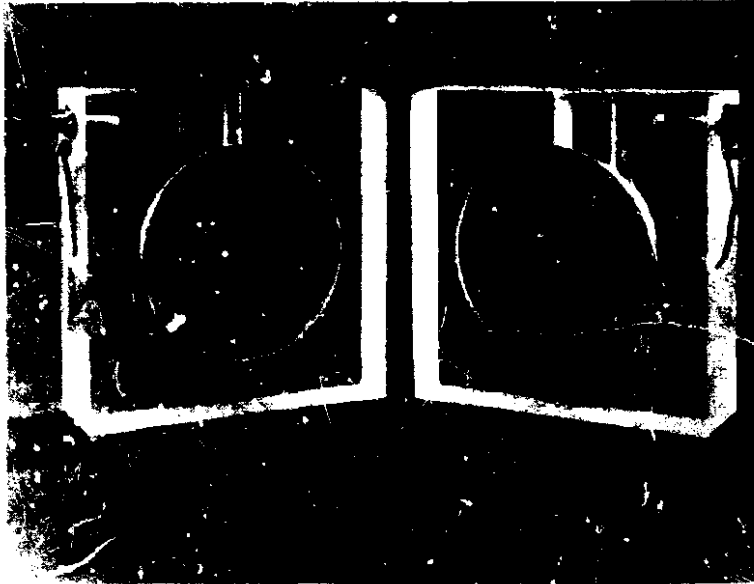


FIGURE 67. APPLIED VOLTAGE CELL-FACE VIEW.



FIGURE 68. SPECIMEN READY FOR TEST.

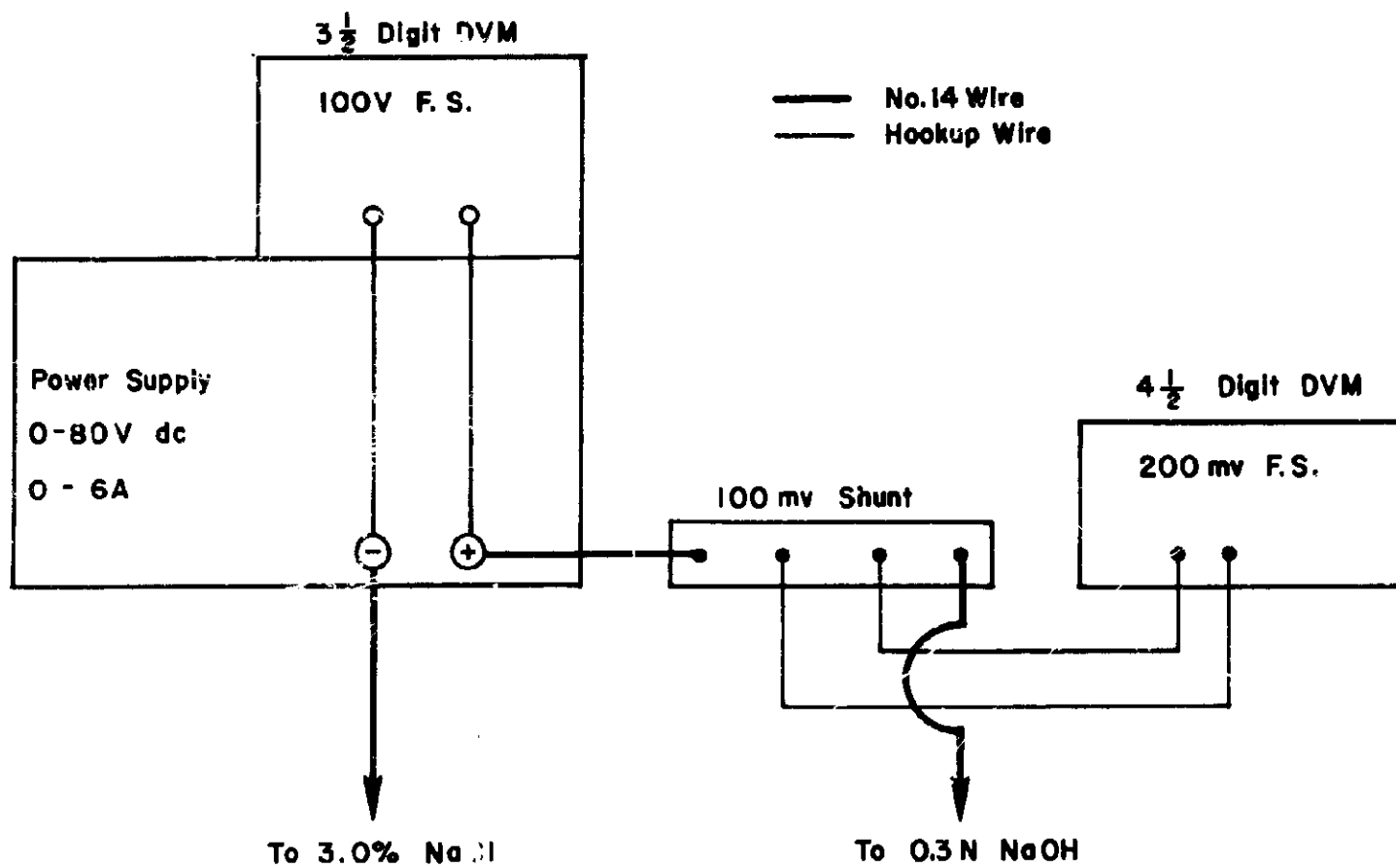


FIGURE 69. ELECTRICAL BLOCK DIAGRAM.

plastic cell. Carefully remove paper disc.

4. Press specimen onto screen; remove excess RTV rubber which flows out of specimen/cell boundary. Cover exposed face of specimen with an impermeable material such as solid rubber sheeting. Place a rubber stopper into cell vent-hole to restrict moisture movement. Allow 10 minutes for rubber to cure.
5. Repeat Steps 3-4 on second half of cell. Allow rubber to cure 10 minutes.
6. Fill left hand (-) side of cell with 3.0% NaCl using a long-stem funnel. Fill right hand (+) side of cell with 0.3N NaOH.
7. Attach lead wires to cell banana posts. Turn on power supply, set to 60.0 V, and record initial current reading.

Note: If a 4-1/2 digit DVM is used in conjunction with the 100 mv shunt, the display can be read directly in milliamps, disregarding the decimal point (i.e., 0.01 mv equals 1 milliamp).

8. Read current every 30 minutes. Monitor temperature inside of cell if desired (thermocouple can be run through 1/8-in. (3 mm) venthole in top of cell).

Note: If temperature exceeds 190°F (88°C), discontinue test in order to avoid damage to cell.

9. Terminate test after 6 hours has elapsed.
10. Remove specimen. Rinse cell thoroughly in running water; strip out and discard residual RTV rubber seal.

Step 5 - Interpretation of Results

1. Construct a plot of current (in amperes) vs. time (in seconds). Draw a smooth curve through the data, and integrate the area underneath the curve in order to obtain the ampere-seconds, or coulombs, of charge passed during the 6-hour test period.

Note: While conventional integration techniques such as planimetry or paper weighing can be used, programmable hand-held calculators are now available which can be used to numerically integrate the plots.

2. Refer to Table 3⁶ for evaluating the test results. These parameters were developed from data on 3.75-in. (95 mm) diameter x 2-in. (51 mm) long core slices taken from laboratory slabs prepared from various types of concretes. They have shown good correlations with 90-day chloride ponding results on companion slabs cast from the same concrete mixes.

Note: The effects of such variables as aggregate type and size, cement content and composition, density, and other factors have not been evaluated. We recommend that persons using this procedure prepare a set of concretes from local materials and use these to establish their own correlation between charge passed and known chloride permeability for their own particular materials. The values given in Table I may be used as estimates until more data has been

TABLE 35
APPLIED VOLTAGE TEST
Interpretation of Results

<u>Chloride Permeability</u>	<u>Charge Passed (coulombs)</u>	<u>Type of Concrete</u>
High	4,000	High water-cement ratios (≥ 0.6)
Moderate	2,000-4,000	Moderate water-cement ratio (0.4-0.5)
Low	1,000-2,000	Low water-cement ratios "Iowa" dense concrete
Very Low	100-1,000	Latex modified concrete Internally sealed concrete
Negligible	100	Polymer impregnated concrete Polymer concrete

developed by a number of agencies on a wider range of concretes.

Notes on Cell Construction - Figure 70

1. Attachment of Lead Wire to Screen

Solder one end of the nylclad lead wire to the outer edge of the brass shim which holds the screen. The nylclad insulation should be removed prior to soldering by burning off with a propane torch and then removing the charred residue with wire wool.

2. Attachment of Screen to Cell

The screen is bonded to the cell by using a high quality waterproof adhesive (Scotch "super-strength adhesive" or equivalent). Scour both the screen shim and the cell lip with medium sandpaper prior to applying adhesive in order to obtain good metal to plastic bond. Apply a coating of adhesive to both cell and screen, run lead wire through 1/16-in. (1.5 mm) hole inside of cell, then gently push screen into place on cell lip. Wipe excess adhesive off face side of screen shim and place a weight on screen until adhesive has fully cured (24 hours).

3. Attachment of Lead Wire to Banana Plug

Solder a 12-10-1/4 ring terminal onto the bare end of the lead wire, keeping excess wire length to a minimum. Run the threaded end of the banana plug through the eyelet of the ring terminal, then thread banana plug into the 1/4-28 threaded hole in the side of the cell, tighten securely. Then fill the 1/6-in. (1.5 mm) hole with clear silicone rubber caulk (Dow Corning No. 732 or equivalent).

4. Materials Quantities and Cost

Some materials may not be available in the small quantities necessary to construct a single cell. In these cases package quantities have been quoted. Lucite sheet stock will probably need to be pre-cut by the suppliers, and the buyer will need to pay cutting charges unless he has another use for the full stock width.

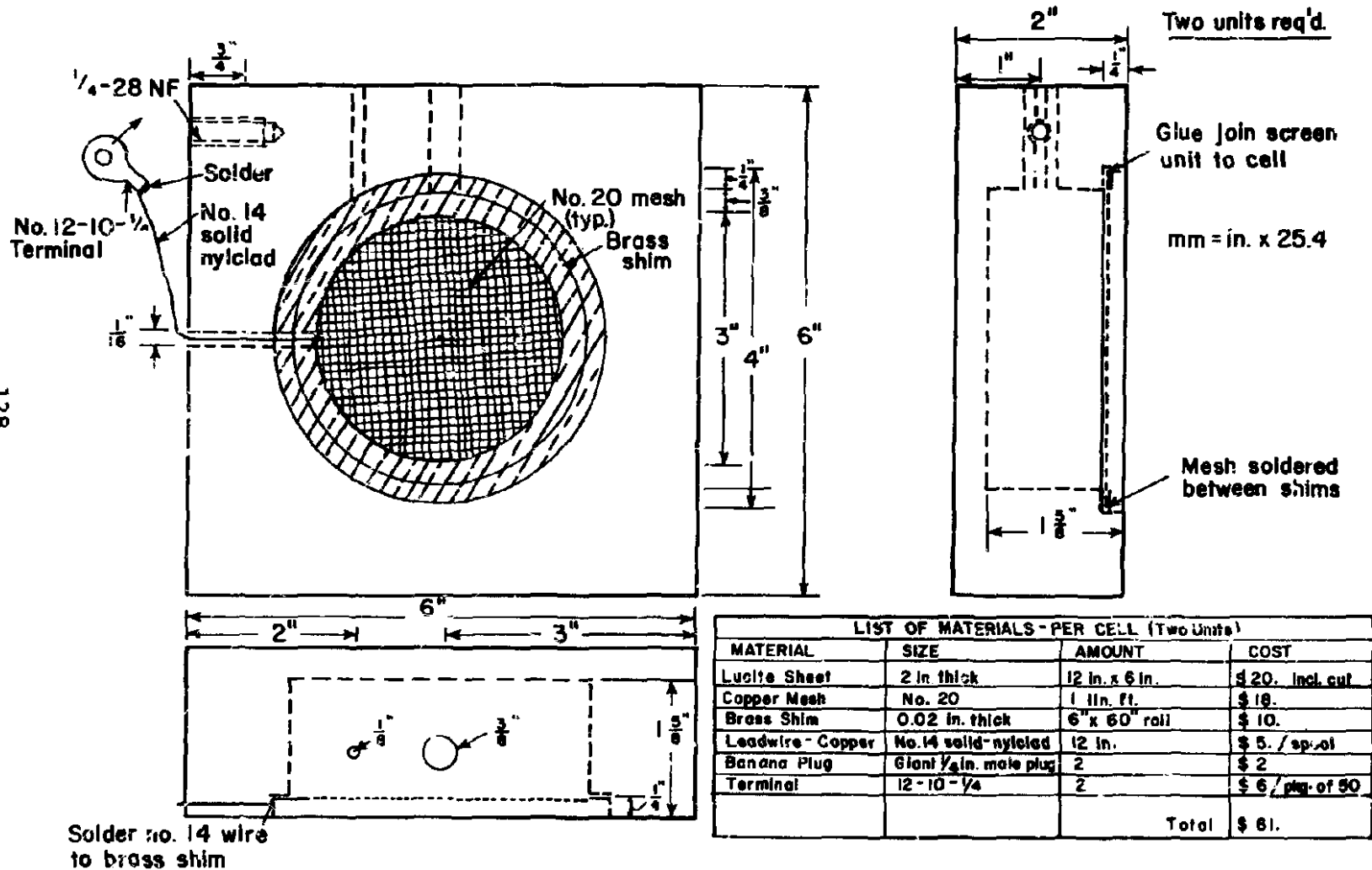


FIGURE 70. APPLIED VOLTAGE CELL (CONSTRUCTION DRAWING).

APPENDIX 2
FIELD TEST PROCEDURE

1. Introduction

The field test procedure can be conveniently broken down into four separate stages, plus clean up.

1. Location of reinforcing steel and bonding of test dike and heating
2. Vacuum saturation of test area
3. Applied voltage test
4. Chloride sampling (optional).

Each test takes two full working days; by use of two dikes four tests can be completed in one working week. The operator should note that stage 2 requires overnight operations; however, the unit may be left unattended during this period. Although the entire test can, in theory, be conducted by one person, an assistant is advisable to help in transporting some of the heavier test equipment and to expedite some of the tasks.

TABLE 36
Field Equipment List

- | <u>No.</u> | <u>Equipment</u> |
|------------|--|
| 1. | <u>Model 158 Electronic Unit</u> |
| | .1 Rain Cover |
| | .2 Light Shield |
| | .3 Pin Connector - For Reinforcing Steel Pin |
| 2. | <u>Vacuum Unit</u> |
| | .1 Limewater Reservoir |
| | .2 Vacuum Oil (Duo-Seal), Funnel |
| | .3 Micro-Stopper (Sargent-Walch S-73460) |
| | .4 Silicone Grease |
| 3. | <u>Screen Unit</u> |
| 4. | <u>Dikes (2)</u> |
| | .1 Plastic Pipe Ends (4) and Caps (3) |

- | | |
|-----|---|
| | .2 Dow Corning No. 732 Silicone Caulk (5 tubes) |
| | .3 Caulking Gun |
| 5. | <u>Generator</u> |
| | .1 6 gal Auxiliary Tank |
| | .2 5 gal Safety Can |
| | .3 5 qts Oil & Filler & Funnel |
| | .4 Oil Pan |
| | .5 Filters & PreCleaner |
| 6. | <u>Chemicals</u> |
| | .1 2 gal 3.0% NaCl |
| | .2 2-1/2 gal Limewater |
| 7. | <u>Tools</u> |
| | .1 Rotary Impact Hammer Kit (Bosch Model 11203K or Equivalent) |
| | .2 Carbide Drill Bits (1.5 in. dia. and 1.375-in. dia.) |
| | .3 Electric Hand Drill and 1/8-in. Bits |
| | .4 Assorted Hand tools (hammers, crescent wrench, 7/8-in. open end wrench, pliers, screwdrivers, chisels) |
| | .5 Electrical Extension Box (100-ft minimum) |
| | .6 Dull Knife, Spatulas, Wire Wool |
| | .7 Small & Large Steel Rules |
| | .8 100-ft Steel Tape |
| 8. | <u>Cover Meter - "R Meter" - James Electronics</u> |
| 9. | <u>Miscellaneous Supplies</u> |
| | .1 Paint Pails |
| | .2 50 ml Plastic Syringe, 2,000 ml Plastic Graduated Cylinder |
| | .3 Large Sponges, Rubber Gloves, Scrub Pad |
| | .4 Sample Container for concrete powder chloride samples |
| | .5 Plastic Bottles for chloride solution samples |
| | .6 Plastic Bags |
| 10. | <u>Vacuum Cleaner (Sears Kenmore or equivalent) and Disposal Bags</u> |

2. Equipment

The major components of the Model 158 Chloride Permeability Test Set have been described in Section 5 of this report. In addition to these components, auxiliary equipment and supplies are needed to carry out a full field test. A complete listing of all necessary supplies is given in Table 36. While some of these may be obvious (such as hand tools), the user is advised to compile a checklist prior to field operations in order to ensure a successful trip. Some of these supplies may be difficult to obtain in isolated areas. The quantities listed are sufficient to perform 1 week of testing (4 tests).

3. Operations

3.1 Location of Reinforcing Steel and Bonding of Test Dike

The objective of this phase is to locate the area of the topmost, steel mat to be used as the positive test electrode. The steel can be located using a magnetic device termed a "cover meter" (James Electronics "R-Meter" or equivalent). Although, at least one of the topmost bars (usually the transverse steel in a bridge deck) must be located, it is preferable to locate^{1/} all steel within the approximately 10.75x10.75-in. (273x273 mm) test area. Once this is done the grid is delineated in pencil on the deck surface and the dike placed

symmetrically^{1/} over the "unit cell", with one uppermost bar running through the center of the test area (see Figure 71). A 1.5-in. (38 mm) diameter hole is then drilled to the center steel bar 5 in. (127 mm) from the outer surface of the dike. Concrete powder extracted from this hole should be retained as a chloride "blank" for the test. A 1/8-in. (3 mm) hole is then drilled into the steel and a knurled 1/8-in. (3 mm) diameter stainless steel pin is driven into this hole. The length of the pin should be such that 2-in. (51 mm) protrudes above the surface of the concrete.

Sand, cement, waste concrete, and other debris should be broomed off the test area. The test area should not be located in spots where oil, paint, or other substances have coated or penetrated the concrete.

A 1/4-in. (6 mm) bead of Silicone Caulk (Dow Corning 732 or equivalent) is then applied to the lower surface of the dike.^{2/} The dike is then pressed onto the test area. Another bead of silicone is then placed around the periphery of the dike and smoothed into place using a wooden spatula.

A 3-in. (75 mm) I.D. X 4-in. (100 mm) long length of schedule 40 PVC pipe is then bonded over the stainless steel pin to the deck surface. A pipe cap having a 3/16-in. (8 mm) groove cut into its surface to allow for the pin leadwire is then placed on the pipe.

All caulking is allowed to cure for 3-4 hours prior to the next phase of operations. If a second dike is available it can also be bonded at this time.

^{1/} In cases where thick overlays (2-in. (51 mm) or more) have been applied to the deck total clear cover may exceed 4-in. (102 mm). Most cover meters are not sufficiently accurate to locate steel at such a depth. In this case, one may need to drill test holes (or cores) into the deck in order to locate a single topmost bar. The locations of the other bars can then be mapped out using the reinforcing details on the deck plans.

^{1/} In some cases, transverse bars are placed skew to the longitudinal steel. In these cases, place the dike perpendicular to the transverse steel.
^{2/} In cases where the concrete surface has been grooved to improve skid resistance, it may be necessary to also fill the grooves with caulk prior to bonding the dike.

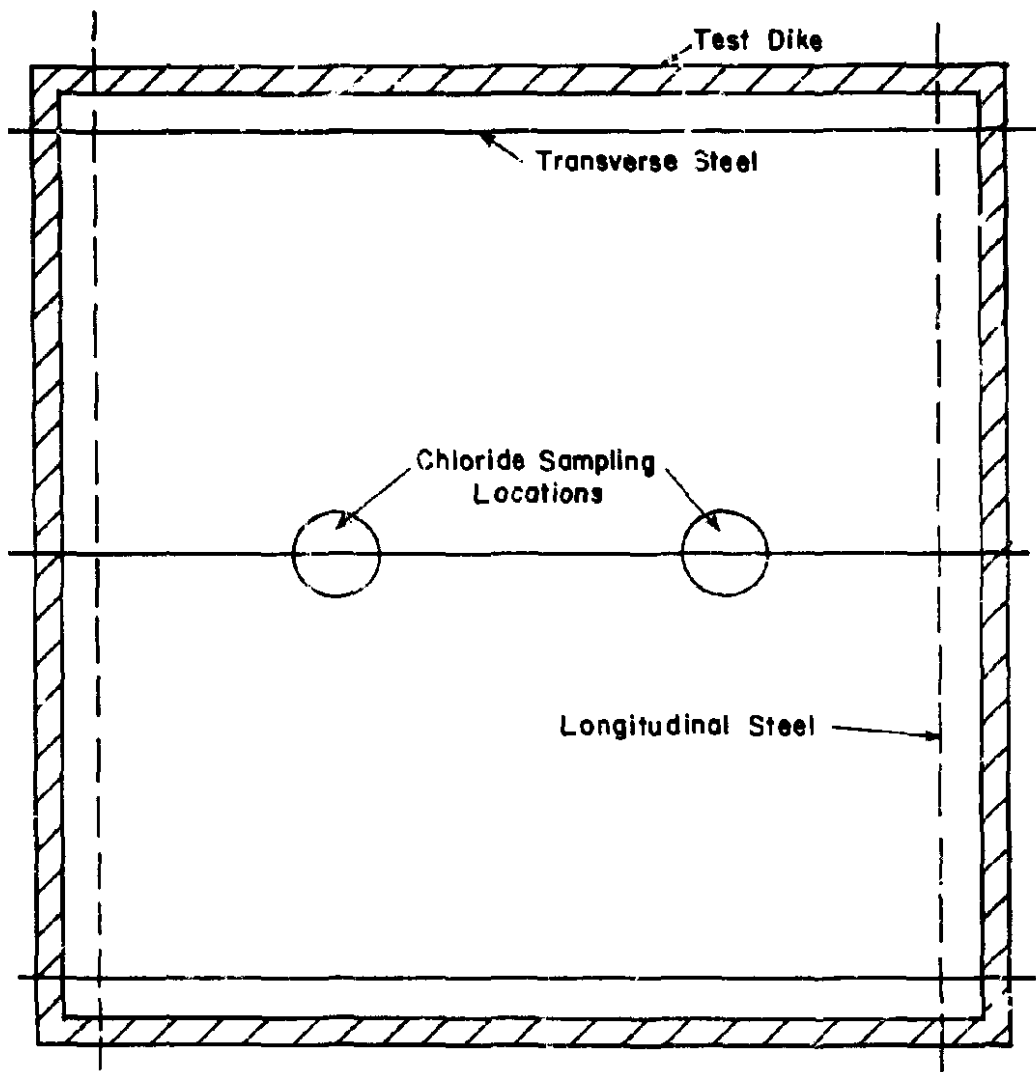


FIGURE 71. EXAMPLE OF DIKE PLACEMENT OVER TEST AREA.

3.2 Vacuum Saturation and Heating of Test Area

After 4 hours have elapsed (3 hours if the weather is warm and dry), the vacuum saturation cover is placed on top the dike and the wing nuts are tightened. The fluid valve is closed and the vacuum pump turned on (the power being supplied by the portable gas generator). The pump is allowed to run for 1 hour; a vacuum of from -28 to -30 in. of Hg (0-6.8 kPa) should be attained. The 1 L reservoir is then attached to the fluid intake pipe and filled to the mark with limewater^{1/} solution. The solution is then slowly let into the chamber. The reservoir is then filled a second time and the process is repeated. The vacuum pump is allowed to run for an additional 1 hour.

The vacuum is then turned off and the fluid entry valve is opened. The stirrer and heater are then turned on. The heater dial setting should initially be set to 75 units and adjusted upwards or downwards so that the pyrometer registers 140°F (60°C). Only a small adjustment (1-2 units) is usually necessary.

If the applied voltage test is scheduled to begin at 0800 hours the following day, the 6-gal auxiliary tank should be connected to the gas generator no earlier than 1800 hours the first day.

3.3 Applied Voltage Test

The following morning the stirrer and heater are turned off and the vacuum top removed from the dike. Most of the hot limewater is removed using a large syringe (commonly termed a "turkey baster") and the remaining water removed with a large sponge. The dike is then covered with a sheet of lucite to prevent further evaporation of moisture.

^{1/} To prepare Limewater solution dissolve 17.5 gm Ca(OH)₂ in 2.5 gal (9.46 l) of cold water.

The 2 L graduate is filled with 1500 ml of 3.0% NaCl solution.^{1/} The solution is transferred to the dike and the screen cover is affixed. The Model 158 instrument leads are connected to the appropriate binding posts on the screen cover. The stainless steel pin connector (+) lead is attached to the pin. The Model 158 instrument is put into operation using the following sequence.

1. Connect the AC Power Cable (yellow cable) to the portable generator.^{2/}
2. Start the generator and allow a few minutes warm up.
3. Turn Test Set Power switch on. Simultaneously press STOP and RESET. All displays should be on and read zeroes.
4. Turn Test Volt switch on and Test Volt Select switch to 80 volts. TEST VOLTS display should read 80.0. Adjust voltage if necessary.
5. Check printer by pushing Manual Print. Printer should print out (1) time, (2) current, and (3) Coulombs, and advance the paper one space.
6. Set test limits.
 - a. Set Test Time (usually 360 minutes) using thumbwheel switches.
 - b. Set Maximum Test Current (usually 7,500 amperes) by holding the Current Read Switch depressed and turning

^{1/} To prepare solution dissolve 0.48 lb (218 gm) of Reagent Grade NaCl in 15.52 lb (7.04 kg) of distilled water. Transfer to a 2-gal (7.6 l) heavy-walled plastic jug.

^{2/} It is a good practice to again run the generator off the 6-gal auxiliary tank, as the 2-gal on-board tank will allow only 5 hours of continuous operation. Therefore, fill the tank prior to starting the applied voltage test.

the Current Adjust pot.
Lock pot.

- c. Set the Auto Print switch to the desired print out interval (usually 30 minutes).
7. Start the test by momentarily pushing the START switch. The current DPM will immediately display test current and the Coulomb display will show coulombs at a rate dependent on the current. The time counter will display time at one count per minute.

No further manipulations other than small voltage adjustments are necessary. The instrument will apply voltage and print out test data for the test time selected (in most cases 360 minutes). It is good practice, however, to maintain a separate hard copy of the data in a field notebook.

The test will self-abort if any one (or more) of the following conditions is encountered.

1. Test solution exceeds 180^oF (82^oC). Over-temperature LED on front panel will light.
2. Test current limit exceeded. Over-current LED on front panel will light.
3. Line voltage drops below 100 volts for an extended (greater than 0.2 msec) time period. Microsecond transient voltage fluctuations will not interfere with the test.
4. Test time is exceeded (normal condition at end of test). Time-out LED will light.

Once the condition has been remedied, the test is put back into operation by depressing RESET, then START. The test will continue from the point in time at which it terminated.^{1/}

During the 6 hour test period a number of other tasks can be performed. The vacuum oil in the vacuum pump must be changed. If one is running more than one test, the vacuum saturation/heating routine can be initiated on the next test area. Other test areas can be located and the steel mapped out.

When the test period is over the unit is turned off and the screen cover removed from the dike. A 200 ml sample of the test solution is placed into the sample bottle. The remaining chloride solution is removed and disposed of. The dike wall is then flushed with approximately 500 ml of fresh water. The dike is removed and the test area is allowed to dry prior to chloride sampling.

4. Chloride Sampling (Optional)

Chloride samples are taken in duplicate directly above the centrally located transverse steel bar (see Figure 71). They are taken 3 in. (76 mm) in from each of the walls of the test chamber. Samples are taken with a 1-3/8-in. (35 mm) diameter carbide bit. A rotary impact hammer (Bosch Model 11203) is used to drill the sample holes. The procedure used follows that prescribed by FHWA (50), with the exception that samples are taken at 1/4-in. (6 mm) increments up to 1 in., and a final 1/2-in. (13 mm) increment for a total of 5 samples per drill hole.

Powder samples are transferred to plastic sample containers and returned

^{1/} While the test clock will run as before, the printer will be out-of-phase with the test clock if the clock stopped at any other point in time than at an exact multiple of 5, 10, or 30 minutes (whichever was chosen for the printer interval). To get the printer back in phase one can let the test run until the clock does reach an exact multiple of the chosen test time, then momentarily disconnect the line cord. When the test is restarted the printer will now again be in-phase with the test clock.

to the laboratory for analysis of total (acid soluble) chloride content. A 3-gram sample is dried to constant weight at 221°F (105°C) and chloride content is determined via Gran Plot Titration (50).

Chloride (as % by weight of sample) is plotted versus the mean sampling depth for each interval (i.e. for 0-1/4-in. (0-6 mm) mean depth is 1/8 in. (3 mm)). A free hand plot is then drawn through the data points, some extrapolation being necessary between 0 and 1/8-in. (0-3 mm) and between the final point and the baseline. The plot can then be numerically integrated, assigning a value of 1 unit for each 0.2 in. (5 mm) on the X-axis of the plot (see Figure 72). The value of the chloride content is then recorded at each of these units. The total integral chloride content is then evaluated using Simpson's Rule (53):

$$\int_{x_0}^{x_n} f(x) dx \approx \frac{h}{3} (f_0 + 4f_1 + 2f_2 + 4f_3 + 2f_4 + \dots + 2f_{n-2} + 4f_{n-1} + f_n) \quad (12)$$

where

$$h = \frac{x_n - x_0}{n} \quad (13)$$

n = number of intervals = 2, 4, 6, 8...

in this case h = 1 and n = 8 so the total uncorrected integral chloride content (I') approximately becomes:

$$\begin{aligned} I' &= \frac{1}{3} (0.105 + 4(0.128) + 2(0.138) + \\ & 4(0.138) + 2(0.085) + 4(0.052) + \\ & 2(0.030) + 4(0.010) + 0.008) \\ I' &= 0.644 \end{aligned}$$

The total integral chloride content is then corrected for the baseline value (0.008 X 8 = 0.064).

$$I = 0.644 - 0.064 = \underline{\underline{0.58}}$$

5. Cleanup

The dike can be removed from the deck by undercutting the silicone seal with a dull knife and then prying the dike off the deck with a heavy gage screwdriver blade. The residual silicone is removed from the dike using a sharp laboratory spatula blade (heavy gloves should be worn during this operation). The lime coating^{1/} can be removed from the dike and the heater coils using steel wool.

All equipment (Dike screen, graduated cylinders, syringe, etc.) coming into contact with the chloride test solution should be washed in clean water and dried prior to the next test.

^{1/} After a number of uses, a permanent discoloration will be noted in the interior dike wall which contacts the test solution. This does not impair the functioning of the dike.

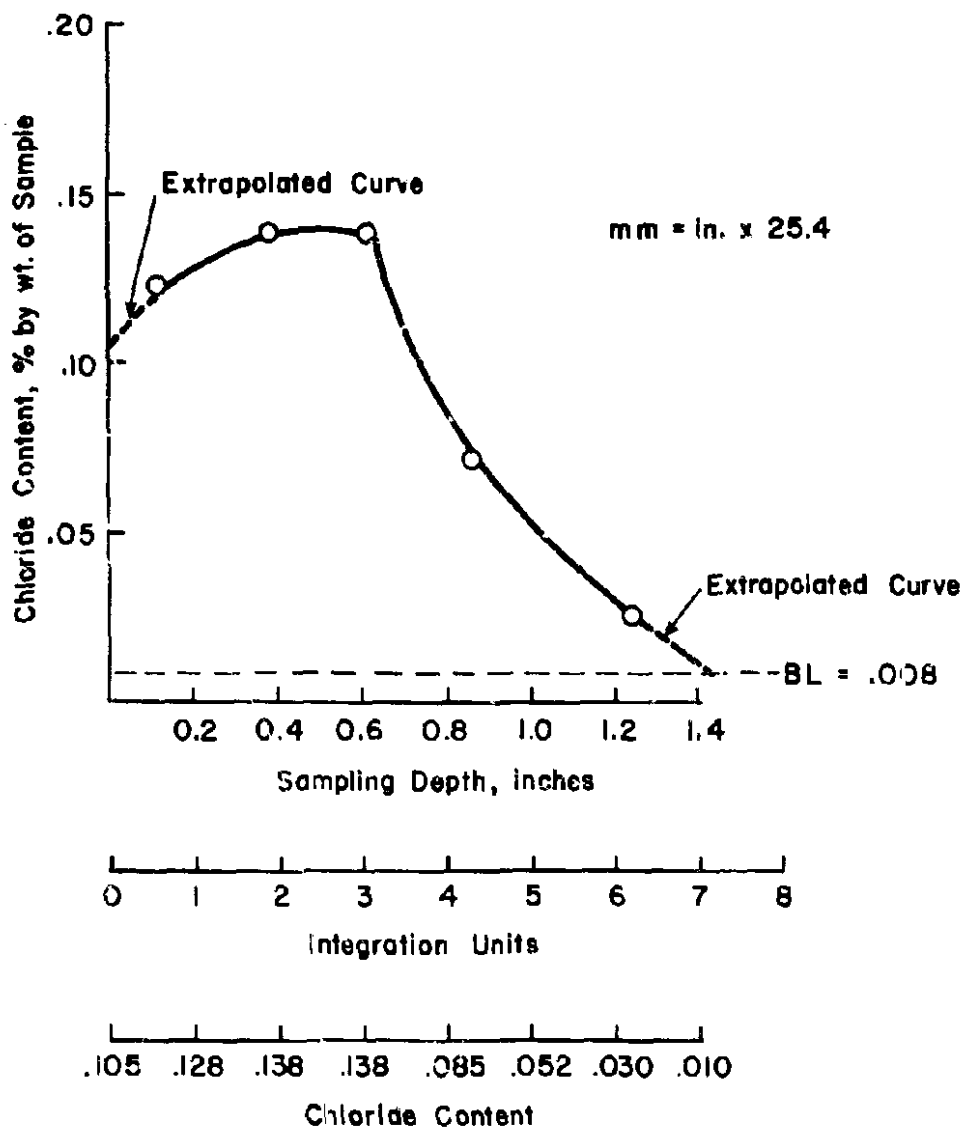


FIGURE 72. CHLORIDE PROFILE DATA PRESENTATION.

APPENDIX 3
CORRELATION ANALYSIS

Correlation analyses between various data sets were performed utilizing the techniques of linear regression analysis. A "statistics package"^{1/} for the Hewlett Packard Model 9825B Calculator was used for calculation and plotting. The following statistics were utilized:

1. Correlation Coefficient (R) - An estimate of the association between the independent variable (X) and the dependent variable (Y). Its square represents the ratio of the variance due to regression to the total variance. When R equals unity all variance can be accounted for by the regression and correlation is "perfect".

2. Standard Error of Estimate (S.E.) - A measure of the scatter of the observed points in the vertical (Y) direction. If populations are normally distributed, then 95 percent of the population will lie within \pm S.E. of the true regression line.

3. Percent Standard Error (% S.E.) - The standard error of estimate divided by the mean Y value. This affords a quantitative estimate of the error to be expected in applying the computed regression line in order to estimate a Y value from a given X value.

4. F Statistic (F) - Ratio of the variance due to regression to the residual (error) variance. If F exceeds the tabulated value for the appropriate degrees of freedom, the probability that the difference between the two variances is due to chance is less than the specified significance level (usually 90, 95, or 99%) and the regression is "significant" at that level. This only implies that the linear relationship between X

and Y is not due to chance alone and does not indicate any causative or associative relationship.

5. 95 Percent Confidence Limits (95% C.L.) - These limits define the X-Y region within which 95 percent of the observations are expected to lie. The limits are asymptotic to the linear regression line, the closest limits occurring at the centroidal point (mean value of X and Y), and the scatter increasing as one nears the extremities. These are shown on Figures 73 through 80 as two dashed curved lines on each side of the linear regression line.

^{1/} General Statistics, Vol. 1, Program No. 10, HP Part No. 09825-15001.

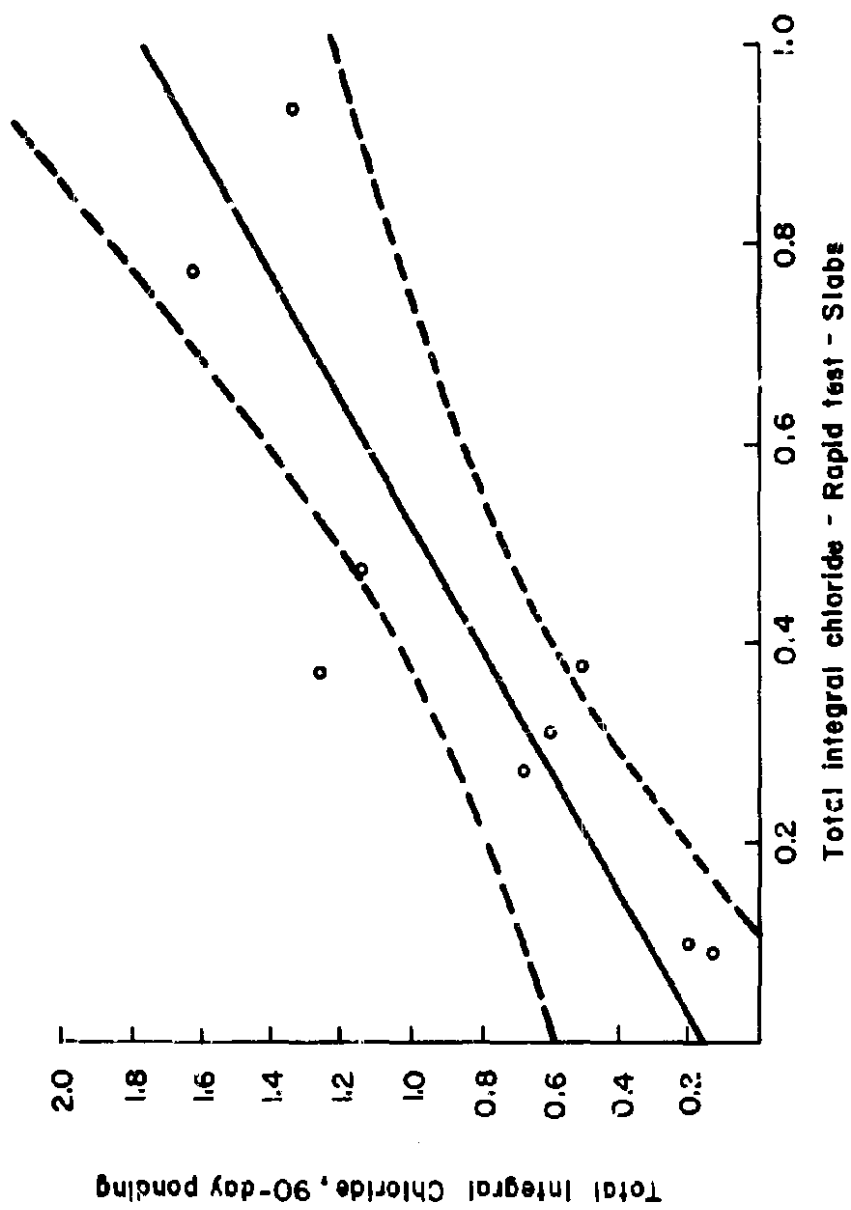


FIGURE 73. RELATIONSHIP BETWEEN TOTAL INTEGRAL CHLORIDE VALUES FOR RAPID TEST RESULTS AND 90-DAY PONDING RESULTS.

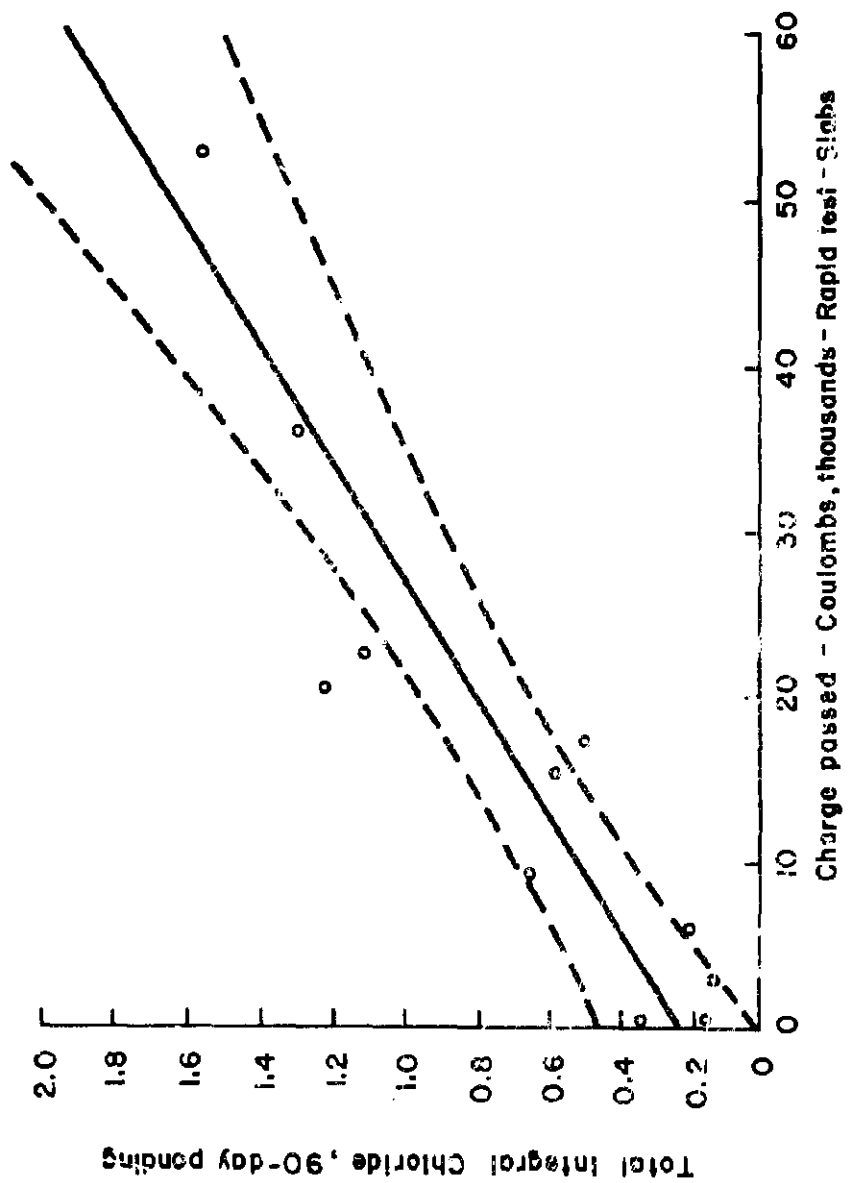


FIGURE 74. RELATIONSHIP BETWEEN CHARGE PASSED DURING RAPID TEST AND TOTAL INTEGRAL CHLORIDE VALUES IN 90-DAY TEST.

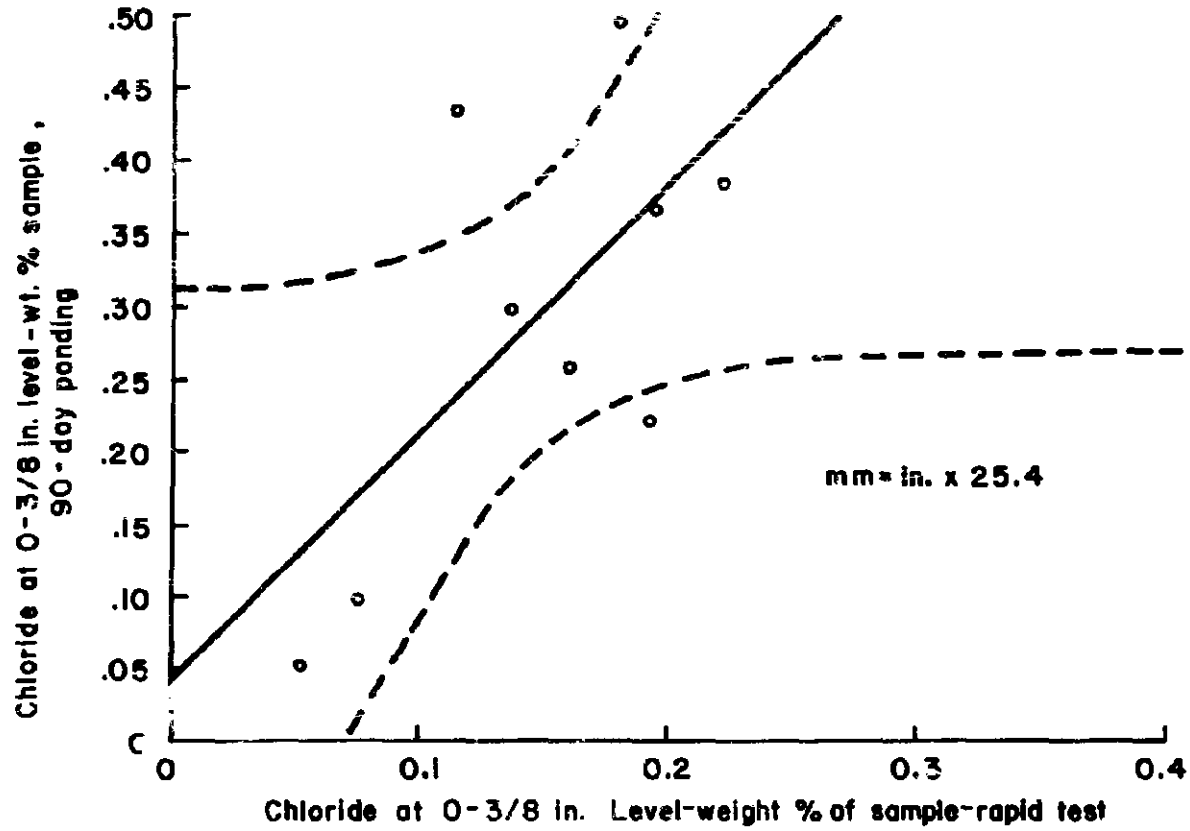


FIGURE 75. RELATIONSHIP BETWEEN CHLORIDE CONTENTS AT THE 0-3/8 IN. LEVEL FOR RAPID AND 90-DAY TEST RESULTS.

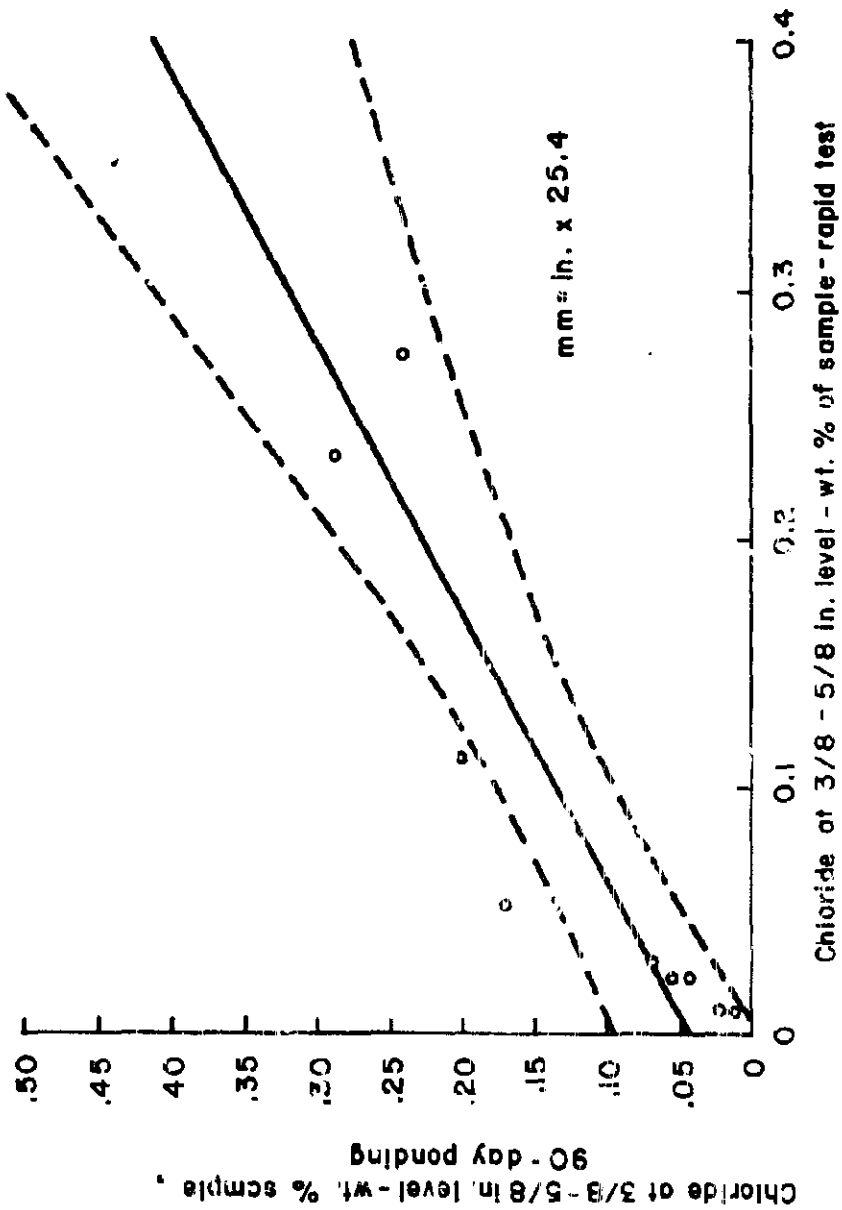


FIGURE 76. RELATIONSHIP BETWEEN CHLORIDE CONTENTS AT THE 3/8 - 5/8 IN. LEVEL FOR RAPID AND 90-DAY TEST RESULTS.

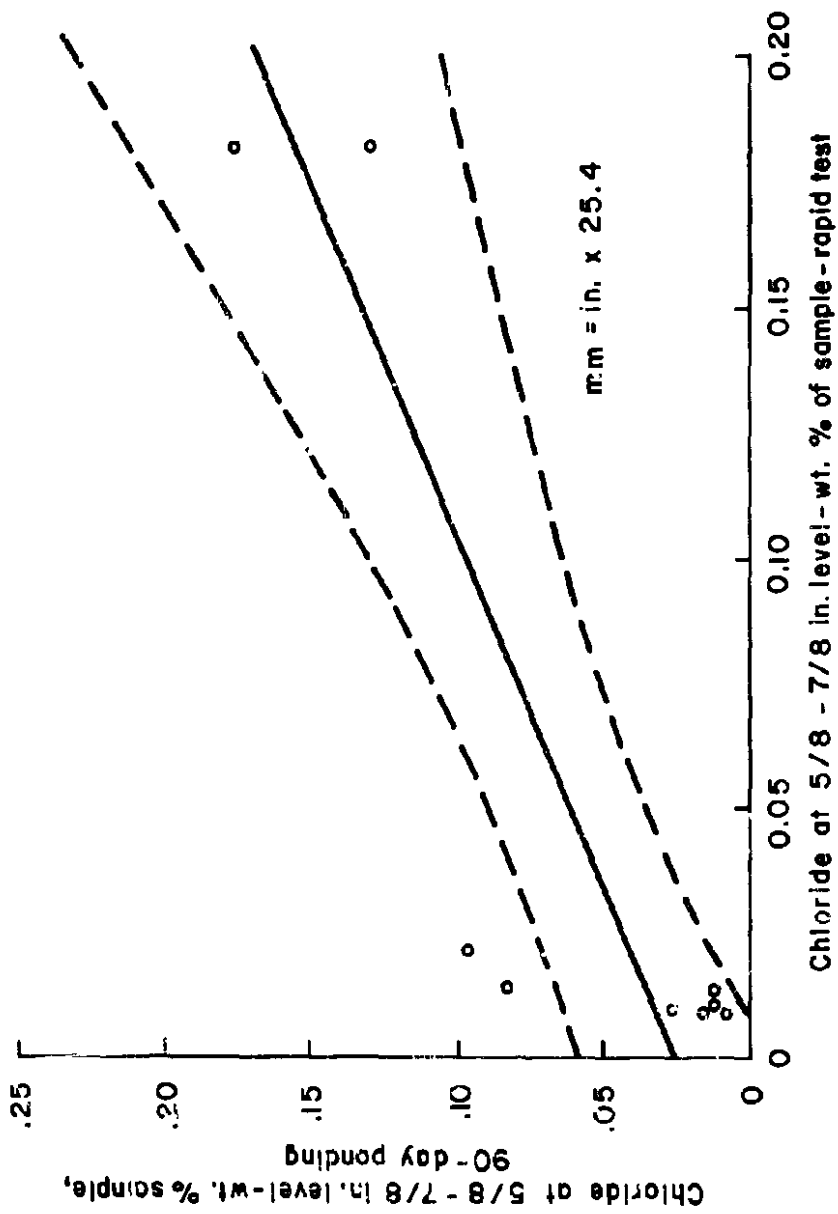


FIGURE 77. RELATIONSHIP BETWEEN CHLORIDE CONTENTS AT THE 5/8-7/8 IN. LEVEL FOR RAPID AND 90-DAY TEST RESULTS.

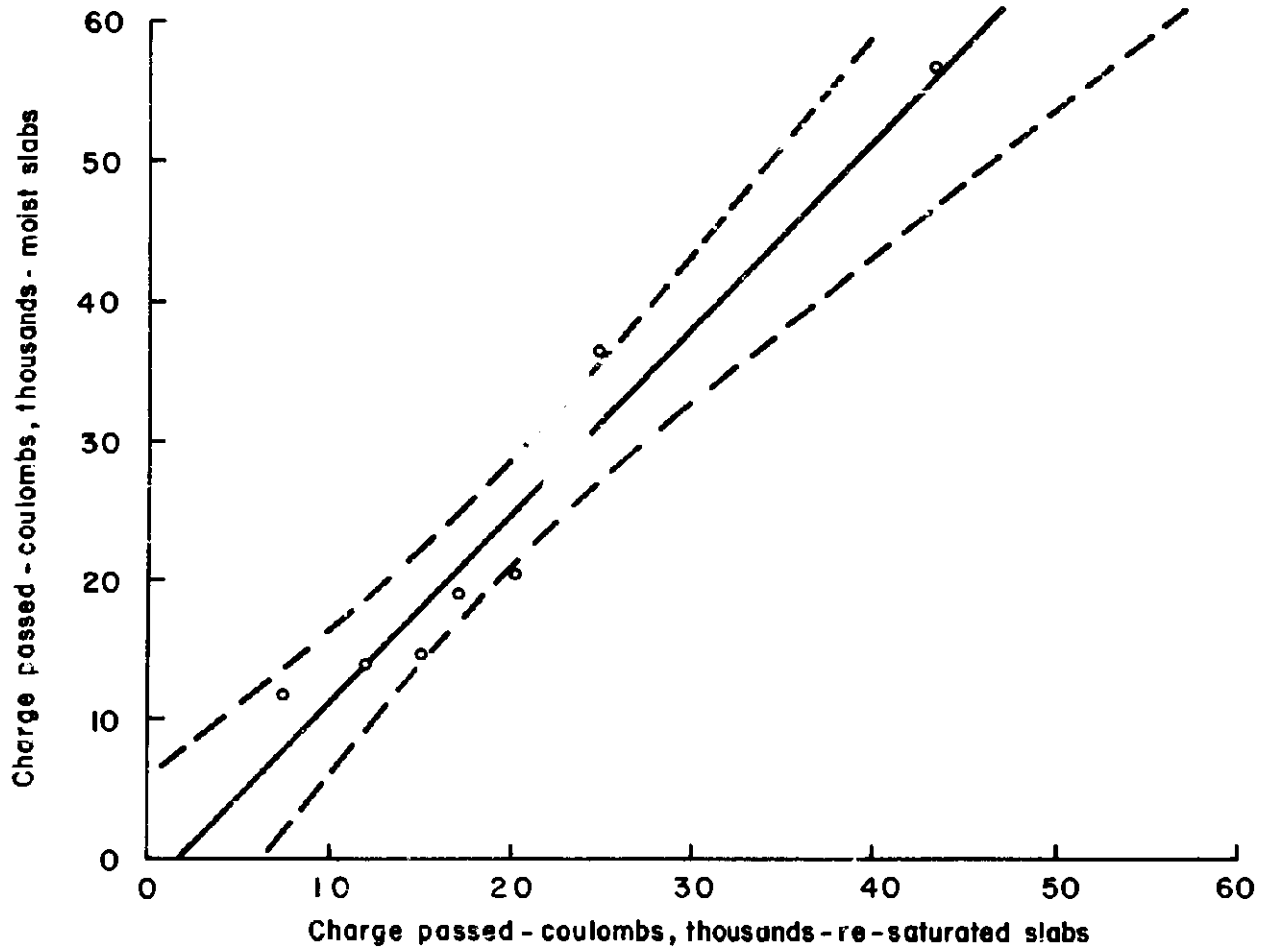


FIGURE 78. RELATIONSHIP BETWEEN CHARGE PASSED FOR RE-SATURATED AND MOIST STORED SLABS.

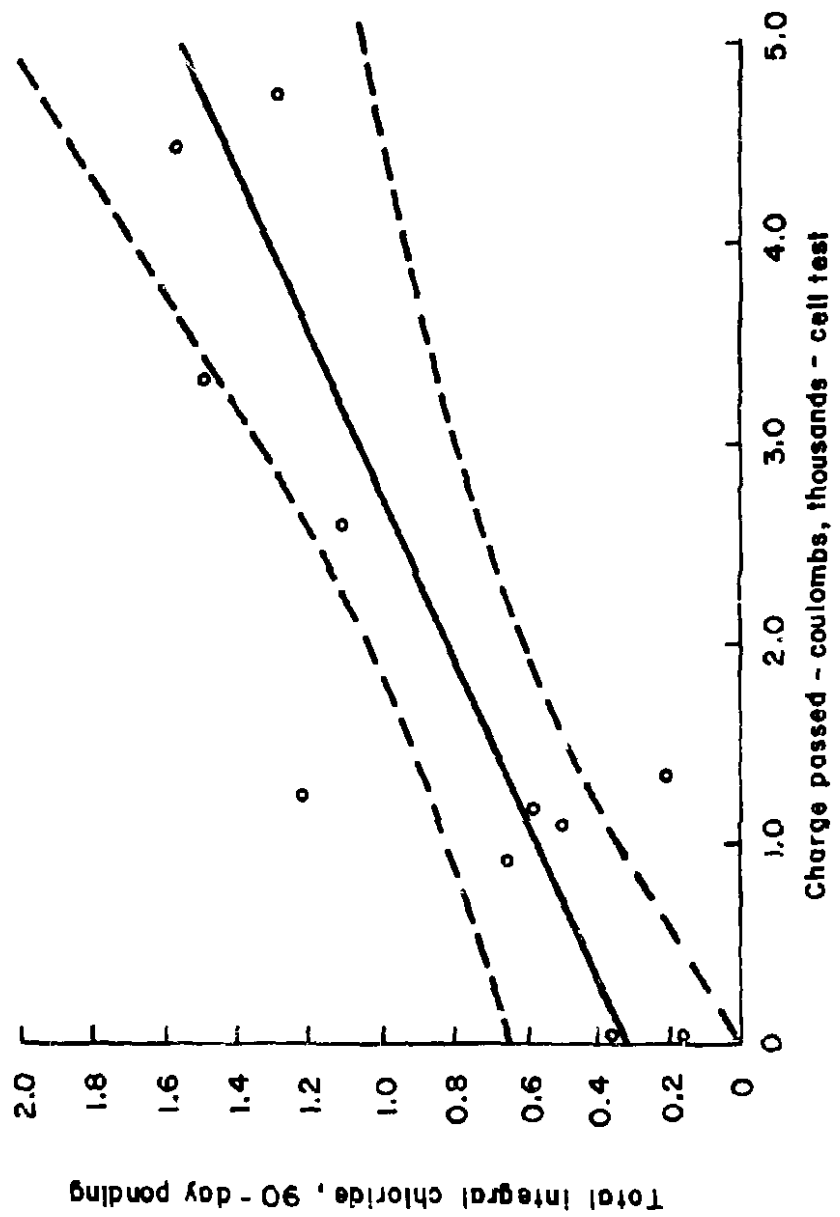


FIGURE 79. RELATIONSHIP BETWEEN CHARGE PASSED DURING CELL TEST ON CORES AND TOTAL INTEGRAL CHLORIDE FROM 90-DAY TEST.

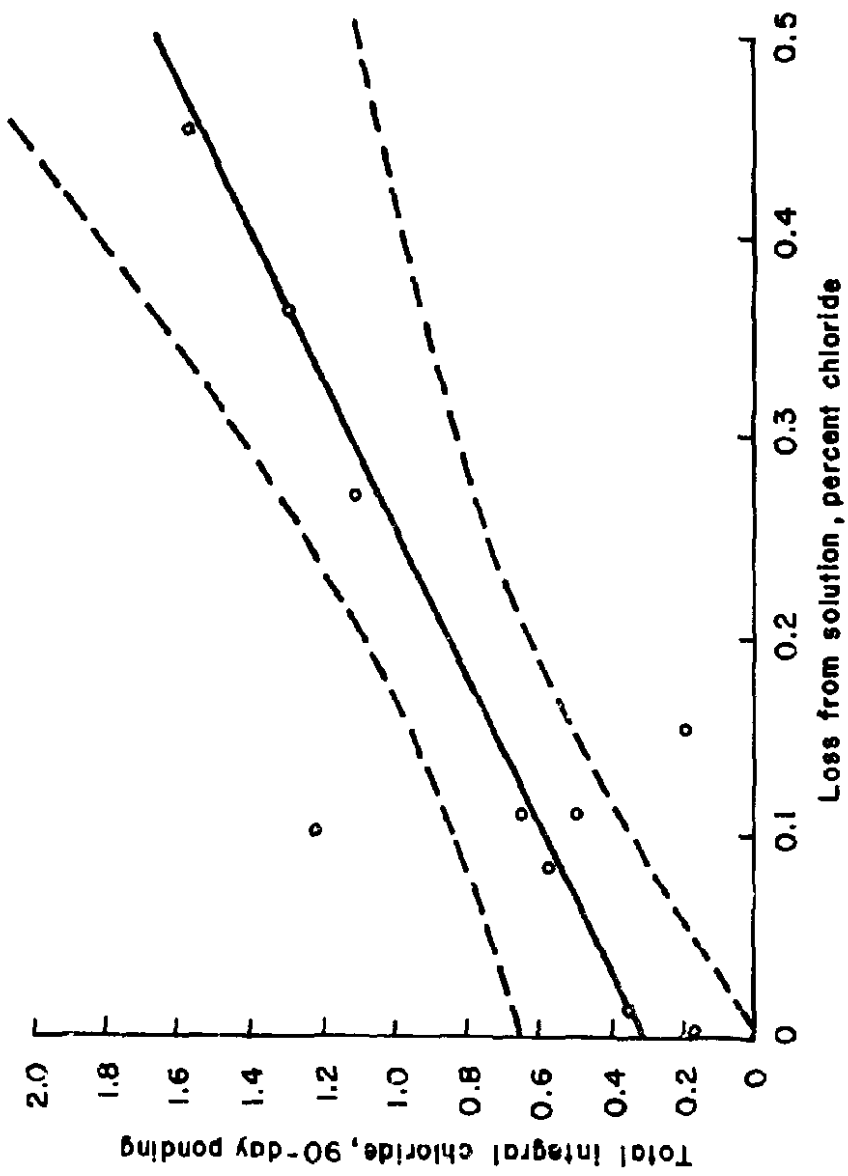


FIGURE 80. RELATIONSHIP BETWEEN LOSS FROM SOLUTION DURING CELL TEST ON CORES AND TOTAL INTEGRAL CHLORIDE FROM 90-DAY TEST.

TABLE 37

CORRELATION ANALYSES - SUMMARY STATISTICS

Relationship X vs Y	Parameters X vs Y	R	S.E. Wt. % Sample	% S.E.	F	Signifi- cance Level
1. As-Rec'd vs. FHWA - 90 days	Total Integral Cl ⁻ vs. Total Integral Cl ⁻	0.86	0.276	+34.6	20.2	99.5%
2. As-Rec'd vs. FHWA - 90 days	Charge Passed-coul. vs. Total Integral Cl ⁻	0.92	0.217	+31.1	46.2	99.9%
3. As-Rec'd vs. FHWA - 90 days	Cl ⁻ at 0-3/8 in. vs. Cl ⁻ at 0-3/8 in.	0.66	0.123	+41.8	5.4	90%
4. As-Rec'd vs. FHWA - 90 days	Cl ⁻ at 3/8-5/8 in. vs. Cl ⁻ at 3/8-5/8 in.	0.90	0.049	+39.6	29.9	99.5%
5. As-Rec'd vs. FHWA - 90 days	Cl ⁻ at 5/8-7/8 in. vs. Cl ⁻ at 5/8-7/8 in.	0.86	0.036	+57.4	19.8	99.5%
6. Re-Sat'd vs. Moist	Charge Passed-coul. vs. Charge Passed-coul.	0.98	3,860 - coul.	+15.8	102.0	99.9%
7. Cell Test vs. FHWA - 90 days	Charge Passed-coul. vs. Total Integral Cl ⁻	0.83	0.294	+38.9	17.7	99.5%
8. Cell Test vs. FHWA - 90 days	Solution Loss - % vs. Total Integral Cl ⁻	0.82	0.299	+39.6	16.9	99.5%

mm = in. X 25.4

TABLE 18
DATA USED FOR CORRELATION ANALYSES

Rapid Test

Depth - Inches^{1/}

Slab	Type	Chloride - Wt. % of Sample					Total Integral Chloride	Charge (coulombs)
		0-3/8	3/8-5/8	5/8-7/8	7/8-9/8	9/8-13/8		
3357	0.6	0.112	0.233	0.181	0.070	0.015	0.77	52,570
3358	0.5	0.193	0.111	0.021	0.010	0.008	0.47	22,500
3393	0.4	0.179	0.050	0.013	0.010	0.008	0.37	20,410
3368	IS-Full	0.220	0.273	0.181	0.022	0.011	0.93	36,070
3397	LTX-Full	0.136	0.022	0.009	0.008	0.008	0.27	8,670
3383	Iowa	0.159	0.022	0.009	0.008	0.008	0.31	15,270
3373	LTX-Over	0.191	0.028	0.008	0.008	0.008	0.37	16,950
3367H	IS-Full	0.072	0.009	0.012	0.008	0.008	0.10	5,770
3362H	IS-Over	0.052	0.008	0.008	0.008	0.008	0.09	3,020
3408	PIC	-	-	-	-	-	-	0
3412	PC	-	-	-	-	-	-	0

90-Day Ponding Test^{2/}

Chloride - Wt. % of Sample

3384	0.6	0.442	0.293	0.179	0.107	0.038	1.56
3354	0.5	0.371	0.201	0.097	0.036	0.013	1.10
3389	0.4	0.503	0.172	0.083	0.025	0.012	1.21
3364	IS-Full	0.390	0.242	0.133	0.057	0.018	1.28
3394	LTX-Full	0.303	0.044	0.025	0.019	0.011	0.64
3379	Iowa	0.261	0.054	0.011	0.008	0.007	0.57
3369	LTX-Over	0.223	0.068	0.013	0.009	0.007	0.49
3357H	IS-Full	0.052	0.013	0.008	0.006	0.007	0.13
3398H	IS-Over	0.099	0.017	0.012	0.010	0.011	0.19
3404	PIC	0.138	0.043	0.009	0.013	0.005	0.337
3409	PC	0.058	0.022	0.011	0.009	0.009	0.161

^{1/} mm = in. X 25.4

^{2/} Each result is the average of three separate samples

APPENDIX 4
PERMEABILITY MEASURING INSTRUMENT
DETAILED REQUIREMENTS

The following is a listing of requirements for a chloride permeability measuring instrument. These specifications were submitted as guidelines and were revised somewhat during the final instrument design.

1. **Size Requirements:** Suggested maximum dimensions are 24-in. long x 12-in. high x 14-in. wide (0.6x0.3x0.35 m).
2. **Weight:** 50 pounds (22.7 kg) or less.
3. **Temperature Range for Operation:** 40° to 140°F (5° to 60°C).
4. **Humidity Range for Operation:** 40% to 95% relative humidity.
5. **Ruggedness:** Must be capable of absorbing the normal handling expected during transportation to and from a typical highway construction site.
6. **Portability:** This instrument will be a portable device. Supporting handles will be located for safe handling by one person but with provision for handling by two persons.
7. **Security:** The instrument case shall be designed so that hazardous components or systems are not readily accessible to personnel.
8. **Duration of Measurement:** Typical measurement time is six (6) hours.
9. **Instrument Configuration:** This instrument shall consist of a measurement and control module, and a separate conditioning element. These two units to be interconnected by removable cable(s).
10. **Control Panel:** The instrument controls shall be located so as to prevent damage during normal handling.
11. **Power Requirements:** 115 V AC \pm 10%, 50 or 60 Hz, single phase. Battery power backup is suggested to preclude data loss in the event of AC power failure.
12. **Voltage Output:** DC voltage must be adjustable to 60 \pm 0.5 and 80 \pm 0.5 V DC.
13. **Current Capacity:** DC current output shall be sufficient to operate one (1) sensing element having approximately one (1) square foot of sensing area. The current requirement is estimated to be in the range of 0 to 5 amperes at 80 V DC.
14. **External Power Requirements:** External AC power requirements are: 115 V AC \pm 10%, 50 or 60 Hz, single phase, with a minimum power output of 1,000 watts.
15. **Circuit Protection:** Fuse protection shall be provided at the AC line input to the instrument.
16. **Voltage Readout:** A meter shall be provided for indication of DC voltage.
17. **Current Readout:** A meter shall be provided for indication of current output to the nearest 0.001 ampere.
18. **Power On Light:** A light shall be provided to indicate that power is applied to the sensing element.
19. **Readout Interval Control:** The interval between data printouts shall be selected by rotary switch or equivalent.
20. **Data Readout:** Printer data should be presented in digital form. "Alpha" numeric printout of data and headings on removable hard copy is preferred.
21. **Data Presentation Interval:** Data readout interval selection shall include 5, 10, and 30 minute periods.

22. Data Printout: Elapsed time, DC current, and the integrated time-current value (coulombs) shall be provided.
23. Materials Measurement Capability: This instrument shall be capable of chloride permeability measurements on conventional portland cement concrete, latex modified concrete, polymer impregnated concrete, internally sealed concrete, and polymer concrete.

APPENDIX 5
APPLICATION OF A FOUR-PIN
RESISTIVITY METHOD FOR DETERMINATION
OF DEPTH OF IMPERMEABILITY

1. Introduction

A four-electrode-resistivity technique has been utilized successfully as a nondestructive means to determine the penetration depth of partially impregnated polymer concrete (42). The validity of this technique is based on the fact that different types of material in a composite may possess distinct electrical resistivities and the resistivity is characteristic of the type of material under well-defined conditions. If the resistivity at all locations in a composite can be accurately measured, it may well indicate the presence and location of certain type of material. The four-electrode-resistivity method provides a way to detect the resistivity at different locations in a composite, and with proper data treatment, a way to determine the location of the interface between two types of material nondestructively. Concrete overlays consisting of portland cement concrete and overlying material may have resistivities so different that the location of the interface, or the thickness of the overlay, can be determined by this technique. The principle of this technique and the result of the measurement will be presented in the following section.

2. The Principle of Four-Electrode-Resistivity Method

The four-electrode-resistivity technique used in this work is a modification of the Wenner-4-pin-surface resistivity test (54) which has been used for measurement of soil resistivity. This technique involves measurement of the resistance to the passage of an electric

current through the selected medium. Four electrodes are equally spaced in a line on the surface of the slab being tested (Figure 81). The current (I) passing through the material between electrodes 1 and 2, and the potential drop (ΔV) between electrodes 3 and 4 are recorded. The average resistivity (ρ) can then be calculated with the following equation:

$$\rho = 2\pi a \frac{\Delta V}{I} \quad (14)$$

where: ρ = resistivity (ohm-cm)
 a = electrode spacing (cm)
 ΔV = potential drop (volts)
 I = current (amperes)

The effective depth of the measurement below the surface is equal to the electrode spacing. This approach is based on the assumption that equipotential hemispheres with radii a are established around electrodes 1 and 2. Every point on the surface of the hemisphere has the same potential. The spacing between the electrodes can be varied and thus the data obtained will reflect the changes in resistivity as a function of the depth from the surface. The measurement at each spacing will be an average value of resistivity of all the material from the surface to depth a . One method of data treatment, an integral method, developed by Moore (55), provides an indication of the thickness of different layers. In this method, the cumulative resistivity is plotted against spacing and a straight line is obtained for each kind of material. If there are two different types of material in a slab, two straight lines will be obtained and the intercept will indicate the location of the interface or the thickness of the overlay.

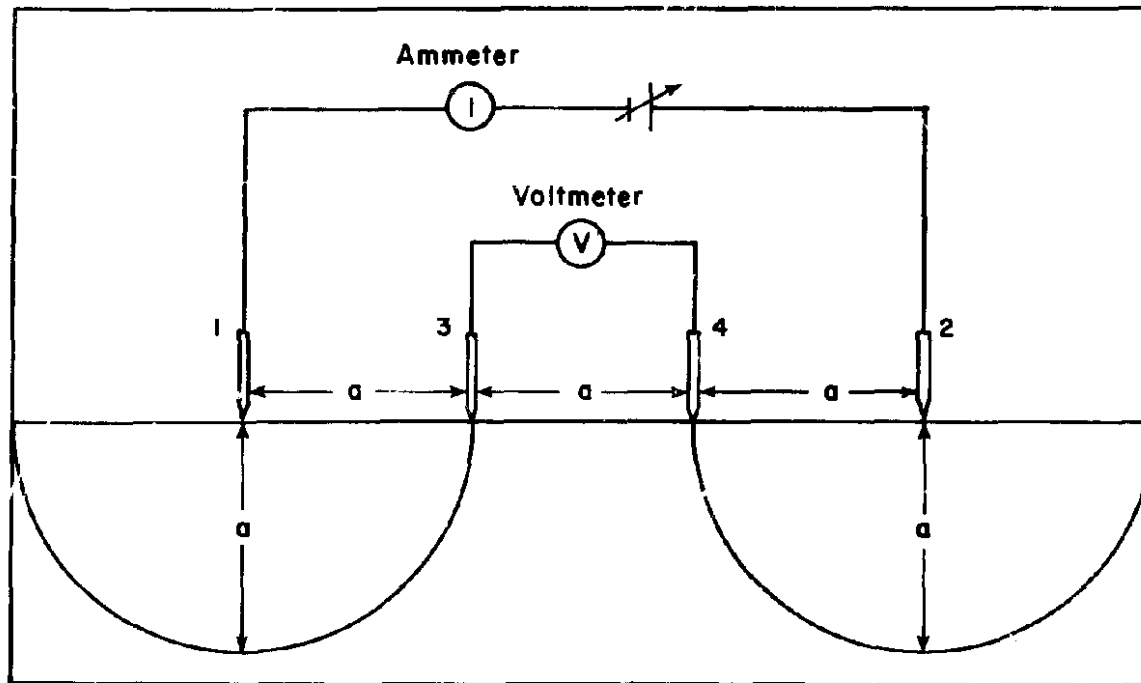


FIGURE 81. WENNER-FOUR-ELECTRODE CONFIGURATION.

3. Experimental

The apparatus used for measurement in this study is shown in Figure 82. Four miniature copper/copper sulfate electrodes manufactured from felt-tip pen bodies were used in this measurement. The sponge rods inside the plastic pen shells were soaked with saturated copper sulfate solution and copper wires were inserted into the sponge rods. Electrodes constructed in this way permit so slow a movement of the copper sulfate solution that the electrodes can be placed at a spacing less than one centimeter while maintaining good electrical contact. The current is supplied by a DC-power source (Hewlett Packard 6116A) to the outside electrodes. The current flowing through the electrodes is measured by an electrometer (Keithley Model 602) and, with the help of a switch, the potential drop between electrodes 3 and 4 is also measured by the same electrometer. The electrode spacing was varied from 7 cm to 1 cm and the resistance data for various spacings were recorded.

The tested slabs are described below. All the tested slabs had the dimensions 12x23-1/2x6 in. (305x597x152 mm). Among the slabs listed below, those which are described as "wet" had been exposed to moisture for a month before being tested. The other slabs were air-dry. Two of these "wet" slabs (#3372 and #3382) had been frozen and were allowed to thaw in plastic bags two days before they were tested. Some of the slabs were reinforced with steel and a few of these reinforced slabs had thermocouples in them. The locations of the reinforcing steel and thermocouples are described in Section 4.1 (page 36).

Full Depth Materials:

- #3356: base concrete (air-dry)
- #3358: base concrete with steel (wet)
- #3402: internally concrete (air-dry)
- #3396: latex concrete (air-dry)

Overlays:

- #3413: polymer concrete overlay with steel (air-dry)
- #3412: polymer concrete overlay with steel and thermocouple (wet)
- #3363: unmelted internally-sealed overlay with steel (air-dry)
- #3362H: partially melted internally-sealed overlay with steel and thermocouple (air-dry)
- #3403H: internally-sealed concrete, partially melted (air-dry)
- #3381: dense concrete overlay (air-dry)
- #3382: dense concrete overlay with steel and thermocouple (air-dry)
- #3383: dense concrete overlay with steel (air-dry)
- #3373: latex overlay with steel (air-dry)
- #3372: latex overlay with steel and thermocouple (wet)

4. Results

4.1 Treatment of Data

Changes in resistivity as a function of depth from the surface (i.e. spacing) for thirteen slabs are shown in Figures 83 through 92. The cumulative resistivity vs spacing plots which are used for determination of overlay thickness are also presented. In the process of calculating cumulative resistivity, the summation can begin with either end, as long as the starting resistivity is higher than the resistivity at the other end. As an example, for this set of data,

spacing	1	2	3	4
resistivity (ohm-cm)	3×10^9	1.1×10^9	2×10^8	7×10^7
spacing	5	6	7	
resistivity (ohm-cm)	6×10^7	5×10^7	4×10^7	

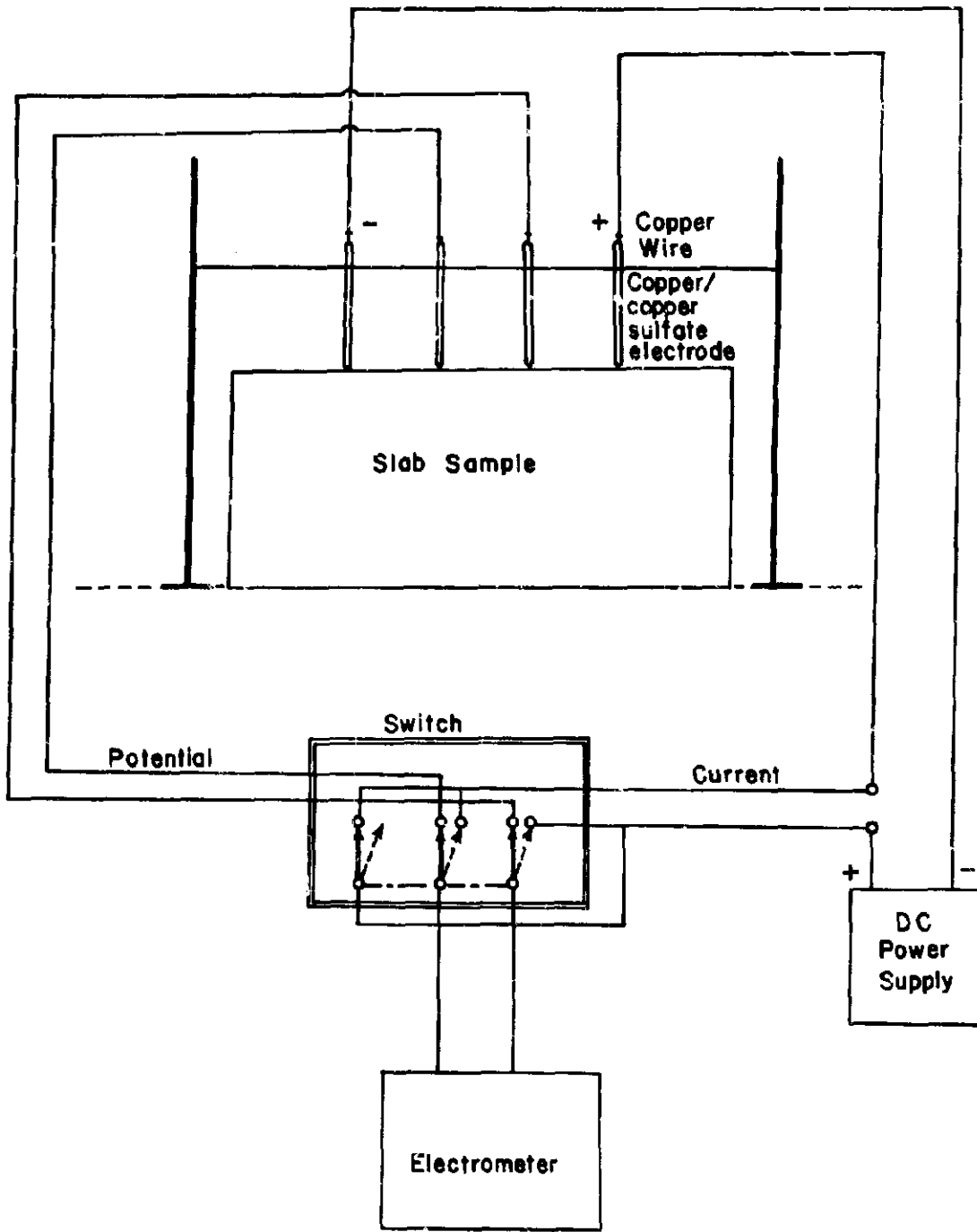


FIGURE 82. APPARATUS FOR RESISTIVITY MEASUREMENT.

the summation starts from the end with higher resistivity, which is the left end, to yield the cumulative resistivity data below.

spacing	1	2	3	4	5
cumulative resistivity ($\times 10^9$ ohm-cm)	3.00	4.10	4.30	4.37	4.43
spacing	6	7			
cumulative	4.48	4.52			

The resistivity data obtained from these slab samples are generally irregular compared to previous data (42). Electrical interference was observed when the resistivity measurement was carried out. A ground current in the magnitude of 10^{-8} - 10^{-9} Amperes was detected even when the power supply was disconnected. This might partly account for the irregularity of the data. The presence of steel rods and thermocouples in some of the slabs might also have complicated the problem. However, the resistivity data still reveal some information on the quality of tested slabs.

The magnitudes of the resistivity data for these tested slabs are generally reasonable. A wet base concrete slab showed a resistivity of the magnitude 10^4 - 10^5 ohm-cm while a dry one showed an average resistivity of 10^7 - 10^8 ohm-cm, as shown in Figure 83. These data are comparable to that obtained at The University of Oklahoma, which showed an average resistivity of 10^4 ohm-cm for wet slabs and 10^6 - 10^{10} ohm-cm for relatively dry slabs, depending on the extent of drying.

4.2 Internally-Sealed Concrete and Overlay

Figure 84 shows the resistivities (in logarithmic scale) of two internally-sealed concrete slabs and two internally-sealed overlay slabs as a function of

spacing. It seems that the resistivity of a internally-sealed concrete slab is slightly lower than that of a laboratory dried base concrete slab, as slab #3402 showed an average resistivity lower than that of a base concrete slab and slab #3363 showed an increase in resistivity with increasing spacing. The high resistivities obtained from the partially melted slabs (#3362H and #3403H) indicates good sealings at least in the surface layers.

In Figure 85, the cumulative resistivity vs spacing diagram indicates an overlay thickness of 1.5 in. (38 mm) (an overlay depth of 2 in. (51 mm) is listed in Table 6). No effect on resistivity due to the presence of reinforcing rods was observed as the location of the steel rods is 3 in. (76 mm) below the surface. The location of the interface of slab #3362H is difficult to tell, possibly because of the presence of steel rods and thermocouples (Figure 86). The cumulative resistivity data are somewhat scattered (Figure 87) for the partially melted internally-sealed concrete slab, #3403H. However, the approximate location of the interface seems to be somewhere around 1.7 in. (43 mm) below the surface.

4.3 Latex Concrete and Overlay

According to Figure 88, the resistivity of a latex concrete slab is also lower than that of a dry base concrete slab. The resistivity of the wet latex overlay slab (#3372) was substantially lower than that of the laboratory dry slab (#3396). This suggests that the latex overlay will absorb water readily. It seems this could be a problem. It is interesting that both latex overlay slabs (#3372 and #3373) showed low resistivity at the same location, 2 in. (51 mm) below the surface. This seems to be an indication of the presence of steel rods, which were 2.25 in. (57 mm) below the surface.

Slab #3356 - Base concrete (laboratory dry) - O
3358 - Base concrete (wet) - - - - - Δ

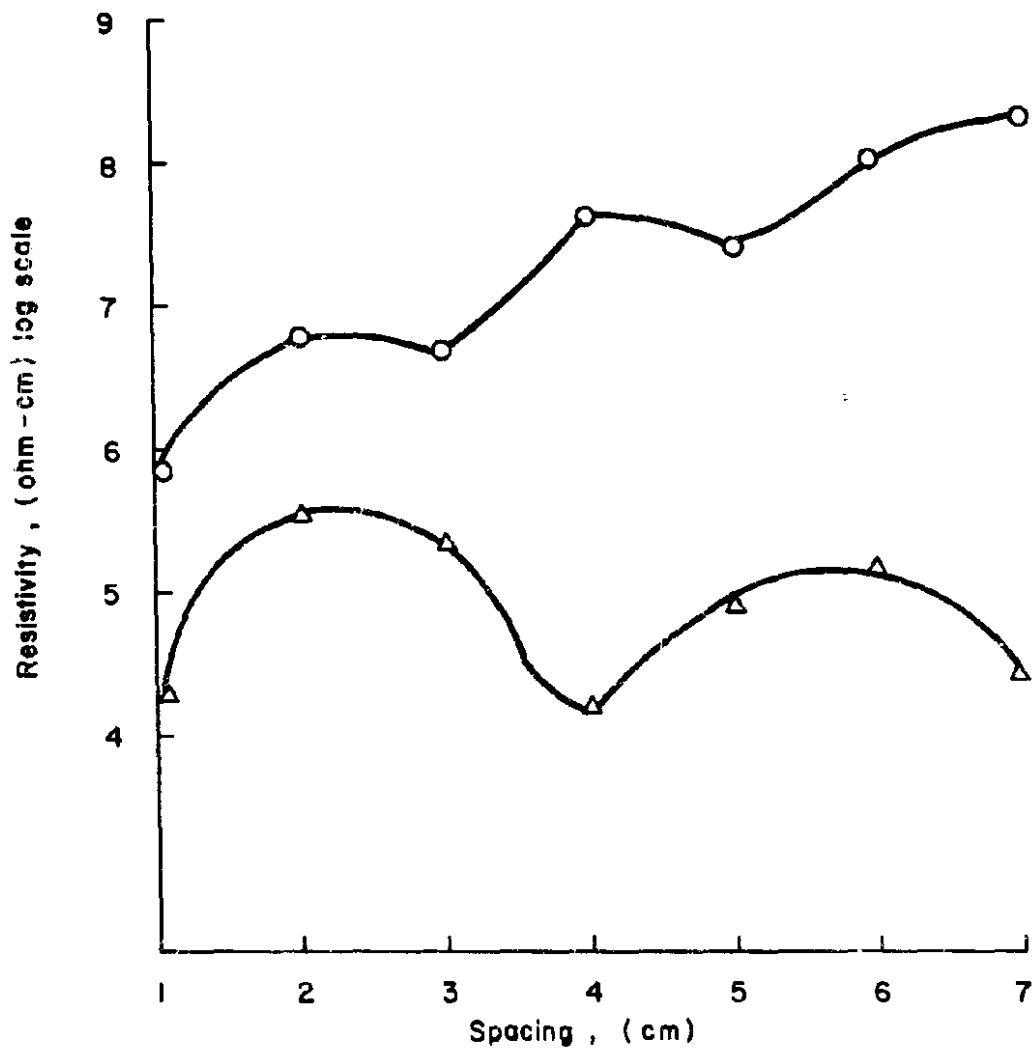


FIGURE 83. RESISTIVITY PROFILES FOR BASE CONCRETE SLABS.

- #3363 - Unmelted internally sealed concrete overlay (with steel) - ○
- #3362H - Partially melted internally sealed overlay - - - - - △
- #3403H - Internally sealed concrete, full depth, partially melted - □
- #3402 - Internally sealed concrete, full depth, unheated - - - - - ●

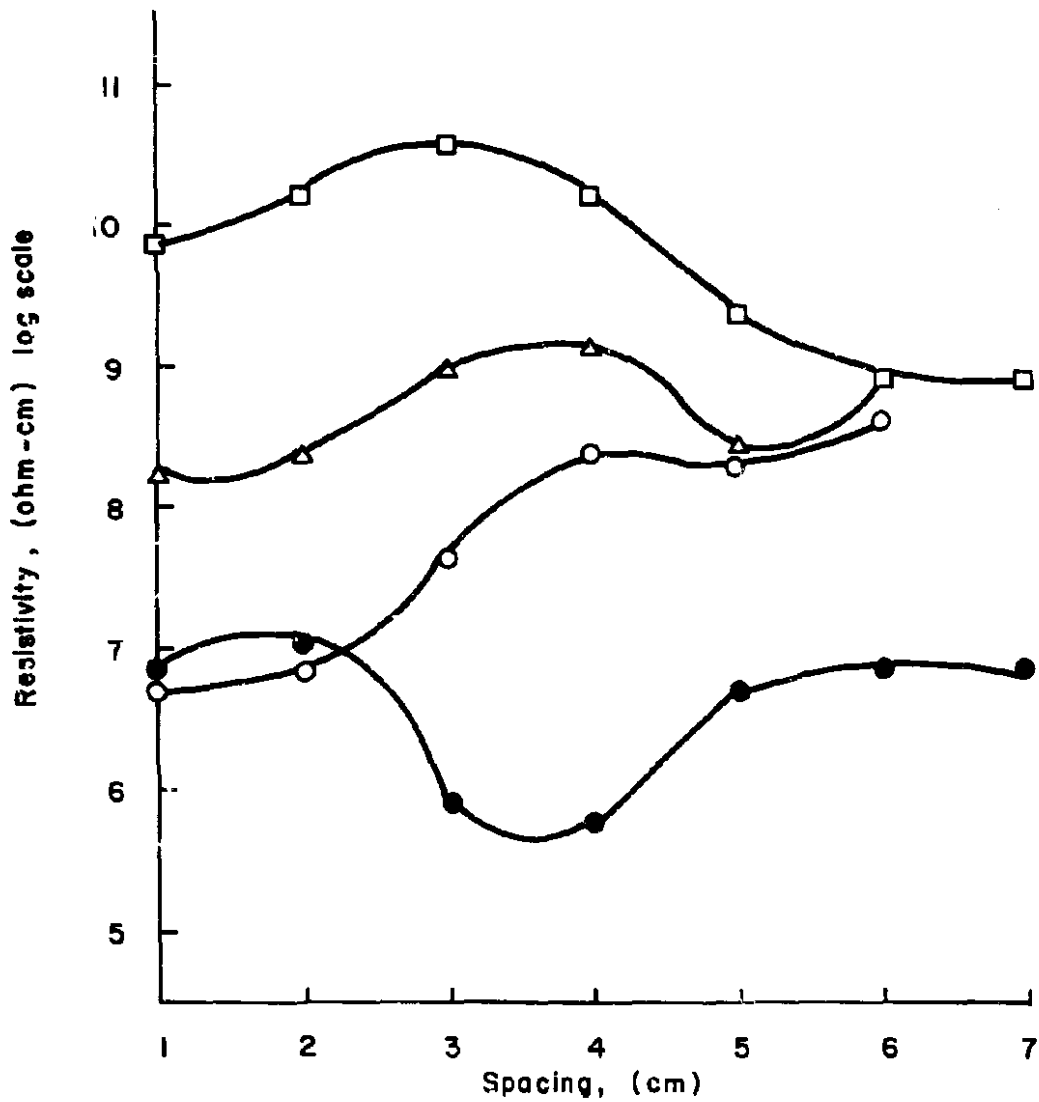


FIGURE 84. RESISTIVITY PROFILES FOR INTERNALLY SEALED CONCRETES.

Slab #3363-Unheated internally sealed overlay (with steel)

Summation starts from right end (a = 6 cm)

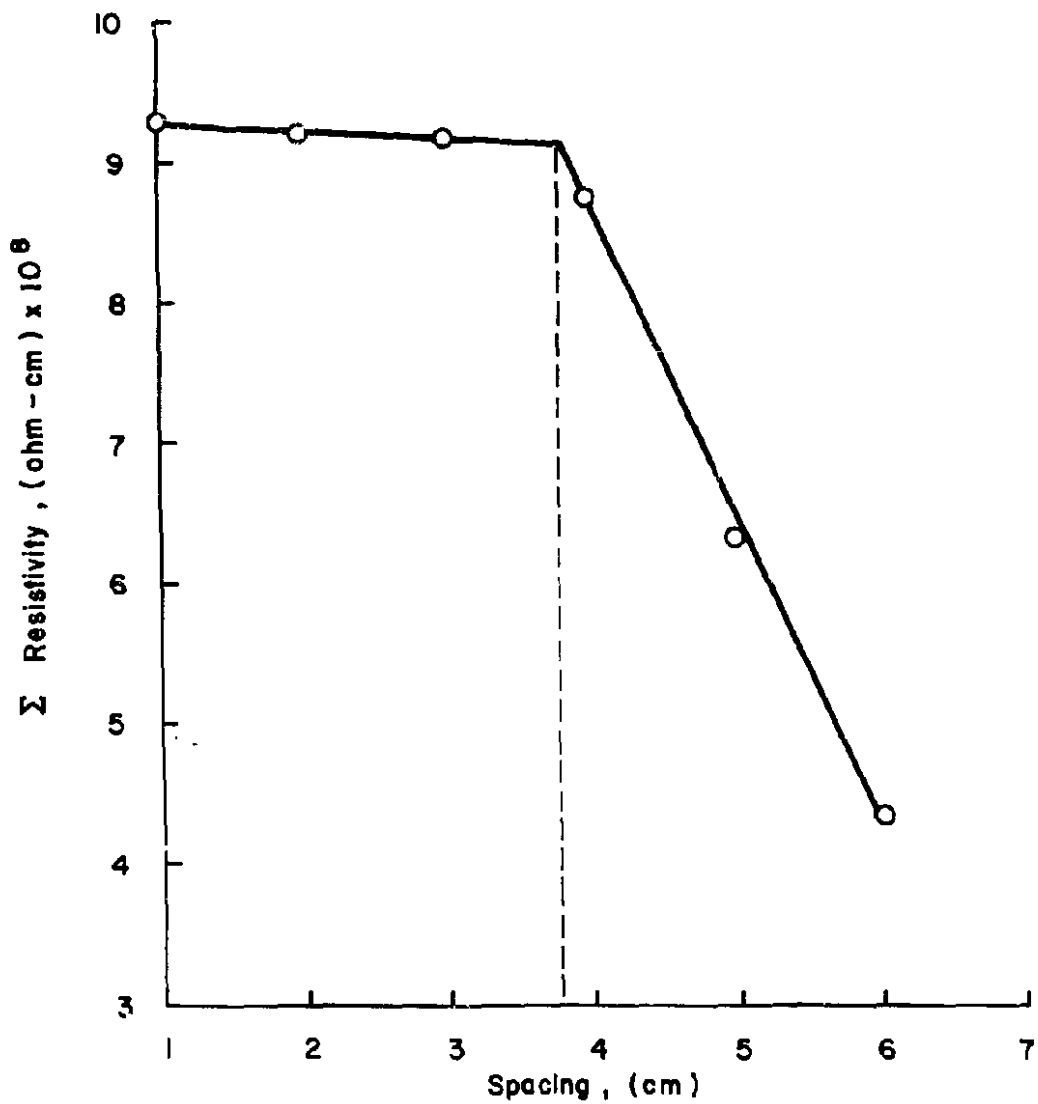


FIGURE 85. RESISTIVITY SUMMATION FOR UNHEATED INTERNALLY SEALED CONCRETE OVERLAY.

Slab#3362H - Partially melted internally sealed overlay (with steel)

Summation starts from right end.

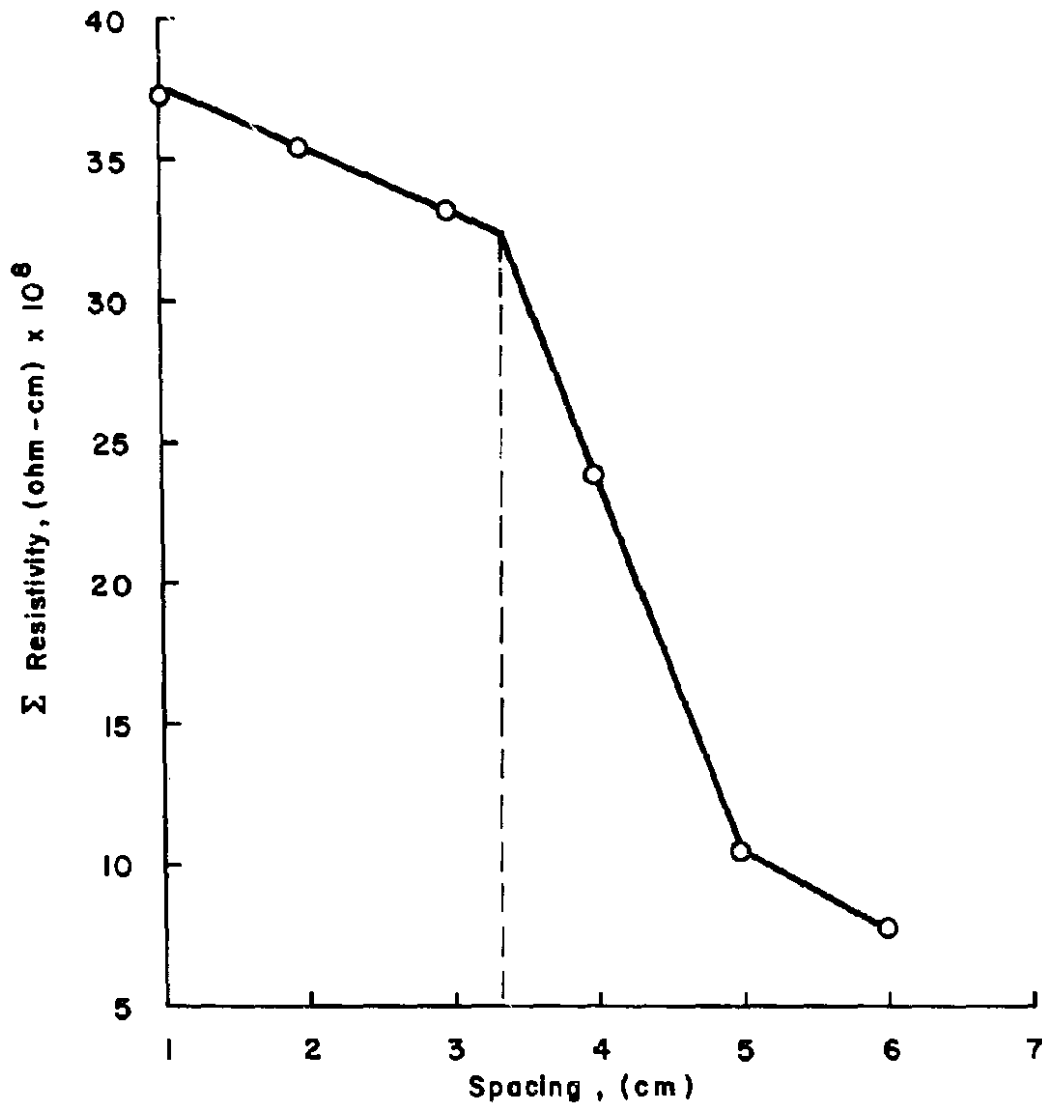


FIGURE 86. RESISTIVITY SUMMATION FOR PARTIALLY MELTED INTERNALLY SEALED CONCRETE OVERLAY.

3403H - Internally sealed concrete , full depth, partially melted

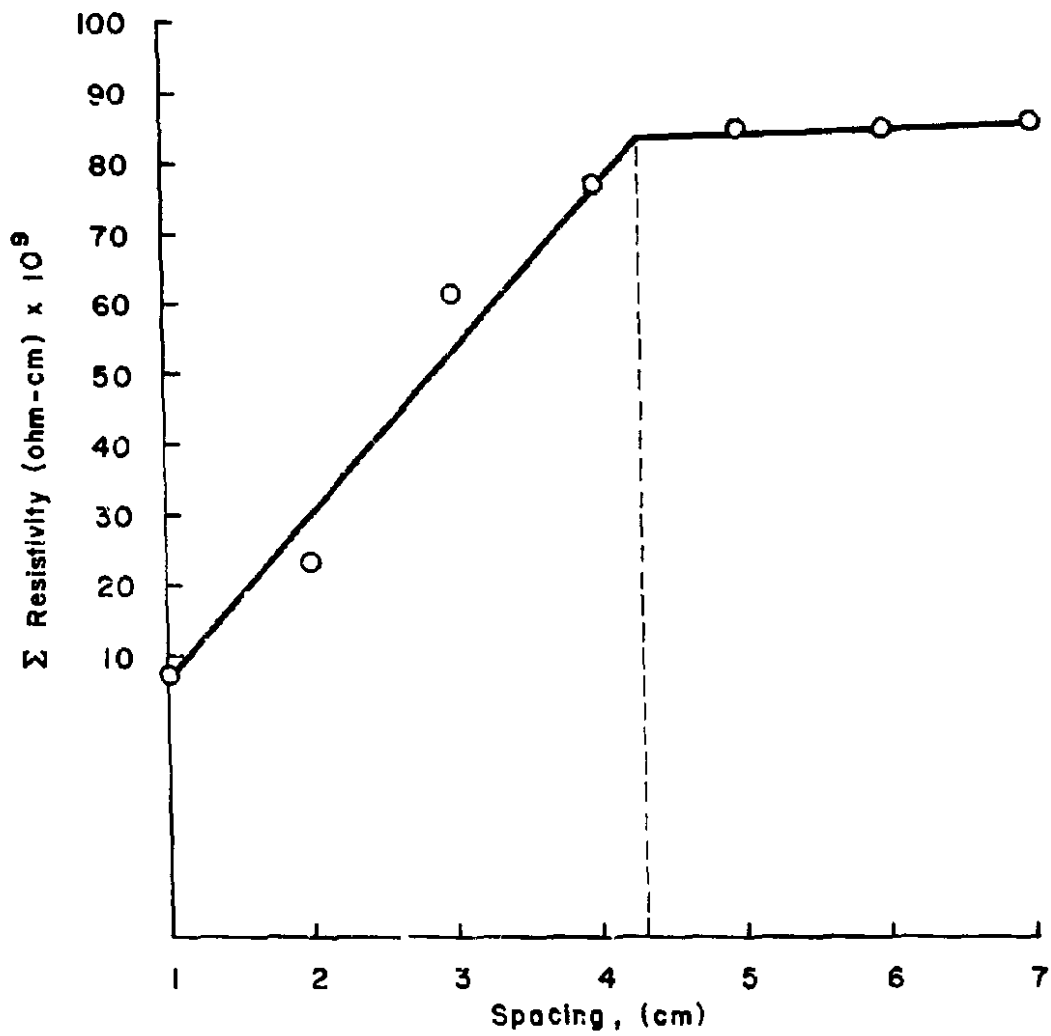


FIGURE 87. RESISTIVITY SUMMATION FOR FULL-DEPTH INTERNALLY SEALED CONCRETE - PARTIALLY MELTED

3396 - Full depth latex concrete, air-dry - ○
 # 3373 - Latex overlay (with steel), air-dry - □
 # 3372 - Latex overlay (with steel), wet - △

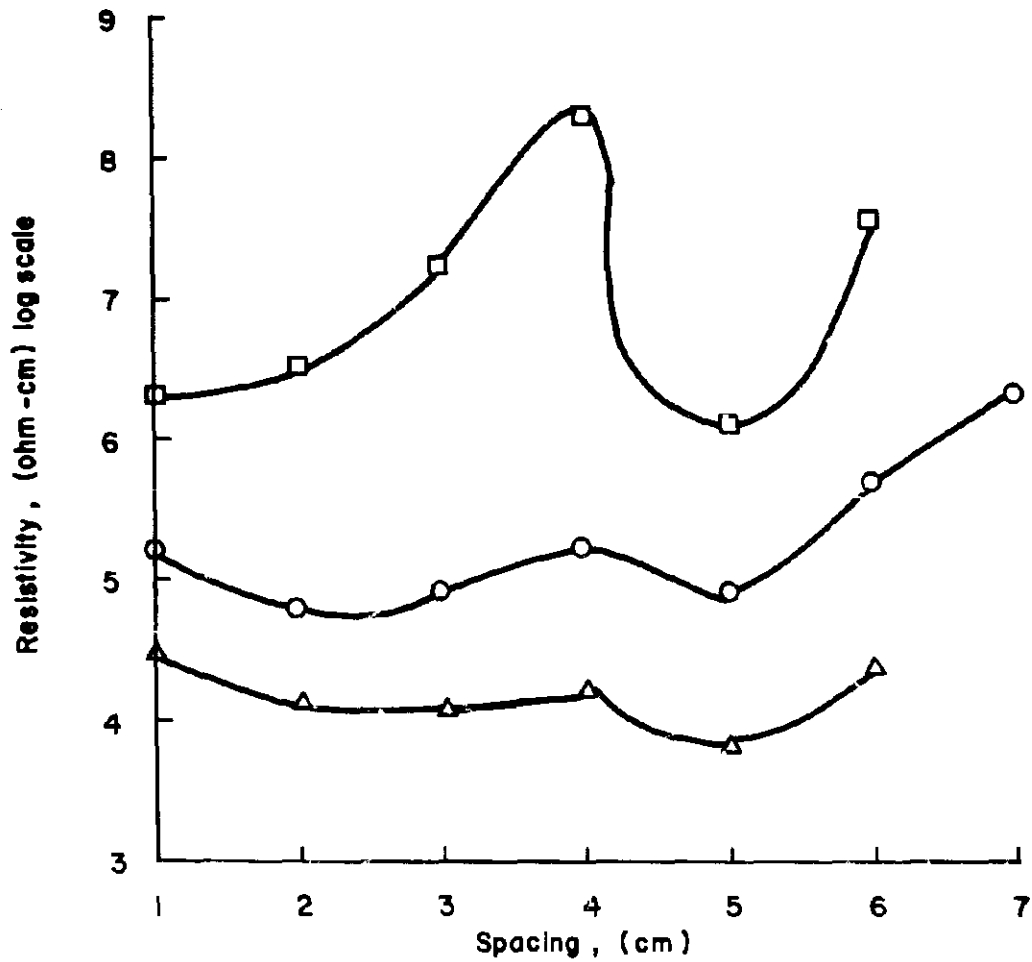


FIGURE 88. RESISTIVITY PROFILES FOR LATEX MODIFIED CONCRETES.

The effect of steel rod on resistivity is pronounced in the dry slab and relatively weak in the wet slab. This fact can be explained by the difference in resistivities between the steel rod and the dry and wet overlay slabs.

The presence of steel rods and thermocouples in #3372 might influence the determination of the overlay depth. The depth is estimated to be 1.45 in. (37 mm) for slab #3372 and 1.56 in. (40 mm) for slab #3373 (listed depth is 1.25 in. (32 mm) for each slab), as shown in Figures 89 and 90.

4.4 Polymer Concrete Overlay

A dry polymer concrete overlay slab (#3413) showed a very high resistivity ($>10^{11}$ ohm-cm) which could not be measured with our instrument with good accuracy. However, resistivity data was obtained for a wet polymer concrete overlay slab (#3412). The resistivity falls into the region of 10^7-10^8 ohm-cm, which is substantially lower than a dry slab (Figure 91). The very thin layer of overlay, 0.5 in. (13 mm), and the presence of thermocouples may be responsible for the resistivity drop. The depth of overlay is difficult to determine, possibly due to the same reasons mentioned above.

Dense Concrete Overlay

A dense concrete also showed a substantial drop in resistivity after exposure to moisture, indicating the infiltration of water (Figure. 92). It appears that after exposure to moisture, there is no significant difference between the resistivity of the high density portion and the base concrete portion. No reasonably accurate determination could be made on the overlay depth in this case.

5. Conclusions

Resistivity data obtained from four-electrode resistivity measurement provide some information which may be helpful in understanding the nature of the overlays and slabs. The experimental results obtained had some inaccuracies which were possibly due to the presence of reinforcing steel, thermocouples and electrical interference.

Based on the results obtained, it seems that this technique may be applicable to measuring the depth of wax-head overlays and partially melted wax-bead layers. This technique may also be effective for depth determination of latex overlays if the effect of steel can be better understood. The depth of polymer concrete overlays and dense concrete overlays probably cannot be measured by this method as the polymer concrete overlay has too high a resistivity and the resistivity difference between dense concrete and base concrete is not significantly large to show the interface.

The major drawbacks of the technique are that there has to be an order of magnitude difference (or more) between the resistivities of the two layers under determination if an interface is to be detected, and that this interface should be relatively sharp. In addition, a very high resistivity material (such as polymer concrete) will prevent any reasonable current from penetrating the overlay, making measurement impossible. This last problem could be overcome, however, by use of higher voltages and/or more sensitive current measurement techniques.

Slab # 3372 - Latex overlay (with steel)

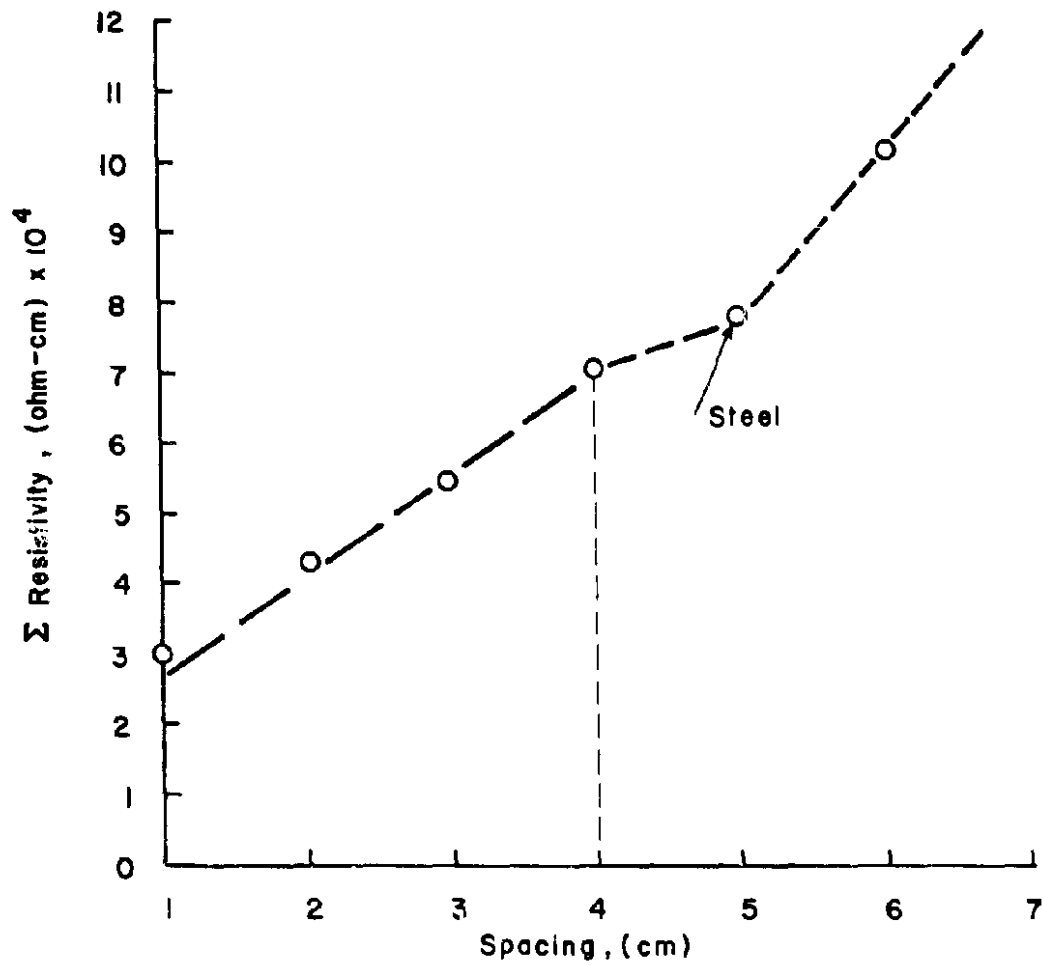


FIGURE 89. RESISTIVITY SUMMATION FOR WET LATEX OVERLAY .

Slab # 3373 - Latex overlay (with steel), air-dry
Summation starts from right end

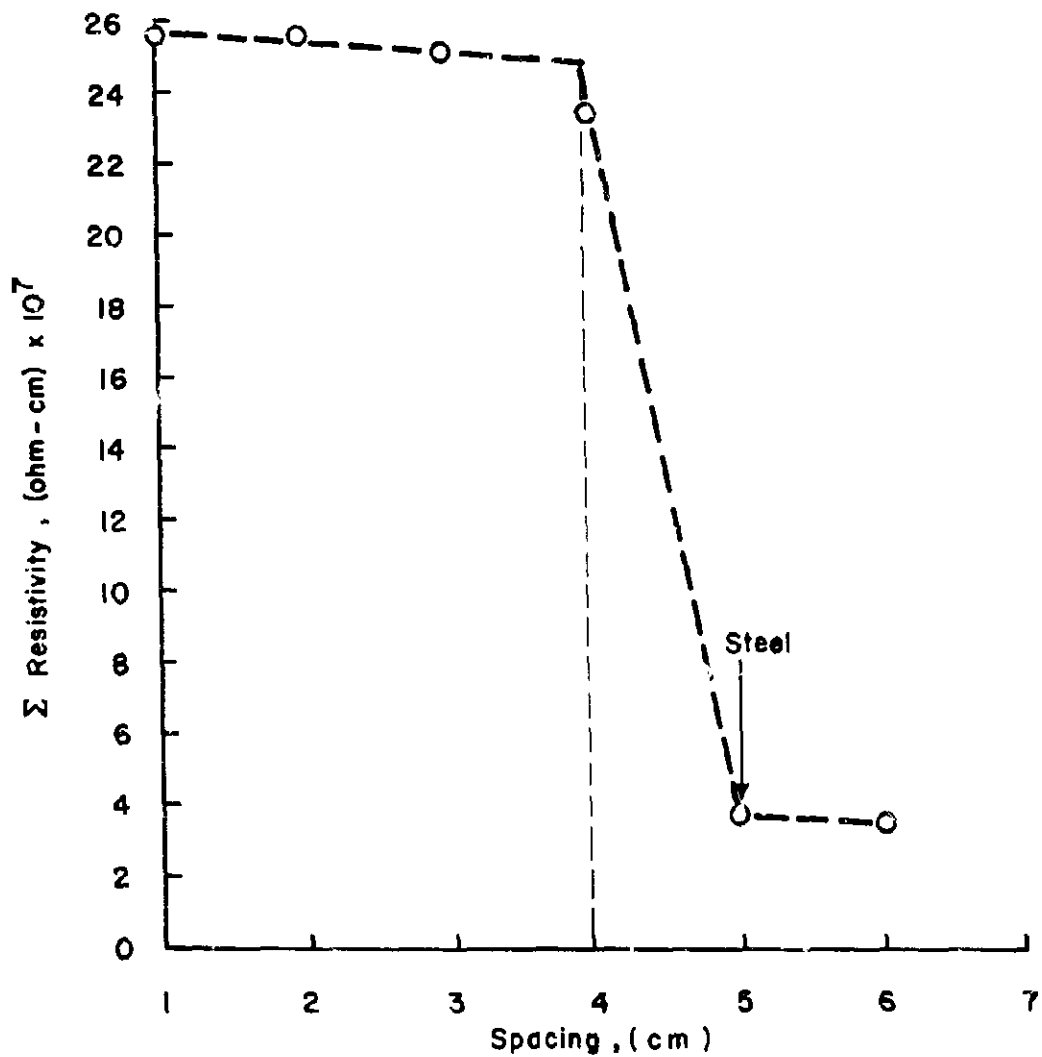


FIGURE 90. RESISTIVITY SUMMATION FOR AIR-DRY LATEX OVERLAY.

Slab # 3412 - Polymer concrete overlay, wet

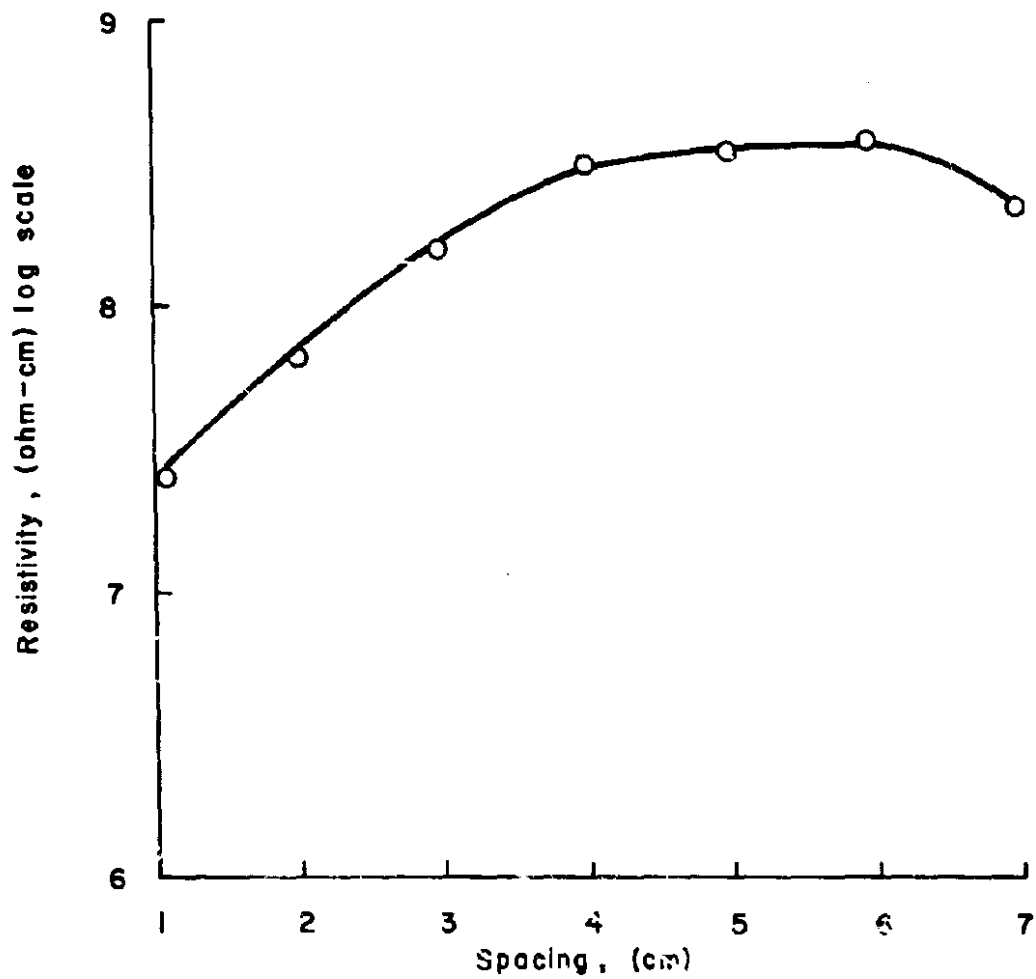


FIGURE 91. RESISTIVITY PROFILE FOR POLYMER CONCRETE OVERLAY.

3381 - Dense concrete overlay , air-dry - O
3382 Dense concrete overlay , wet - - Δ

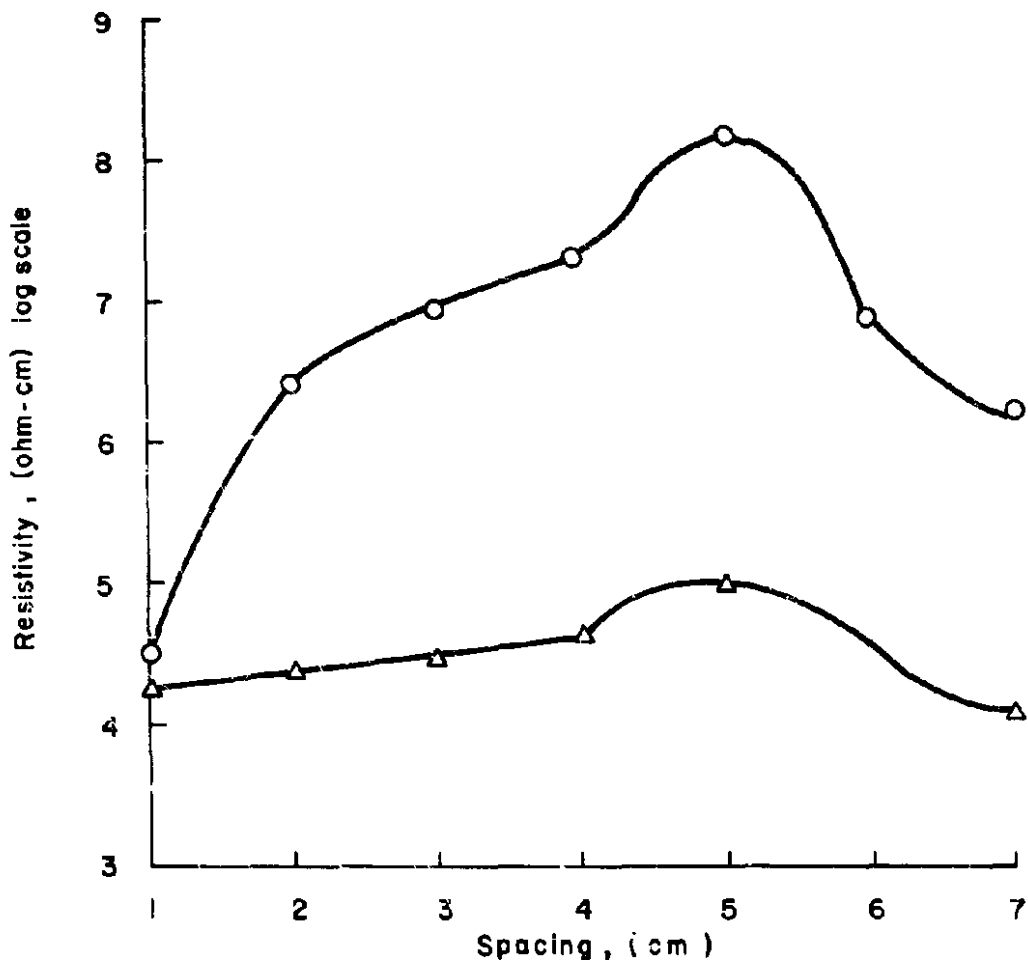


FIGURE 92. RESISTIVITY PROFILES FOR AIR-DRY AND WET DENSE CONCRETE OVERLAYS.

APPENDIX 6

TABLE 39

STRUCTURAL DETAILS

BRIDGE NO. 1

1. NAME: B-36-73 at Manitowoc Rapids, Wisconsin, Northbound lanes over Manitowoc River
2. DESCRIPTION:

Length: 504'-11.5" (153.9 m)

Width: 43'0" (13.1 m) total
12'0" (3.66 m) driving lanes
10'-0" (3.05 m) outside shoulder
6'0" (1.83 m) inside shoulder

Type: Continuous I beam unit 499' (152 m) long having four spans
124'-4.5" (37.9 m), 125' (38.1 m), 125' (38.1 m),
124'-4.5" (37.9 m)

Concrete Deck Slab:
500'-0.5" (152.4 m) long
42'-10" (13.06 m) wide
4,000 psi (27.6 MPa) concrete

Slab Reinforcement: Grade 60 Reinforcement

Top Mat:
No. 4 (13 mm) transverse (20° skew) at 6.5" (165 mm) centers
No. 4 (13 mm) longitudinal at 12.0" (305 mm) centers

Bottom Mat:
No. 4 (13 mm) transverse (20° skew) at 6.5" (165 mm) centers
No. 4 (13 mm) longitudinal at 6.0" (152 mm) centers

Slab Thickness: 7.5" (191 mm)

Plan Cover: 2.0" (51 mm)

Grade: Approaches +1.99% and -2.20%
Main span 1,400' (427 m) vertical curvature arch
3. SALT EXPOSURE: None

TABLE 40

STRUCTURE DETAILS

BRIDGE NO. 2

1. NAME: B-41-62 at Lincoln, Wisconsin, Eastbound lanes over C&NW R.R. Track
2. DESCRIPTION:

Original Deck
Length: 189'-7" (57.8 m)
Width: 42'0" (12.8 m) total
22'0" (6.7 m) driving lane
12'-0" (3.7 m) passing lane
6'0" (1.83 m) shoulder

Type: Continuous I beam unit 186.5' (56.8 m) long having three spans:
62' (18.9 m)
62.5' (19.1 m)
62' (18.9 m)

Concrete Deck Slab:
188.7' (57.5 m) long
41.5' (12.6 m) wide
Grade AA Concrete

Slab Reinforcement: Grade 20 Reinforcement

Top Mat:
No. 6 (19 mm) transverse at 7.5" (191 mm) centers
No. 5 (16 mm) longitudinal at 13" (330 mm) centers

Bottom Mat:
No. 6 (19 mm) transverse at 7.5" (191 mm) centers
No. 5 (16 mm) longitudinal at 6.5" (165 mm) centers

Slab Thickness: 6.5" (165 mm)

Plan Cover: 2.0" (51 mm)

Grade: +0.75% E. to W.

APPENDIX 7

TABLE 41
SLAB IDENTIFICATION AND STORAGE CONDITIONS

<u>Description</u>	<u>Storage</u>		
	<u>Moist</u> <u>(73°F-100% RH)^{2/}</u>	<u>Frozen- As Received^{1/}</u> <u>(0°F)</u>	<u>Air</u> <u>(73°F-50% RH)</u>
w/c = 0.60	3388	3387	3386
w/c = 0.50	3357	3358	3356
w/c = 0.40	3392	3393	3391
Latex Modified-Full Depth	3399	3397	3396
Internally-Sealed-Full Depth-Heated	3367H	-	3366H, 3403H
Internally-Sealed-Full Depth-Unheated	-	3368	3365, 3402
Polymer Impregnated Concrete	3408	3407	3406
Latex Modified-Overlay	3372	3373	3371
Internally-Sealed-Overlay-Heated	3362H	-	-
Internally-Sealed-Overlay-Unheated	-	3363	3361
10% Overlay	3382	3383	3381
Polymer Concrete Overlay	3412	3413	3411

^{1/} Specimens were sealed in heavy plastic bags prior to freezing
^{2/} °C = 5/9(°F - 32)

FEDERALLY COORDINATED PROGRAM (FCP) OF HIGHWAY RESEARCH AND DEVELOPMENT

The Offices of Research and Development (R&D) of the Federal Highway Administration (FHWA) are responsible for a broad program of staff and contract research and development and a Federal-aid program, conducted by or through the State highway transportation agencies, that includes the Highway Planning and Research (HP&R) program and the National Cooperative Highway Research Program (NCHRP) managed by the Transportation Research Board. The FCP is a carefully selected group of projects that uses research and development resources to obtain timely solutions to urgent national highway engineering problems.*

The diagonal double stripe on the cover of this report represents a highway and is color-coded to identify the FCP category that the report falls under. A red stripe is used for category 1, dark blue for category 2, light blue for category 3, brown for category 4, gray for category 5, green for categories 6 and 7, and an orange stripe identifies category 0.

FCP Category Descriptions

1. Improved Highway Design and Operation for Safety

Safety R&D addresses problems associated with the responsibilities of the FHWA under the Highway Safety Act and includes investigation of appropriate design standards, roadside hardware, signing, and physical and scientific data for the formulation of improved safety regulations.

2. Reduction of Traffic Congestion, and Improved Operational Efficiency

Traffic R&D is concerned with increasing the operational efficiency of existing highways by advancing technology, by improving designs for existing as well as new facilities, and by balancing the demand-capacity relationship through traffic management techniques such as bus and carpool preferential treatment, motorist information, and rerouting of traffic.

3. Environmental Considerations in Highway Design, Location, Construction, and Operation

Environmental R&D is directed toward identifying and evaluating highway elements that affect

the quality of the human environment. The goals are reduction of adverse highway and traffic impacts, and protection and enhancement of the environment.

4. Improved Materials Utilization and Durability

Materials R&D is concerned with expanding the knowledge and technology of materials properties, using available natural materials, improving structural foundation materials, recycling highway materials, converting industrial wastes into useful highway products, developing extender or substitute materials for those in short supply, and developing more rapid and reliable testing procedures. The goals are lower highway construction costs and extended maintenance-free operation.

5. Improved Design to Reduce Costs, Extend Life Expectancy, and Insure Structural Safety

Structural R&D is concerned with furthering the latest technological advances in structural and hydraulic designs, fabrication processes, and construction techniques to provide safe, efficient highways at reasonable costs.

6. Improved Technology for Highway Construction

This category is concerned with the research, development, and implementation of highway construction technology to increase productivity, reduce energy consumption, conserve dwindling resources, and reduce costs while improving the quality and methods of construction.

7. Improved Technology for Highway Maintenance

This category addresses problems in preserving the Nation's highways and includes activities in physical maintenance, traffic services, management, and equipment. The goal is to maximize operational efficiency and safety to the traveling public while conserving resources.

0. Other New Studies

This category, not included in the seven-volume official statement of the FCP, is concerned with HP&R and NCHRP studies not specifically related to FCP projects. These studies involve R&D support of other FHWA program office research.

* The complete seven-volume official statement of the FCP is available from the National Technical Information Service, Springfield, Va. 22161. Single copies of the introductory volume are available without charge from Program Analysis (HRD-3), Offices of Research and Development, Federal Highway Administration, Washington, D.C. 20590.